



UNIVERSITA' DELLA CALABRIA

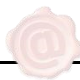
Dipartimento di Chimica e Tecnologie Chimiche


*Scuola di Dottorato in
Scienze e Ingegneria dell'Ambiente, delle Costruzioni e dell'Energia
(SIACE)*

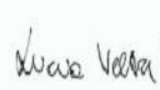
XXXIII CICLO

Settore Scientifico Disciplinare CHIM06 (Chimica Organica)


***New Catalyzed Approaches For The One-Step Synthesis
Of
High Value-Added Products***

Coordinatore: Ch.mo Prof. Salvatore Critelli
CRITELLI SALVATORE
Firma  12.05.2021 07:26:25 UTC

Supervisore: Ch.mo Prof. Bartolo Gabriele
Firma


Supervisore: Dott.ssa Lucia Veltri
Firma


Dottoranda: Dott.ssa Roberta Amuso

Firma 

Contents

ABSTRACT	3
CHAPTER 1	5
<i>Synthesis of Thiadiazafluorenones by a Palladium-Catalyzed Cyclocarbonylation Approach</i>	5
1.1 INTRODUCTION	6
1.2 RESULTS AND DISCUSSION	14
1.3 CONCLUSIONS	22
1.4 EXPERIMENTAL SECTION	23
1.5 CHARACTERIZATION DATA	26
1.6 REFERENCES	35
CHAPTER 2	37
<i>α-Alkylation of Ketones with Alcohols by Cyclometalated Ruthenium Pincer Complexes as Catalysts</i>	37
2.1 INTRODUCTION	38
2.2 RESULTS AND DISCUSSION	46
2.3 CONCLUSIONS	54
2.4 EXPERIMENTAL SECTION	55
2.5 CHARACTERIZATION DATA	62
2.6 REFERENCES	72
CHAPTER 3	75
<i>Cyclometalated Ruthenium Complexes as Catalyst for Efficient Alkylation of Anilines with Alcohols</i>	75
3.1 INTRODUCTION	76
3.2 RESULTS AND DISCUSSION	78
3.3 CONCLUSIONS	85
3.4 EXPERIMENTAL SECTION	86
3.5 CHARACTERIZATION DATA	88
3.6 REFERENCES	94
CHAPTER 4	97
<i>Synthesis of 1,3-Oxazine-2,4-Diones by DBU-Catalyzed Incorporation of Carbon Dioxide Into 3-Ynamides</i>	97
4.1 INTRODUCTION	98
4.2 RESULTS AND DISCUSSION	104
4.3 CONCLUSIONS	111
4.4 EXPERIMENTAL SECTION	112
4.5 CHARACTERIZATION DATA	114
4.6 REFERENCES	121
CHAPTER 5	123
<i>Synthesis of Oxazinobenzimidazolone Derivatives by $ZnCl_2$-Promoted Cyclization</i>	123
5.1 INTRODUCTION	124
5.2 RESULTS AND DISCUSSION	129
5.3 CONCLUSIONS	137
5.4 EXPERIMENTAL SECTION	138
5.5 CHARACTERIZATION DATA	140
5.6 REFERENCES	150
CHAPTER 6	153
Conclusions	153

Abstract

Heterocyclic compounds play an important role in synthetic and bioorganic chemistry, as they represent a structural motif in a large number of biologically active natural and non-natural compounds. The synthesis of new heterocycles possessing biological activity and the development of innovative and accessible synthetic pathways are currently a very widespread research area.

In the present PhD thesis is reported the development of new synthetic, simple and innovative methodologies in one step for the direct formation of high value-added compounds by the catalytic activation of simple building blocks, CO and CO₂.

CO is a simplest and most available C-1 unit, which meets the requirements of “atom economy”, step economy and “green chemistry”; the possibility to synthesize molecules of important pharmacological interest by a direct carbonylation procedure involving the use of carbon monoxide represent a very attractive alternative synthetic approach.

CO₂ is the main component of greenhouse gases, responsible for the increase in the earth's temperature and anomalous climate changes. Thus, post-combustion CO₂ capture and its conversion into high value-added chemicals are integral parts of today's green energy industry. In fact, carbon dioxide can be considered as a ubiquitous, cheap, abundant, non-toxic, non-flammable and renewable C1 source, which has great importance from the viewpoint of both environmental protection and resource utilization.

In the first chapter is reported a new example of an additive cyclocarbonylation process leading to 1-thia-4a,9-diazafluoren-4-ones, an important class of polyheterocyclic compounds known to possess important pharmacological activities.

Part of this PhD was spent at Leibniz Institute for Catalysis in Rostock University. Here, ruthenium PNP pincer complexes bearing supplementary cyclometalated C,N-bound ligands have been prepared and fully characterized for the first time. The advantages of the new catalysts are demonstrated in the general *green* α -alkylation of ketones with alcohols following a hydrogen autotransfer protocol. Furthermore, other cyclometalated ruthenium complexes bearing bidentate ligand were obtained for methylation of anilines with methanol to selectively give *N*-methylanilines. The hydrogen autotransfer procedure has been applied under mild conditions (60 °C) in a practical manner (NaOH as base).

A new process for the utilization of carbon dioxide to give high value-added 1,3-oxazine-2,4-diones is presented in the fourth chapter. It is based on the catalytic carboxylative heterocyclization of readily available 3-ynamides, using 1,8-diazabicyclo[5.4.0]undec-7-ene (DBU) as organocatalyst. The reaction, which takes place under relatively mild conditions [80 °C for 15 h in a 3:1 mixture (v/v) of MeCN-HC(OMe)₃, under 30 atm of CO₂] proceeds through an ordered sequence of steps, involving substrate deprotonation by DBU, nucleophilic attack to CO₂, 6-*exo-dig* cyclization, and isomerization, to give the final products in 44-85% yields over 16 examples.

Finally, the synthesis of high value-added polycyclic heterocyclic derivatives by metal-promoted annulation of acyclic precursors is one of the most important area of research in heterocyclic chemistry and a straightforward approach to new polycyclic heterocycles, 1*H*-benzo[4,5]imidazo[1,2-*c*][1,3]oxazin-1-ones is described in the last part. It is based on the ZnCl₂-promoted deprotective 6-*endo-dig* heterocyclization of *N*-Boc-2-alkynylbenzimidazoles under mild conditions (CH₂Cl₂, 40 °C for 3 h).

Chapter 1

Synthesis of Thiadiazafluorenones by a Palladium-Catalyzed Cyclocarbonylation Approach

1.1 Introduction

1.1.1 Incorporation of the simplest C-1 unit (carbon monoxide) for the direct formation of high value-added carbonylated products

Carbon monoxide is a cheap, abundant, and readily available C-1 source. For many years particularly attractive to academia and the chemical industry has been the opportunity to activate CO for efficient incorporation into an organic substrate. Indeed, a process like this, called carbonylation, is considered the most attractive and sustainable way for the direct synthesis of carbonyl compounds starting from readily available substrates (alkenes, alkynes, alcohols, amines, and so on), thanks to the elevated atom economy and the continuous development of catalytic systems able to promote the process under mild conditions and with high selectivity.¹

1.1.2 Carbonylation reactions

Carbonylation² is the incorporation of carbon monoxide into an organic substrate, for example by the insertion of CO into an existing bond, such as C–X (X=Cl, Br, I), or by the addition of CO to unsaturated compounds, such as alkynes or olefins and alkylic, vinylic, aryl species in the presence of nucleophiles (NuH). The carbonyl compounds can be directly synthesized starting from the simplest C-1 unit, which also meets the requirements of “atom economy”³, step economy⁴ and “green chemistry”⁵. The advantages of carbonylation reactions are very interesting and distinguishable: the carbon chain can be easily increased after the insertion of carbon monoxide; carbonyl-containing compounds are important synthetic intermediates in organic synthesis, which significant applications in advanced materials, agro-chemicals, dyes, pharmaceuticals, and so on; being a fundamental and promising transformation, the carbonylation process introduces a new approach for constructing synthetically versatile cyclic-acyclic carbonylated derivatives with high efficiency and selectivity⁶.

Carbon monoxide (CO) was discovered in the 18th century by de Lassone from the reaction of zinc oxide with coke. The initial work in the field of carbonylations was done by W. Reppe at BASF in the 1930s and 1940s; who coined the term “carbonylation”^{7b}, since then, carbonylation reactions have gained great importance in Chemical industry. 80 years of

research and development in the field of carbonylation, today made it possible to synthetic chemist to routinely employ CO as an inexpensive and easily available C1 source to synthesize all kinds of carbonyl compounds. Nowadays, academic and industrial laboratories have broadly explored CO's use in chemical reactions⁷. Alcohols, amines, ethers, carboxylic acids and halides can be converted to acids, amides, esters, ketones, alkyones, alkenones, anhydrides and acid halides with the assistance of transition metal catalysts in the presence of a CO source. The CO sources used can be carbon monoxide gas, metal carbonyls such as $\text{Mo}(\text{CO})_6$, $\text{Co}(\text{CO})_6$, formic acid, aldehyde.

Among the different catalytic reactions, carbonylation is of particular importance, which represents industrial core technologies for converting various bulk chemicals into a diverse set of useful products of our daily life. In fact, today the largest applications of homogeneous catalysis in bulk chemical industry (regarding scale) are carbonylation reactions, especially hydroformylations. The most successful example of industrial carbonylation process is the synthesis of acetic acid via carbonylation of methanol [by Rh catalysis (Monsanto process) or Ir catalysis (Cativa process)]⁸. Not only carboxylic acids, esters and amides are accessible by carbonylation, but anhydrides, acid fluorides, aldehydes, and ketones can also be easily synthesized. Which of these products are obtained depends on the nucleophile: water (hydroxycarbonylation), alcohols (alkoxycarbonylation), amines (aminocarbonylation), carboxylate salts; fluorides, hydrides, or organometallic reagents can be used.

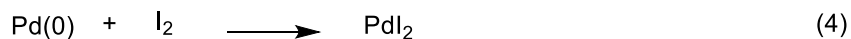
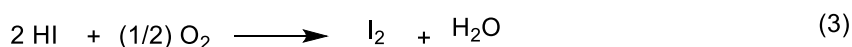
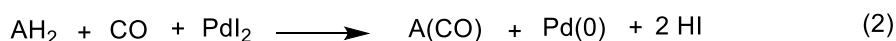
A variety of carbonylation products can be prepared from the same aromatic substrate simply by changing the nucleophile, an advantage with respect to biologically active compound libraries. In addition to intermolecular carbonylations, intramolecular reactions are also possible, which allow for the synthesis of heterocycles. A prominent example is the intramolecular alkoxy- or aminocarbonylation (cyclocarbonylation) of hydroxy- or amino-substituted aryl/vinyl halides which enables the synthesis of lactones, lactams, oxazoles, thiazoles, imidazoles, and other heterocycles⁶.

On the basis of the reaction mechanism, it is possible to distinguish four types of carbonylation reactions: *Substitutive Carbonylation*, *Additive Carbonylation*, *Reductive Carbonylation* and *Oxidative Carbonylation*.

1.1.3 Palladium-catalyzed carbonylation reaction

Palladium metal based catalytic system has been routinely employed in carbonylation reactions preferably for oxidative carbonylation and carbonylative coupling reactions than hydroformylation reactions. Palladium catalyzed oxidative carbonylation reactions require the coupling of organic nucleophiles or electrophiles in the presence of CO and an oxidant to prepare various carbonyl-containing compounds¹⁰. Under oxidative carbonylation conditions palladium can lead to the formation of mono and double carbonylated products¹¹. Most commonly Pd(II) catalyst reacts with the organic substrates of electron-rich species, such as olefins, alkynes, and arenes¹². Numerous Pd(II) complexes of the type L_2PdX_2 can be easily formed from $PdCl_2$ and the appropriate ligand L. The well-known Pd(II) complexes¹³ are $PdCl_2(PPh_3)_2$, $Pd(OAc)_2$, and $PdCl_2(RCN)_2$ and PdI_2 ^{2,14}. Various carbonylation reactions catalyzed by palladium metal have been reported in literature.

One of the most versatile and efficient catalysts in diverse kinds of carbonylation processes (oxidative carbonylations as well as additive and substitutive carbonylations)² is the catalytic system PdI_2 in conjunction with KI, developed, about 20 years ago¹⁴, by Prof Gabriele. PdI_2 catalyst in conjunction with an excess of iodide anions from KI, constitutes an exceptionally efficient, selective and versatile catalyst for promoting a variety of oxidative carbonylation processes, leading to important acyclic as well as heterocyclic carbonyl compounds under mild conditions and with high selectivity. The main characteristics of this system are its simplicity, the only ligands for Pd(II) being electron rich iodide anions which also provides efficient mechanism of re-oxidation of Pd(0) to Pd(II) by the use of oxygen directly as the external oxidant. PdI_4^{2-} , formed in situ (Scheme 1.1.1, Eq. 1) from the reaction between PdI_2 and KI, is an active species to carry out the effective carbonylation process, also responsible for solubility of catalyst in the solvent which tends to perform carbonylation under homogeneous catalytic conditions. Carbonylation of the organic substrate (AH_2) results into formation of carbonylated product and reduced Pd(0) species along with liberated two moles of HI (Scheme 1.1.1, Eq. 2, in the following scheme anionic iodide ligands are omitted for clarity). Reaction of HI with oxygen present in gas mixture occurs along with production of water as product (Scheme 1.1.1, Eq. 3). Pd(0) reoxidation occurs through oxidative addition of I_2 (Scheme 1.1.1, Eq. 4).



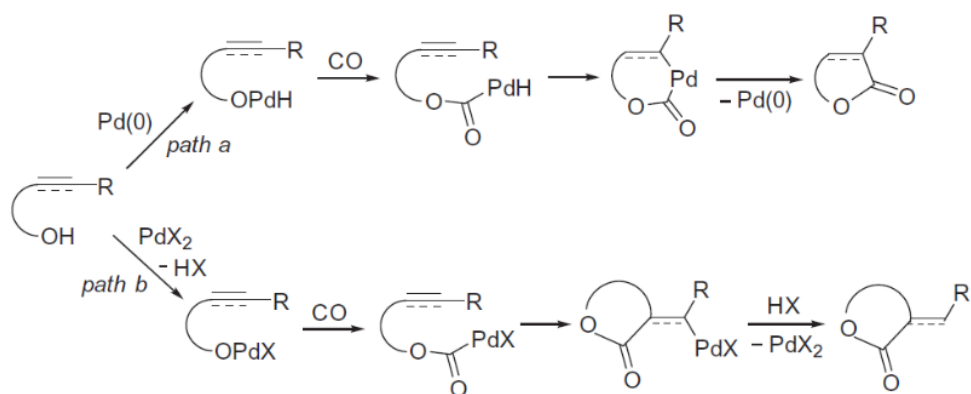
Scheme 1.1.1 Mechanism of Pd(0) reoxidation in PdI₂/KI-catalysed oxidative carbonylation reactions. Anionic iodide ligands are omitted for clarity. AH₂ = organic substrate; A (CO) = carbonylated product.

PdI₄²⁻ is generally a more active catalyst species than PdCl₄²⁻, which was, in turn, more active than neutral complexes, such as (PhCN)₂PdCl₂ or Pd(OAc)₂. These results indicate that the active catalytic species is stabilized by halide ligands. Moreover, the better results obtained with iodide rather than chloride can be interpreted in view of the higher electron-releasing power of I⁻ compared with Cl⁻.

1.1.4 Palladium-Catalyzed Cyclocarbonylations Leading to Heterocycles Under Nonoxidative Conditions

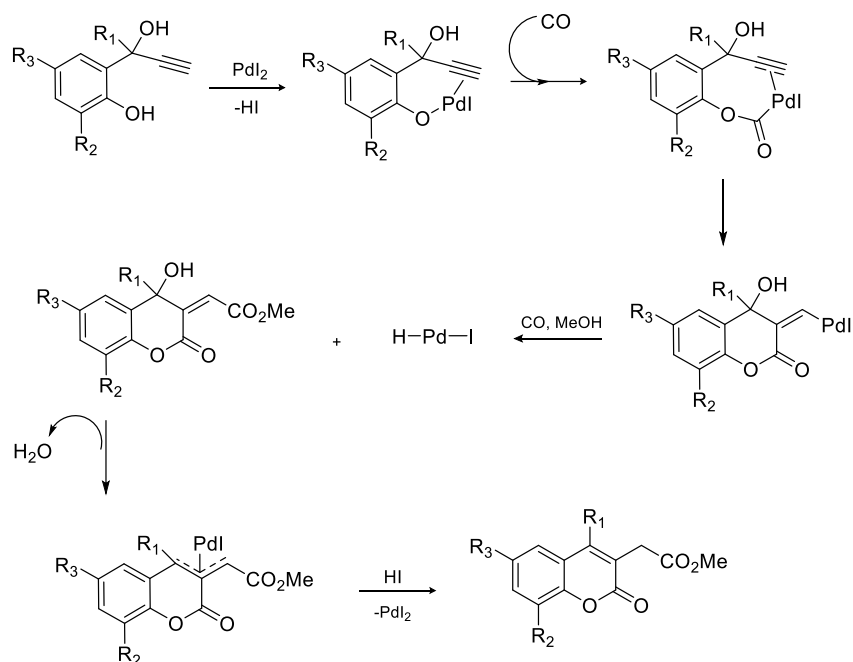
In the palladium-catalyzed carbonylative heterocyclization reactions, a palladium-based species is able to promote both the heterocyclization of a suitably functionalized substrate and the incorporation of one or more CO molecules, with formation of carbonylated heterocycles in a single catalytic process. These processes can occur in two different pathways: *a) under oxidative conditions* and *b) under nonoxidative conditions*. In this section will be discussed and explained the heterocyclization under nonoxidative conditions¹⁵.

Non only halides but other substrates can be cyclocarbonylated to afford heterocycles. Alkenes and alkynes functionalized with a suitably placed nucleophilic group are excellent substrates for the synthesis of heterocycles by cyclocarbonylation reactions. These processes can be catalyzed either by Pd(0) or Pd(II) species, through different mechanistic pathways, as exemplified in Scheme 1.1.2 in the case of unsaturated alcohols.



Scheme 1.1.2 Possible mechanistic pathways leading to oxygen heterocycles by Pd(0)- or Pd (II)-catalyzed (pathways a and b, respectively) cyclocarbonylation of unsaturated alcohols.

The Gabriele's group reported an innovative synthesis of coumarins under conditions of Pd(II) catalysis, using the PdI₂/KI catalyst. The method was based on carbonylation of 2-(1-hydroxyprop-2-ynyl)phenols carried out in MeOH as solvent and external nucleophile and under 90 atm of CO. As shown in Scheme 1.1.3, formation of coumarin derivative could be interpreted as occurring through an ordered sequence of steps, involving: CO insertion into a palladium phenate bond, followed by intramolecular triple bond insertion, alkoxy carbonylation of the ensuing vinylpalladium complex to give an intermediate bearing an allyl alcoholic moiety and a palladium hydride species, formation of a π-allyl complex with elimination of water, and protonolysis. As can be seen from Scheme 1.1.3, Pd(II) was regenerated in the last step, so the process occurred without need for palladium reoxidation, and therefore under nonoxidative conditions. These new coumarin derivatives thus obtained possess interesting phytotoxic and herbicidal activity.

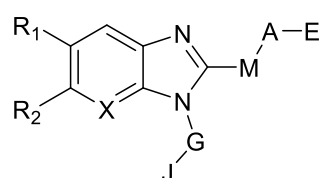


Scheme 1.1.3 Synthesis of coumarin derivatives by cyclocarbonylation of 2-(1-hydroxyprop-2-ynyl)phenols ($R_1=H, Me, Ph$; $R_2=H, OMe$; $R_3=H, OMe, Cl$).

1.1.5 Pharmacological importance of thiadiazafluorenes

The incorporation of benzimidazole nucleus, a biologically accepted pharmacophore in medicinal compounds, has made it a versatile heterocyclic moiety possessing wide spectrum of biological activities¹⁶, in particular strong cardiotonic activity and other derivatives are known to be anti-hypersecretion agents.

A benzimidazole derivative or its medically acceptable salt, represented by the following formula shown in figure 1.1.1, is a human chymase activity inhibitor capable of being applied clinically:



$R_1, R_2 = H, -R, OR$;
 $X = -CH=, N$;
 $G =$ alkylene group;
 $J =$ heterocyclic group;
 $M = -CH_2-, -S(O)m-$;
 $A =$ alkylene group or an alkenylene group;
 $E = -COOR, -SOR, CONHR$ or $-SONHR$, etc.

Fig. 1.1.1 Heterocyclic moiety of benzimidazole derivative

Chymase is a neutral protease present in mast cell granules, and is intimately involved in various biological reactions participated in by mast cells. For example, chymase has been reported to have various actions, including the promotion of degranulation from mast cells, activation of Interleukin-1B (IL-1B), activation of matrix protease, decomposition of fibronectin and type IV collagen, promotion of the liberation of transforming growth factor-B (TGF B), activation of Substance P and vasoactive intestinal polypeptide (VIP), conversion from angiotensin I (Ang I) to angiotensin II (Ang II), and conversion of endothelin. On the basis of the above, inhibitors of said chymase activity are considered to be promising as preventive and/or therapeutic agents against respiratory diseases such as bronchial asthma, inflammatory and allergic diseases such as allergic rhinitis, atopic dermatitis and urticaria, cardiovascular diseases such as Sclerosing vascular lesions, vasoconstriction, peripheral circulatory disorders, renal insufficiency and cardiac insufficiency, and bone and cartilage metabolic diseases such as rheumatoid arthritis and osteoarthritis¹⁷.

In previous studies¹⁸, *Brukstus, A. B., Garaliene, V. N., Sirvidyte, A. P. et al.*, have found that benzo[d]imidazole derivatives (figure 1.1.2) possess strong cardiotoxic activity and their mechanisms of action should be studied:

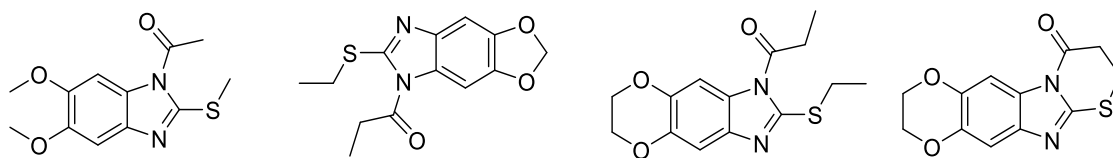


Fig.1.1.2 Benzo[d]imidazole derivatives studied by *Brukstus, A. B* and company

Afterwards, *Garaliene, V. N. et al.*,¹⁹ performed investigations on the effect of compounds shown in fig. 1.1.2 on the action potential duration (APD) and contractile force in atrium activated by carbamylcholine chloride (carbachol) and in guinea pig heart papillary muscles. This study was shown that these compounds possessed positive inotropic effects and in concentration-dependent manner significantly increased the contraction force in the guinea pig papillary muscle and atrium.

A series of 2,3-dihydro-thiazolo- and thiazinobenzimidazoles²⁰ (figure 1.1.3) has been found which possesses pharmaceutical activity, in particular antiulcer activity and/or antisecretory activity and hence is useful in the treatment of ulcers or gastric hypersecretion. In particular the compounds are useful in the treatment of peptic ulcer disease.

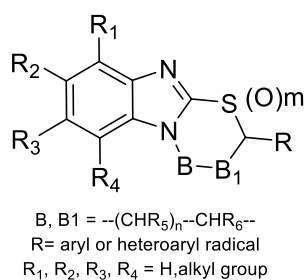
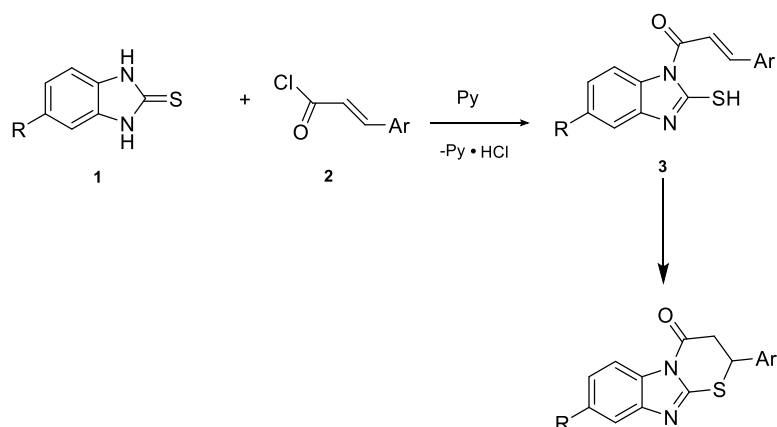


Fig. 1.1.3 2,3-dihydro-thiazolo- and thiazinobenzimidazoles structure

1.1.6 Synthesis of thiadiazafluorenones derivatives

There are many synthetic strategies known in literature to obtain substituted thiadiazafluorenones derivatives. A recent procedure²¹ includes the reaction of 2-mercaptobenzimidazole (**1**) and 5-ethoxy-2-mercaptobenzimidazole (**1**) and substituted **2** without isolation of intermediate N-cinnamoylimidazoles **3** to obtain 2-Aryl-2,3-dihydro-4H-[1,3]thiazino[3,2-a]benzimidazol-4-ones **4** (scheme 1.1.4).



Scheme 1.1.4 Synthesis of 2-Aryl-2,3-dihydro-4H-[1,3]thiazino[3,2-a]benzimidazol-4-ones **4**

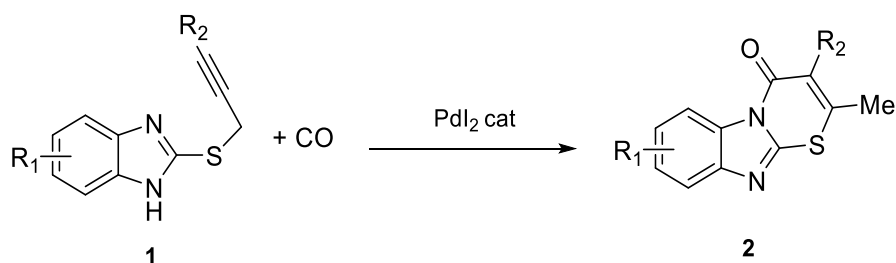
The reaction proceeds under mild conditions by heating the reagents in pyridine–benzene at reflux for 2 h.

The thiadiazafluorenones derivatives are also prepared by intramolecular amidation of 3-(1H-benzo[d]imidazol-2-ylthio)-propanoic acid and its derivatives.²¹

1.2 Results and Discussion

As known in the literature, palladium-catalyzed cyclocarbonylation reactions of unsaturated substrates bearing a nucleophilic group in a suitable position for cyclization have been proven to be particularly significant for the synthesis of carbonylated heterocycles, as outlined in the section 1.1.

In this PhD thesis, we report a novel PdI₂ catalyzed cyclocarbonylation route²² to 1-thia-4a,9-diazafluoren-4-one **2** starting from readily available 2-(prop-2-ynylthio)-1H-benzo[d]imidazoles **1**, bearing an internal and terminal triple bond (Scheme 1.2.1).



Scheme 1.2.1 Synthesis of 1-thia-4a,9-diazafluoren-4-one **2** from 2-(Alkynylthio)benzimidazole **1** by Palladium-Catalyzed Cyclocarbonylation.

The research work started with the synthesis of the substrate 2-(pent-2-yn-1-ylthio)-1H-benzo[d]imidazole **1a**. The first reaction was carried out in EtOH (concentration of **1a** = 0.2 mmol/mL) at 100 °C in the presence of PdI₂(0.02 eq), KI (1 eq) under 30 atm of CO for 5 h. The reaction afforded to 3-ethyl-2-methyl-1-thia-4a,9-diazafluoren-4-one **2a** in a 36% yield (isolated yield based on starting **1a**) with a complete substrate conversion (Table 1.1, entry 1). The structure of the product **2a** was established as well as by NMR and IR spectroscopy, and further determined by XRD analysis (figure 1.2.1).

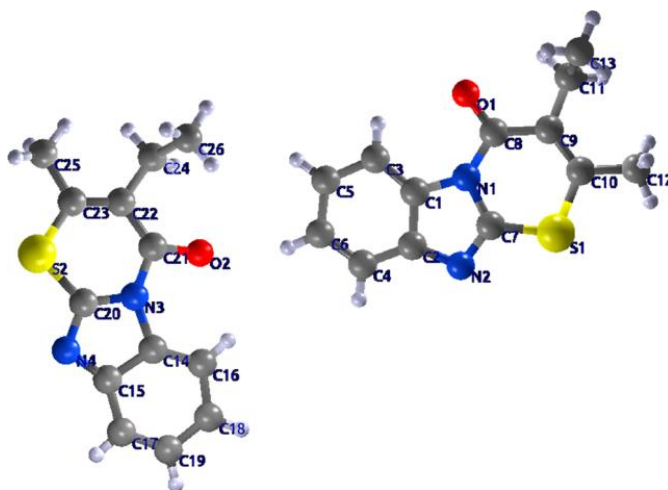
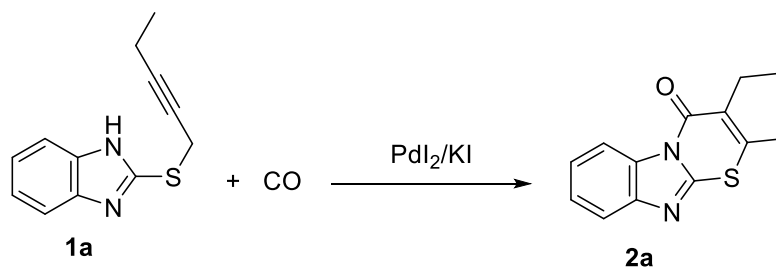


Fig. 1.2.1 X-ray structure of 3-ethyl-2-methyl-1-thia-4a,9-diazafluoren-4-one **2a**

To improve the initial result, we carried out several experiments in different conditions. Initially we tested different catalytic system such us Pd(CF₃COO)₂ and PdCl₂/KCl (table 1.1, entries 2-3) but we obtained a mixture of heavy products (as showed by TLC analysis) and low yields of product **2a**. We tested the possibility to use Pd(PPh₃)₄ as catalyst together PdI₂/KI and we carried out also an experiment adding water to reaction mixture in order to move the initial redox reaction. However, in both the experiment, we didn't obtain the desired result (table 1.1, entries 4-5). Then we carried out the reaction using different solvent and at different concentration of substrate **1a** (Table 1.1, entries 6-10). As can be seen, the use of dioxane and acetonitrile afforded to low yield of the desidered product as well as the decrease of concentration. A better result was instead obtained using methanol (Table 1.1, entry 8). Carrying out the reaction with less KI (table 1.1, entry 11) and with a pressure of CO of 50 atm (table 1.1, entry 12), the yield of **2a** remained unchanged, while an increase of the yield was observed when the process was carried out at 80°C (entries 14-15). Finally carrying out the reaction in MeOH (**1a** concentration = 0.2 mmol/mL) at 80 °C for 20 h, in presence of 0.02 eq di PdI₂ and 1 eq of KI, under 30 atm of carbon monoxide, the substrate conversion reached 100% and was obtained the product **2a** in 50% isolated yield (entry 16).

Table 1.1 Carbonylation Reactions of 2-(pent-2-yn-1-ylthio)-1*H*-benzo[*d*]imidazole **1a** under Different Conditions

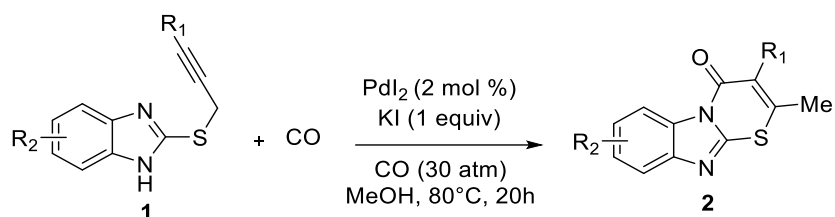


Entry	Catalytic system	Solvent	Concn of 1a ^a	T(°C)	P _{CO} (atm)	t (h)	Conv. of 1a ^b (%)	GLC yield of 2a ^c (%)
1	PdI ₂ (0.02 eq) / KI (1 eq)	EtOH	0.2	100	30	5	100	38 (36)
2	Pd(CF ₃ CO ₂ H) ₂ (0.02 eq)	EtOH	0.2	100	30	5	100	8
3	PdCl ₂ (0.02 eq) / KCl (1 eq)	EtOH	0.2	100	30	5	100	16
4	PdI ₂ (0.02 eq) / KI (1 eq) Pd(PPh ₃) ₄ (0.02 eq)	EtOH	0.2	100	30	5	100	36
5 ^d	PdI ₂ (0.02 eq) / KI (1 eq)	EtOH	0.2	100	30	5	100	30
6	PdI ₂ (0.02 eq) / KI (1 eq)	dioxane	0.2	100	30	5	100	18
7	PdI ₂ (0.02 eq) / KI (1 eq)	CH ₃ CN	0.2	100	30	5	100	27
8	PdI ₂ (0.02 eq) / KI (1 eq)	MeOH	0.2	100	30	5	100	42
9	PdI ₂ (0.02 eq) / KI (1 eq)	EtOH	0.1	100	30	5	100	17
10	PdI ₂ (0.02 eq) / KI (1 eq)	EtOH	0.4	100	30	5	100	38
11	PdI ₂ (0.02 eq) / KI (0.4 eq)	EtOH	0.2	100	30	5	100	37
12	PdI ₂ (0.02 eq) / KI (1 eq)	EtOH	0.2	100	50	5	100	37
13	PdI ₂ (0.02 eq) / KI (1 eq)	EtOH	0.2	80	30	6	63	30
14	PdI ₂ (0.02 eq) / KI (1 eq)	EtOH	0.2	80	30	15	94	44
15	PdI ₂ (0.02 eq) / KI (1 eq)	EtOH	0.2	80	30	20	100	48
16	PdI ₂ (0.02 eq) / KI (1 eq)	MeOH	0.2	80	30	20	100	51(50)

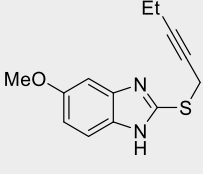
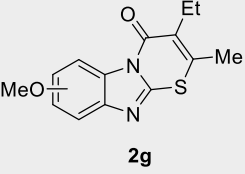
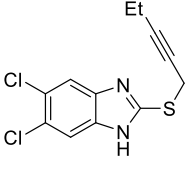
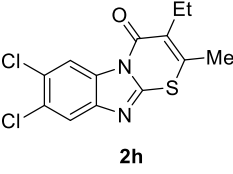
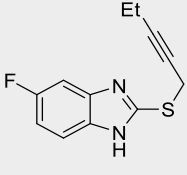
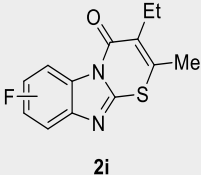
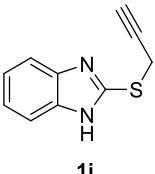
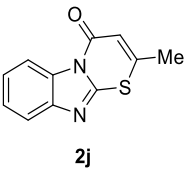
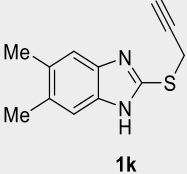
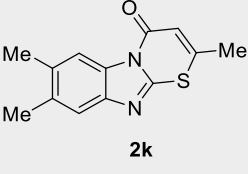
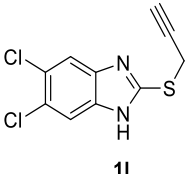
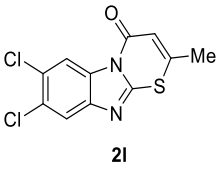
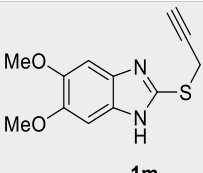
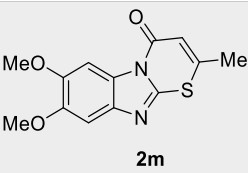
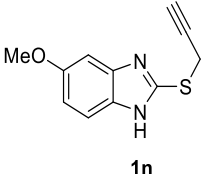
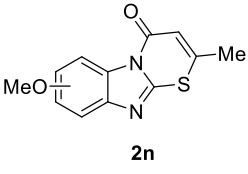
^a Mmol of **1a** per mL of solvent. ^b Isolated conversion based on starting **1a**. ^c GLC yield (isolated yield) based on starting **1a**. ^d The reaction was carried out in presence of H₂O (10 eq)

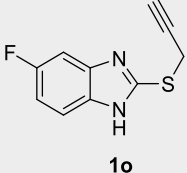
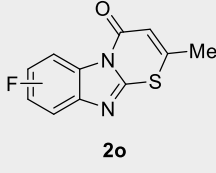
The process was then generalized to other differently substituted substrates **1b–i**, bearing various alkyl groups on the triple bond and electron-withdrawing as well as π -donating groups on the aromatic ring (Table 1.2). The reaction also worked nicely with substrates **1j–o**, bearing a terminal triple bond, as shown by entries 10-16. The structures of the products were further confirmed by XRD analysis of compounds **2f** and **2j** (figure 1.2.2).

Table 1.2. Synthesis of 3-Alkyl-2-methyl-1-thia-4a,9-diazafluoren-4-ones **2a-o** by Palladium-Catalyzed Carbonylation of 2-(prop-2-ynylthio)-1*H*-benzo[*d*]imidazoles **1a-i** Bearing an Internal Triple Bond and **1j-o** Bearing a Terminal Triple Bond^a



Entry	1	2	Yield of 2^b (%)
1	 1a	 2a	60
2	 1b	 2b	55
3	 1c	 2c	57
4	 1d	 2d	55
5	 1e	 2e	56
6	 1f	 2f	50

7	 <p>1g</p>	 <p>2g</p>	57 ^c
8	 <p>1h</p>	 <p>2h</p>	59
9	 <p>1i</p>	 <p>2i</p>	57 ^d
10	 <p>1j</p>	 <p>2j</p>	65
11	 <p>1k</p>	 <p>2k</p>	72
12	 <p>1l</p>	 <p>2l</p>	71
13	 <p>1m</p>	 <p>2m</p>	67
14	 <p>1n</p>	 <p>2n</p>	74 ^e

15			78 ^{f,g}
----	---	--	-------------------

^aAll reactions were carried out at 80 °C for 20 h under 30 atm (at 25 °C) of CO, in MeOH as the solvent (substrate concentration: 0.2 mmol of 1/mL of solvent), and in the presence of 2 mol % of PdI₂ and 1 equiv of KI. ^bIsolated yield, based on starting material **1**. ^cMixture of regioisomers (~3/1 by ¹H NMR). ^dMixture of regioisomers (~1.1/1 by ¹H NMR). ^eMixture of regioisomers (~1.2/1, by GLC). ^fMixture of regioisomers (~1.4/1, by ¹H NMR). ^gThe reaction was carried out with 5 mol % of PdI₂ for 15 h.

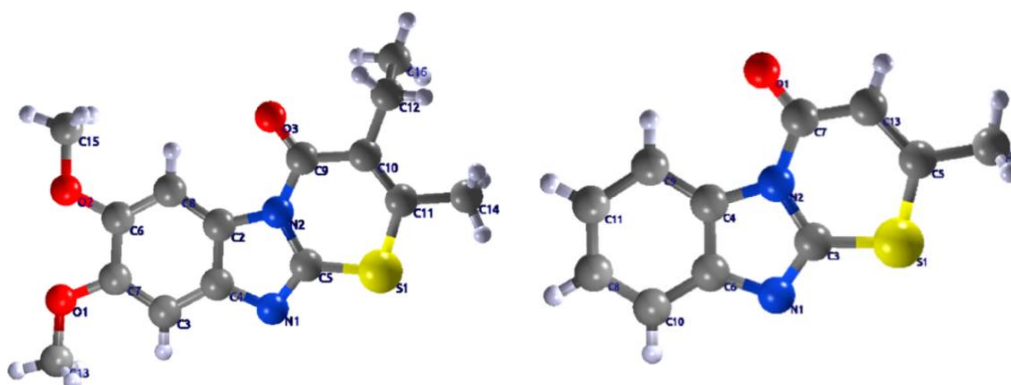
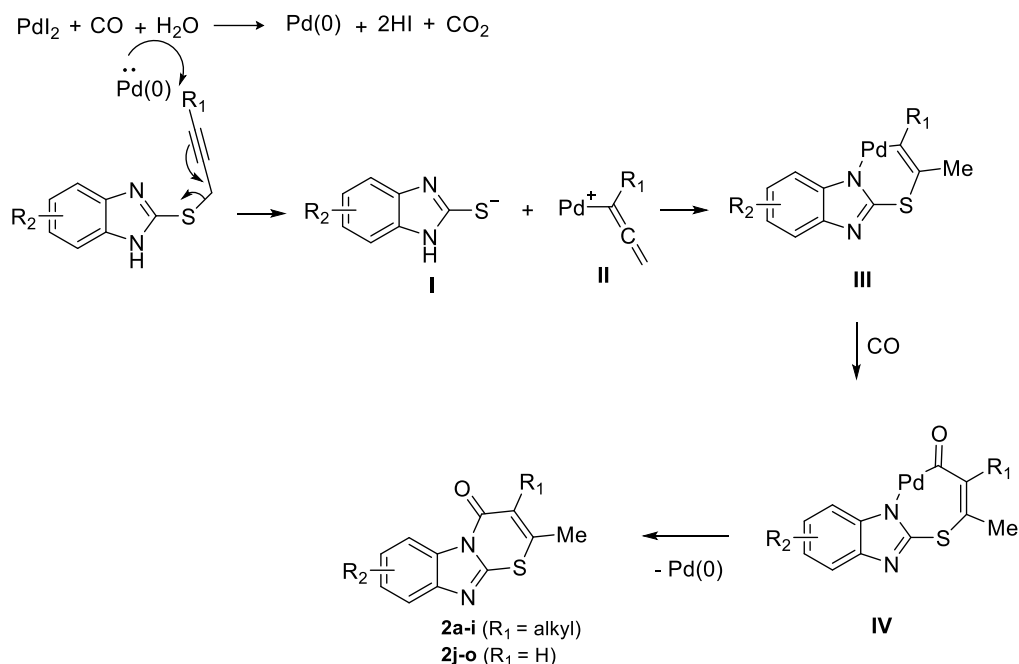


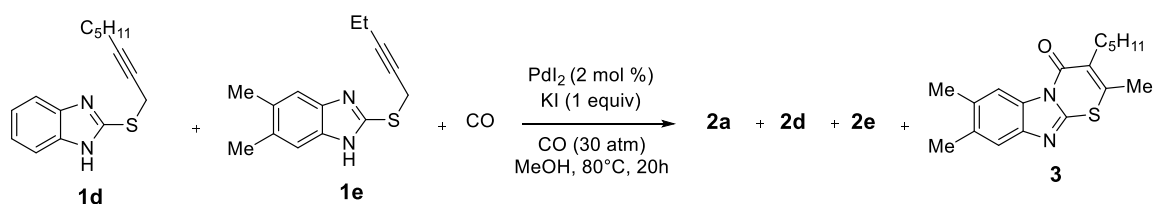
Fig.1.2.2 X-ray structure of 3-ethyl-6,7-dimethoxy-2-methyl-1-thia-4a,9-diazafluoren-4-one **2f** and 2-methyl-1-thia-4a,9-diazafluoren-4-one **2j**.

Mechanistically, the formation of 2-methyl-substituted products **2a–o** (Table 1.2) takes place by Pd(0)-promoted propargyl–allene rearrangement, occurring through a formal Pd(0) attack to the terminal carbon of the triple bond, with elimination of a thiolate **I** and formation of the allenylpalladium intermediate **II** (Scheme 1.2.2). Formation of an iodide-stabilized palladium(0) species under our conditions may take place by the water–gas shift reaction between PdI₂, CO, and traces of water present in the reaction mixture, as already observed by us under similar conditions. Addition of the thiolate **I** to the allenic moiety of **II** then leads to palladacycle intermediate **III**. The latter undergoes carbon monoxide insertion to give **IV**, from which the final product is formed by reductive elimination (Scheme 1.2.2).



Scheme 1.2.2 Proposed Mechanistic Pathway for the Palladium-Catalyzed Cyclocarbonylation of 2-(prop-2-ynylthio)-1H-benzo[d]imidazoles **1a-i** and **1j-o** Leading to 2-Methyl-1-thia-4a,9-diazafluoren-4-ones **2a-i** and **2j-o**, respectively.

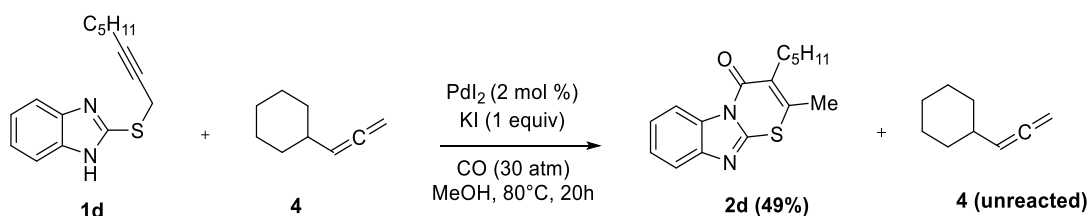
The mechanistic hypothesis has been confirmed carrying out a crossover experiment by allowing an equimolar mixture of substrates 2-(oct-2-yn-1-ylthio)-1H-benzo[d]imidazole **1d** and 5,6-dimethyl-2-(pent-2-yn-1-ylthio)-1H-benzo[d]imidazole **1e** to react under the optimized conditions (Scheme 1.2.3).



Scheme 1.2.3 Crossover Experiment: Formation of a Mixture of Thiadiazafluorenones **2a**, **2d**, **2e**, and **3** from Carbonylation of a Mixture of Substrates **1d** and **1e**.

The GLC-MS analysis of the reaction mixture evidenced the formation of four products (**2a**, **2d**, **2e**, and **3**) (Scheme 1.2.3) from the addition of two different thiolates to two different allenylpalladium complexes, derived from **1d** and **1e**, which is clearly in agreement with the proposed mechanism (Scheme 1.2.2).

We also verified if free allenes (possibly derived from protonolysis of complex **II**) were involved as intermediates in the formation of final bicyclic products. However, as shown in Scheme 1.2.4, the carbonylation of 2-(oct-2-yn-1-ylthio)-1*H*-benzo[*d*]imidazole **1d** together with commercially available cyclohexylallene **4** only gave the product 2-methyl-3-pentyl-4*H*-benzo[4,5]imidazo[2,1-*b*][1,3]thiazin-4-one **2d** (49% yield) without any formation of the mixed product resulting from allene incorporation. This result strongly suggests that protonolysis of complex **II** to give a free allene does not occur in our process, and that, according to Scheme 1.2.2, this intermediate preferentially undergoes direct attack by thiolate **I**.



Scheme 1.2.4 Carbonylation of **1d** in the Presence of Cyclohexylallene **4**

1.3 Conclusions

In conclusion, we developed a novel cyclocarbonylative method for the direct synthesis of thiadiazafuorenones **2** starting from readily available 2-(propynylthio)benzimidazoles **1** bearing internal and terminal triple bond. The process is catalyzed by the simple catalytic system PdI₂/KI and occurs in MeOH under relatively mild conditions (80 °C, under 30 atm of CO). Product formation, whose structure has been confirmed by XRD analysis by the most representative products, must ensue from some unexpected kind of structural rearrangement, most likely occurring through palladium-promoted propargyl–allene rearrangement to give a thiolate and an allenylpalladium intermediate, followed by thiolate addition to the central allenic carbon and cyclocarbonylation. To the best of our knowledge, this is the first example of synthesis of polyheterocycles **2** by a direct additive carbonylation approach.

1.4 Experimental Section

1.4.1 Preparation of 2-(Prop-2-ynylthio)-1*H*-benzo[*d*]imidazoles **1a–i**, bearing an internal triple bond and **1j–o** bearing a terminal triple bond

To a solution of the 1*H*-imidazole-2-thione derivative (16.7 mmol) [2.5 g of 1,3-dihydrobenzoimidazole-2-thione (commercially available), 2.97 g of 5,6-dimethyl-1,3-dihydrobenzoimidazole-2-thione (commercially available), 3.65 g of 5,6-dichloro-1,3-dihydrobenzoimidazole-2-thione (commercially available), 3.51 g of 5,6-dimethoxy-1,3-dihydrobenzoimidazole-2-thione²³, 3.00 g of 5-methoxy-1,3-dihydrobenzoimidazole-2-thione (commercially available), 2.81 g of 5-fluoro-1,3-dihydrobenzoimidazole-2-thione²³ in anhydrous acetone (100 mL), were added, under nitrogen, K₂CO₃ (2.3 g, 16.7 mmol) and the 1-bromoalk-2-yne derivative (25.1 mmol) [3.69 g of 1-bromopent-2-yne (commercially available); 3.34 g of 1-bromobut-2-yne (commercially available), 4.04 g of 1-bromohex-2-yne²³, 11 4.75 g of 1-bromooct-2-yne^{24,25}]. The mixture was stirred at room temperature for 20 h. After evaporation of the solvent, dichloromethane (30 mL) and water (30 mL) were sequentially added, and the phases were separated. The aqueous phase was extracted again with dichloromethane (20 mL), and finally, the collected organic phases were dried over Na₂SO₄. After filtration and evaporation of the solvent, products **1a–i** were purified by column chromatography on silica gel using as eluent 9:1 hexane–AcOEt for **1b**, **1d**, and **1h**; 8:2 hexane–AcOEt for **1c**; or 7:3 hexane–AcOEt for **1a**, **1e**, **1f**, **1g**, and **1i**.

Also, for the 2-(prop-2-ynylthio)-1*H*-benzo[*d*]imidazoles bearing a terminal triple bond **1j–o** the same procedure was followed. To a solution of the 1,3-dihydrobenzimidazole-2-thione derivative (16.7 mmol) [1,3-dihydrobenzimidazole-2-thione: 2.50 g; 5,6-dimethyl-1,3-dihydrobenzimidazole-2-thione: 2.97 g; 5,6-dichloro-1,3-dihydrobenzimidazole-2-thione: 3.65 g; 5,6-dimethoxy-1,3-dihydrobenzimidazole-2-thione²³: 3.51 g; 5-methoxy-1,3-dihydrobenzimidazole-2-thione: 3.00 g; 5-fluoro-1,3-dihydrobenzimidazole-2-thione²³: 2.81 g] in anhydrous acetone (100 mL) was added, under nitrogen, K₂CO₃ (2.3 g, 16.7 mmol) followed by propargyl bromide (2.96 g, corresponding to 2.8 mL of a 80 wt % solution in toluene, 25.1 mmol). The mixture was stirred at room temperature for 20 h. After evaporation of the solvent, dichloromethane (30 mL) and water (30 mL) were sequentially added, and the phases were separated. The aqueous phase was extracted again with dichloromethane (20 mL), and

finally the collected organic phases were dried over Na₂SO₄. After filtration and evaporation of the solvent, products **1j–o** were purified by column chromatography on silica gel using as eluent 9/1 hexane-AcOEt for **1j–k** and **1n** and 7/3 hexane-AcOEt for **1m** and **1o**.

1.4.2 General Procedure for the Synthesis of Thiadiazafuorenones **2a–o**

A 35 mL stainless steel autoclave was charged in the presence of air with PdI₂ (5.8 mg, 1.61 × 10⁻² mmol), KI (133 mg, 0.81 mmol), MeOH (4 mL), and the 2-prop-2-ynylthiobenzimidazole (0.81 mmol; 175 mg of **1a**, 164 mg of **1b**, 187 mg of **1c**, 209 mg of **1d**, 198 mg of **1e**, 224 mg of **1f**, 200 mg of **1g**, 231 mg of **1h**, 190 mg of **1i**, 153 mg of **1j**; 175 mg of **1k**; 208 of **1l**; 201 mg of **1m**; 177 mg of **1n** and 167 mg of **1o**). The autoclave was purged at room temperature several times with CO under stirring (5 atm) and eventually pressurized with CO (30 atm). After being stirred at 80 °C for 20 h, the autoclave was cooled, degassed, and opened. After evaporation of the solvent, products **2** were purified by column chromatography on neutral alumina using 98:2 hexane–AcOEt as eluent.

1.4.3 Crossover Experiment

A 35 mL stainless steel autoclave was charged in the presence of air with PdI₂ (11.6 mg, 3.22 × 10⁻² mmol), KI (267 mg, 1.61 mmol), MeOH (8 mL), **1d** (208.7mg, 0.81 mmol), and **1e** (197.6 mg, 0.81 mmol). The autoclave was purged at room temperature several times with CO under stirring (5 atm) and eventually pressurized with CO (30 atm). After being stirred at 80 °C for 20 h, the autoclave was cooled, degassed, and opened. The resulting crude inseparable mixture was analyzed by GLC and LC-MS, which evidenced the formation of a ratio of **2a/2d/2e/3** = 1:1.2:3:1.9 (determined by GLC): GC-MS (5) *m/z* = 314 (M⁺,100), 271 (14), 257 (46), 230 (48), 178 (16), 137 (73).

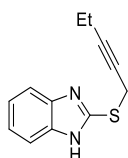
1.4.4 Carbonylation of 2-(oct-2-yn-1-ylthio)-1*H*-benzo[d]imidazole **1d** in the presence of Cyclohexylallene

A 35 mL stainless steel autoclave was charged in the presence of air with PdI₂ (8.3 mg, 2.30 × 10⁻² mmol), KI (191.24 mg, 1.15 mmol), MeOH (5.8 mL), **1d** (148.8 mg, 0.58 mmol), and

cyclohexylallene **4** (commercially available; 70.4 mg, 0.58 mmol). The autoclave was purged at room temperature several times with CO under stirring (5 atm) and eventually pressurized with CO (30 atm). After being stirred at 80 °C for 20 h, the autoclave was cooled, degassed, and opened. The crude mixture was analyzed in GLC to determinate the cyclohexylallene conversion (54%). After evaporation of the solvent, the crude mixture was purified by column chromatography on neutral alumina (98:2 hexane–AcOEt as eluent), affording **2d** in 49% yield (81.8 mg).

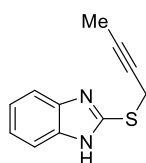
1.5 Characterization Data

1.5.1 Characterization of 2-(prop-2-ynylthio)-1H-benzo[d]imidazoles (**1a–o**) and Thiadiazafluorenones (**2a–o**)



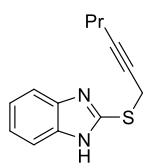
2-(Pent-2-yn-1-ylthio)-1H-benzo[d]imidazole (**1a**).

Yield 2.75 g, starting from 2.50 g of 1,3-dihydrobenzoimidazole-2-thione (76%); colorless solid, mp = 139–141 °C; IR (KBr) ν = 2972 (s), 2181 (vw), 1445 (s), 1402 (s), 1270 (m), 1228 (m), 980 (m), 737 (s) cm^{-1} ; ^1H NMR (300 MHz, DMSO- d_6) δ = 12.74 (s, br, 1 H), 7.63–7.40 (m, 2 H), 7.24–7.13 (m, 2 H), 4.16 (t, J = 2.3, 2 H), 2.16 (qt, J = 7.5, 2.3, 2 H), 1.00 (t, J = 7.5, 3 H); $^{13}\text{C}\{^1\text{H}\}$ NMR (75 MHz, DMSO- d_6) δ = 149.0, 143.4 (br), 135.7 (br), 122.0, 117.6 (br), 111.0 (br), 85.5, 75.2, 20.8, 13.9, 12.0; GC-MS m/z = 216 (M^+ , 77), 201 (100), 187 (27), 150 (27), 122 (42); HRMS (ESI-TOF) m/z [$\text{M}+\text{Na}$] $^+$ calcd for $\text{C}_{12}\text{H}_{12}\text{N}_2\text{SNa}^+$ 239.0613; found 239.0609.



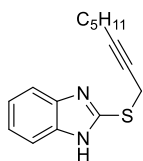
2-(But-2-yn-1-ylthio)-1H-benzo[d]imidazole (**1b**).

Yield 2.70 g, starting from 2.50 g of 1,3-dihydrobenzoimidazole-2-thione (80%); colorless solid, mp = 169–171 °C; IR (KBr) ν = 2972 (m, br), 2239 (vw), 1445 (m), 1402 (s), 1269 (m), 1229 (m), 980 (m) cm^{-1} ; ^1H NMR (300 MHz, DMSO- d_6) δ = 12.59 (s, br, 1 H), 7.51–7.41 (m, 2 H), 7.18–7.09 (m, 2 H), 4.12 (q, J = 2.5, 2 H), 1.77 (t, J = 2.5, 3 H); $^{13}\text{C}\{^1\text{H}\}$ NMR (75 MHz, DMSO- d_6) δ = 148.8, 121.5, 79.4, 74.8, 20.3, 3.2 (Note: the signals of quaternary carbons were too broad to be detected); GC-MS m/z = 202 (M^+ , 100), 201 (72), 187 (31), 169 (81), 149 (42), 122 (77); HRMS (ESI-TOF) m/z [$\text{M}+\text{Na}$] $^+$ calcd for $\text{C}_{11}\text{H}_{10}\text{N}_2\text{SNa}^+$ 225.0457; found 225.0451.



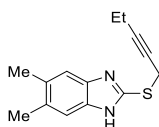
2-(Hex-2-yn-1-ylthio)-1H-benzo[d]imidazole (**1c**).

Yield 2.00 g, starting from 2.50 g of 1,3-dihydrobenzoimidazole-2-thione (52%); colorless solid, mp = 140–142 °C; IR (KBr) ν = 2959 (m, br), 2234 (vw), 1441 (m), 1400 (m), 1269 (m), 1242 (m), 737 (s) cm^{-1} ; ^1H NMR (300 MHz, CD_3OD) δ = 7.54–7.44 (m, 2 H), 7.24–7.15 (m, 2 H), 4.98 (s, br, 1 H), 4.03–3.98 (m, 2 H), 2.13–2.02 (m, 2 H), 1.46–1.29 (m, 2 H), 0.81 (t, J = 7.3, 3 H); $^{13}\text{C}\{^1\text{H}\}$ NMR (75 MHz, CD_3OD) δ = 150.3, 140.4 (br), 123.5, 115.0 (br), 85.4, 75.7, 23.0, 22.5, 21.4, 13.6; GC-MS m/z = 230 (M^+ , 60), 201 (100), 187 (24), 169 (28), 150 (28), 122 (29); HRMS (ESI-TOF) m/z [$\text{M}+\text{Na}$] $^+$ calcd for $\text{C}_{13}\text{H}_{14}\text{N}_2\text{SNa}^+$ 253.0770; found 253.0769.



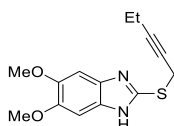
2-(Oct-2-yn-1-ylthio)-1H-benzo[d]imidazole (1d).

Yield 3.45 g, starting from 2.50 g of 1,3-dihydrobenzoimidazole-2-thione (80%); colorless solid, mp = 108–111 °C; IR (KBr) ν = 2957 (m br), 2234 (w), 1445 (m), 1402 (s), 1267 (m), 1227 (m), 980 (m), 739 (s) cm^{-1} ; ^1H NMR (500 MHz, DMSO- d_6) δ = 12.61 (s, br, 1 H), 7.50–7.41 (m, br, 2 H), 7.15–7.10 (m, 2 H), 4.12 (t, J = 2.3, 2 H), 2.12 (tt, J = 7.0, 2.3, 2 H), 1.36–1.31 (m, 2 H), 1.25–1.13 (m, 4 H), 0.77 (t, J = 7.0, 3 H); $^{13}\text{C}\{^1\text{H}\}$ NMR (125 MHz, DMSO- d_6) δ = 148.6, 121.5, 83.7, 75.7, 30.2, 27.7, 21.5, 20.5, 17.9, 13.7 (Note: the signals of two quaternary carbons were too broad to be detected); GC-MS m/z = 258 (M^+ , 100), 202 (97), 201 (100), 187 (14), 169 (14), 143 (41); HRMS (ESI-TOF) m/z [$\text{M}+\text{Na}$] $^+$ calcd for $\text{C}_{15}\text{H}_{18}\text{N}_2\text{SNa}^+$ 281.1083; found 281.1085.



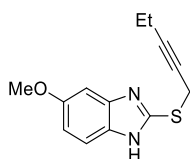
5,6-Dimethyl-2-(pent-2-yn-1-ylthio)-1H-benzo[d]imidazole (1e)

Yield 2.45 g, starting from 2.97 g of 5,6-dimethyl-1,3-dihydrobenzoimidazole-2-thione (60%); colorless solid, mp = 164–166 °C; IR (KBr) ν = 2974 (m), 2232 (vw), 1449 (m), 1391 (s), 1227 (m), 982 (m); ^1H NMR (300 MHz, DMSO- d_6) δ = 7.26 (s, 2 H), 4.12 (t, J = 2.2, 2 H), 2.28 (s, 6 H), 2.14 (qt, J = 7.5, 2.2, 2 H), 0.99 (t, J = 7.5, 3 H) (Note: the NH signal was too broad to be detected); $^{13}\text{C}\{^1\text{H}\}$ NMR (75 MHz, DMSO- d_6) δ = 147.1, 137.4, 130.2, 114.1, 85.2, 75.0, 20.8, 19.9, 13.6, 11.7 (Note: the signals of two quaternary carbons were too broad to be detected); GC-MS m/z = 244 (M^+ , 100), 243 (23), 229 (53), 171 (6); HRMS (ESI-TOF) m/z [$\text{M}+\text{Na}$] $^+$ calcd for $\text{C}_{14}\text{H}_{16}\text{N}_2\text{SNa}^+$ 267.0926; found 267.0925.



5,6-Dimethoxy-2-(pent-2-yn-1-ylthio)-1H-benzo[d]imidazole (1f).

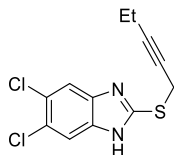
Yield 3.46 g, starting from 3.51 g of 5,6-dimethoxy-1,3-dihydrobenzoimidazole-2-thione (75%); colorless solid, mp = 102–105 °C; IR (KBr) ν = 2950 (m), 2234 (vw), 1393 (s), 1331 (s), 1200 (s), 1138 (s), 1007 (m), 849 (m) cm^{-1} ; ^1H NMR (300 MHz, CD_3OD) δ = 7.05 (s, 2 H), 4.95 (s, br); 3.90 (t, J = 2.4, 2 H), 3.85 (s, 6 H), 2.10 (qt, J = 7.5, 2.4, 2 H), 0.98 (t, J = 7.5, 3 H); $^{13}\text{C}\{^1\text{H}\}$ NMR (75 MHz, CD_3OD) δ = 148.6, 146.9, 97.8 (br), 86.9, 75.0, 56.8, 23.4, 14.1, 13.0 (Note: the signal of a quaternary carbon was too broad to be detected); GC-MS m/z = 276 (M^+ , 100), 261 (43), 243 (26), 209 (14), 174 (5); HRMS (ESI-TOF) m/z [$\text{M}+\text{Na}$] $^+$ calcd for $\text{C}_{14}\text{H}_{16}\text{N}_2\text{O}_2\text{SNa}^+$ 299.0825; found 299.0825.



5-Methoxy-2-(pent-2-yn-1-ylthio)-1H-benzo[d]imidazole (1g).

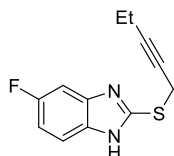
Yield 3.29 g, starting from 3.00 g of 5-methoxy-1,3-dihydrobenzoimidazole-2-thione (80%); colorless solid, mp = 112–116 °C; IR (KBr) ν = 2875 (m), 2230 (vw), 1628 (m), 1393 (s), 1204 (s), 1161 (s), 1034 (m), 980 (m), 806 (s) cm^{-1} ; ^1H NMR (300 MHz, CDCl_3) δ = 7.48 (d, J = 8.8, 1 H),

7.08 (d, $J = 2.3$, 1 H), 6.87 (dd, $J = 8.8$, 2,3, 1 H), 4.01 (t, $J = 2.4$, 2 H), 3.82 (s, 3 H), 2.12 (qt, $J = 7.5$, 2.4, 2 H), 1.04 (t, $J = 7.5$, 3 H) (Note: the NH signal was too broad to be detected); $^{13}\text{C}\{^1\text{H}\}$ NMR (75 MHz, CDCl_3) $\delta = 156.4$, 148.1, 139.5 (br), 134.3 (br), 115.3, 111.9, 97.2, 86.5, 74.1, 55.8, 22.5, 13.6, 12.5; GC-MS $m/z = 246$ (M^+ , 100), 231 (51), 217 (25), 174 (15), 120 (18); HRMS (ESI-TOF) m/z [$\text{M} + \text{Na}$] $^+$ calcd for $\text{C}_{13}\text{H}_{14}\text{N}_2\text{OSNa}^+$ 269.0719; found 269.0717.



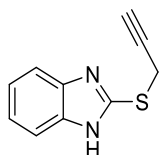
5,6-Dichloro-2-(pent-2-yn-1-ylthio)-1H-benzo[d]imidazole (1h).

Yield 3.33 g, starting from 3.65 g of 5,6-dichloro-1,3-dihydrobenzimidazole-2-thione (70%); yellow solid, mp = 188–193 °C; IR (KBr) $\nu = 2920$ (m), 2234 (vw), 1377 (s), 1319 (m), 1096 (m), 961 (m), 868 (m) cm^{-1} ; ^1H NMR (300 MHz, DMSO-d_6) $\delta = 7.74$ (s, 2 H), 4.15 (t, $J = 2.4$, 2 H), 2.16 (qt, $J = 7.5$, 2.4, 2 H), 1.00 (t, $J = 7.5$, 3 H) (Note: the NH signal was too broad to be detected); $^{13}\text{C}\{^1\text{H}\}$ NMR (75 MHz, DMSO-d_6) $\delta = 152.5$, 124.0, 114.8 (br), 85.3, 74.8, 20.4, 13.6, 11.8 (Note: the signal of a quaternary carbon was too broad to be detected); GC-MS $m/z = 288$ [$(\text{M}^+ 4)^+$, 13], 286 [$(\text{M}^+ 2)^+$, 69], 285 [$(\text{M}^+ 1)^+$, 21], 284 (M^+ , 100), 271 (27), 269 (39), 257 (55), 255 (76), 220 (39), 167 (32); HRMS (ESI-TOF) m/z [$\text{M} + \text{H}$] $^+$ calcd for $\text{C}_{12}\text{H}_{11}\text{Cl}_2\text{N}_2\text{S}^+$ 285.0015; found 285.0015.



5-Fluoro-2-(pent-2-yn-1-ylthio)-1H-benzo[d]imidazole (1i).

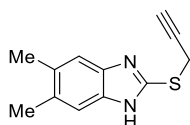
Yield 1.56 g, starting from 2.81 g of 5-fluoro-1,3-dihydrobenzimidazole-2-thione (40%); colorless solid, mp = 175–177 °C; IR (KBr) $\nu = 2914$ (m, br), 2237 (vw), 1397 (s), 1142 (s), 988 (m), 845 (s), 799 (s) cm^{-1} ; ^1H NMR (300 MHz, DMSO-d_6) $\delta = 12.79$ (s, br, 1 H), 7.62–7.20 (m, 2 H), 7.01 (t, $J = 9.7$, 1 H), 4.18–4.12 (m, 2 H), 2.22–2.11 (m, 2 H), 1.01 (t, $J = 7.5$, 3 H); $^{13}\text{C}\{^1\text{H}\}$ NMR (75 MHz, DMSO-d_6) $\delta = 158.2$ (d, $J = 233.9$, C-6 bonded to F), 150.7 (tautomer A), 149.5 (tautomer B), 144.0 (tautomer A or B), 140.2 (tautomer B or A), 135.5 (tautomer A or B), 132.1 (tautomer B or A), 118.1 (tautomer A or B), 110.9 (tautomer B or A), 109.7 (d, $J = 25.3$, C-5 or C-7, tautomer A or B), 109.3 (d, $J = 25.3$, C-5 or C-7, tautomer B or A), 103.3 (d, $J = 24.3$, C-7 or C-5, tautomer A or B), 97.2 (d, $J = 25.5$, C-7 or C-6, tautomer B or A), 85.1, 74.9, 20.4, 13.6, 11.7 (Note: some carbon signals were doubled owing to slow tautomerization of the imidazole ring); ^{19}F NMR (471 MHz, DMSO-d_6) $\delta = -120.0$ (s, tautomer A or B), -121.4 (s, tautomer B or A); GC-MS $m/z = 234$ (M^+ , 76), 219 (100), 205 (32), 168 (27), 140 (47), 108 (37); HRMS (ESI-TOF) m/z [$\text{M} + \text{Na}$] $^+$ calcd for $\text{C}_{12}\text{H}_{11}\text{FN}_2\text{SNa}^+$ 257.0519; found 257.0513



2-(Prop-2-ynylthio)-1H-benzo[d]imidazole (1j).

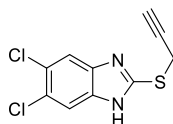
Yield: 2.51 g starting from 2.50 g of 1,3-dihydrobenzimidazole-2-thione (80%). Colorless solid, mp: 165–167 °C, lit.²⁶: 164–165 °C and 165–167, lit.²⁷; IR (KBr) ν 3048 (m), 2958 (m), 2888 (m), 2106 (vw), 1506 (w), 1444 (m), 1405 (s), 1351 (m), 1267 (m), 1227 (m), 1012 (m), 977 (m), 745 (s), 657 (m) cm^{-1} ; ^1H NMR (300 MHz, DMSO-d_6): δ 12.7 (s, br, 1 H), 7.56–7.42 (m, 2 H), 7.21–7.10 (m, 2 H), 4.16 (d, $J = 2.6$, 2 H), 3.22 (t, $J = 2.6$, 1 H); ^{13}C NMR (75 MHz, DMSO-d_6): δ 148.3,

121.5, 114.3 (br), 80.0, 73.9, 19.7; MS (ESI⁺, direct infusion): m/z 189 [(M+H)⁺]; Anal. calcd for C₁₀H₈N₂S (188.25): C, 63.80; H, 4.28; N, 14.88; S, 17.03; found C, 63.89; H, 4.30; N, 14.85; S, 16.96.



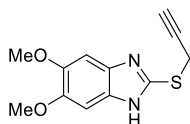
5,6-Dimethyl-2-(prop-2-ynylthio)-1H-benzo[d]imidazole (1k).

Yield: 3.25 g starting from 2.97 g of 5,6-dimethyl-1,3-dihydrobenzimidazole-2-thione (90%). Colorless solid, mp: 163–164 °C; IR (KBr) ν 3051 (m), 2920 (m), 2122 (vw), 1451 (s), 1415 (m), 1389 (s), 1299 (w), 1234 (w), 974 (m), 854 (m) cm⁻¹; ¹H NMR (300 MHz, CD₃OD): δ 7.24 (s, 2 H), 4.92 (s, br, 1 H), 3.99–3.93 (m, 2 H), 2.65–2.57 (m, 1 H), 2.32 (s, 6 H); ¹³C NMR (75 MHz, CD₃OD): δ 148.5, 139.2, 132.8, 115.4, 79.8, 73.2, 22.3, 20.2; MS (ESI⁺, direct infusion): m/z 217 [(M+H)⁺]; Anal. calcd for C₁₂H₁₂N₂S (216.30): C, 66.63; H, 5.59; N, 12.95; S, 14.82; found C, 66.29; H, 5.61; N, 12.90; S, 15.20.



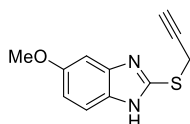
5,6-Dichloro-2-(prop-2-ynylthio)-1H-benzo[d]imidazole (1l).

Yield: 3.21 g starting from 3.65 g of 5,6-dichloro-1,3-dihydrobenzimidazole-2-thione (75%). Colorless solid, mp: 185–188 °C; IR (KBr) ν 3270 (m), 2923 (m), 2122 (w), 1492 (w), 1402 (m), 1332 (m), 1260 (m), 1095 (m), 967 (m), 866 (m), 660 (s) cm⁻¹; ¹H NMR (300 MHz, CD₃OD): δ 7.60 (s, 2 H), 4.92 (s, br, 1 H), 4.07 (d, J = 2.6, 2 H), 2.68 (t, J = 2.6, 1 H); ¹³C NMR (75 MHz, CD₃OD): δ 153.5, 140.3, 127.4, 116.5, 79.2, 73.5, 21.6; MS (ESI⁺, direct infusion): m/z 257 [(M+H)⁺]; Anal. calcd for C₁₀H₆Cl₂N₂S (257.139): C, 46.71; H, 2.35; Cl, 27.57; N, 10.89; S, 12.47; found C, 46.79; H, 2.33; Cl, 27.61; N, 10.86; S, 12.41.



5,6-Dimethoxy-2-(prop-2-ynylthio)-1H-benzo[d]imidazole (1m).

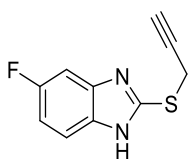
Yield: 3.43 g starting from 3.51 g of 5,6-dimethoxy-1,3-dihydrobenzimidazole-2-thione (83%). Yellow solid, mp: 95–97 °C; IR (KBr) ν 3287 (m), 2116 (w), 1665 (m), 1632 (m), 1597 (m), 1511 (m), 1497 (m), 1453 (m), 1368 (m), 1339 (m), 1243 (m), 1216 (m), 1147 (m), 1012 (m), 989 (m), 857 (m), 734 (s) cm⁻¹; ¹H NMR (300 MHz, DMSO-*d*₆): δ 12.45 (s, br, 1 H), 7.03 (s, 2 H), 4.06 (d, J = 1.9, 2 H), 3.77 (s, 6 H), 3.22–3.16 (m, 1 H); ¹³C NMR (75 MHz, DMSO-*d*₆): δ 146.2, 144.9, 133.5, (br), 97.2 (br), 80.2, 73.9, 55.9, 20.5; MS (ESI⁺, direct infusion): m/z 249 [(M+H)⁺]; Anal. calcd for C₁₂H₁₂N₂O₂S (248.30): C, 58.05; H, 4.87; N, 11.28; S, 12.91; found C, 57.91; H, 4.89; N, 11.26; S, 12.88.



5-Methoxy-2-(prop-2-ynylthio)-1H-benzo[d]imidazole (1n).

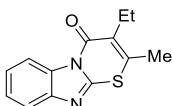
Yield: 2.20 g starting from 3.00 g of 5-methoxy-1,3-dihydrobenzimidazole-2-thione (60%). Colorless solid, mp: 140–142 °C; IR (KBr) ν 3262 (m), 2122 (vw), 1622 (m), 1456 (m), 1396 (s), 1342 (m), 1301 (m), 1272 (w), 1227 (m), 1158 (m), 1113 (w), 981 (m), 815 (m) cm⁻¹; ¹H NMR (300 MHz, DMSO-*d*₆): δ 12.6 (s, br, 1 H), 7.50–7.34 (m, 1 H), 7.17–6.93 (m, 1 H), 6.81 (dd, J = 8.6, 2.3, 1 H), 4.15 (d, J = 2.5, 2 H), 3.79 (s, 3 H), 3.22 (t, J = 2.5, 1 H); ¹³C NMR (75 MHz, DMSO-

d₆): δ 155.4, 147.0, 137.1, 117.9, 110.7, 100.2, 94.5, 80.1, 73.9, 55.4, 20.0; MS (ESI⁺, direct infusion): m/z 219 [(M+ H)⁺]; Anal. calcd for C₁₁H₁₀N₂OS (218.27): C, 60.53; H, 4.62; N, 12.83; S, 14.69; found C, 60.32; H, 4.60; N, 12.88; S, 14.72.



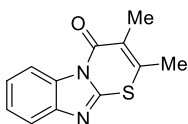
5-Fluoro-2-(prop-2-ynylthio)-1H-benzimidazole (1o).

Yield: 2.10 g starting from 2.81 g of 5-fluoro-1,3-dihydrobenzimidazole-2-thione (61%). Yellow solid, mp: 132–134 °C; IR (KBr) ν 3303 (m), 1633 (m), 1498 (s), 1461 (m), 1427 (m), 1362 (m), 1274 (m), 1242 (m), 1159 (m), 997 (m), 860 (m), 677 (m) cm⁻¹; ¹H NMR (300 MHz, CD₃OD): δ 7.44 (dd, J = 8.8, 4.7, 1 H), 7.20 (dd, J = 9.1, 2.3, 1 H), 7.06–6.92 (m, 1 H), 4.06–4.01 (m, 2 H), 2.69–2.63 (m, 1 H); ¹³C NMR (75 MHz, CD₃OD): δ 161.1 (d, J = 238), 151.5, 141.1 (br), 137.4 (br), 116.0 (br), 111.5 (d, J = 26), 101.4 (d, J = 26), 79.8, 73.5, 73.4, 22.0; ¹⁹F NMR (471 MHz, CD₃OD): δ -113.5 (s); MS (ESI⁺, direct infusion): m/z 207 [(M+H)⁺]; Anal. calcd for C₁₀H₇FN₂S (206.24): C, 58.24; H, 3.42; F, 9.21; N, 13.58; S, 15.55; found C, 58.29; H, 3.40; F, 9.18; N, 13.61; S, 15.52.



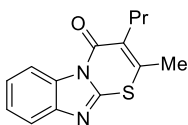
3-Ethyl-2-methyl-1-thia-4a,9-diazafluoren-4-one (2a).

Yield 119 mg, starting from 175 mg of **1a** (60%); colorless solid, mp = 132–134 °C; IR (KBr) ν = 1675 (s), 1475 (s), 1432 (s), 1358 (m), 1313 (m), 1148 (m), 760 (m) cm⁻¹; ¹H NMR (500 MHz, CDCl₃) δ = 8.57 (d, J = 8.1), 7.74 (d, J = 8.1), 7.50–7.44 (m, 1 H), 7.44–7.38 (m, 1 H), 2.76 (q, J = 7.5, 2 H), 2.43 (s, 3 H), 1.18 (t, J = 7.5, 3 H); ¹³C{¹H} NMR (125 MHz, CDCl₃) δ = 160.4, 146.2, 142.4, 140.7, 131.6, 127.8, 125.7, 123.8, 118.4, 116.1, 21.3, 20.6, 13.0; GCMS m/z = 244 (M⁺, 100), 229 (51), 211 (16), 201 (16); HRMS (ESI-TOF) m/z [M+Na]⁺ calcd for C₁₃H₁₂N₂OSNa⁺ 267.0563; found 267.0557.



2,3-Dimethyl-1-thia-4a,9-diazafluoren-4-one (2b).

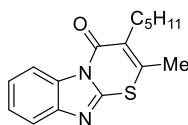
Yield 103 mg, starting from 164 mg of **1b** (55%); colorless solid, mp = 178–183 °C; IR (KBr) ν = 1674 (s), 1474 (m), 1435 (m), 1354 (w), 1312 (m), 1150 (m), 768 (s) cm⁻¹; ¹H NMR (300 MHz, CDCl₃) δ = 8.59 (d, J = 8.0), 7.73 (d, J = 7.7), 7.50–7.30 (m, 2 H), 2.36 (s, 3 H), 2.21 (s, 3 H); ¹³C{¹H} NMR (75 MHz, CDCl₃) δ = 160.7, 146.1, 142.3, 140.6, 131.4, 125.7, 123.8, 121.8, 118.3, 116.0, 21.3, 13.4; GC-MS m/z = 230 (M⁺, 100), 201 (27), 169 (15), 150 (15); HRMS (ESI-TOF) m/z [M-H]⁻ calcd for [C₁₂H₉N₂OS]⁻ 229.0441; found 229.0452.



2-Methyl-3-propyl-1-thia-4a,9-diazafluoren-4-one (2c).

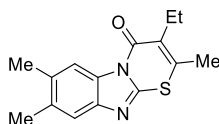
Yield 119 mg, starting from 187 mg of **1c** (57%); colorless solid, mp = 111–112 °C; IR (KBr) ν = 1684 (s), 1466 (s), 1431 (s), 1350 (s), 1311 (s), 1152 (m), 746 (s) cm⁻¹; ¹H NMR (300 MHz, CDCl₃) δ = 8.57 (d, J = 8.0), 7.74 (d, J = 7.8, 1 H), 7.52–7.35 (m, 2 H), 2.70 (t, J = 7.6, 2 H), 2.43 (s, 3 H), 1.59 (sext, J = 7.6, 2 H), 1.03 (t, J = 7.6, 3 H); ¹³C{¹H} NMR (125 MHz, CDCl₃) δ = 160.5, 146.2,

142.3, 141.0, 131.5, 126.4, 125.7, 123.8, 118.4, 116.1, 29.8, 22.0, 20.9, 14.1; GC-MS m/z = 258 (M^+ , 96), 243 (14), 229 (100), 201 (16), 143 (12); HRMS (ESI-TOF) m/z [$M-H$] $^-$ calcd for $C_{14}H_{13}N_2OS^-$ 257.0754; found 257.0764.



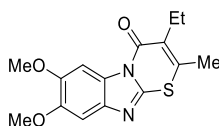
2-Methyl-3-pentyl-1-thia-4a,9-diazafluoren-4-one (2d).

Yield 128 mg, starting from 209 mg of **1d** (55%); colorless solid, mp = 56–58 °C; IR (KBr) ν = 1684 (s), 1474 (s), 1443 (s), 1383 (s), 1315 (m), 1225 (m), 1155 (m), 760 (s) cm^{-1} ; 1H NMR (300 MHz, $CDCl_3$) δ = 8.51 (d, J = 7.6, 1 H), 7.68 (d, J = 7.9), 7.44–7.28 (m, 2 H), 2.62 (t, J = 7.8, 2 H), 2.34 (s, 3 H), 1.57–1.22 (m, 6 H), 0.87 (t, J = 6.5, 3 H); $^{13}C\{^1H\}$ NMR (125 MHz, $CDCl_3$) δ = 160.4, 146.1, 142.3, 140.8, 131.4, 126.5, 125.6, 123.7, 118.3, 116.0, 31.8, 28.4, 27.9, 22.5, 20.8, 14.0; GC-MS m/z = 286 (M^+ , 47), 229(37), 202 (31), 137 (100); HRMS (ESI-TOF) m/z [$M+Na$] $^+$ calcd for $C_{16}H_{18}N_2OSNa^+$ 309.1032; found 309.1036.



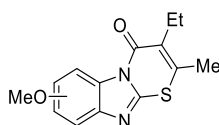
2,6,7-Trimethyl-3-ethyl-1-thia-4a,9-diazafluoren-4-one (2e).

Yield 124 mg, starting from 198 mg of **1e** (56%); colorless solid, mp = 154–158 °C; IR (KBr) ν = 1667 (s), 1477 (m), 1442 (s), 1350 (s), 1169 (m), 883 (m), 768 (m) cm^{-1} ; 1H NMR (300 MHz, $CDCl_3$) δ = 8.27 (s, 1 H), 7.43 (s, 1 H), 2.70 (q, J = 7.4, 2 H), 2.38 (s, 3 H), 2.36 (s, 6 H), 1.15 (t, J = 7.4, 3 H); $^{13}C\{^1H\}$ NMR (75 MHz, $CDCl_3$) δ = 160.2, 144.9, 140.8, 140.4, 134.7, 132.9, 129.7, 127.4, 118.3, 116.1, 21.2, 20.52, 20.46, 13.0; GC-MS m/z = 272 (M^+ , 100), 257 (44), 239 (13), 229 (19); HRMS (ESI-TOF) m/z [$M+Na$] $^+$ calcd for $C_{15}H_{16}N_2OSNa^+$ 295.0876; found 295.0871.



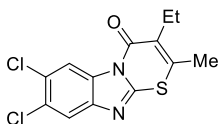
3-Ethyl-6,7-dimethoxy-2-methyl-1-thia-4a,9-diazafluoren-4-one (2f).

Yield 123 mg, starting from 224 mg of **1f** (50%) ; colorless solid, mp = 167–169 °C; IR (KBr) ν = 1667 (s), 1462 (s), 1427 (s), 1373 (m), 1318 (s), 1007 (m), 841 (m), 756 (m) cm^{-1} ; 1H NMR (300 MHz, $CDCl_3$) δ = 8.13 (s, 1 H), 7.20 (s, 1 H), 4.01 (s, 3 H), 3.97 (s, 3 H) 2.76 (q, J = 7.5, 2 H), 2.44 (s, 3 H), 1.18 (t, J = 7.5, 3 H); $^{13}C\{^1H\}$ NMR (75 MHz, $CDCl_3$) δ = 160.5, 148.6, 147.1, 143.6, 140.8, 136.3, 127.2, 125.1, 100.1, 98.7, 56.4, 56.2, 21.3, 20.6, 13.1; GC-MS m/z = 304 (M^+ , 100), 289 (60), 261 (9), 167 (32); HRMS (ESI-TOF) m/z [$M+Na$] $^+$ calcd for $C_{15}H_{16}N_2O_3SNa^+$ 327.0774; found 327.0767.



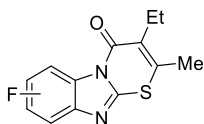
Mixture of Regioisomers 3-Ethyl-7-methoxy-2-methyl-1-thia-4a,9-diazafluoren-4-one (A) and 3-Ethyl-6-methoxy-2-methyl-1-thia-4a,9-diazafluoren-4-one (B) (1g; A/B Ratio = 3.0, by 1H NMR) (2g). Yield 127 mg, starting from 200 mg of **1g** (57%); colorless solid, mp = 114–119 °C; IR (KBr) ν = 1670 (s), 1477 (s), 1431 (s), 1358 (m), 1018 (m), 845 (m), 764 (m) cm^{-1} ; 1H NMR (300 MHz, $CDCl_3$) δ = 8.40 (d, J = 8.9, 1 H, B), 8.09 (d, J = 2.4, 1 H, A), 7.59 (d, J = 8.8, 1 H, A), 7.17 (d, J = 2.3, 1 H, B), 7.05 (dd, J = 8.8, 2.4, 1 H, A), 6.97 (dd, J = 8.9, 2.3, 1 H, B), 3.90 (s, 3 H, A), 3.87 (s, 3 H, B), 2.72 (q, J = 7.4, 2 H, A+B), 2.40 (s, 3 H, A+B), 1.16 (t, J =

7.4, 3 H, A+B); $^{13}\text{C}\{^1\text{H}\}$ NMR (75 MHz, CDCl_3) δ = 160.6 (A), 160.0 (B), 158.3 (B), 157.0 (A), 146.4 (B), 144.2 (A), 143.6 (B), 141.0 (A), 140.3 (B), 136.6 (A), 132.1 (A), 127.6 (B), 127.3 (A), 125.8 (B), 118.7 (A), 116.4 (B), 115.3 (A), 112.7 (B), 101.1 (B), 99.4 (A), 55.92 (A), 55.89 (B), 21.3 (A+B), 20.6 (A+B), 13.1 (A+B); GC-MS [A] m/z = 274 (M^+ , 100), 259 (55), 231 (18), 180 (10), 165(11); GC-MS [B] m/z = 274 (M^+ , 100), 259 (56), 231 (17), 180 (10), 165 (11); HRMS (ESI-TOF) m/z [$\text{M} + \text{Na}$] $^+$ calcd for $\text{C}_{14}\text{H}_{14}\text{N}_2\text{O}_2\text{SNa}^+$ 297.0668; found 297.0663.



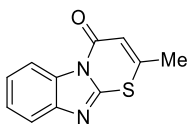
6,7-Dichloro-3-ethyl-2-methyl-1-thia-4a,9-diazafluoren-4-one (2h).

Yield 150 mg, starting from 231 mg of **1h** (59%); colorless solid, mp = 200–202 °C; IR (KBr) ν = 1670 (s), 1466 (m), 1427 (s), 1350 (m), 914 (m), 872 (m) cm^{-1} ; ^1H NMR (300 MHz, CDCl_3) δ = 8.63 (s, 1 H), 7.75 (s, 1 H), 2.75 (q, J = 7.5, 2 H), 2.46 (s, 3 H), 1.17 (t, J = 7.5, 3 H); $^{13}\text{C}\{^1\text{H}\}$ NMR (75 MHz, CDCl_3) δ = 159.7, 148.1, 141.5, 141.4, 130.3, 129.9, 127.84, 127.82, 119.4, 117.3, 21.3, 20.7, 12.9; GC-MS m/z = 316 [$(\text{M}^+ 4)^+$, 13], 314 [$(\text{M}^+ 2)^+$, 65], 312 (M^+ , 100), 299 (22), 297 (30), 279 (17), 277 (18), 271(11), 269 (16); HRMS (ESI-TOF) m/z [$\text{M} + \text{H}$] $^+$ calcd for $\text{C}_{13}\text{H}_{11}\text{Cl}_2\text{N}_2\text{OS}^+$ 312.9964; found 312.9949.



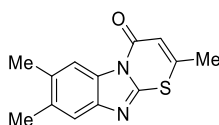
Mixture of Regioisomers 3-Ethyl-6-fluoro-2-methyl-1-thia-4a,9-diazafluoren-4-one (A) and 3-Ethyl-7-fluoro-2-methyl-1-thia-4a,9-diazafluoren-4-one (B) (A/B Ratio = 1.1, by ^1H NMR) (2i).

Yield 121 mg, starting from 190 mg of **1i** (57%); colorless solid, mp = 107–109 °C; IR (KBr) ν = 1670 (s), 1468 (s), 1437 (s), 1358 (m), 1130 (m), 845 (m), 814 (m) cm^{-1} ; ^1H NMR (300 MHz, CDCl_3) δ = 8.46 (dd, J = 8.9, 5.0, 1 H, A), 8.24 (dd, J = 8.9, 2.4, 1 H, B), 7.63 (dd, J = 8.9, 4.8, 1 H, B), 7.36 (dd, J = 8.9, 2.3, 1 H, A), 7.18 (td, J = 8.9, 2.4, 1 H, B), 7.09 (dd, J = 8.9, 2.3, 1 H, A), 2.79–2.67 (m, 2 H, A+B), 2.43 (s, 3 H, A), 2.43 (s, 3 H, B), 1.22–1.12 (m, 3 H, A+B); $^{13}\text{C}\{^1\text{H}\}$ NMR (75 MHz, CDCl_3) δ = 160.9 (d, J = 242.6, A), 160.09 (B), 159.95 (A), 159.6 (d, J = 241.6, B), 147.8 (A+B), 146.2 (B), 143.2 (d, J = 12.8, A), 141.0 (d, J = 28.9, B), 138.67 (A or B), 138.65 (B or A), 131.4 (d, J = 14.2, B), 128.8 (A), 127.6 (d, J = 22.0, A), 118.9 (d, J = 9.9, B), 116.7 (d, J = 9.9, A), 113.8 (d, J = 25.1, B), 111.7 (d, J = 25.2, A), 104.5 (d, J = 24.8, A), 103.3 (d, J = 29.6, B), 21.28 (A+B), 20.64 (A), 20.60 (B), 12.99 (A+B); ^{19}F NMR (471 MHz, CD_3Cl) δ = -115.8 (s, A), -117.4 (s, B); GC-MS (A+B) m/z = 262 (M^+ , 100), 247 (52), 229 (16), 219 (21), 168 (9); HRMS (ESI-TOF) m/z [$\text{M} + \text{Na}$] $^+$ calcd for $\text{C}_{13}\text{H}_{11}\text{FN}_2\text{OSNa}^+$ 285.0468; found 285.0468.



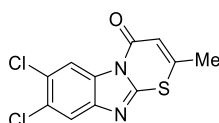
2-Methyl-1-thia-4a,9-diazafluoren-4-one (2j).

Yield: 114 mg, starting from 153 mg of **1j** (65%) Colorless solid, mp: 170–172 °C; IR (KBr): ν 1680 (s), 1639 (m), 1618 (m), 1472 (m), 1401 (m), 1360 (m), 1310 (m), 1200 (w), 771 (m) cm^{-1} ; ^1H NMR (300 MHz, CDCl_3): δ 8.54 (d, J = 7.8, 1 H), 7.76 (d, J = 7.7, 1 H), 7.54–7.36 (m, 2 H), 6.56–6.51 (m, 1 H), 2.48 (d, J = 0.9, 3 H); ^{13}C NMR (75 MHz, CDCl_3): δ 159.6, 148.8, 146.7, 142.5, 131.2, 125.8, 124.2, 118.6, 116.1, 115.6, 22.8; GC-MS: m/z 216 (M^+ , 100), 188 (29), 175 (4), 150 (33), 143 (6), 129 (4), 122 (5), 108 (4), 90 (9); Anal. calcd for $\text{C}_{11}\text{H}_8\text{N}_2\text{OS}$ (216.26): C, 61.09; H, 3.73; N 12.95; S, 14.83; found C, 61.35; H, 3.71; N 12.91; S, 14.89.



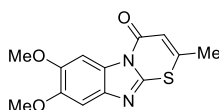
2,6,7-Trimethyl-1-thia-4a,9-diazafluoren-4-one (2k).

Yield: 142 mg, starting from 175 mg of **1k** (72%). Colorless solid, mp: 115–121 °C; IR (KBr): ν 1677 (s), 1377 (m), 1347 (m), 1315 (m), 1286 (m), 1184 (m), 1094 (w), 846 (m) cm^{-1} ; ^1H NMR (300 MHz, CDCl_3): δ 8.24 (s, 1 H), 7.45 (s, 1 H), 6.48–6.43, (m, 1 H), 2.44 (d, $J = 1.1$, 3 H), 2.39 (s, 3 H), 2.38 (s, 3 H); ^{13}C NMR (75 MHz, CDCl_3): δ 159.6, 148.2, 145.6, 141.6, 134.9, 133.5, 130.0, 119.0, 116.1, 115.8, 22.5, 20.2; GC-MS: m/z 244 (M^+ , 100), 229 (20), 216 (16), 201 (7), 178 (23), 163 (10), 157 (3), 122 (7), 91 (7), 67 (10); Anal. calcd for $\text{C}_{13}\text{H}_{12}\text{N}_2\text{OS}$ (244.31): C, 63.91; H, 4.95; N 11.47; S, 13.12; found C, 63.80; H, 4.96; N 11.49; S, 13.09.



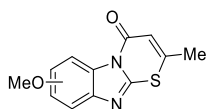
6,7-Dichloro-2-methyl-1-thia-4a,9-diazafluoren-4-one (2l).

Yield 164 mg, starting from 208 mg of **1l** (71%). Yellow solid, mp: 153–155 °C; IR (KBr): ν 1692 (s), 1467 (w), 1375 (m), 1340 (m), 1297 (m), 1190 (m), 1095 (m), 842 (m) cm^{-1} ; ^1H NMR (300 MHz, CDCl_3): δ 8.64 (s, 1 H), 7.82 (s, 1 H), 6.56 (q, $J = 1.2$, 1 H), 2.52 (d, $J = 1.2$, 3 H); ^{13}C NMR (75 MHz, CDCl_3): δ 153.5, 140.3, 127.4, 116.5, 79.2, 73.5, 21.6; GC-MS: m/z 286 [$(\text{M}^+ 2)^+$, 69], 284 (M^+ , 100), 258 (23), 256 (33), 220 (18), 218 (25), 199(3), 181 (8), 158 (4), 142 (4), 100 (4), 88 (6), 67 (61); Anal. calcd for $\text{C}_{11}\text{H}_6\text{Cl}_2\text{N}_2\text{OS}$ (285.15): C, 46.33; H, 2.12; Cl, 24.87; N 9.82; S, 11.24; found C, 46.21; H, 2.14; N 9.86; S, 11.27.



6,7-Dimethoxy-2-methyl-1-thia-4a,9-diazafluoren-4-one (2m).

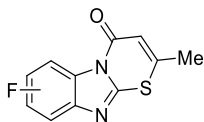
Yield: 150 mg, starting from 201 mg of **1m** (67%). Yellow solid, mp: 187–188 °C; IR (KBr): ν 1678 (s), 1465 (s), 1436 (s), 1340 (m), 1307 (m), 1193 (m), 1153 (m), 1016 (m), 862 (m), 830 (m) cm^{-1} ; ^1H NMR (300 MHz, CDCl_3): δ 8.02 (s, 1 H), 7.18 (s, 1 H), 6.48 (s, 1 H), 3.99 (s, 3 H), 3.96 (s, 3 H), 2.47 (s, 3 H); ^{13}C NMR (75 MHz, CDCl_3): δ 159.7, 149.6, 148.4, 144.2, 137.1, 132.2, 125.4, 115.5, 101.7, 100.0, 56.9, 56.6, 22.5; GC-MS: m/z 276 (M^+ , 100), 261 (28), 233 (6), 207 (11), 193 (5), 167 (5), 135 (5), 73(6); Anal. calcd for $\text{C}_{13}\text{H}_{12}\text{N}_2\text{O}_3\text{S}$ (276.31): C, 56.51; H, 4.38; N 10.14; S, 11.60; found C, 56.66; H, 4.36; N 10.17; S, 11.64.



Mixture of 6-Methoxy-2-methyl-1-thia-4a,9-diazafluoren-4-one and 7-Methoxy-2-methyl-1-thia-4a,9-diazafluoren-4-one (1.2/1 Mixture of Isomers A/B, by GLC)(2n).

Yield: 148 mg, starting from 177 mg of **1n** (74%). Yellow solid, mp: 125–130 °C; IR (KBr): ν 1689 (s), 1594 (w), 1478 (s), 1432 (m), 1366 (m), 1303 (m), 1277 (m), 1200 (m), 1155 (m), 1023 (m), 839 (m) cm^{-1} ; ^1H NMR (300 MHz, CDCl_3): δ 8.37 (d, $J = 9.0$, A), 8.05 (d, $J = 2.5$, B), 7.61 (d, $J = 8.8$, B), 7.19 (d, $J = 2.4$, 1 H, A), 7.07 (dd, $J = 8.8, 2.5$, 1 H, B), 7.01 (dd, $J = 9.0, 2.4$, A), 6.51 (q, $J = 1.1$, 1 H, B), 6.48 (q, $J = 1.1$, 1 H, A), 3.91 (s, 3 H, B), 3.88 (s, 3 H, A), 2.48 (d, $J = 1.2$, 3 H, A), 2.47 (d, $J = 1.1$, 3 H, B) (Note: The A/B isomer assignments are based on ^1H NMR peak integration data: A refers to the major isomer and B refers to the minor isomer); ^{13}C NMR (75 MHz, CDCl_3): δ 159.5, 158.79, 158.75, 157.5, 149.1, 148.5, 147.1, 144.9, 135.3, 131.7, 130.9, 128.8, 125.0, 118.5, 116.7, 115.7, 115.4, 114.1, 100.3, 99.5, 56.0, 55.8, 29.7, 22.8; GC-MS [A (major isomer)]:

m/z 246 (M^+ , 100), 231 (42), 218 (7), 203 (14), 180 (21), 165 (29), 152 (4), 137 (4), 67 (36); GCMS [B (minor isomer)]: m/z 246 (M^+ , 100), 231 (41), 218 (9), 203 (10), 180 (15), 165 (27), 152 (4), 137 (6), 123 (3), 89 (4), 67 (34); Anal. calcd for $C_{12}H_{10}N_2O_2S$ (246.28): C, 58.52; H, 4.09; N 11.37; S, 13.02; found C, 58.37; H, 4.07; N 11.39; S, 13.05.



Mixture of 6-Fluoro-2-methyl-1-thia-4a,9-diazafluoren-4-one and 7-Fluoro-3-methyl-1-thia-4a,9-diazafluoren-4-one (1.4:1 mixture of isomers A:B, by 1H NMR) (**2o**). Yield: 129 mg, starting from 167 mg of **1o** (68%). Colorless solid, mp: 125–128°C; IR (KBr): ν 1679 (s), 1466 (s), 1429 (s), 1355 (m), 1305 (m), 1135 (m), 958 (m), 862 (m), 813 (m) cm^{-1} ; 1H NMR (300 MHz, $CDCl_3$): δ 8.47 (dd, $J = 9.0, 5.0, 1$ H, A), 8.24 (dd, $J = 8.8, 2.4, 1$ H, B), 7.67 (dd, $J = 8.9, 4.8, 1$ H, B), 7.40 (dd, $J = 8.6, 2.3, 1$ H, A), 7.28–7.09 (m, 1 H, A + 1 H, B), 6.55 (s, br, 1 H, A), 6.52 (s, br, 1 H, B), 2.50 (s, 3 H, A + 3 H, B) (Note: The A/B isomer assignments are based on 1H NMR peak integration data: A refers to the major isomer and B refers to the minor isomer); ^{13}C NMR (75 MHz, $CDCl_3$): δ 160.9 (d, $J = 243$), 159.8 (d, $J = 243$), 159.4, 159.3, 149.3, 148.9, 143.3 (d, $J = 12.5$), 138.3 (d, $J = 1.4$), 131.1 (d, $J = 13.9$), 127.6 (d, $J = 1.4$), 119.2 (d, $J = 9.7$), 116.8 (d, $J = 9.7$), 115.5, 115.3, 114.1 (d, $J = 25.0$), 112.2 (d, $J = 25.0$), 104.8 (d, $J = 25.0$), 103.3 (d, $J = 29.8$), 22.9, 22.8; ^{19}F NMR (471 MHz, $CDCl_3$): δ -108.5 (s), -109.7 (s); GC-MS [A+B]: m/z 234 (M^+ , 100), 206 (32), 191 (3), 168 (32), 162 (8), 147 (5), 136 (4), 108 (16), 95 (5); Anal. calcd for $C_{11}H_7FN_2OS$ (234.25): C, 56.40; H, 3.01; F 8.11; N, 11.96; S, 13.69; found C, 56.29; H, 3.02; N 11.99; S, 13.65.

1.6 References

- [1] B. Gabriele; *Targets Heterocycl Syst.* **2018**, *22*, 41–55.
- [2] a) B. Gabriele, G. Salerno, M. Costa, G. P. Chiusoli, *J. Organomet. Chem.* **2003**, *687*, 219; (b) B. Gabriele, G. Salerno, M. Costa, G. P. Chiusoli, *Curr. Org. Chem.* **2004**, *8*, 919; (c) B. Gabriele, G. Salerno, M. Costa, *Synlett* **2004**, 2468; (d) B. Gabriele, G. Salerno, M. Costa, *Top. Organomet. Chem.* **2006**, *18*, 239; (e) B. Gabriele, R. Mancuso, G. Salerno *Eur. J. Org. Chem.* **2012**, 6825; (f) Q. Liu, H. Zhang, A. Lei; *Angew. Chem. Int. Ed.* **2011**, *50*, 10788; (g) X.-F. Wu, H. Neumann, M. Beller, *Chem. Soc. Rev.* **2011**, *40*, 4986; (h) I. Omae, *Coord. Chem. Rev.* **2011**, *255*, 139; (i) R. Grigg, S. P. Mutton, *Tetrahedron* **2010**, *66*, 5515; (j) M. Beller and X.-F. Wu, *Springer-Verlag Berlin Heidelberg* **2013**.
- [3] (a) B. M. Trost; *Science* **1991**, *254*, 1471; (b) B. M. Trost; *Angew. Chem. Int. Ed. Engl.* **1995**, *34*, 259; (c) B. M. Trost, *Acc. Chem. Res.* **2002**, *35*, 695.
- [4] (a) P. A. Wender, B. L. Miller, *Nature*, **2009**, *460*, 197; (b) P. A. Wender, V. A. Verma, T. J. Paxton, T. H. Pillow, *Acc. Chem. Res.* **2008**, *41*, 40.
- [5] (a) P. Anastas, N. Eghbali, *Chem. Soc. Rev.* **2010**, *39*, 301; (b) R. A. Sheldon, I. Arends, H. Ulf, *Green Chemistry and Catalysis*, Wiley-VCH, Weinheim, **2008**; (c) R. A. Sheldon, *Chem. Commun.* **2008**, 3352; (d) R. A. Sheldon, *Green Chem.* **2007**, *9*, 1273.
- [6] G. Vasapollo, G. Mele; *Current Organic Chemistry*, **2006**, *10*, 1397.
- [7] (a) M. Beller; *Acc. Chem. Res.* **2014**, *47*, 1041; (b) J. Falbe, *Springer*, Berlin, **1980**.
- [8] M. Beller, X. F. Wu, *Springer: Amsterdam*, **2013**.
- [9] X.-F. Wu, H. Neumann, & M. Beller, *Chemical Reviews*, **2012**, *113(1)*, 1–35.
- [10] (a) X.-F. Wu, H. Neumann and M. Beller, *ChemSusChem*, **2013**, *6*, 229–241; (b) Q. Liu, H. Zhang and A. Lei, *Angew. Chem., Int. Ed.*, **2011**, *50*, 10788.
- [11] S.T. Gadge and B.M. Bhanage, *RSC Adv.*, **2014**, *4*, 10367.
- [12] R. C. Larock, *Chem. Rev.* **2006**, *106*, 4644.
- [13] (a) F. R. Hartley, *Applied Science: London*, **1972**; (b) T. Hosokawa, S. Miyagi, S. Murahashi, A. Sonoda, *J. Org. Chem.* **1978**, *43*, 2752.
- [14] a) B. Gabriele, M. Costa, G. Salerno, G. P. Chiusoli, *J. Chem. Soc., Chem. Commun.* **1992**, 1007; (b) B. Gabriele, M. Costa, G. Salerno, G. P. Chiusoli, *J. Chem. Soc. Perkin Trans. 1* **1994**, 83.
- [15] B. Gabriele, Chapter 3 - Synthesis of Heterocycles by Palladium-Catalyzed Carbonylative Reactions, *Advances in Transition-Metal Mediated Heterocyclic Synthesis*, Academic Press, **2018**, 55-127,
- [16] Narasimhan, B., Sharma, D. & Kumar, *Med Chem Res* **21**, **2012**, 269–283.
- [17] N. Tsuchiya, Hino (JP); Y. Matsumoto, Hino (JP); H. Saitou, Hino (JP); T. Mizuno, Hino (JP), Benzimidazole Derivative, *United States Patent, US 7,176,320*, **2007**.
- [18] (a) A. B. Brukshtus, V. N. Garalene, A. R.-R. Sirvidite, and V. K. Daukshas ; (b) A. B. Brukshtus, V. N. Garalene, A. R.-R. Sirvidite, and V. K. Daukshas, *Pharmaceutical Chemistry Journal*, **1994**, Vol. 28(6).
- [19] Garaliene et al., *Arzneim.Forsch./Drug Res.* **2006**, *56*, No. 4, 282–287

- [20] R. Crossley, *Patent Number: 4873237*, **Oct. 10, 1989**.
- [21] (a) Khalil, A. K. Phosphorus, *Sulfur Silicon Relat. Elem.* **2007**, *182*, 815–823. (b) Britsun, V. N.; Lozinskii, M. O. *Chem. Heterocycl. Compd.* **2003**, *39*, 960–964. (c) Bell, S. C.; Wei, P. H. L. J. *Med. Chem.* **1976**, *19*, 524–530.
- [22] L. Veltri, R. Amuso, C. Cuocci, P. Vitale, B. Gabriele, *J. Org. Chem.*, **2019**, *84*, 8743–8749
- [23] L. Veltri, V. Paladino; P. Plastina; B. Gabriele, *J. Org. Chem.* **2016**, *81*, 6106–6111.
- [24] Carless, H. A. J.; Batten, R. J.; *J. Chem. Soc., Perkin Trans. 1* **1987**, 1999–2007.
- [25] M. Rosenberger, (Hoffmann-La Roche Inc.) *U.S. Patent Appl. US4311645*, **1982**.
- [26] T.I Yaroshenko, A.S.Nakhmanovich, L.I Larina, V.N. Elokhina, S.V. Amosova, *Chem. Heterocycl. Compd.* **2008**, *44*, 1129–1134.
- [27] L. Veltri; G. Grasso; R. Rizzi; R. Mancuso; B. Gabriele; *Asian J. Org. Chem.*, **2016**, *5*, 560–567.

Chapter 2

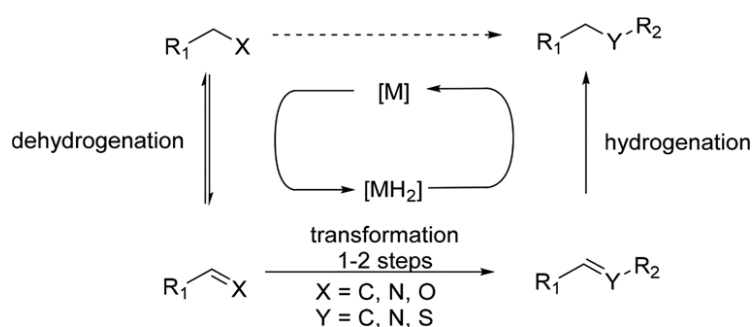
α -Alkylation of Ketones with Alcohols by Cyclometalated Ruthenium Pincer Complexes as Catalysts

2.1 Introduction

2.1.1 The borrowing hydrogen (BH) principle¹

The *borrowing hydrogen (BH) principle* or *hydrogen auto-transfer* consists in the transfer hydrogenation (avoiding the direct use of molecular hydrogen) with one or more intermediate reactions to form more complex molecules. This is an effective procedure because occurs without need tedious separation or isolation processes. Basically, the key concept is that the hydrogen from a donor molecule will be stored by a catalytic metal fragment to be released in a final hydrogenation step, hence the reaction name. Wherefore, an appropriate catalytic system in borrowing hydrogen catalysis requires metal complexes or stabilized metal particles in which H₂ dissociation and recombination is simple, preferably without requiring severe reaction conditions¹.

Typical homogeneous complexes that have been reported for these reactions are Ruthenium (Ru), Iridium (Ir), and Rhodium (Rh) complexes, among others. The borrowing hydrogen strategy is point out in the following Scheme 2.1.1: the start is a metal-catalyzed dehydrogenation, by virtue of which a usually less reactive donor molecule is temporarily converted into a more reactive substrate (e.g., an alkane transforms into an alkene, an alcohol into an aldehyde, or a ketone and an amine into an imine).



Scheme 2.1.1 Basic Scheme of the BH Methodology

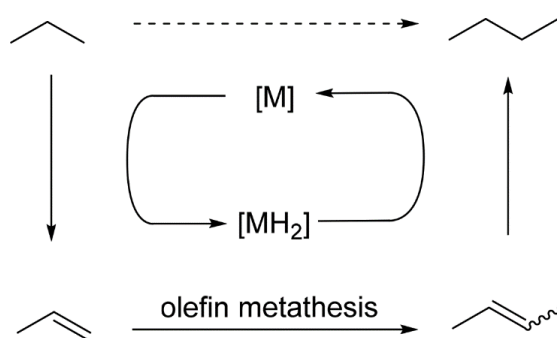
At this point, the more activated intermediate by further transformations gives an unsaturated compound that will be reduced with the intervention of the metal hydrides generated during the first dehydrogenation step. As shown in Scheme 2.1.1, the strategy

typically consists of three steps: (i) dehydrogenation, (ii) intermediate reaction, and (iii) hydrogenation. The borrowing hydrogen catalysis is a powerful process because is synthetic, economic and environmental and in the past few years the BH reactions have received much attention. The Borrowing Hydrogen Methodology can be applied in both homogeneous and heterogeneous catalysis but in this chapter, we will focus on BH methodology in homogeneous catalysis.

2.1.2 Borrowing Hydrogen Process in Homogeneous Catalysis¹

In the BH methodology in Homogeneous Catalysis, is worth considering three main subheadings based on the source of the electrophile (alkanes, alcohols, and amines) and the type of bond formed (carbon-carbon, carbon heteroatom). This has been taken into account to end-up with the intermediate reaction working in tandem with the metalcatalyzed hydrogenation/dehydrogenation step¹.

Activation of Alkanes with Formation of C-C Bonds: alkane dehydrogenation in the borrowing hydrogen catalysis can be an efficient and powerful route to activate alkanes; indeed, alkane metathesis is an efficient BH strategy to form new alkanes and, because it is similar to olefin metathesis, is based on a tandem operational combination of alkane dehydrogenation/hydrogenation and olefin metathesis reactions, as shown in Scheme 2.1.2.



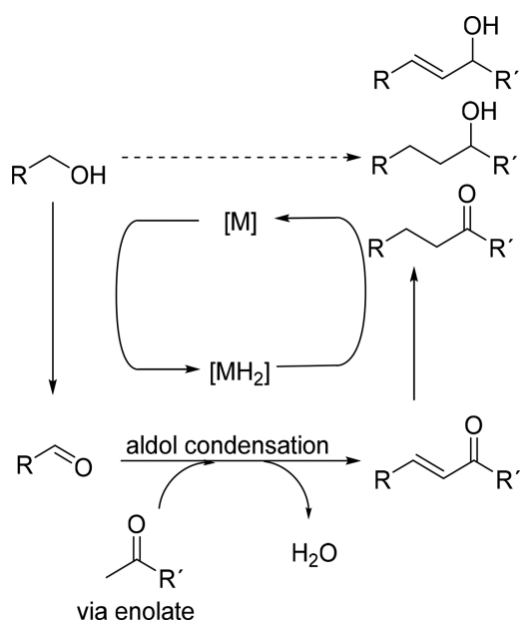
Scheme 2.1.2 Borrowing Hydrogen and Olefin Metathesis Working in Tandem

In 2006 by Goldman et al. reported one of the first homogeneous catalytic systems for transforming a specific alkane into a higher homologue by BH process combining one iridium complex as dehydrogenation/ hydrogenation catalyst and the Schrock's molybdenum imido

olefin catalyst. The process was able to transform n-hexane into a range of C12 to C15 n-alkanes.

Activation of Alkanes with Formation of C–N Bonds: compared to the traditional alkylation methods to get amines, BH processes are definitely superior from an environmental point of view (utilization of hazardous chemicals and solvents). In a recent literature review², there is only an example of N-arylations via BH catalysis from reaction initiated by alkane activation.

Activation of Alcohols with Formation of C–C Bonds: carbonyl compounds, deriving originally from an alcohol, give the corresponding alkenes through ulterior C–C forming reactions via borrowing hydrogen methods. Thus, the resulting olefins will be hydrogenated in situ to afford saturated alkanes through a net alkylation process. Aldol Condensation is the Intermediate Reaction in the BH strategy and allows access to more complex structures starting from simple alcohols. As highlighted in the scheme 2.1.3, global reaction starts with dehydrogenation of hydroxylic compound to give corresponding aldehyde or ketone. Just formed the corresponding carbonyl compound, the aldol condensation takes place the corresponding α,β -unsaturated compound through an enol or enolate intermediate. At this point, metal hydrides would reduce the unsaturated compound to the corresponding alcohol.



Scheme 2.1.3 Hydrogen Autotransfer Process with Aldol Condensation as the Intermediate Reaction

Depending on the starting reagent, three different reaction routes can carry out in hydrogen autotransfer processes through aldolic condensation: (a) α -alkylation of carbonyl compounds with alcohols, (b) β -alkylation of secondary alcohols to give β -alkylated alcohols or β -alkylated ketones, and (c) β -alkylation of primary alcohols with primary alcohols to yield β -alkylated alcohols (figure 2.1.1).

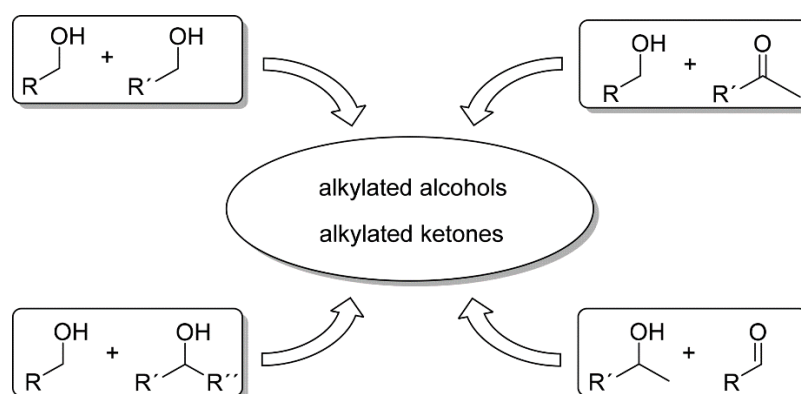


Fig. 2.1.1 Different routes for the indirect aldol condensation through the BH strategy.

Among many groups of representative catalysts which were successfully applied in these C–C forming reactions, the use of ruthenium and iridium complexes must be focused of attention. In particular, ruthenium-based complexes have been widely applied for the α -alkylation of ketones or amides with primary alcohols, whereas iridium complexes have proved appropriate in α -alkylations starting from ketones and esters.

2.1.3 Pincer Complexes in Homogeneous Catalysis³

In organometallic chemistry and organic synthesis pincer complexes are developing considerably in the past two decades. Indeed, pincer complexes are a satisfactory alternative, because improving selectivity and specific activities with the possibility to realize different fine-tuning steps. In recent times, the use of pincer catalysts for chemical transformations has increased greatly as play an important role in the synthesis of numerous organometallic compounds, like imines, amines, peptides, pyridines, pyrroles, and acetals, as well as carboxylic acid derivatives, such as esters and amides, also cross-coupling reactions, allyl-,

alkyl- and arylations, Diels–Alder and Michael reactions, reductions, (de)hydrogenations, activation of ammonia, water and CO₂, and borylations, as well as hydrocarboxylations³.

In 1976, pincer ligands were introduced for the first time by Shaw and co-workers and in addition, pioneering work on pincer complexes was reported by Van Koten and Noltes in 1978.

In general, pincer complexes are a tridentate ligand that is bound at flanking, coplanar sites to the metal center which allows the stability, selectivity, and reactivity to be influenced by metal or ligand modifications. The most common modifications to obtain high selectivity and activity are variations in the ring size and the ring nature (aromatic vs. non-aromatic ring or elimination of the ring) and besides geometric properties, electronic effects also need to be taken into consideration.

A generic structure for pincer complexes is shown in figure 2.1.2: M is a metal center, Z is a spacer, and YXY is a symmetric ligand (identical Y), where Y and X are coordinated to the metal center to form two stable five- or six-membered rings or hybrids of five or six membered rings.

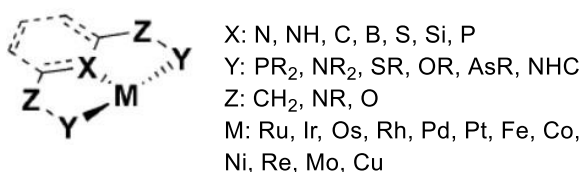


Fig. 2.1.2 Generic structure for pincer complexes³.

YXY can be neutral, charged, Lewis acidic or basic. Are also known asymmetric pincer ligands of the type YXY' and the differences between Y and Y' are basically three: a) the use of soft vs. hard donors, b) the rigidity of their binding to the metal center, and c) steric limitation of the substituents, which leads to congested metal centers. In addition, an appropriate control of reactivity is obtained through ligand design by incorporating bulky substituents to prevent coordination with free positions. Changes of X can be control electronic effects, whereas different spacers Z have direct control of electronic and indirect control of steric properties and also an influence on the behavior during complex formation and catalysis.

2.1.4 (De)hydrogenation reactions with Ru pincer complexes³

Recent publications point out the use of ruthenium complexes for (de)hydrogenation of miscellaneous substrates.

The homogeneously catalyzed hydrogenation of carboxylic acid derivatives is a much-investigated topic. The ruthenium-based pincer-type complex (figure 2.1.3), submitted by Milstein and coworkers, proved to be highly efficient in ester reduction and indeed is regarded as state of the art in the field³.

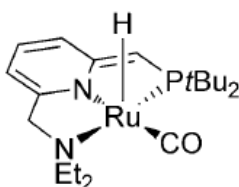


Fig. 2.1.3 Ruthenium-based pincer-type complex by Milstein and coworkers³.

Further progress was achieved by Kuriyama and co-workers using ruthenium PNP pincer complex, that today is commonly known as Ru-MACHO (figure 2.1.4), characterized by high hydrogenation activity in methanol.

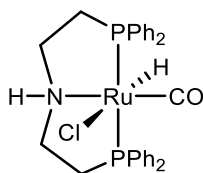


Fig. 2.1.4 Ru-MACHO

2.1.5 Selection of Pincer Ligand⁴

As mentioned above, the pincer ligands are tridentate with a central aromatic ring *ortho* or *ortho-disubstituted* with two electron-donor substituents. The pincer ligand can be changed via modification of the central moiety, the donor sites and electronic/steric effects on both. The main changes of the central group consist in the different type of ring (benzene, pyridine, acridine, etc.), in the size of ring (five-, six- or seven-membered), in the ring nature (aromatic versus aliphatic) or replacing the ring itself with an acyclic pincer ligand. The side arms stabilize

the pincer complexes and their property can also be varied to design pincer ligands with certain electronic and steric properties. The donor centers (E) could be a heteroatom, part of a heterocyclic moiety or an N-heterocyclic carbene (NHC) (figure 2.1.5). If these donor sites are similar, give rise to a symmetrical pincer (EZE), or an unsymmetrical pincer (EZE') if different from each other. The main differences are various and could be soft vs. hard donors, the rigidity with which they bind to the metal center, the steric constraints brought on by their substituents, the ligand type, i.e., neutral, charged, Lewis acidic, Lewis basic, etc.

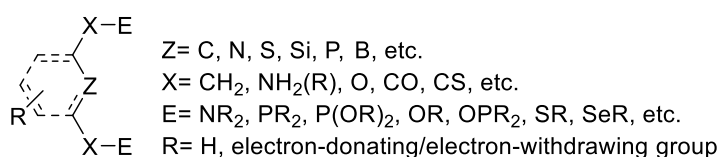


Fig.2.1.5 Pincer ligand structure's modification⁴.

The donor groups (E) are connected to the central backbone by spacers (X), such as methylene groups (-CH₂-), amines (-NR-), or oxygen atoms (-O-), etc. These different variations can generate chiral pincers, so altering the spacers controls the enantioselectivity of the pincer-based catalyst. Also, the length affects the coordination pocket of the pincer binder and its own spatial behavior on coordination. Pincer complexes with aromatic backbones enable them to induce remote electronic effects by substitution on the aryl moiety with electron-donating or electron-withdrawing groups. The overall properties of the metal complex strongly depend on the nature of the central donor atom (Z), indeed replacement of the central carbanion by isoelectronic nitrogen, silicon, phosphorus, or boron anions sometimes leads to important achievements in the catalytic activity.

2.1.6 Synthesis of Ruthenium Pincer Complexes⁴

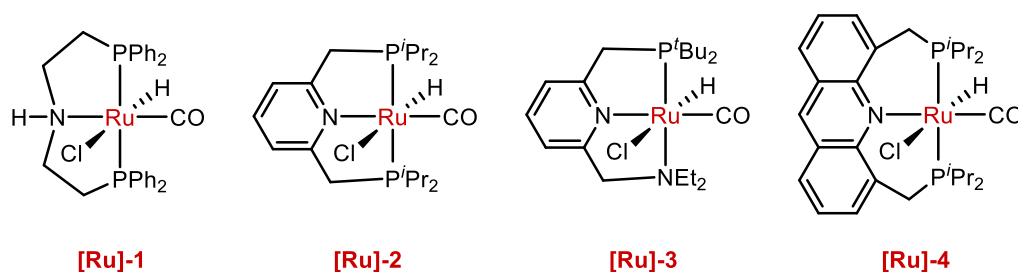
The development of pincer complexes-based catalysis requires conscious pincer ligand design. Generally, the introduction of the ruthenium source to a predesigned pincer ligand begins the synthesis of ruthenium pincer complexes. The pincer ligand structure controls the complexation of pincer ligands to ruthenium ions i.e., whether direct metallation, C(Si)-H activation, transmetallation or transcyclometallation depends on the pincer ligand precursor and the adopted protocol for the reaction.

Direct metallation probably is the simplest and most efficient way to synthesize pincer complexes, even if limited to the synthesis of those complexes incorporating heteroatoms (or sometimes in-situ generated free carbenes) in the three coordination sites. In direct metallation, the predesigned ligand bearing constantly available free electrons ready for bonding in pincer coordination sites is introduced to the ruthenium source. The straightforwardness of the direct metallation is the best way for the synthesis of pyridine-based pincer ligands, having heteroatoms on both of the side arms, e.g., PNP, PNN, PNS, PONOP, PNNNP, PNNCN, and NNN.

In general, the pincer complex is generated by the reaction between stoichiometric amounts of the pincer ligand and the suitable ruthenium source, refluxed in solvents such as THF or toluene under an inert atmosphere. Thereby, for pincer ligands incorporating NHC, treatment with a strong base such as KHMDS or LiHMDS at low temperature is required first to generate the free carbene followed by addition of the ruthenium source.

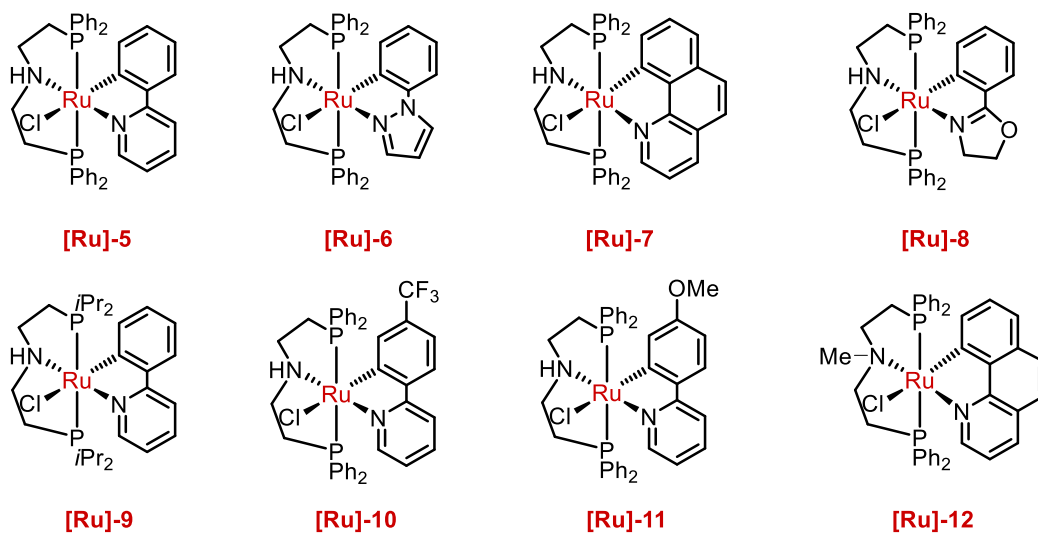
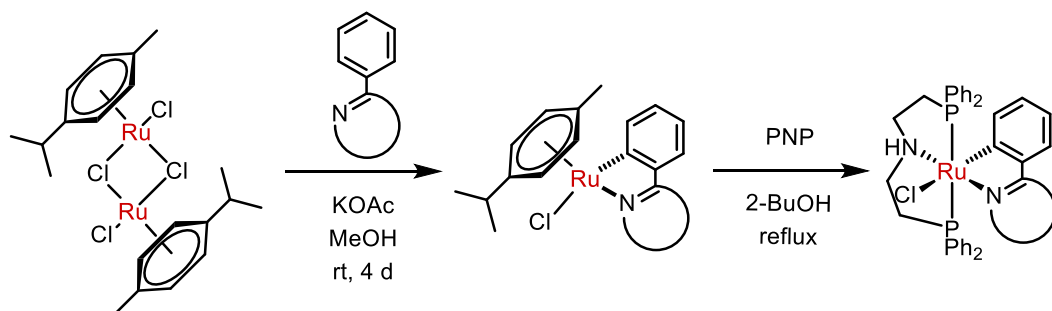
2.2 Results and Discussion

As said previously, the many Ru PNP pincer complexes used are shown in the scheme 2.2.1: Ru-MACHO ($[\text{RuHCl}(\text{CO})(\text{HN}(\text{CH}_2\text{CH}_2\text{PPh}_2)_2]$), **[Ru]-1**, introduced for the catalytic hydrogenation of esters⁵, organic carbonates⁶, nitriles⁷, and others as well as for dehydrogenation reactions of compounds like methanol⁸ or ethanol⁹. Additionally, in the scheme 2.2.1 the pyridine-based Ru pincer complexes **[Ru]-2** and **[Ru]-3** are also included, developed by Milstein and co-workers as efficient catalysts for numerous (de)hydrogenation reactions¹⁰.



Scheme 2.2.1 Frequently used Ru PNP pincer complexes³

In this study¹¹, we have put in place the synthesis of complexes **[Ru]-5–[Ru]-12** through cyclometalation of $[\text{Ru}(p\text{-cym})\text{Cl}_2]_2$ with 2-phenylpyridine¹² and an array of further heterocycles to get ready the corresponding intermediates, which were reacted with aliphatic pincer ligands in 2-butanol. The expected complexes **[Ru]-5–[Ru]-12** yielded powdery solids ranging from bright yellow to ruby-red in color (Scheme 2.2.2).



Scheme 2.2.2 Preparation of ruthenium pincer complexes bearing C,N-bound heterocycle ligands.

Afterwards, all these complexes were characterized by NMR, IR, MS analyses and X-ray structural analyses only for representative examples, like see figure 2.2.1.

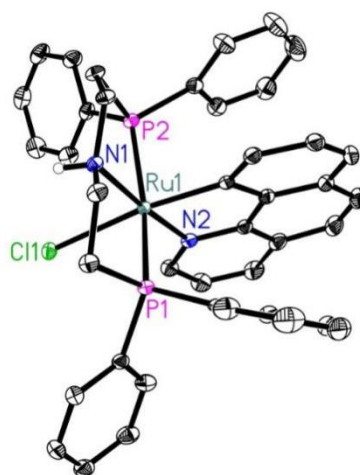


Fig. 2.2.1 Crystal structure of **[Ru]-7**. Displacement ellipsoids correspond to 30% probability. Hydrogen atoms (except the N-bound) and co-crystallized solvent are omitted for clarity.

Once ready these novel complexes, we applied them in hydrogen borrowing reactions and in particular, the α -alkylation of ketones with alcohols was of interest¹³.

To compare the reactivity of the novel catalysts with the parent Ru-MACHO system, the first investigations concerned the reaction of acetophenone with 2-methoxyethanol in *tert*-amyl alcohol at 130 °C in the presence of catalytic amounts of cesium carbonate as base. As can be seen from the Table 2.1, in these conditions, **[Ru]-1** only yielded in 16% of the desired product (entry 1), otherwise under the same reaction conditions, higher yields up to 48% were obtained with the newly synthesized catalysts (Table 2.1, entries 2–8). Hence, noting that the introduced phenyl heterocycle ligands can be beneficial for catalysis, we used the complex **[Ru]-7**, with benzo[h]quinoline as additional ligand, for optimizing the reaction conditions. Indeed, like see Table 2.1, entry 19, an optimal yield of 68% was obtained. Notably, no product formation at all is observed carrying out the reaction without any catalyst or without base. Interestingly, the application of **[Ru]-12**, in which the NH is replaced by a N-methyl group gave 46% of the desired product. This comparably high yield suggests that the NH proton is not essential for the catalyst performance. For the **[Ru]-12** an outer-sphere mechanism cannot be put forward, therefore can be suggested that the strong *trans* influence of the C-Ru bond very likely promotes labilization of the Ru-Cl bond and its substitution by the alkoxide. Even if in the absence of a mechanism to support the following hypothesis, likely subsequent β -hydride elimination could generate a Ru-hydride complex with ensuing formation of the aldehyde.

Table 2.1: Catalyst comparison and optimization for α -alkylation of acetophenone with 2-methoxyethanol.

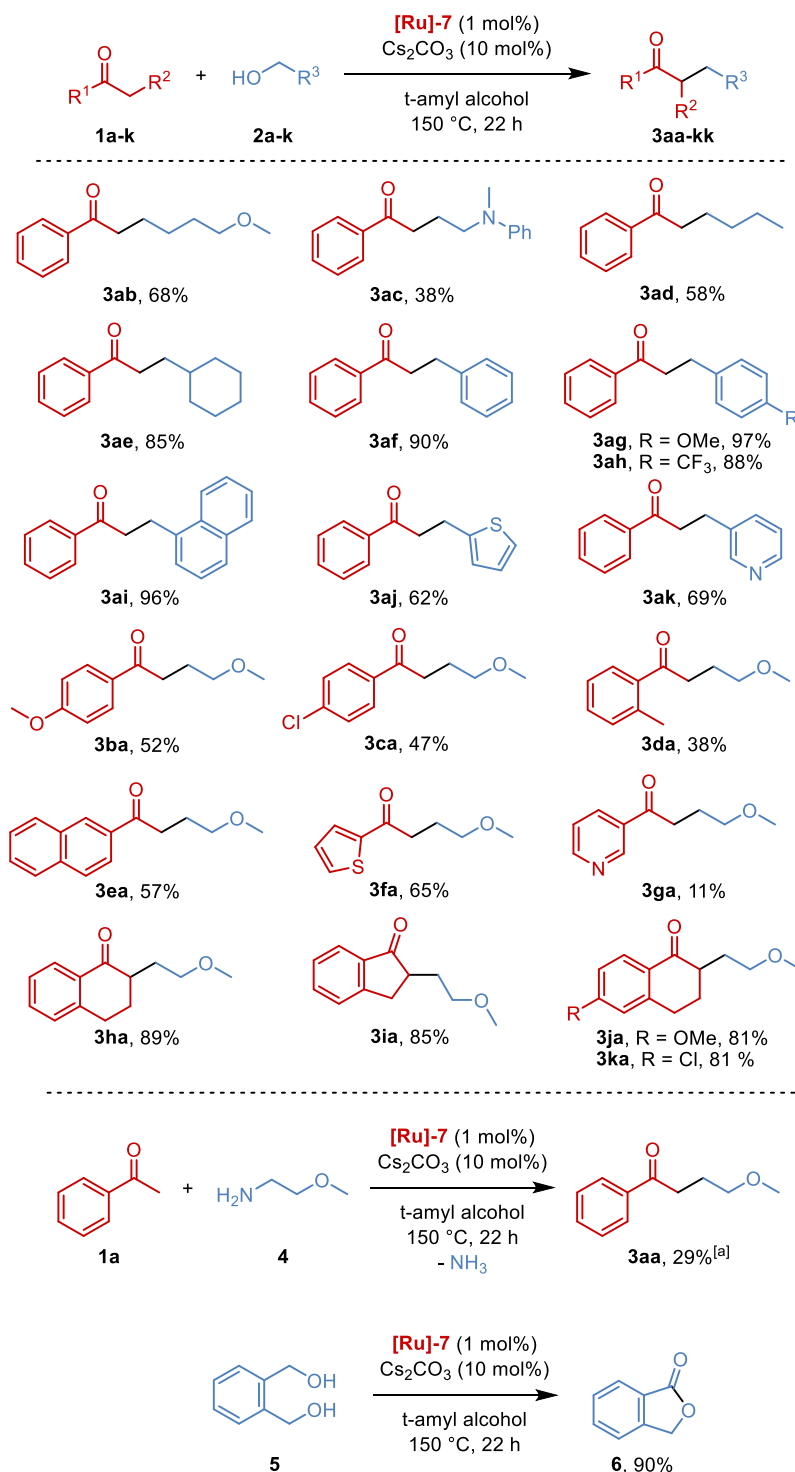
Ph-C(=O)-CH_3 (1a) + $\text{HO-CH}_2\text{-CH}_2\text{-O-CH}_3$ (2a) $\xrightarrow[\text{base, solvent, T, t}]{\text{[Ru]}}$ $\text{Ph-C(=O)-CH}_2\text{-CH}_2\text{-O-CH}_3$ (3aa)

#	[Ru]	Base	Base Loading	Solvent	T (°C)	Yield (%)
1	[Ru]-1	CS ₂ CO ₃	10 mol%	<i>t</i> -amyl alc.	130	16
2	[Ru]-5	CS ₂ CO ₃	10 mol%	<i>t</i> -amyl alc.	130	42
3	[Ru]-6	CS ₂ CO ₃	10 mol%	<i>t</i> -amyl alc.	130	44
4	[Ru]-7	CS ₂ CO ₃	10 mol%	<i>t</i> -amyl alc.	130	48
5	[Ru]-8	CS ₂ CO ₃	10 mol%	<i>t</i> -amyl alc.	130	32
6	[Ru]-9	CS ₂ CO ₃	10 mol%	<i>t</i> -amyl alc.	130	22

7	[Ru]-10	Cs ₂ CO ₃	10 mol%	<i>t</i> -amyl alc.	130	38
8	[Ru]-11	Cs ₂ CO ₃	10 mol%	<i>t</i> -amyl alc.	130	43
9	[Ru]-7	Cs ₂ CO ₃	10 mol%	<i>t</i> -amyl alc.	140	58
10	[Ru]-7	Cs ₂ CO ₃	10 mol%	<i>t</i> -amyl alc.	150	65
11	[Ru]-7	KOtBu	10 mol%	<i>t</i> -amyl alc.	150	44
12	[Ru]-7	NaOtBu	10 mol%	<i>t</i> -amyl alc.	150	45
13	[Ru]-7	NaOH	10 mol%	<i>t</i> -amyl alc.	150	38
14	[Ru]-7	K ₂ CO ₃	10 mol%	<i>t</i> -amyl alc.	150	36
15	[Ru]-7	NEt ₃	10 mol%	<i>t</i> -amyl alc.	150	-
16	[Ru]-7	Cs ₂ CO ₃	20 mol%	<i>t</i> -amyl alc.	150	66
17	[Ru]-7	Cs ₂ CO ₃	30 mol%	<i>t</i> -amyl alc.	150	64
18 ^[a]	[Ru]-7	Cs ₂ CO ₃	10 mol%	<i>t</i> -amyl alc.	150	57
19^[b]	[Ru]-7	Cs₂CO₃	10 mol%	<i>t</i>-amyl alc.	150	68
20 ^[c]	[Ru]-7	Cs ₂ CO ₃	10 mol%	<i>t</i> -amyl alc.	150	60
21 ^[b]	[Ru]-7	Cs ₂ CO ₃	10 mol%	heptane	150	41
22 ^[b]	[Ru]-7	Cs ₂ CO ₃	10 mol%	toluene	150	38
23 ^[b]	[Ru]-7	Cs ₂ CO ₃	10 mol%	THF	150	53
24 ^[b]	[Ru]-7	Cs ₂ CO ₃	10 mol%	1,4-dioxane	150	37
25 ^[b]	[Ru]-7	Cs ₂ CO ₃	10 mol%	water	150	10
26 ^[b]	[Ru]-7	-	-	<i>t</i> -amyl alc.	150	-
27	-	Cs ₂ CO ₃	10 mol%	<i>t</i> -amyl alc.	150	-
28	[Ru]-12	Cs ₂ CO ₃	10 mol%	<i>t</i> -amyl alc.	150	46
29	[Ru]-1	Cs ₂ CO ₃	10 mol%	<i>t</i> -amyl alc.	150	31

Unless otherwise specified, reactions were carried out with **1a** (1.0 mmol), **2a** (1.2 mmol), the catalyst (0.02 mmol), and the base (0.1 mmol) in 1 ml of solvent at the indicated temperature for 22 h; ^[a] catalyst loading: 0.5 mol%; ^[b] catalyst loading: 1 mol%; ^[c] catalyst loading: 3 mol%; yields determined by GC using n-hexadecane as internal standard.

Definitely, the optimal conditions have been identified in the reaction with **1a** (1.0 mmol), **2a** (1.2 mmol), **[Ru]-7** (0.01 mmol), and Cs₂CO₃ (0.1 mmol) in 1 mL of *t*-amyl alcohol at 150°C and these have been applied for testing different substrates (Scheme 2.2.3).



Scheme 2.2.3 Substrate scope of the Ru-catalyzed α -alkylation of ketones and related reactions. Yields of isolated material; ^[a]yield determined by GC using hexadecane as internal standard.

Reaction of 4-methoxybutanol (**2b**) gave 68% of the desired product **3ab** and exchanging the ether group for a tertiary amine, the corresponding product **3ac** was obtained in 38% yield. Additionally, the reaction with simple, aliphatic alcohols like 1-butanol **2d** or cyclohexylmethanol **2e**, acetophenone was alkylated in satisfying yields (58 and 85%,

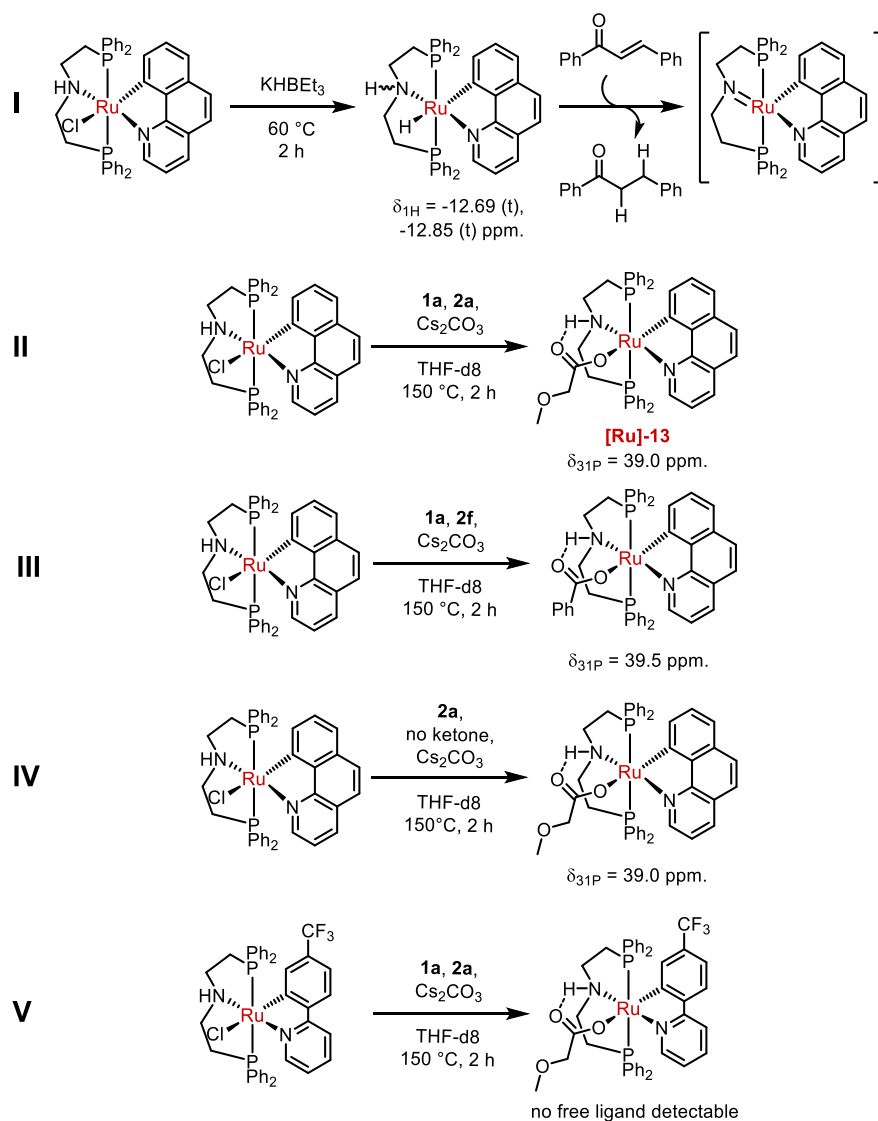
respectively). Surprising, the yield rises to 90 % when benzyl alcohol **2f** is applied. At this point, substituted benzyl alcohols were applied to give alkylated ketones **3ag** and **3ah** in 97 and 88% yield, respectively. Furthermore, the desired product **3ai** deriving from 1-naphthyl methanol **2i** was obtained with an excellent 96% yield. Finally, 2-thiophenemethanol **2j** and 3-pyridylmethanol **2k** were applied as representatives of heterocycle-bearing alcohols. Here, the corresponding products were obtained in 62 and 69% yield, respectively.

Afterwards, the reactions were carried out with differently substituted acetophenone derivatives and proceeded smoothly affording 38 to 58% of the corresponding products **3ba** to **3da**. In line with this, 2-acetonaphthone was converted into **3ea** in 57% yield and 2-acetyl heterocycles **1f** and **1g** gave 65 and 11%, respectively. Next, the products coming from acetone **1h** or 1-indanone **1i** were obtained in good yields of 89 and 85%, respectively. In line with this, when substituted tetralone-derivates **1j** and **1k** are employed, the corresponding products are generated in 81% yield in both cases.

This new class of complexes are as well able to dehydrogenate amines allowing for their application in alkylating ketones. To confirm this, instead of the alcohol **2a**, the reaction carried out with 2-methoxyethylamine **4** giving **3aa**. Moreover, with these reaction conditions, diols like 1,2-benzenedimethanol **5** undergo cyclization to yield the corresponding cyclic lactone **6** under C-O bond formation with 90 %.

After leading a satisfactory substrate scope, the focus was on investigating of the reaction mechanism. First, it has been studied if the applied complex is capable of forming stable ruthenium hydride species, because it would be possible that these species spontaneously release the hydride and the aryl heterocycle ligand through reductive elimination. Nevertheless, a treatment of **[Ru]-7** with KHBET_3 led to the obtaining two hydridic species, detected by ^1H NMR spectroscopy, shown in scheme 2.2.4, reaction I. In a follow-up experiment, one of these hydride complexes is able to promptly hydrogenate benzylideneacetophenone which corresponds to the last step of the alkylation of ketones with alcohols. Next, to find out which catalyst species are actually present under reaction conditions, the reaction was carried out in a pressure-resistant NMR tube (adapting the reaction conditions with use of $[\text{D}_8]\text{THF}$ as solvent, shortened reaction times and higher catalyst loadings). At this point, one major species was detected in ^{31}P NMR, besides starting complex **[Ru]-7** (scheme 2.2.4, reaction II). To verify the nature of this species, in the reaction III, the NMR-scale experiment was carried out with benzyl alcohol instead of 2-

methoxyethanol. This resulted in a slightly shifted ^{31}P NMR signal suggesting that a different complex is formed herein, when a different alcohol is deployed. Therefore, in the reaction IV the reaction was repeated without addition of the ketone. Here, a similar species was detected by ^{31}P NMR, whereas it was not observed in a comparison experiment without alcohol or ketone. The species formed in this reaction was further characterized by NMR spectroscopy as well as X-ray structural analysis. This revealed that the complex predominantly present during catalysis is ruthenium carboxylate complex **[Ru]-13** (figure 2.2.2) and, under reaction conditions, this species is probably generated by hydration of the in situ formed aldehyde followed by catalytic dehydrogenation of the so-formed gem-diol.



Scheme 2.2.4 Investigation experiments of catalyst species involved in the reaction.

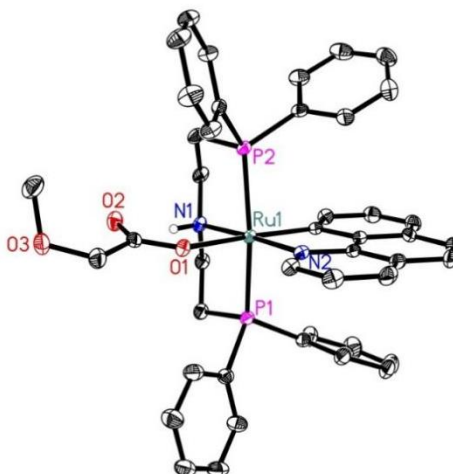


Fig. 2.2.2 Crystal structure of **[Ru]-13**. Displacement ellipsoids correspond to 30% probability. Only one molecule of the asymmetric unit is shown. Hydrogen atoms (except the N-bound) and co-crystallized solvent are omitted for clarity.

The aldol condensation occurring during catalysis or the moisture present in the alcohols, not dried before the use, probably form the water required for this process. Attempts to synthesize **[Ru]-13** independently in the best case yielded in a mixture of 78% of it and the starting complex **[Ru]-7**. However, when this mixture was applied in the standard reaction, the product was obtained in similar 68%. Due to this, **[Ru]-13** likely depicts a catalyst reservoir and can be activated by base probably through deprotonation of the NH group and formation of a further N-Ru bond with displacement of the carboxylate group, the same way chloride is displaced from **[Ru]-7**. Finally, experiments were performed concerning the stability of the phenyl heterocycle ligand during catalysis. For this, the NMR reaction was carried out under use of **[Ru]-10** as catalyst to investigate species involving this ligand by ^{19}F NMR. Here again, a species fitting to the corresponding carboxylate complex and the starting material were observed. Besides this, only small traces of other fluorine-containing species were detected, indicating that the applied cyclometalated ligands in fact remain bound to the complex during catalysis.

2.3 Conclusions

In conclusion, cyclometalated aryl heterocycles can be used as a tunable mimic of carbonyl and hydride ligands in popular ruthenium pincer complexes. Following this concept, a series of novel potent catalysts for (de)hydrogenations have been obtained. The general advantage of such catalysts compared to the parent complex is demonstrated for the *green* α -alkylation of ketones with alcohols. Plausible reaction intermediates were investigated for this, all still involving the intact phenyl heterocycle and the pincer ligand. This catalyst design can be used as a guideline for the creation of a variety of other pincer complexes, too; thus, opening the door for more effective catalysis.

2.4 Experimental section

2.4.1 General procedure for the synthesis of cyclometalated ruthenium complexes [Ru(C^N)(*p*-cym)Cl]

According to literature procedures¹⁴, [Ru(*p*-cym)Cl₂]₂ (1.0 mmol), the aryl-substituted heterocycle (2.0 mmol) and KOAc (4.0 mmol) were dissolved in 50 ml of methanol and the resulting suspension stirred at room temperature for 4 days. Evaporation of the solvent provided the crude product as an orange solid which was purified either by column chromatography or washing with a suitable solvent mixture to remove impurities.

[Ru(2-phenyl pyridine)(*p*-cym)Cl]¹⁴: Following the general procedure, the reaction of [Ru(*p*-cym)Cl₂]₂ with 2-phenyl pyridine provided [Ru(2-phenyl pyridine)(*p*-cym)Cl] as an orange solid. The crude product was washed with a solution of heptane/ethyl acetate (1:1, 3 x 10 ml). The remaining solid was then dissolved in CH₂Cl₂ and the resulting solution filtered to remove insoluble impurities. After evaporation of the solvent, the pure product was obtained as an orange solid (742.4 mg, 87%).

[Ru(1-phenyl pyrazole)(*p*-cym)Cl]¹⁴: Following the general procedure, the reaction of [Ru(*p*-cym)Cl₂]₂ with 1-phenyl pyrazole provided [Ru(1-phenyl pyrazole)(*p*-cym)Cl] as a yellowish orange solid. The crude product was washed with a solution of heptane/ethyl acetate (1:1, 3 x 10 ml). The remaining solid was then dissolved in CH₂Cl₂ and the resulting solution filtered to remove insoluble impurities. After evaporation of the solvent, the pure product was obtained as a yellowish orange solid (556.6 mg, 67%).

[Ru(benzo[h]quinone)(*p*-cym)Cl]¹⁴: Following the general procedure, the reaction of [Ru(*p*-cym)Cl₂]₂ with benzo[h]quinone provided [Ru(benzo[h]quinone)(*p*-cym)Cl] as a dark green solid. The crude product was purified by column chromatography under an argon atmosphere using heptane/ethyl acetate (1:1) with 1% NEt₃ as eluent (738.9 mg, 82%).

[Ru(2-phenyl-2-oxazoline)(*p*-cym)Cl]¹⁴: Following the general procedure, the reaction of [Ru(*p*-cym)Cl₂]₂ with 2-phenyl-2-oxazoline provided [Ru(2-phenyl-2-oxazoline)(*p*-cym)Cl] as an orange solid. The crude product was purified by column chromatography under an argon atmosphere using heptane/ethyl acetate (1:1) with 1% NEt₃ as eluent (412.2 mg, 49%).

[Ru(2-(4-trifluoromethyl phenyl) pyridine)(*p*-cym)Cl]¹⁴: Following the general procedure, the reaction of [Ru(*p*-cym)Cl₂]₂ with 2-(4-trifluoromethyl phenyl) pyridine provided [Ru(2-(4-trifluoromethyl phenyl) pyridine)(*p*-cym)Cl] as an orange solid. The crude product was washed

with MeOH (3 x 5 ml). The remaining solid was then dissolved in CH₂Cl₂ and the resulting solution filtered to remove insoluble impurities. After evaporation of the solvent, the pure product was obtained as an orange solid (731.2 mg, 74%).

*[Ru(2-(4-methoxy phenyl) pyridine)(p-cym)Cl]*¹⁴: Following the general procedure, the reaction of [Ru(*p*-cym)Cl₂]₂ with 2-(4-methoxy phenyl) pyridine provided [Ru(2-(4-methoxy phenyl) pyridine)(*p*-cym)Cl] as an orange solid. The crude product was washed with MeOH (3 x 5 ml). The remaining solid was then dissolved in CH₂Cl₂ and the resulting solution filtered to remove insoluble impurities. After evaporation of the solvent, the pure product was obtained as an orange solid (612.1 mg, 67%).

2.4.2 Experimental procedure for the synthesis of cyclometalated ruthenium PNP complexes [Ru(CN)(PNP)Cl]

[Ru(CN)(*p*-cym)Cl] (0.4 mmol) and HN(CH₂CH₂PR₂)₂ (0.42 mmol) were suspended in 10 ml of 2-butanol. NEt₃ (0.8 mmol) was added and the suspension was heated under reflux for 18 h during which the product precipitates out of the reaction mixture as a brightly colored solid. After cooling down, the solvent was decanted via syringe and the remaining solid was washed with *i*PrOH (3 x 5 ml) and dried in high vacuum.

[Ru(2-phenyl pyridine)(HN(CH₂CH₂PPh₂)₂)Cl] (**[Ru]-5**): Following the general procedure, the reaction of [Ru(2-phenyl pyridine)(*p*-cym)Cl] with HCl·HN(CH₂CH₂PPh₂)₂ provided [Ru(2-phenyl pyridine)(HN(CH₂CH₂PPh₂)₂)Cl] as an orange solid (228.4 mg, 78%). Crystals suitable for X-ray crystal structure analysis were obtained by slow vapor diffusion of pentane into a saturated solution of the product in chloroform at 6 °C. The solid-state analysis shows that the crystals are of the ClC-trans, ClH-cis isomer.

[Ru(1-phenyl pyrazole)(HN(CH₂CH₂PPh₂)₂)Cl] (**[Ru]-6**): Following the general procedure, the reaction of [Ru(1-phenyl pyrazole)(*p*-cym)Cl] with HCl·HN(CH₂CH₂PPh₂)₂ provided [Ru(1-phenyl pyrazole)(HN(CH₂CH₂PPh₂)₂)Cl] as a yellow solid (173.6 mg, 60%).

[Ru(benzo[h]quinone)(HN(CH₂CH₂PPh₂)₂)Cl] (**[Ru]-7**): Following the general procedure, the reaction of [Ru(benzo[h]quinone)(*p*-cym)Cl] with HCl·HN(CH₂CH₂PPh₂)₂ provided [Ru(benzo[h]quinone)(HN(CH₂CH₂PPh₂)₂)Cl] as a ruby solid (222.9 mg, 74%). Crystals suitable for X-ray crystal structure analysis were obtained by slow vapor diffusion of pentane into a

saturated solution of the product in chloroform at 6 °C. The solid-state analysis shows that the crystals are of the ClC-trans, ClH-cis isomer.

[Ru(2-phenyl-2-oxazoline)(HN(CH₂CH₂PPh₂)₂)Cl] (**[Ru]-8**): Following the general procedure, the reaction of [Ru(2-phenyl-2-oxazoline)(*p*-cym)Cl] with HCl·HN(CH₂CH₂PPh₂)₂ provided [Ru(2-phenyl-2-oxazoline)(HN(CH₂CH₂PPh₂)₂)Cl] as an orange solid (132.9 mg, 46%).

[Ru(2-phenyl pyridine)(HN(CH₂CH₂PiPr₂)₂)Cl] (**[Ru]-9**): Following the general procedure, the reaction of [Ru(2-phenyl pyridine)(*p*-cym)Cl] with HN(CH₂CH₂PiPr₂)₂ (added as commercially available solution in THF; NEt₃ not necessary in this case) provided [Ru(2-phenyl pyridine)(HN(CH₂CH₂PiPr₂)₂)Cl] as a reddish orange solid (120.4 mg, 50%).

[Ru(2-(4-trifluoromethyl phenyl) pyridine)(HN(CH₂CH₂PPh₂)₂)Cl] (**[Ru]-10**): Following the general procedure, the reaction of [Ru(2-(4-trifluoromethyl phenyl)pyridine)(*p*-cym)Cl] with HCl·HN(CH₂CH₂PPh₂)₂ provided [Ru(2-(4-trifluoromethylphenyl) pyridine)(HN(CH₂CH₂PPh₂)₂)Cl] as a red solid (207.2 mg, 65%).

[Ru(2-(4-methoxy phenyl) pyridine)(HN(CH₂CH₂PPh₂)₂)Cl] (**[Ru]-11**): Following the general procedure, the reaction of [Ru(2-(4-methoxy phenyl) pyridine)(*p*-cym)Cl] with HCl·HN(CH₂CH₂PPh₂)₂ provided [Ru(2-(4-methoxy phenyl) pyridine)(HN(CH₂CH₂PPh₂)₂)Cl] as an orange solid (223.5 mg, 73%).

*[Ru(benzo[*h*]quinone)(MeN(CH₂CH₂PPh₂)₂)Cl]* (**[Ru]-12**): Following the general procedure, the reaction of [Ru(benzo[*h*]quinone)(*p*-cym)Cl] with HCl·MeN(CH₂CH₂PPh₂)₂ provided [Ru(benzo[*h*]quinone)(HN(CH₂CH₂PPh₂)₂)Cl] as a ruby solid (81.2 mg, 26%).

2.4.3 Experimental procedure for the ruthenium-catalyzed α -alkylation of ketones with alcohols

In a glass pressure tube (25 mL) under an argon atmosphere, ruthenium complex (7.3 mg, 0.01 mmol), Cs₂CO₃ (32.6 mg, 0.1 mmol), ketone (1.0 mmol), and alcohol (1.2 mmol) were dissolved in *tert*-amyl alcohol (1 mL). The resulting mixture was stirred at 150 °C in an aluminium block for 22 hours. After cooling down to room temperature, the crude was directly purified by flash chromatography on silica gel to afford, after concentration and high-vacuum drying, the

relative products in the reported yields: 4-methoxy-1-phenylbutan-1-one (**3aa**)¹⁵ was obtained as brownish oil (123.0 mg, 68%); 4-methoxy-1-phenylhexan-1-one (**3ab**)¹⁶ was obtained as purple oil (140.1 mg, 68%); 4-(methyl(phenyl)amino)-1-phenylbutan-1-one (**3ac**) was obtained as light brown oil (95.0 mg, 38%); 1-phenylhexan-1-one (**3ad**)¹⁷ was obtained as colorless oil (103.0 mg, 58%); 3-cyclohexyl-1-phenylpropan-1-one (**3ae**)¹⁸ was obtained as white solid (183.2 mg, 85%); 1,3-diphenylpropan-1-one (**3af**)¹⁸ was obtained as white solid (114.3 mg; 54%); 3-(4-methoxyphenyl)-1-phenylpropan-1-one (**3ag**)¹⁸ was obtained as reddish solid (232.2, 97%); 1-phenyl-3-(4-(trifluoromethyl)phenyl)propan-1-one (**3ah**)¹⁸ was obtained as beige solid (243.7 mg; 88%); 3-(naphthalen-1-yl)-1-phenylpropan-1-one (**3ai**)¹⁸ was obtained as colorless oil (249.7 mg, 97%); 1-phenyl-3-(thiophen-2-yl)propan-1-one (**3aj**)¹⁹ was obtained as dark purple oil (133.5 mg; 62%); 1-phenyl-3-(pyridin-3-yl)propan-1-one (**3ak**)²⁰ was obtained as greyish solid (146.2 mg; 69%); 4-methoxy-1-(4-methoxyphenyl)butan-1-one (**3ba**)²¹ was obtained as white solid (107.9, 52%); 1-(4-chlorophenyl)-4-methoxybutan-1-one (**3ca**) was obtained as white solid (99.3 mg, 47%); 4-methoxy-1-(o-tolyl)butan-1-one (**3da**) was obtained as yellow oil (73.4 mg, 38%); 4-methoxy-1-(naphthalen-2-yl)butan-1-one (**3ea**) was obtained as violet oil (129.5 mg, 57%); 4-methoxy-1-(thiophen-2-yl)butan-1-one (**3fa**) was obtained as brown oil (119.2 mg, 65%); 4-methoxy-1-(pyridin-3-yl)butan-1-one (**3ga**)²² was obtained as yellow oil (20.4 mg, 11%); 2-(2-methoxyethyl)-3,4-dihydronaphthalen-1(2H)-one (**3ha**) was obtained as yellow oil (181.6 mg; 89%); 2-(2-methoxyethyl)-2,3-dihydro-1H-inden-1-one (**3ia**) was obtained as yellow oil (162.3 mg; 85%); 6-methoxy-2-(2-methoxyethyl)-3,4-dihydronaphthalen-1(2H)-one (**3ja**) obtained as brownish oil (189.1 mg; 81%); 6-chloro-2-(2-methoxyethyl)-3,4-dihydronaphthalen-1(2H)-one (**3ka**) obtained as brown oil (193.7 mg; 81%);

2.4.4 Procedure for the ruthenium-catalyzed α -alkylation of ketones with amines

In a glass pressure tube (25 mL) under an argon atmosphere, ruthenium complex [**Ru**]-**7** (7.3 mg, 0.01 mmol), Cs₂CO₃ (32.6 mg, 0.1 mmol), ketone (1.0 mmol), and amine (2.0 mmol) were dissolved in *tert*-amyl alcohol (1 mL). The resulting mixture was stirred at 150 °C in an aluminium block for 22 hours. After cooling down to room temperature, the crude was analyzed by GC using hexadecane as internal standard.

2.4.5 Procedure for the ruthenium-catalyzed lactone formation

In a glass pressure tube (25 mL) under an argon atmosphere, the ruthenium complex **[Ru]-7** (7.3 mg, 0.01 mmol), Cs₂CO₃ (32.6 mg, 0.1 mmol), and 1,2-benzenedimethanol (1.0 mmol) were dissolved in *tert*-amyl alcohol (1 mL). The resulting mixture was stirred at 150 °C in an aluminium block for 22 hours. After cooling down to room temperature, the crude was directly purified by flash chromatography on silica gel to afford, after concentration and high-vacuum drying, the corresponding product isobenzofuran-1(3H)-one (**6**)²³ was obtained as a white solid (120.5 mg, 90%).

2.4.6 Experiments for Mechanistic Investigations

I. Reaction to generate Ru-H complexes (I)

To a stirred solution of **[Ru]-7** (21.0 mg, 0.027 mmol) in 2 ml of THF-d₈, KHBet₃ (30 µl of a 1 M solution in THF, 0.030 mmol, 1.08 eq) was added. The resulting red solution was heated to 60 °C for 2 h, causing a slight darkening of the solution. After cooling to room temperature, 1 ml of the solution was taken, filtered and transferred into an NMR tube and, immediately, ¹H and ³¹P was recorded. ¹H NMR (400 MHz, THF) δ = -12.74 (t, *J*=23.0, minor hydride complex), -12.58 (t, *J*=22.7, major hydride complex) ppm. ³¹P NMR (162 MHz, THF) δ = 35.9 (s, 54%, starting material), 55.1 (s, 16%, major hydride complex), 55.5 (s, 9%, minor hydride complex), {33.9 (d, *J*=11.4), 44.3 (d, *J*=11.4), 13%}, 36.9 (s, 5%); 41.9 (s, 2%), 39.1 (s, 1%) ppm.

Herein, two hydride species can be detected, having very similar chemical shifts, while generally, the formation of hydride complexes from the starting complex **[Ru]-7** could have resulted in four different species assuming that the pincer ligand remains equatorially coordinated. To the remaining solution, 2-benzylideneacetophenone (14.4 mg, 0.69 mmol, 5 eq with respect to the amount of catalyst in the remaining solution) dissolved in 0.5 ml of THF-d₈ was added. After stirring for 5 min at room temperature, 1 ml of the solution was taken, filtered and transferred into an NMR tube and, immediately, ¹H and ³¹P NMR spectra were recorded. The remaining solution was filtered and investigated by GC-MS. ¹H NMR (300 MHz, THF) δ = 2.97 – 3.02 (m, 2H), 3.26 – 3.34 (m, 2H) ppm.

^{31}P NMR (122 MHz, THF) δ = ^{31}P NMR (162 MHz, THF) δ = 35.9 (s, 61%, starting material), 55.5 (s, 8%, minor hydride complex), {33.9 (d, $J=11.4$), 44.3 (d, $J=11.4$), 16%}, 42.1 (s, 5%), 36.9 (s, 4%), 39.3 (s, 2%), 39.1 (s, 2%), 36.0 (s, 2%) ppm.

Following the addition, the signal of the major hydride at -12.58 ppm had disappeared and the listed ^1H NMR signals fit to 3-phenylpropiophenone, as would be the product of the hydrogenation of 2-benzylideneacetophenone. Additionally, the formation of 3-phenylpropiophenone was confirmed by GC-MS.

II. NMR reaction

In a Schlenk flask (5 mL) under an argon atmosphere, ruthenium complex **[Ru]-7** (14.0 mg, 0.02 mmol), Cs_2CO_3 (18.2 mg, 0.05 mmol), acetophenone (58 μl , 0.5 mmol), and 2-methoxyethanol (67 μl , 0.6 mmol) were dissolved in THF-d_8 (1 mL). Next the suspension was transferred into a pressure resistant NMR tube via syringe. Subsequently, the mixture was heated to 150 $^\circ\text{C}$ in an oil bath for 2 hours. After cooling down to room temperature, ^{31}P NMR spectrum was recorded immediately. ^{31}P NMR (122 MHz, THF) δ = 39.0 (s, 74%), 35.8 (s, 24%, starting material), 40.7 (s, 1%), 43.0 (s, 1%) ppm.

To confirm, that the alkylation of acetophenone took place, after recording NMR, the reaction solution was analyzed by GC using hexadecane as internal standard. Here, 18.9 mg (22%) of 4-methoxy-1-phenylbutan-1-one were detected.

III. NMR reaction using benzyl alcohol

In a Schlenk flask (5 mL) under an argon atmosphere, ruthenium complex **[Ru]-7** (14.0 mg, 0.02 mmol), Cs_2CO_3 (18.2 mg, 0.05 mmol), acetophenone (58 μl , 0.5 mmol), and benzyl alcohol (62 μl , 0.6 mmol) were dissolved in THF-d_8 (1 mL). Next the suspension was transferred into a pressure resistant NMR tube via syringe. Subsequently, the mixture was heated to 150 $^\circ\text{C}$ in an oil bath for 2 hours. After cooling down to room temperature, a ^{31}P NMR spectrum was recorded immediately. ^{31}P NMR (122 MHz, THF) δ = ^{31}P NMR (122 MHz, THF) δ = 39.5 (major product), 35.8 (starting material), 38.4, 39.2, 41.2, 46.4, 48.8, 51.6, 51.8, 57.0, 57.3 ppm.

To confirm, that the alkylation of acetophenone took place, after recording NMR, the reaction solution was analyzed by GC using hexadecane as internal standard. Here, 27.4 mg (26%) of 3-phenylpropiophenone were detected.

IV. NMR reaction without addition of ketone

In a Schlenk flask (5 mL) under an argon atmosphere, ruthenium complex **[Ru]-7** (14.0 mg, 0.02 mmol), Cs₂CO₃ (18.2 mg, 0.05 mmol), and 2-methoxyethanol (67 μl, 0.6 mmol) were dissolved in THF-d₈ (1 mL). Next the suspension was transferred into a pressure resistant NMR tube via syringe. Subsequently, the mixture was heated to 150 °C in an oil bath for 2 hours. After cooling down to room temperature, a ³¹P NMR spectrum was recorded immediately.

³¹P NMR (122 MHz, THF) δ = 38.8 (s, 5%), 39.0 (s, 90%), 40.7 (s, 2%), 46.2 (s, 1%), 49.8 (s, 1%), 56.0 (s, 1%) ppm.

V. NMR reaction using [Ru]-10 (V)

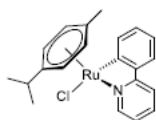
In a Schlenk flask (5 mL) under an argon atmosphere, ruthenium complex **[Ru]-7** (14.0 mg, 0.02 mmol), Cs₂CO₃ (18.2 mg, 0.05 mmol), acetophenone (58 μl, 0.5 mmol), and 2-methoxyethanol (67 μl, 0.6 mmol) were dissolved in THF-d₈ (1 mL). Next the suspension was transferred into a pressure resistant NMR tube via syringe. Subsequently, the mixture was heated to 150 °C in an oil bath for 2 hours. After cooling down to room temperature, ¹⁹F and ³¹P NMR were recorded immediately. ¹⁹F NMR (282 MHz, THF) δ = -63.4 ppm. ³¹P NMR (122 MHz, THF) δ = 38.6 (major signal), 35.4 (starting material), 40.6, 50.0 ppm.

After recording the NMR spectrum, 2-(4-(trifluoromethyl)phenyl)pyridine (3.0 mg, solved in 0.3 ml of THF-d₈) were added to the solution and ¹⁹F NMR was recorded again. ¹⁹F NMR (282 MHz, THF) δ = -63.2 (free ligand), -63.4 ppm.

Here, a new signal appeared for the free ligand, confirming that none of this was detectable in the first NMR spectrum. To confirm, that the alkylation of acetophenone took place, after recording NMR, the reaction solution was analyzed by GC using hexadecane as internal standard. Here, 21.8 mg (24%) of 4-methoxy-1-phenylbutan-1-one were detected.

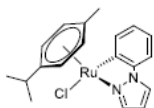
2.5 Characterization Data

2.5.1 Characterization of cyclometalated ruthenium complexes [Ru(C[^]N)(*p*-cym)Cl], cyclometalated ruthenium PNP complexes [Ru(CN)(PNP)Cl] and ketone (**3**)



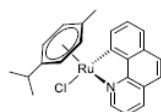
[Ru(2-phenyl pyridine)(p-cym)Cl]: orange solid.

¹H NMR (400 MHz, CDCl₃) δ = 0.88 (d, *J* = 6.9 Hz, 3H), 0.98 (d, *J* = 6.9 Hz, 3H), 2.04 (s, 3H), 2.43 (hept, *J* = 6.9 Hz, 1H), 4.98 (dd, *J* = 5.9, 1.3 Hz, 1H), 5.17 (dd, *J* = 5.9, 1.2 Hz, 1H), 5.57 (ddd, *J* = 10.4, 6.0, 1.2 Hz, 2H), 6.98 – 7.08 (m, 2H), 7.17 (td, *J* = 7.4, 1.4 Hz, 1H), 7.57 – 7.74 (m, 3H), 8.15 (ddd, *J* = 7.5, 1.2, 0.5 Hz, 1H), 9.23 (ddd, *J* = 5.7, 1.6, 0.8 Hz, 1H) ppm. ¹³C NMR (101 MHz, CDCl₃) δ = 18.9 (CH₃), 21.9 (CH₃), 22.7 (CH₃), 30.9 (CH), 82.3 (CH), 84.2 (CH), 89.8 (CH), 90.9 (CH), 100.6 (C), 100.8 (C), 118.9 (CH), 121.5 (CH), 122.6 (CH), 124.0 (CH), 129.6 (CH), 136.7 (CH), 139.7 (CH), 143.4 (C), 154.7 (CH), 165.5 (C), 181.5 (Ru-C) ppm.



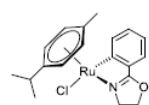
[Ru(1-phenyl pyrazole)(p-cym)Cl]: orange solid.

¹H NMR (400 MHz, CDCl₃) δ = 0.94 (dd, *J* = 14.2, 6.9, 6H), 2.04 (s, 3H), 2.43 (hept, *J* = 6.9, 1H), 5.05 – 5.10 (m, 1H), 5.26 – 5.30 (m, 1H), 5.55 (dd, *J* = 5.8, 1.2, 2H), 6.46 (dd, *J* = 2.8, 2.2, 1H), 6.99 – 7.05 (m, 1H), 7.10 (td, *J* = 7.3, 1.4, 1H), 7.16 (dd, *J* = 7.7, 1.3, 1H), 7.90 (dd, *J* = 2.8, 0.7, 1H), 8.05 (dd, *J* = 2.2, 0.7, 1H), 8.13 (dd, *J* = 7.3, 1.3, 1H) ppm. ¹³C NMR (101 MHz, CDCl₃) δ = 18.9 (CH₃), 22.0 (CH₃), 22.5 (CH₃), 30.8 (CH), 82.3 (CH), 84.2 (CH), 88.2 (CH), 88.7 (CH), 100.1 (C), 100.1 (C), 108.4 (CH), 111.5 (CH), 123.2 (CH), 125.0 (CH), 126.1 (CH), 140.2 (CH), 141.9 (C), 142.2 (CH), 161.9 (Ru-C) ppm.



*[Ru(benzo[*h*]quinone)(p-cym)Cl]*: dark green solid.

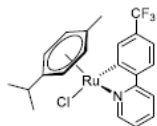
¹H NMR (400 MHz, CD₂Cl₂) δ = 0.80 (d, *J* = 6.9, 3H), 0.93 (d, *J* = 6.9, 3H), 2.00 (s, 3H), 2.44 (hept, *J* = 6.9, 1H), 5.12 (dd, *J* = 5.9, 1.2, 1H), 5.30 (dd, *J* = 5.9, 1.2, 1H), 5.67 (dd, *J* = 5.9, 1.2, 1H), 5.73 (dd, *J* = 5.9, 1.3, 1H), 7.47 (dd, *J* = 8.0, 5.3, 1H), 7.53 – 7.62 (m, 3H), 7.79 (d, *J* = 8.7, 1H), 8.21 (dd, *J* = 8.0, 1.3, 1H), 8.38 (dd, *J* = 6.4, 1.7, 1H), 9.47 (dd, *J* = 5.3, 1.3, 1H) ppm. ¹³C NMR (101 MHz, CD₂Cl₂) δ = 19.0 (CH₃), 21.9 (CH₃), 22.7 (CH₃), 31.3 (CH), 82.6 (CH), 84.0 (CH), 89.7 (CH), 90.3 (CH), 100.3 (C), 101.6 (C), 120.9 (CH), 121.6 (CH), 123.3 (CH), 127.1 (C), 129.3 (CH), 129.7 (CH), 134.1 (C), 135.9 (CH), 136.9 (CH), 140.9 (C), 153.2 (CH), 155.5 (C), 179.3 (Ru-C) ppm.



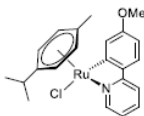
[Ru(2-phenyl-2-oxazoline)(p-cym)Cl]: orange solid.

¹H NMR (400 MHz, CDCl₃) δ = 0.97 (d, *J* = 6.8, 3H), 1.08 (d, *J* = 6.9, 3H), 2.03 (s, 3H), 2.53 (hept, *J* = 6.9, 1H), 4.02 – 4.24 (m, 2H), 4.58 – 4.78 (m, 2H), 4.96 (dd, *J* = 5.8, 1.2, 1H), 5.17 (dd, *J* = 5.9,

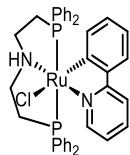
1.2, 1H), 5.43 (dd, $J=5.9, 1.2, 1\text{H}$), 5.53 (dd, $J=5.8, 1.2, 1\text{H}$), 6.96 (td, $J=7.4, 1.1, 1\text{H}$), 7.19 (td, $J=7.4, 1.5, 1\text{H}$), 7.33 (ddd, $J=7.5, 1.5, 0.6, 1\text{H}$), 8.13 (ddd, $J=7.6, 1.1, 0.5, 1\text{H}$) ppm. ^{13}C NMR (101 MHz, CDCl_3) $\delta = 19.0$ (CH_3), 22.1 (CH_3), 22.7 (CH_3), 31.1 (CH), 54.4 (CH_2), 70.7 (CH_2), 80.9 (CH), 81.7 (CH), 87.5 (CH), 88.0 (CH), 99.2 (C), 101.3 (C), 122.3 (CH), 126.4 (CH), 130.6 (CH), 130.8 (C), 139.3 (CH), 174.2 (CH), 182.7 (CH) ppm.



[Ru(2-(4-trifluoromethyl phenyl) pyridine)(p-cym)Cl]: orange solid. ^1H NMR (300 MHz, CDCl_3) $\delta = 0.86$ (d, $J=6.9, 3\text{H}$), 0.97 (d, $J=6.9, 3\text{H}$), 2.06 (s, 3H), 2.41 (hept, $J=6.9, 1\text{H}$), 5.01 (dd, $J=6.0, 1.2, 1\text{H}$), 5.20 (dd, $J=6.0, 1.1, 1\text{H}$), 5.56 – 5.63 (m, 2H), 7.12 (ddd, $J=7.3, 5.7, 1.7, 1\text{H}$), 7.24 (ddd, $J=8.1, 1.8, 0.7, 1\text{H}$), 7.62 – 7.72 (m, 2H), 7.75 (ddd, $J=8.3, 1.7, 0.8, 1\text{H}$), 8.38 (dd, $J=1.8, 0.9, 1\text{H}$), 9.25 (ddd, $J=5.7, 1.5, 0.8, 1\text{H}$) ppm; ^{13}C NMR (75 MHz, CDCl_3) $\delta = 18.9$ (CH), 21.8 (CH_3), 22.6 (CH_3), 31.0 (CH), 82.2 (CH), 84.6 (CH), 89.9 (CH), 91.1 (CH), 101.4 (C), 101.7 (C), 119.6 (q, $J=4.0, \text{CH}$), 119.7 (CH), 122.6 (CH), 123.5 (CH), 130.0 (q, $J=30.3, \text{CCF}_3$), 135.6 (q, $J=3.5, \text{CH}$), 137.1 (CH), 146.7 (q, $J=1.6, \text{C}$), 154.9 (CH), 164.1 (C), 181.4 (Ru-C) ppm, CF_3 not detectable; ^{19}F NMR (282 MHz, CDCl_3) $\delta = -62.0$ ppm.



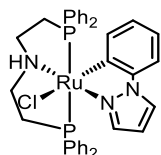
[Ru(2-(4-methoxy phenyl) pyridine)(p-cym)Cl]: orange solid. ^1H NMR (300 MHz, CDCl_3) $\delta = 0.88$ (d, $J=6.9, 3\text{H}$), 0.98 (d, $J=6.9, 3\text{H}$), 2.04 (s, 3H), 2.44 (hept, $J=7.0, 1\text{H}$), 3.90 (s, 3H), 4.97 (dd, $J=6.0, 1.2, 1\text{H}$), 5.17 (dd, $J=6.0, 1.2, 1\text{H}$), 5.50 – 5.59 (m, 2H), 6.58 (dd, $J=8.5, 2.5, 1\text{H}$), 6.95 (ddd, $J=6.2, 5.7, 2.3, 1\text{H}$), 7.52 – 7.63 (m, 3H), 7.70 (d, $J=2.5, 1\text{H}$), 9.10 – 9.19 (m, 1H) ppm; ^{13}C NMR (75 MHz, CDCl_3) $\delta = 18.9$ (CH_3), 21.8 (CH_3), 22.7 (CH_3), 30.9 (CH), 55.3 (CH_3), 82.4 (CH), 84.4 (CH), 89.6 (CH), 90.6 (CH), 100.4 (C), 100.6 (C), 108.8 (CH), 118.2 (CH), 120.4 (CH), 124.0 (CH), 125.0 (CH), 136.5 (CH), 136.7 (C), 154.5 (CH), 159.7 (C), 165.0 (C), 183.4 (C-Ru) ppm.



[Ru(2-phenyl pyridine)(HN(CH₂CH₂PPh₂)₂)Cl] (**[Ru]-5**): orange solid. ^1H NMR (300 MHz, CD_2Cl_2) $\delta = 10.07 - 9.98$ (ddt, $J=5.8, 1.5, 0.8, 1\text{H}$), 7.76 – 7.60 (m, 4H), 7.59 – 7.43 (m, 2H), 7.35 – 7.17 (m, 6H), 7.11 – 6.99 (m, 1H), 6.97 – 6.83 (m, 3H), 6.82 – 6.69 (ddp, $J=7.4, 6.5, 1.0, 5\text{H}$), 6.62 – 6.50 (m, 2H), 6.52 – 6.30 (m, 4H), 6.20 – 6.07 (ddd, $J=7.7, 7.1, 1.2, 0.6, 1\text{H}$), 6.06 – 5.94 (ddd, $J=7.6, 7.0, 1.5, 1\text{H}$), 4.71 – 4.53 (t, $J=12.4, 1\text{H}$), 3.56 – 3.31 (m, 2H), 3.09 – 2.85 (m, 4H), 2.44 – 2.25 (m, 2H) ppm. ^{13}C NMR (75 MHz, CD_2Cl_2) $\delta = 31.0$ (t, $J=11.0, 2 \times \text{CH}_2$), 52.9 (t, $J=3.8, 2 \times \text{CH}_2$), 117.3 (CH), 117.7 (CH), 119.9 (CH), 123.5 (CH), 126.8 (CH), 127.6 (d, $J=3.8, 4 \times \text{CH}$), 127.7 (CH), 128.2 (t, $J=4.6, 4 \times \text{CH}$), 129.6 (2 \times CH), 130.5 (t, $J=5.3, 4 \times \text{CH}$), 133.5 (CH), 134.3 (t, $J=6.2, 4 \times \text{CH}$), 135.6 (C), 135.8 (C), 137.5 (t, $J=17.0, \text{CH}$), 139.3 (CH), 146.3

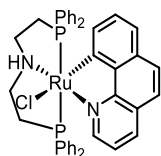
(C), 154.9 (CH), 168.0 (C), 186.9 (C) ppm. ^{31}P NMR (122 MHz, CD_2Cl_2) δ = 35.5 (s, 89%), 36.2 (s, 6%), 38.9 (s, 5%) ppm.

Elemental Anal. calcd. for $\text{C}_{39}\text{H}_{37}\text{ClN}_2\text{P}_2\text{Ru}$: C, 63.97; H, 5.09; N, 3.83; P, 8.46; Ru, 13.80; found: C, 63.97; H, 4.99; N, 3.96; P, 8.27; Ru, 13.97. HRMS (ESI-TOF): m/z : calcd for $[\text{M}-\text{Cl}]^+$: 697.1475, found 697.1473.



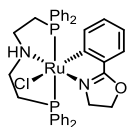
$[\text{Ru}(1\text{-phenyl pyrazole})(\text{HN}(\text{CH}_2\text{CH}_2\text{PPh}_2)_2)\text{Cl}]$ (**[Ru]-6**): yellow solid.

^1H NMR (400 MHz, CD_2Cl_2) Isomer 1 ($\delta^{31}\text{P}$ = 37.60 ppm) δ = 2.19 – 2.40 (m, 2H), 2.83 – 3.04 (m, 3H), 3.12 – 3.23 (m, 2H), 3.68 – 3.86 (m, 1H), 3.95 – 4.09 (m, 1H), 5.20 (dd, J =2.8, 2.2, 1H), 6.16 (dd, J =2.1, 1.1, 1H), 6.56 – 6.59 (m, 3H), 6.80 – 6.90 (m, 3H), 6.90 – 6.97 (m, 3H), 7.00 (dd, J =7.8, 1.4, 1H), 7.14 – 7.17 (m, 1H), 7.19 (dd, J =7.1, 1.4, 1H), 7.26 (dtd, J =6.4, 5.1, 4.3, 1.9, 6H), 7.28 – 7.30 (m, 2H), 7.84 – 7.88 (m, 4H), 8.87 – 8.94 (m, 1H); Isomer 2 ($\delta^{31}\text{P}$ = 37.67 ppm) δ = 2.19 – 2.40 (m, 2H), 2.83 – 3.04 (m, 3H), 3.35 – 3.53 (m, 2H), 3.68 – 3.86 (m, 1H), 4.16 – 4.29 (m, 1H), 5.90 (td, J =7.4, 1.3, 1H), 6.11 (t, J =7.5, 1H), 6.40 – 6.51 (m, 6H), 6.53 – 6.56 (m, 1H), 6.76 (tt, J =7.3, 1.3, 4H), 6.80 – 6.90 (m, 3H), 7.30 – 7.33 (m, 4H), 7.78 – 7.83 (m, 4H), 7.88 – 7.92 (m, 2H), 8.48 (dd, J =2.1, 1.1, 1H) ppm. ^{13}C NMR (101 MHz, CD_2Cl_2) δ = 30.1, 31.0, 52.0, 52.8, 105.9, 106.9, 109.3, 109.8, 117.6, 118.4, 122.5, 122.7, 123.2, 123.5, 127.0, 127.2 (t, J =4.2), 127.4 – 127.6 (m), 127.6 – 127.8 (m), 129.2, 129.4, 129.4 – 129.7 (m), 134.2 (dt, J =9.6, 6.4), 135.1, 135.8, 136.6, 138.7, 139.4, 141.3 (d, J =2.1), 141.7, 143.9 ppm, ipso-C and C-Ru not detectable. ^{31}P NMR (162 MHz, CD_2Cl_2) δ = 37.60 (s, 46%), 37.67 (s, 54%) ppm. Elemental Anal. calcd. for $\text{C}_{37}\text{H}_{36}\text{ClN}_3\text{P}_2\text{Ru}$: C, 61.62; H, 5.03; N, 5.83; P, 8.59; Ru, 14.01; found: C, 61.51; H, 5.21; N, 5.99; P, 8.31; Ru, 14.51. HRMS (ESI-TOF): m/z : calcd for $[\text{M}]^+$: 721.1127, found 721.1133.



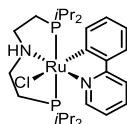
$[\text{Ru}(\text{benzo}[h]\text{quinone})(\text{HN}(\text{CH}_2\text{CH}_2\text{PPh}_2)_2)\text{Cl}]$ (**[Ru]-7**): ruby solid.

^1H NMR (400 MHz, CD_2Cl_2) δ = 2.35 (tdt, J =14.7, 5.7, 2.0, 2H), 2.99 (dq, J =14.0, 4.5, 2H), 3.03 – 3.17 (m, 2H), 3.45 – 3.61 (m, 2H), 4.63 (t, J =12.5, 1H), 5.93 – 6.00 (m, 4H), 6.35 – 6.46 (m, 6H), 6.61 (d, J =7.7, 1H), 6.64 – 6.70 (m, 2H), 6.78 – 6.82 (m, 1H), 7.20 – 7.27 (m, 6H), 7.28 – 7.42 (m, 2H), 7.46 (dd, J =7.9, 5.3, 1H), 7.71 (dtd, J =7.8, 4.7, 1.8, 4H), 7.98 – 8.03 (m, 1H), 10.22 (ddt, J =5.4, 1.5, 0.8, 1H) ppm. ^{13}C NMR (101 MHz, CD_2Cl_2) δ 30.8 (t, J = 10.2 Hz), 53.2 (t, J = 3.8 Hz), 116.0, 119.7, 122.3, 126.8, 127.1 (t, J = 4.3 Hz), 127.4, 128.2 (t, J = 4.7 Hz), 129.3, 129.6 (t, J = 5.4 Hz), 129.6, 132.1, 133.6, 134.4 (t, J = 6.1 Hz), 135.0, 135.2, 136.8, 137.4, 143.3, 153.4 ppm, ipso-C not detectable; ^{31}P NMR (162 MHz, CD_2Cl_2) δ = 35.7 (s, 91%), 36.8 (s, 9%) ppm. Elemental Anal. calcd. for $\text{C}_{41}\text{H}_{37}\text{ClN}_2\text{P}_2\text{Ru}$: C, 65.12; H, 4.93; N, 3.70; P, 8.19; Ru, 13.37; found: C, 65.05; H, 4.84; N, 3.99; P, 7.52; Ru, 12.17. HRMS (ESI-TOF): m/z : calcd for $[\text{M}]^+$: 756.1175, found 756.1193.



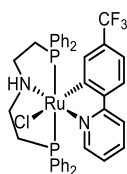
[Ru(2-phenyl-2-oxazoline)(HN(CH₂CH₂PPh₂)₂)Cl] (**[Ru]-8**): orange solid.

¹H NMR (400 MHz, CD₂Cl₂) δ = 1.91 (dd, *J*=9.7, 8.7, 2H), 2.29 (tdt, *J*=14.7, 5.4, 1.8, 2H), 2.71 – 2.86 (m, 2H), 2.97 (dd, *J*=9.6, 8.9, 2H), 3.24 (dq, *J*=13.6, 4.1, 2H), 3.63 – 3.79 (m, 2H), 3.93 – 4.06 (m, 1H, NH), 6.73 – 6.80 (m, 4H), 6.85 – 6.91 (m, 1H), 7.10 – 7.19 (m, 6H), 7.21 – 7.29 (m, 8H), 7.82 – 7.91 (m, 4H), 8.96 (ddd, *J*=7.6, 1.3, 0.7, 1H) ppm. ¹³C NMR (101 MHz, CD₂Cl₂) δ 31.2 (t, *J* = 10.8 Hz), 52.4 (t, *J* = 3.7 Hz), 52.8, 68.2, 118.3, 125.4, 127.9, 128.2 (t, *J* = 4.9 Hz), 128.5 (t, *J* = 4.0 Hz), 128.7, 129.9, 130.1 (t, *J* = 5.4 Hz), 134.5, 134.8 (t, *J* = 6.6 Hz), 136.0 (t, *J* = 18.3 Hz), 136.5 (t, *J* = 15.7 Hz), 141.9 ppm, ipso-C not detectable. ³¹P NMR (162 MHz, CD₂Cl₂) δ 37.2 ppm (s). Elemental Anal. calcd. for C₃₇H₃₇ClN₂OP₂Ru: C, 61.37; H, 5.15; N, 3.87; P, 8.55; Ru, 13.96; found: C:61.36; H, 5.13; N, 3.94; P, 8.29, Ru, 13.06. HRMS (ESI-TOF): *m/z*: calcd for [M]⁺: 724.1113, found 7224.1147.



[Ru(2-phenyl pyridine)(HN(CH₂CH₂PiPr₂)₂)Cl] (**[Ru]-9**): reddish orange solid.

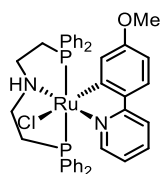
¹H NMR (400 MHz, CD₂Cl₂) δ = 0.16 (q, *J*=7.2, 6H), 0.66 (dt, *J*=7.1, 5.5, 6H), 1.17 (td, *J*=7.1, 5.9, 6H), 1.25 – 1.34 (m, 10H), 2.03 – 2.12 (m, 2H), 2.70 – 2.81 (m, 2H), 2.99 – 3.17 (m, 4H), 3.35 (s, 1H), 6.69 – 6.78 (m, 1H), 6.81 (ddd, *J*=7.3, 5.8, 1.5, 1H), 6.86 (td, *J*=7.3, 1.5, 1H), 7.21 – 7.27 (m, 1H), 7.41 (ddd, *J*=8.1, 7.2, 1.6, 1H), 7.60 (dt, *J*=7.6, 1.4, 2H), 9.86 (ddd, *J*=5.9, 1.7, 0.8, 1H) ppm; ¹³C NMR (101 MHz, CD₂Cl₂) δ = 18.6, 19.3, 19.9, 20.5, 23.8 (t, *J* = 7.4 Hz), 26.6 (t, *J* = 10.0 Hz), 27.2 (t, *J* = 8.4 Hz), 51.9 (t, *J* = 4.0 Hz), 116.6, 117.6, 119.2, 124.2, 127.1, 132.1, 133.9, 137.4, 148.0, 155.6, 168.8 ppm. ³¹P NMR (162 MHz, CD₂Cl₂) δ = 31P NMR (162 MHz, CD₂Cl₂) δ = 42.1 (s, 89%), 40.1 (s, 7%), {44.5 (d, *J*=296.6), 56.1 (d, *J*=296.6), 4%} ppm. Elemental Anal. calcd. for C₂₇H₄₅ClN₂P₂Ru: C, 54.40; H, 7.61; N, 4.70; P, 10.39; Ru, 16.95; found: C, 54.53; H, 7.73; N, 4.67; P, 10.20; Ru, 17.00. HRMS (ESI-TOF): *m/z*: calcd for [M-Cl]⁺: 561.2101, found 561.2112.



[Ru(2-(4-trifluoromethyl phenyl) pyridine)(HN(CH₂CH₂PPh₂)₂)Cl] (**[Ru]-10**): red solid.

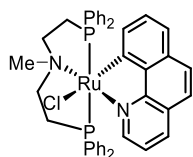
¹H NMR (300 MHz, CD₂Cl₂) major isomer (δ_{31P} = 35.4 ppm): δ = 2.24 – 2.41 (m, 2H), 2.82 – 3.07 (m, 4H), 3.36 – 3.59 (m, 2H), 4.62 – 4.80 (m, 1H), 6.24 – 6.40 (m, 4H), 6.65 – 6.82 (m, 5H), 6.87 (ddd, *J*=7.5, 5.9, 2.3, 4H), 7.14 (tdd, *J*=8.8, 6.6, 1.8, 1H), 7.20 – 7.34 (m, 5H), 7.45 – 7.63 (m, 3H), 7.75 (ddt, *J*=9.6, 7.4, 3.3, 4H), 10.05 – 10.28 (m, 1H) ppm; minor isomer (δ_{31P} = 36.9 ppm): δ = 2.40 – 2.54 (m, 2H), 2.82 – 3.07 (m, 2H), 3.06 – 3.24 (m, 2H), 3.67 (t, *J*=15.8, 2H), 4.35 – 4.50 (m, 1H), 5.77 (ddd, *J*=7.4, 5.7, 1.5, 1H), 6.35 – 6.48 (m, 4H), 6.65 – 6.82 (m, 6H), 6.87 (ddd, *J*=7.5, 5.9, 2.3, 4H), 6.99 – 7.09 (m, 1H), 7.20 – 7.34 (m, 6H), 7.81 (dd, *J*=5.2, 2.6, 4H), 9.36 (s, 1H) ppm. ¹³C NMR (75 MHz, CD₂Cl₂): Assignment of ¹³C shifts was not possible due to isomers, poor solubility, and ¹⁹F-¹³C coupling. ³¹P NMR (122 MHz, CD₂Cl₂) δ = 35.4 (s, 58%), 36.9 (s, 41%), 39.1 (s, 1%) ppm. ¹⁹F NMR (282 MHz, CD₂Cl₂) δ = -63.2 (s, 62%), -62.0 (s, 37%), -62.6 (s, 1%) ppm. Elemental Anal. calcd. for C₄₀H₃₆ClF₃N₂P₂Ru: C, 60.04; H, 4.53; N, 3.50;

P, 7.74; Ru, 12.63; found: C, 60.04; H, 4.09; N, 3.70; P, 7.41; Ru, 11.64. HRMS (ESI-TOF): m/z : calcd for $[M]^{1+}$: 800.1038, found 800.1046.



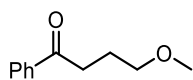
$[Ru(2-(4-methoxy phenyl) pyridine)(HN(CH_2CH_2PPh_2)_2)Cl]$ (**[Ru]-11**): orange solid.

1H NMR (300 MHz, CD_2Cl_2) δ = 2.22 – 2.42 (m, 2H), 2.83 – 3.03 (m, 4H), 3.37 (s, 3H), 3.33 – 3.55 (m, 2H), 4.65 (t, $J=12.2$, 1H), 5.68 (dd, $J=8.5$, 2.4, 1H), 5.94 – 6.02 (m, 1H), 6.39 – 6.50 (m, 4H), 6.79 (ddt, $J=8.3$, 7.1, 1.0, 4H), 6.84 (d, $J=8.5$, 1H), 6.88 – 6.95 (m, 2H), 6.99 (ddd, $J=7.2$, 5.8, 1.5, 1H), 7.20 – 7.33 (m, 6H), 7.33 – 7.39 (m, 1H), 7.44 – 7.53 (m, 1H), 7.71 (dtd, $J=7.7$, 4.8, 1.8, 4H), 9.98 (ddd, $J=5.7$, 1.5, 0.7, 1H) ppm; ^{13}C NMR (75 MHz, CD_2Cl_2) δ 31.0, 53.0 (t, $J = 3.8$ Hz), 105.2, 113.3 – 115.7 (m), 116.5, 118.9, 123.0, 124.6, 127.6 (t, $J = 4.4$ Hz), 127.6, 128.2 (t, $J = 4.7$ Hz), 129.7, 130.4 (t, $J = 5.2$ Hz), 133.5, 134.4 (t, $J = 6.2$ Hz), 135.6, 137.3 (t, $J = 17.0$ Hz), 139.7, 154.7, 158.0, 167.5 ppm; ^{31}P NMR (122 MHz, CD_2Cl_2) δ = 35.2 ppm (s). Elemental Anal. calcd. for $C_{40}H_{39}ClN_2OP_2Ru$: C, 63.03; H, 5.16; N, 3.68; P, 8.13; Ru, 13.26; found: C, 63.11; H, 4.96; N, 3.86; P, 7.61; Ru, 12.43. HRMS (ESI-TOF): m/z : calcd for $[M-Cl-2H]^+$: 725.1425, found 725.1433.



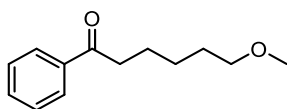
$[Ru(benzo[h]quinone)(MeN(CH_2CH_2PPh_2)_2)Cl]$ (**[Ru]-12**): ruby solid.

1H NMR (400 MHz, CD_2Cl_2) ($\delta^{31}P = 37.5$ ppm) δ = 2.56 – 2.72 (m, 2H), 2.86 – 2.91 (m, 2H), 2.99 (s, 3H), 3.04 – 3.10 (m, 2H), 4.18 – 4.31 (m, 2H), 6.22 (ddt, $J=8.0$, 4.8, 2.3, 4H), 6.58 (t, $J=7.6$, 8H), 6.83 (d, $J=7.4$, 2H), 7.10 (d, $J=7.6$, 1H), 7.27 (dd, $J=5.3$, 2.2, 8H), 7.43 – 7.52 (m, 2H), 7.59 (d, $J=8.7$, 1H), 7.96 (dd, $J=7.8$, 1.3, 1H), 9.45 – 9.59 (m, 1H) ppm. ^{13}C NMR (75 MHz, CD_2Cl_2): Assignment of ^{13}C shifts was not possible due to isomers, poor solubility, and ^{31}P - ^{13}C coupling. ^{31}P NMR (162 MHz, CD_2Cl_2) δ = 34.4 (s, 50%), 37.5 (s, 50%) ppm. Elemental Anal. calcd. for $C_{42}H_{39}ClN_2P_2Ru$: C, 65.49; H, 5.10; N, 3.64; Cl, 4.60; P, 8.04; Ru, 13.12; found: C, 65.79; H, 4.23; N, 3.50; Cl, 4.88; P, 7.98; Ru, 13.13. HRMS (ESI-TOF): m/z : calcd for $[M-Cl]^+$: 735.1642, found 735.1632.



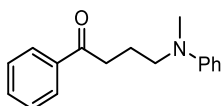
4-methoxy-1-phenylbutan-1-one (**3aa**): brownish oil.

1H NMR (400 MHz, $CDCl_3$) δ = 2.02 (tt, $J=7.2$, 6.1, 2H), 3.07 (t, $J=7.2$, 2H), 3.33 (s, 3H), 3.46 (t, $J=6.1$, 2H), 7.42 – 7.48 (m, 2H), 7.52 – 7.57 (m, 1H), 7.94 – 8.00 (m, 2H); ^{13}C NMR (101 MHz, $CDCl_3$) δ = 24.3 (CH_2), 35.2 (CH_2), 58.6 (CH_3), 71.9 (CH_2), 128.1 (2 x CH), 128.7 (2 x CH), 133.1 (CH), 137.1 (CH), 200.1 (C=O); GCMS (EI): m/z (%): 77 (45), 78 (11), 105 (100), 120 (98), 178 (2) $[M]^+$; HRMS(ESI-TOF): m/z : calcd for $C_{11}H_{14}O_2$: 178.09883 $[M+H]^+$; found: 178.09873.



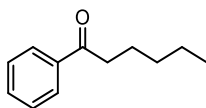
4-methoxy-1-phenylhexan-1-one (3ab): purple oil.

^1H NMR (300 MHz, CDCl_3) δ = 1.38 – 1.51 (m, 2H), 1.57 – 1.68 (m, 2H), 1.71 – 1.82 (m, 2H), 2.91 – 3.03 (m, 2H), 3.32 (s, 3H), 3.38 (t, $J=6.5$, 2H), 7.41 – 7.49 (m, 2H), 7.51 – 7.58 (m, 1H), 7.92 – 7.98 (m, 2H) ppm; ^{13}C NMR (75 MHz, CDCl_3) δ = 24.3 (CH_2), 26.1 (CH_2), 29.6 (CH_2), 38.6 (CH_2), 58.7 (CH_3), 72.7 (CH_2), 128.2 (2 x CH), 128.7 (2 x CH), 133.0 (CH), 137.2 (CH), 200.4 (C=O) ppm; GCMS (EI): m/z (%): 77 (34), 105 (100), 120 (72), 174 (10); HRMS (ESI-TOF): m/z : calcd for $\text{C}_{13}\text{H}_{18}\text{O}_2$: 206.13013 [M] $^+$; found: 206.13063.



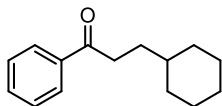
4-(methyl(phenyl)amino)-1-phenylbutan-1-one (3ac): brown oil.

^1H NMR (300 MHz, CDCl_3) δ = 2.27 – 2.40 (m, 2H), 3.23 (s, 3H), 3.30 (t, $J=7.0$, 2H), 3.67 – 3.75 (m, 2H), 6.98 (tt, $J=7.3$, 1.0, 1H), 7.01 – 7.07 (m, 2H), 7.47 – 7.56 (m, 2H), 7.70 – 7.78 (m, 2H), 7.81 – 7.88 (m, 1H), 8.20 – 8.26 (m, 2H) ppm; ^{13}C NMR (75 MHz, CDCl_3) δ = 21.5 (CH_2), 35.7 (CH_2), 38.4 (CH_3), 52.1 (CH_2), 112.4 (2 x CH), 116.3 (CH), 128.1 (2 x CH), 128.7 (2 x CH), 129.3 (2 x CH), 133.1 (CH), 137.0 (C), 149.5 (C), 199.8 (C=O) ppm; GCMS (EI): m/z (%): 219 (2), 220 (2), 253 (100) [M] $^+$, 254 (19); HRMS (ESITOF): m/z : calcd for $\text{C}_{17}\text{H}_{19}\text{NO}$: 254.1539 [$\text{M}+\text{H}$] $^+$; found: 254.1548.



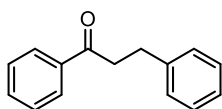
1-phenylhexan-1-one (3ad): colorless oil.

^1H NMR (300 MHz, CDCl_3) δ = 0.87 – 0.95 (m, 3H), 1.29 – 1.45 (m, 4H), 1.67 – 1.81 (m, 2H), 2.91 – 3.00 (m, 2H), 7.41 – 7.49 (m, 2H), 7.51 – 7.58 (m, 1H), 7.93 – 7.99 (m, 2H) ppm; ^{13}C NMR (75 MHz, CDCl_3) δ = 14.1 (CH_3), 22.7 (CH_2), 24.2 (CH_2), 31.7 (CH_2), 38.7 (CH_2), 128.2 (2 x CH), 128.7 (2x CH), 133.0 (CH), 137.2 (C), 200.7 (C=O) ppm; GCMS (EI): m/z (%): 77 (33), 105 (100), 106 (8), 120 (68), 133 (7), 176 (9) [M] $^+$; HRMS (ESI-TOF): m/z : calcd for $\text{C}_{12}\text{H}_{16}\text{O}$: 176.11957 [M] $^+$; found: 176.11963.



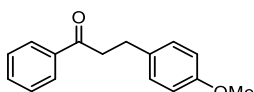
3-cyclohexyl-1-phenylpropan-1-one (3ae): white solid.

^1H NMR (300 MHz, CDCl_3) δ = 0.85 – 1.03 (m, 2H), 1.07 – 1.40 (m, 4H), 1.58 – 1.82 (m, 7H), 2.91 – 3.03 (m, 2H), 7.41 – 7.49 (m, 2H), 7.50 – 7.58 (m, 1H), 7.90 – 8.00 (m, 2H) ppm; ^{13}C NMR (75 MHz, CDCl_3) δ = 26.4 (2 x CH_2), 26.7 (CH_2), 31.9 (CH_2), 33.3 (2 x CH_2), 36.3 (CH_2), 37.6 (CH), 128.2 (2 x CH), 128.7 (2 x CH), 132.9 (CH), 137.2 (C), 201.0 (C=O) ppm; GCMS (EI): m/z (%): 77 (22), 78 (5), 105 (69), 106 (5), 120 (100), 121 (17), 133 (20), 216 (6) [M] $^+$; HRMS (ESI-TOF): m/z : calcd for $\text{C}_{15}\text{H}_{20}\text{O}$: 216.15087 [M] $^+$; found: 216.15081.



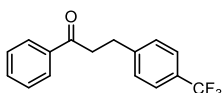
1,3-diphenylpropan-1-one (3af): white solid.

^1H NMR (400 MHz, CDCl_3) δ = 3.11 (dd, J =8.5, 6.9, 2H), 3.30 – 3.37 (m, 2H), 7.21 – 7.27 (m, 1H), 7.27 – 7.36 (m, 4H), 7.45 – 7.52 (m, 2H), 7.56 – 7.62 (m, 1H), 7.97 – 8.02 (m, 2H) ppm; ^{13}C NMR (101 MHz, CDCl_3) δ = 30.3 (CH_2), 40.6 (CH_2), 126.3 (CH), 128.2 (2 x CH), 128.6 (2 x CH), 128.7 (2 x CH), 128.7 (2 x CH), 133.2 (CH), 137.0 (C), 141.4 (C), 199.3 (C=O) ppm; GCMS (EI): m/z (%): 77 (30), 105 (100), 210 (68) $[\text{M}]^+$, 211 (11); HRMS (ESI-TOF): m/z : calcd for $\text{C}_{15}\text{H}_{14}\text{O}$: 210.10392 $[\text{M}]^+$; found: 210.10340.



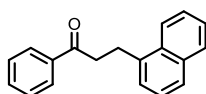
3-(4-methoxyphenyl)-1-phenylpropan-1-one (3ag): reddish solid.

^1H NMR (400 MHz, CDCl_3) δ = 3.02 (dd, J =8.4, 6.9, 2H), 3.24 – 3.31 (m, 2H), 3.79 (s, 3H), 6.82 – 6.88 (m, 2H), 7.15 – 7.20 (m, 2H), 7.43 – 7.49 (m, 2H), 7.53 – 7.59 (m, 1H), 7.94 – 7.98 (m, 2H) ppm; ^{13}C NMR (101 MHz, CDCl_3) δ = 29.4 (CH_2), 40.8 (CH_2), 55.4 (CH_3), 114.0 (2 x CH), 128.2 (2 x CH), 128.7 (2 x CH), 129.5 (2 x CH), 133.1 (CH), 133.4 (C), 137.0 (C), 158.1 (C), 199.5 (C=O) ppm; GCMS (EI): m/z (%): 207 (2), 209 (3), 224 (3), 239 (3), 240 (100) $[\text{M}]^+$, 241 (17), 242 (2); HRMS (ESI-TOF): m/z : calcd for $\text{C}_{16}\text{H}_{16}\text{O}_2$: 240.11448 $[\text{M}]^+$; found: 240.11440.



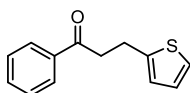
1-phenyl-3-(4-(trifluoromethyl)phenyl)propan-1-one (3ah): beige solid.

^1H NMR (300 MHz, CDCl_3) δ = 3.14 (t, J =7.4, 2H), 3.33 (ddd, J =7.9, 7.0, 0.9, 2H), 7.37 (ddt, J =8.0, 1.4, 0.8, 2H), 7.42 – 7.50 (m, 2H), 7.52 – 7.61 (m, 3H), 7.93 – 7.96 (m, 1H), 7.93 – 8.06 (m, 1H); ^{13}C NMR (101 MHz, CDCl_3) δ = 29.8 (CH_2), 39.9 (CH_2), 124.4 (q, J =271.8, CCF_3), 125.5 (q, J =3.8, 2 x CH), 128.1 (2x CH), 128.7 (2 x CH), 128.9 (2 x CH), 133.3 (CH), 136.7 (C), 145.6 (C), 198.6 (C=O) ppm, CF_3 not detectable; ^{19}F NMR (282 MHz, CDCl_3) δ = -62.4; GCMS (EI): m/z (%): 77 (26), 105 (100), 259 (11), 278 (87) $[\text{M}]^+$, 279 (15); HRMS (ESI-TOF): m/z : calcd for $\text{C}_{16}\text{H}_{13}\text{OF}_3$: 278.09130 $[\text{M}]^+$; found: 278.09134.



3-(naphthalen-1-yl)-1-phenylpropan-1-one (3ai): colorless oil.

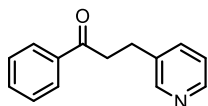
^1H NMR (300 MHz, CDCl_3) δ = 3.40 – 3.48 (m, 2H), 3.51 – 3.61 (m, 2H), 7.40 – 7.49 (m, 4H), 7.49 – 7.59 (m, 3H), 7.72 – 7.79 (m, 1H), 7.86 – 7.91 (m, 1H), 7.94 – 8.00 (m, 2H), 8.04 – 8.10 (m, 1H) ppm; ^{13}C NMR (75 MHz, CDCl_3) δ = 27.3 (CH_2), 39.9 (CH_2), 123.6 (CH), 125.7 (CH), 125.8 (CH), 126.2 (CH), 126.3 (CH), 127.1 (CH), 128.2 (2 x CH), 128.7 (2 x CH), 129.1 (CH), 131.8 (C), 133.2 (CH), 134.1 (C), 136.9 (C), 137.5 (C), 199.4 (C=O) ppm; GCMS (EI): m/z (%): 152 (10), 153 (16), 154 (15), 155 (44), 260 (100) $[\text{M}]^+$, 261 (21); HRMS (ESI-TOF): m/z : calcd for $\text{C}_{19}\text{H}_{16}\text{O}$: 260.11957 $[\text{M}]^+$; found: 260.11941.



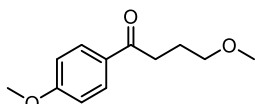
1-phenyl-3-(thiophen-2-yl)propan-1-one (3aj): dark purple oil.

^1H NMR (300 MHz, CDCl_3) δ = 3.27 – 3.34 (m, 2H), 3.34 – 3.41 (m, 2H), 6.87 (dq, J =3.5, 1.0, 1H),

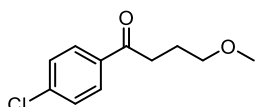
6.93 (dd, $J=5.1, 3.4, 1\text{H}$), 7.13 (dd, $J=5.1, 1.2, 1\text{H}$), 7.43 – 7.51 (m, 2H), 7.53 – 7.61 (m, 1H), 7.95 – 7.98 (m, 1H), 7.98 – 8.01 (m, 1H) ppm; ^{13}C NMR (75 MHz, CDCl_3) $\delta = 24.3$ (CH_2), 40.7 (CH_2), 123.5 (CH), 124.8 (CH), 127.0 (CH), 128.1 (2 x CH), 128.7 (2 x CH), 133.3 (CH), 136.9 (C), 144.0 (C), 198.7 (C=O) ppm; GCMS (EI): m/z (%): 77 (40), 97 (43), 105 (83), 110 (11), 111 (50), 216 (100) $[\text{M}]^+$, 217 (15); HRMS (ESITOF): m/z : calcd for $\text{C}_{13}\text{H}_{12}\text{OS}$: 216.06034 $[\text{M}]^+$; found: 216.06026.



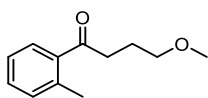
1-phenyl-3-(pyridin-3-yl)propan-1-one (**3ak**): greyish solid. ^1H NMR (300 MHz, CDCl_3) $\delta = 3.07$ (dd, $J=8.0, 6.9, 2\text{H}$), 3.31 (ddd, $J=7.8, 7.1, 0.7, 2\text{H}$), 7.20 (ddd, $J=7.8, 4.8, 0.9, 1\text{H}$), 7.39 – 7.49 (m, 2H), 7.51 – 7.61 (m, 2H), 7.90 – 7.98 (m, 2H), 8.45 (dd, $J=4.8, 1.7, 1\text{H}$), 8.52 (dt, $J=2.2, 0.7, 1\text{H}$) ppm; ^{13}C NMR (75 MHz, CDCl_3) $\delta = 27.2$ (CH_2), 39.9 (CH_2), 123.5 (CH), 128.1 (2 x CH), 128.8 (2 x CH), 133.4 (CH), 136.1 (CH), 136.7 (C), 136.7 (C), 147.8 (CH), 150.1 (CH), 198.5 (C=O) ppm; GCMS (EI): m/z (%): 182 (79), 183 (14), 193 (7), 194 (7), 196 (6), 210(26), 211 (100) $[\text{M}]^+$, 212 (16); HRMS (ESI-TOF): m/z : calcd for $\text{C}_{14}\text{H}_{13}\text{NO}$: 211.09917 $[\text{M}]^+$; found: 211.09852.



4-methoxy-1-(4-methoxyphenyl)butan-1-one (**3ba**): white solid. ^1H NMR (300 MHz, CDCl_3) $\delta = 2.0$ (ddt, $J=7.6, 7.0, 6.1, 2\text{H}$), 3.0 (dd, $J=7.5, 7.0, 2\text{H}$), 3.3 (s, 3H), 3.5 (t, $J=6.1, 2\text{H}$), 3.9 (s, 3H), 6.9 – 7.0 (m, 2H), 7.9 – 8.0 (m, 2H) ppm; ^{13}C NMR (75 MHz, CDCl_3) $\delta = 24.5$ (CH_2), 34.8 (CH_2), 55.6 (CH_3), 58.7 (CH_3), 72.0 (CH_2), 113.8 (2 x CH), 130.3 (C), 130.4 (2 x CH), 163.5 (C), 198.7 (C=O) ppm; GCMS (EI): m/z (%): 77 (12), 92 (9), 107 (8), 135 (96), 136 (9), 150 (100), 151 (10), 208 (1) $[\text{M}]^+$; HRMS (ESI-TOF): m/z : calcd for $\text{C}_{12}\text{H}_{16}\text{O}_3$: 208.10940 $[\text{M}]^+$; found: 208.10930.

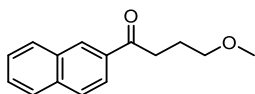


1-(4-chlorophenyl)-4-methoxybutan-1-one (**3ca**): white solid. ^1H NMR (300 MHz, CDCl_3) $\delta = 1.95$ – 2.06 (m, 2H), 3.04 (dd, $J=7.4, 6.9, 2\text{H}$), 3.33 (s, 3H), 3.46 (t, $J=6.0, 2\text{H}$), 7.40 – 7.47 (m, 2H), 7.88 – 7.94 (m, 2H) ppm; ^{13}C NMR (75 MHz, CDCl_3) $\delta = 24.2$ (CH_2), 35.2 (CH_2), 58.7 (CH_3), 71.8 (CH_2), 129.0 (2 x CH), 129.6 (2 x CH), 135.5 (C), 139.5 (C), 198.9 (C=O) ppm; GCMS (EI): m/z (%): 75 (10), 111 (29), 139 (95), 141 (31), 154 (100), 156 (34), 212 (1) $[\text{M}]^+$; HRMS (ESI-TOF): m/z : calcd for $\text{C}_{11}\text{H}_{13}\text{O}_2\text{Cl}$: 214.05691 $[\text{M}]^+$; found: 214.05692.



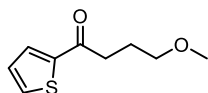
4-methoxy-1-(o-tolyl)butan-1-one (**3da**): yellow oil. ^1H NMR (300 MHz, CDCl_3) $\delta = 2.01$ (tt, $J=7.1, 6.1, 2\text{H}$), 2.48 – 2.53 (m, 3H), 3.00 (t, $J=7.2, 2\text{H}$), 3.34 (s, 3H), 3.47 (t, $J=6.1, 2\text{H}$), 7.22 – 7.30 (m, 2H), 7.34 – 7.40 (m, 1H), 7.64 – 7.69 (m, 1H) ppm; ^{13}C NMR (75 MHz, CDCl_3) $\delta = 21.3$ (CH_3), 24.4 (CH_2), 38.2 (CH_2), 58.6 (CH_3), 71.9 (CH_2), 125.7 (CH), 128.5 (CH), 131.2 (CH), 132.0 (CH), 138.0 (C), 138.3 (C), 204.2 (C=O) ppm; GCMS

(EI): m/z (%): 65 (7), 91 (33), 119 (100), 120 (9), 134 (31), 192 (5) $[M]^+$; HRMS (ESI-TOF): m/z : calcd for $C_{12}H_{16}O_2$: 192.11448 $[M]^+$; found: 192.11443.



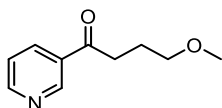
4-methoxy-1-(naphthalen-2-yl)butan-1-one (3ea): violet oil.

1H NMR (300 MHz, $CDCl_3$) δ = 2.09 (tt, $J=7.0, 6.0, 2H$), 3.21 (t, $J=7.2, 2H$), 3.36 (s, 2H), 3.51 (t, $J=6.1, 2H$), 7.50 – 7.63 (m, 2H), 7.83 – 7.92 (m, 2H), 7.93 – 7.99 (m, 1H), 8.05 (dd, $J=8.6, 1.8, 1H$), 8.48 – 8.52 (m, 1H) ppm; ^{13}C NMR (75 MHz, $CDCl_3$) δ = 24.4 (CH_2), 35.3 (CH_2), 58.7 (CH_3), 71.9 (CH_2), 124.0 (CH), 126.8 (CH), 127.9 (CH), 128.5 (CH), 128.5 (CH), 129.7 (CH), 129.8 (CH), 132.7 (C), 134.5 (C), 135.7 (C), 200.0 (C=O) ppm; GCMS (EI): m/z (%): 155 (58), 170 (100), 171 (13), 228 (7) $[M]^+$; HRMS (ESI-TOF): m/z : calcd for $C_{15}H_{16}O_2$: 228.11448 $[M]^+$; found: 228.11450.



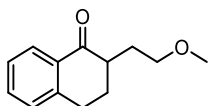
4-methoxy-1-(thiophen-2-yl)butan-1-one (3fa): brown oil.

1H NMR (400 MHz, $CDCl_3$) δ = 2.00 (dddd, $J=7.6, 7.0, 6.3, 5.7, 2H$), 2.99 (ddd, $J=7.5, 7.0, 0.6, 2H$), 3.31 (d, $J=0.6, 111, 3H$), 3.44 (td, $J=6.1, 0.6, 2H$), 7.09 – 7.13 (m, 1H), 7.61 (ddd, $J=5.0, 1.2, 0.6, 1H$), 7.72 (ddd, $J=3.8, 1.2, 0.6, 1H$) ppm; ^{13}C NMR (101 MHz, $CDCl_3$) δ = 24.5 (CH_2), 35.9 (CH_2), 58.6 (CH_3), 71.7 (CH_2), 128.1 (CH), 131.9 (CH), 133.5 (CH), 144.5 (C), 193.0 (C=O) ppm; GCMS (EI): m/z (%): 83 (5), 84 (4), (67), 112 (4), 126 (100), 127 (8), 128 (5), 184 (2) $[M]^+$; HRMS (ESI-TOF): m/z : calcd for $C_9H_{12}O_2S$: 184.05525 $[M]^+$; found: 184.05485.



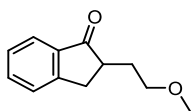
4-methoxy-1-(pyridin-3-yl)butan-1-one (3ga): yellow oil.

1H NMR (300 MHz, $CDCl_3$) δ = 1.94 – 2.09 (m, 2H), 3.07 (t, $J=7.1, 2H$), 3.31 (s, 3H), 3.45 (t, $J=6.0, 2H$), 7.39 (ddd, $J=8.0, 4.8, 0.9, 1H$), 8.22 (ddd, $J=8.0, 2.3, 1.8, 1H$), 8.75 (dd, $J=4.8, 1.7, 1H$), 9.16 (dd, $J=2.3, 0.9, 1H$) ppm; ^{13}C NMR (75 MHz, $CDCl_3$) δ = 24.0 (CH_2), 35.5 (CH_2), 58.7 (CH_3), 71.6 (CH_2), 123.7 (CH), 132.3 (C), 135.4 (CH), 149.7 (CH), 153.5 (CH), 198.9 (C=O) ppm; GCMS (EI): m/z (%): 51 (12), 78 (44), 106 (93), 121 (100), 122 (13), 135 (16), 179 (1) $[M]^+$; HRMS (ESI-TOF): m/z : calcd for $C_{10}H_{13}NO_2$: 180.1019 $[M+H]^+$; found: 180.1024.

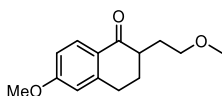


2-(2-methoxyethyl)-3,4-dihydronaphthalen-1(2H)-one (3ha): yellow oil.

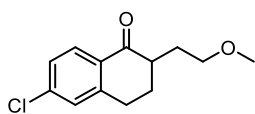
1H NMR (300 MHz, $CDCl_3$) δ = 1.67 (dq, $J=14.2, 6.4, 1H$), 1.89 (dddd, $J=13.3, 11.8, 9.9, 5.7, 1H$), 2.19 – 2.39 (m, 2H), 2.64 (dddd, $J=11.8, 6.7, 6.0, 4.4, 1H$), 2.92 – 3.11 (m, 2H), 3.34 (s, 3H), 3.55 (td, $J=6.4, 0.8, 2H$), 7.22 (ddq, $J=7.6, 1.4, 0.7, 1H$), 7.22 – 7.34 (m, 1H), 7.44 (td, $J=7.5, 1.5, 1H$), 7.98 – 8.04 (m, 1H) ppm; ^{13}C NMR (75 MHz, $CDCl_3$) δ = 28.9 (CH_2), 29.1 (CH_2), 29.8 (CH_2), 44.8 (CH), 58.6 (CH_3), 70.7 (CH_2), 126.6 (CH), 127.5 (CH), 128.8 (CH), 132.6 (C), 133.2 (CH), 144.0 (C), 200.2 (C=O) ppm; GCMS (EI): m/z (%): 131 (21), 145 (21), 146 (100), 147 (10), 204 (1) $[M]^+$; HRMS (ESI-TOF): m/z : calcd for $C_{13}H_{16}O_2$: 204.11448 $[M]^+$; found: 204.11348.



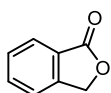
2-(2-methoxyethyl)-2,3-dihydro-1H-inden-1-one (3ia): yellow oil. ^1H NMR (300 MHz, CDCl_3) δ = 1.71 (ddt, $J=14.0, 9.1, 6.2, 1\text{H}$), 2.25 (dtd, $J=14.0, 6.6, 4.8, 1\text{H}$), 2.71 – 2.82 (m, 1H), 2.82 – 2.92 (m, 1H), 3.30 – 3.42 (m, 1H), 3.33 (s, 3H), 3.49 – 3.63 (m, 2H), 7.32 – 7.39 (m, 1H), 7.41 – 7.47 (m, 1H), 7.57 (ddd, $J=7.8, 7.2, 1.2, 1\text{H}$), 7.71 – 7.77 (m, 1H) ppm; ^{13}C NMR (75 MHz, CDCl_3) δ = 31.3 (CH_2), 33.2 (CH_2), 44.9 (CH), 58.7 (CH_3), 70.9 (CH_2), 124.0 (CH), 126.6 (CH), 127.4 (CH), 134.8 (CH), 136.7 (C), 153.7 (C), 208.7 (C=O) ppm; GCMS (EI): m/z (%): 115 (14), 131 (18), 132 (100), 133 (10), 145 (15), 190 (2) [M] $^+$; HRMS (ESI-TOF): m/z : calcd for $\text{C}_{12}\text{H}_{14}\text{O}_2$: 190.09883 [M] $^+$; found: 190.09841.



6-methoxy-2-(2-methoxyethyl)-3,4-dihydronaphthalen-1(2H)-one (3ja): brownish oil. ^1H NMR (300 MHz, CDCl_3) δ = 1.58 – 1.73 (m, 1H), 1.87 (dddd, $J=13.2, 11.5, 9.8, 5.6, 1\text{H}$), 2.17 – 2.37 (m, 2H), 2.58 (dddd, $J=11.4, 6.9, 5.9, 4.4, 1\text{H}$), 2.86 – 3.06 (m, 2H), 3.34 (s, 3H), 3.54 (td, $J=6.5, 0.8, 2\text{H}$), 3.84 (s, 3H), 6.67 (dd, $J=2.5, 1.1, 1\text{H}$), 6.80 (ddt, $J=8.7, 2.6, 0.6, 1\text{H}$), 7.98 (dd, $J=8.8, 0.4, 1\text{H}$) ppm; ^{13}C NMR (75 MHz, CDCl_3) δ = 29.2, 29.2, 29.9, 44.5, 55.5, 58.6, 70.8, 112.5, 113.2, 126.3, 129.9, 146.5, 163.5, 198.9 ppm; GCMS (EI): m/z (%): 161 (18), 175 (22), 176 (100), 177 (12); HRMS (ESI-TOF): m/z : calcd for $\text{C}_{14}\text{H}_{18}\text{O}_3$: 257.1153 [$\text{M}+\text{Na}$] $^+$; found: 257.1156



6-chloro-2-(2-methoxyethyl)-3,4-dihydronaphthalen-1(2H)-one (3ka): brown oil. ^1H NMR (300 MHz, CDCl_3) δ = 1.61 – 1.75 (ddt, $J=14.2, 6.8, 6.2, 1\text{H}$), 1.82 – 1.99 (dddd, $J=13.3, 11.8, 10.1, 5.4, 1\text{H}$), 2.21 – 2.41 (m, 2H), 2.59 – 2.71 (dddd, $J=11.8, 6.8, 5.9, 4.5, 1\text{H}$), 2.95 – 3.04 (m, 2H), 3.32 – 3.37 (s, 3H), 3.51 – 3.60 (m, 2H), 7.22 – 7.30 (m, 2H), 7.93 – 7.99 (dq, $J=8.3, 0.5, 1\text{H}$) ppm; ^{13}C NMR (75 MHz, CDCl_3) δ = 28.7 (CH_2), 28.8 (CH_2), 29.7 (CH_2), 44.6 (CH), 58.6 (CH_3), 70.6 (CH_2), 127.2 (CH), 128.6 (CH), 129.2 (CH), 131.1 (C), 139.5 (C), 145.6 (C), 199.1 (C=O) ppm; GCMS (EI): m/z (%): 152 (8), 165 (8), 179 (14), 180 (100), 181 (15), 182 (32); HRMS (ESI-TOF): m/z : calcd for $\text{C}_{13}\text{H}_{15}\text{O}_2\text{ClNa}$: 261.0658 [$\text{M}+\text{Na}$] $^+$; found: 261.0666.



isobenzofuran-1(3H)-one (6): white solid. ^1H NMR (400 MHz, CDCl_3) δ = 5.32 (s, 3H), 7.47 – 7.57 (m, 2H), 7.69 (td, $J=7.5, 1.1, 1\text{H}$), 7.92 (dt, $J=7.6, 1.0, 1\text{H}$) ppm; ^{13}C NMR (101 MHz, CDCl_3) δ = 69.8 (CH_2), 122.2 (CH), 125.9 (C), 125.9 (CH), 129.2 (CH), 134.1 (CH), 146.6 (C), 171.2 (C=O) ppm; GCMS (EI): m/z (%): 77 (33), 105 (100), 133 (15), 134 (46) [M] $^+$; HRMS (ESI-TOF): m/z : calcd for $\text{C}_8\text{H}_6\text{O}_2$: 134.03623 [M] $^+$; found: 134.03596.

2.6 References

- [1] A. Corma, J. Navas, and M. J. Sabater; *Chem. Rev.*, **2018**, *118*, 1410–1459.
- [2] Q. Yang; Q. Wang; Z. Yu, *Chem. Soc. Rev.* **2015**, *44*, 2305–2329.
- [3] S. Werkmeister, J. Neumann, K. Junge, and M. Beller, *Chem. Eur. J.* **2015**, *21*, 12226 – 12250.
- [4] H.A. Younus, W. Su, N. Ahmad, S. Chen, and F. Verpoort, *Adv. Synth. Catal.*, **2014**
- [5] W. Kuriyama, T. Matsumoto, Y. Ino, O. Ogata (Takasago International Corporation), WO20110487227, **2011**.
- [6] Z. Han, L. Rong, J. Wu, L. Zhang, Z. Wang, K. Ding, *Angew. Chem. Int. Ed.* **2012**, *51*, 13041 – 13045; *Angew. Chem.* **2012**, *124*, 13218 –13222.
- [7] J. Neumann, C. Bornschein, H. Jiao, K. Junge, M. Beller, *Eur. J. Org. Chem.* **2015**, 5944–5948.
- [8] a) M. Nielsen, E. Alberico, W. Baumann, H.-J. Drexler, H. Junge, S. Gladioli, M. Beller, *Nature* **2013**, *495*, 85– 89; b) A. Monney, E. Barsch, P. Sponholz, H. Junge, R. Ludwig, M. Beller, *Chem. Commun.* **2014**, *50*, 707 – 709; c) E. Alberico, A. J. J. Lennox, L. K. Vogt, H. Jiao, W. Baumann, H.-J. Drexler, M. Nielsen, A. Spannenberg, M. P. Checinski, H. Junge, M. Beller, *J. Am. Chem. Soc.* **2016**, *138*, 14890– 14904.
- [9] M. Nielsen, H. Junge, A. Kammer, M. Beller, *Angew. Chem. Int. Ed.* **2012**, *51*, 5711 – 5713; *Angew. Chem.* **2012**, *124*, 5809 –5811.
- [10] a) J. Zhang, M. Gandelman, L. J. W. Shimon, H. Rozenberg, D. Milstein, *Organometallics* **2004**, *23*, 4026 –4033; b) J. Zhang, G. Leitus, Y. Ben- David, D. Milstein, *J. Am. Chem. Soc.* **2005**, *127*, 10840 –10841; c) H. Zeng, Z. Guan, *J. Am. Chem. Soc.* **2011**, *133*, 1159– 1161; d) P. Hu, Y. Diskin-Posner, Y. Ben-David, D. Milstein, *ACS Catal.* **2014**, *4*, 2649 –2652; e) E. Khaskin, M. A. Iron, L. J. W. Shimon, J. Zhang, D. Milstein, *J. Am. Chem. Soc.* **2010**, *132*, 8542 – 8543; f) E. Balaraman, C. Gunanathan, J. Zhang, L. J. W. Shimon, D. Milstein, *Nat. Chem.* **2011**, *3*, 609; g) C. Gunanathan, M. Hçlscher, W. Leitner, *Eur. J. Inorg. Chem.* **2011**, 3381– 3386; h) C. A. Huff, M. S. Sanford, *ACS Catal.* **2013**, *3*, 2412 –2416.
- [11] P. Piehl, R. Amuso, E. Alberico, H. Junge, B. Gabriele, H. Neumann, M. Beller, *Chem. Eur. J.* **2020**, *26*, 6050.
- [12] B. Li, T. Roisnel, C. Darcel, P. H. Dixneuf, *Dalton Trans.* **2012**, *41*, 10934 –10937.
- [13] a) R. Martnez, G. J. Brand, D. J. Ramòn, M. Yus, *Tetrahedron Lett.* **2005**, *46*, 3683– 3686; b) R. Martnez, D. J. Ramòn, M. Yus, *Tetrahedron* **2006**, *62*, 8988 –9001; c) C. Schleppehorst, B. Maji, F. Glorius, *ACS Catal.* **2016**, *6*, 4184 –4188; d) C. Xu, X.-M. Dong, Z.-Q. Wang, X.-Q. Hao, Z. Li, L.-M. Duan, B.-M. Ji, M.-P. Song, *J. Organomet. Chem.* **2012**, *700*, 214–218; e) F. Li, J. Ma, N. Wang, *J. Org. Chem.* **2014**, *79*, 10447 –10455; f) D. Wang, K. Zhao, P. Ma, C. Xu, Y. Ding, *Tetrahedron Lett.* **2014**, *55*, 7233 – 7235; g) S. Elangovan, J.-B. Sortais, M. Beller, C. Darcel, *Angew. Chem. Int. Ed.* **2015**, *54*, 14483 –14486; *Angew. Chem.* **2015**, *127*, 14691 – 14694; h) C. Seck, M. D. Mbaye, S. Coufourier, A. Lator, J. F. Lohier, A. Poater, T. R. Ward, S. Gaillard, J. L. Renaud, *ChemCatChem* **2017**, *9*, 4410 –4416; i) L. Bettoni, C. Seck, M. D. Mbaye, S. Gaillard, J.-L. Renaud, *Org. Lett.* **2019**, *21*, 3057 – 3061; j) M. Peça-Lpez, P. Piehl, S. Elangovan, H. Neumann, M. Beller, *Angew. Chem. Int. Ed.* **2016**, *55*, 14967– 14971; *Angew. Chem.* **2016**, *128*,

- 15191 –15195; k) A. Bruneau-Voisine, L. Pallova, S. Bastin, V. Csar, J.-B. Sortais, *Chem. Commun.* **2019**, *55*, 314–317; l) D. Banerjee, L. M. Kabadwal, J. Das, *Chem. Commun.* **2018**, *54*, 14069 –14072; m) G. Zhang, J. Wu, H. Zeng, S. Zhang, Z. Yin, S. Zheng, *Org. Lett.* **2017**, *19*, 1080 –1083; n) P. Piehl, M. Pena-Lopez, A. Frey, H. Neumann, M. Beller, *Chem. Commun.* **2017**, *53*, 3265 –3268.
- [14] B. Li, T. Roisnel, C. Darcel, P. H. Dixneuf, *Dalton Trans.* **2012**, *41*, 10934-10937.
- [15] J. Barrios-Rivera, Y. Xu, M. Wills, *Org. Lett.* **2019**, *21*, 7223-7227.
- [16] T. Shimada, Y. Yamamoto, *J. Am. Chem. Soc.* **2002**, *124*, 12670-12671.
- [17] F. Li, J. Ma, N. Wang, *J. Org. Chem.* **2014**, *79*, 10447-10455.
- [18] R. Wang, J. Ma, F. Li, *J. Org. Chem.* **2015**, *80*, 10769-10776.
- [19] D. Weickmann, B. Plietker, *ChemCatChem* **2013**, *5*, 2170-2173.
- [20] D. W. Tay, H. Jong, Y. H. Lim, W. Wu, X. Chew, E. G. Robins, C. W. Johannes, *J. Org. Chem.* **2015**, *80*, 4054-4063.
- [21] H. G. Yayla, H. Wang, K. T. Tarantino, H. S. Orbe, R. R. Knowles, *J. Am. Chem. Soc.* **2016**, *138*, 10794-10797.
- [22] T. E. Spratt, L. A. Peterson, W. L. Confer, S. S. Hecht, *Chem. Res. Toxicol.* **1990**, *3*, 350-356.
- [23] A. B. Leduc, T. F. Jamison, *Org. Process Res. Dev.* **2012**, *16*, 1082-1089.

Chapter 3

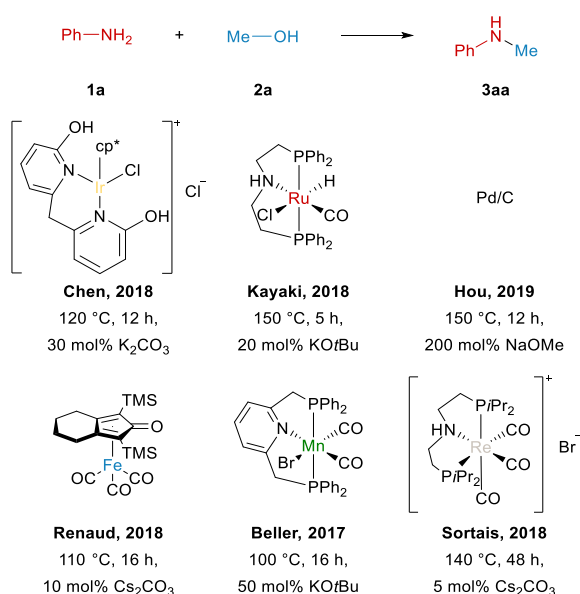
Cyclometalated Ruthenium Complexes as Catalyst for Efficient Alkylation of Anilines with Alcohols

3.1 Introduction

The selective N-alkylation of amines continues to be an important and widely applied chemical transformation in organic synthesis¹⁻³, especially for the synthesis of bio-active compounds, e.g. in the pharmaceutical industry⁴⁻⁶. In this respect, particularly N-methylation of amines is interesting, since this transformation is regularly used to influence the lipophilicity of such compounds, thus making them more biologically accessible^{7,8}. While classical methods for N-alkylation rely mainly on toxic and waste-generating alkylating agents like formaldehyde and alkyl halides, modern hydrogen autotransfer reactions offer an attractive alternative (see introduction 2.1 in the chapter “ α -Alkylation of Ketones with Alcohols by Cyclometalated Ruthenium Pincer Complexes as Catalysts” for Borrowing Hydrogen principle).

In recent years methylation of anilines with methanol was typically achieved at elevated temperatures in the presence of either molecularly-defined complexes or heterogenous materials. Most of the known catalysts are based on noble transition metal complexes, e.g. iridium⁹⁻¹¹ and specifically ruthenium¹²⁻¹⁷. However, more recently, first row transition metals like iron^{18,19} or manganese²⁰⁻²³ and others were developed, too²⁴⁻²⁷.

Notably, most of the currently known catalysts rely on sophisticated ligands and only work above 100 °C in the presence of large amounts of strong bases, which create additional environmental concern (scheme 3.1.1).

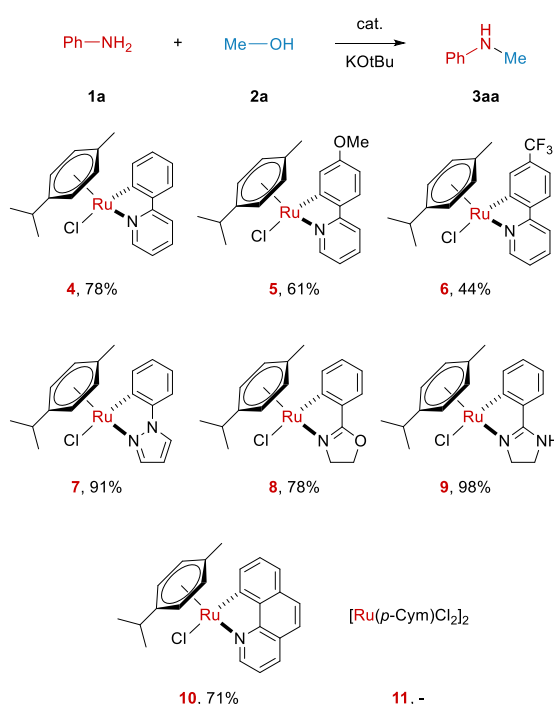


Scheme 3.1.1 Selected catalysts used for the N-methylation of aniline.

Based on the work²⁸ discussed in the chapter 2, from which it was discovered that cyclometalated ligands can have a positive influence on the reactivity of ruthenium pincer complexes, in this work²⁹ we have focused on the further applications of these types of catalysts and I was interested in developing simple cyclometalated ruthenium complexes for the N-methylation of anilines with methanol.

3.2 Results and discussion

First, different cyclometalated ruthenium complexes of the general structure $\text{Ru}(\text{C}^{\wedge}\text{N})(p\text{-cymene})\text{Cl}$ (**4-10** in scheme 3.2.1) were synthesized following modified literature procedures^{30,31}. All these complexes were then tested in the *N*-methylation of aniline as a model system. In order to get an idea on the catalytic potential of these complexes, initial test reactions were carried out at 70 °C with 2 mol% of the respective complex, albeit in the presence of 1 equiv. of KOtBu as strong base (see scheme 3.2.1).



Scheme 3.2.1 *N*-methylation of aniline with Cyclometalated Ru-complexes tested. All reactions were carried out with **1a** (1.0 mmol), Ru catalyst (0.02 mmol), KOtBu (1.0 mmol) in MeOH (1.5 ml) at 70 °C for 22h. Yields determined by GC using hexadecane as internal standard.

Surprisingly, all the investigated Ru complexes were able to deliver the desired product. Notably, the main precursor of these complexes, $[\text{Ru}(p\text{-cymene})\text{Cl}_2]_2$, does not catalyse this reaction. The highest yield herein was gained when using the novel ruthenium complex **9** bearing a phenyl imidazole ligand. The molecular structure of this complex is depicted in figure 3.2.1.

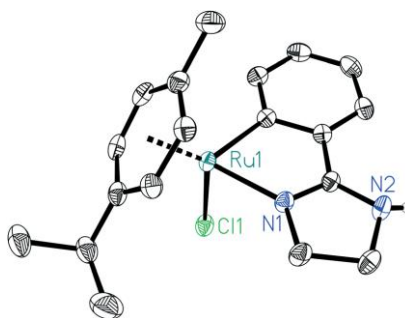


Fig.3.2.1 Molecular structure of ruthenium complex **9**. Displacement ellipsoids correspond to 50% probability. Carbon-bound hydrogen atoms are omitted for clarity.

Next, we tried to perform more systematic variations of critical reaction parameters. Gratifyingly, the base loading could be reduced to only 10 mol% without a significant decrease in reactivity (Table 3.1, entry 2). Furthermore, it was possible to replace the strong base KOtBu with cheaper sodium hydroxide (Table 3.1, entry 5). Interestingly, the reaction turned out to work best in only 0.5 ml of undried methanol (Table 3.1, entry 12). In addition, after defining 60 °C as the optimal reaction temperature, control experiments revealed that no product was formed when the reaction was carried out in the absence of catalyst or base. Interestingly, by scaling up the reaction to 5 mmol, the catalyst loading could be decreased to only 0.4 mmol%, while retaining a high yield of 88% *N*-methylaniline (Table 3.1, entry 17).

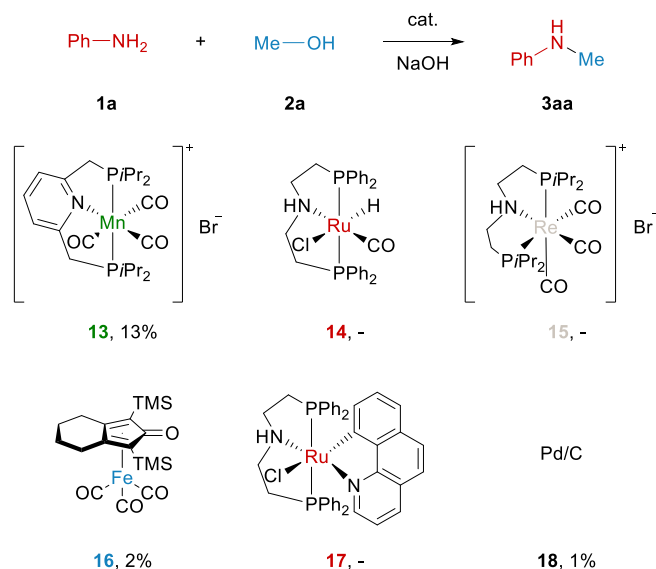
Table 3.1. Ruthenium-catalysed *N*-methylation of aniline with methanol: variation of reaction conditions.

#	catalyst loading [mol%]	base	base loading [mol %]	temp. [°C]	MeOH [ml]	yield ^[a] [%]
1	2	KOtBu	100	70	1.5	98
2	2	KOtBu	10	70	1.5	91
3	2	KOtBu	5	70	1.5	85
4	2	Cs ₂ CO ₃	10	70	1.5	88
5	2	NaOH	10	70	1.5	87
6	2	K ₂ CO ₃	10	70	1.5	84
7	2	NEt ₃	10	70	1.5	-
8	3	NaOH	10	70	1.5	87
9	1	NaOH	10	70	1.5	75
10	2	NaOH	10	70	0.5	88
11	2	NaOH	10	70	2.0	68
12	2	NaOH	10	70	0.5 ^[b]	91

13	2	NaOH	10	60	0.5 ^[b]	96
14	2	NaOH	10	50	0.5 ^[b]	51
15	-	NaOH	10	60	0.5 ^[b]	-
16	2	-	-	60	0.5 ^[b]	-
17^[c]	0.4	NaOH	10	80	2.5 ^[b]	88

Unless otherwise stated, reactions were carried out with **1a** (1.0 mmol), catalyst **9**, base in methanol for 22 h; ^[a] Yields determined by GC using hexadecane as internal standard; ^[b] technical grade methanol was used without drying prior to use; ^[c] reaction was performed in 5 mmol scale.

With optimal reaction conditions (1 mmol aniline **1a**, 0.02 mmol of catalyst **9** and 0.1 mmol of sodium hydroxide in 0.5 ml of methanol at 60 °C for 22 h) in hand, the new reaction system to some state-of-the-art catalysts for this transformation is compared (see Scheme 3.2.2). Surprisingly, only a Mn PNP pincer complex previously developed in the Beller's group³² was able to produce *N*-methylaniline under such mild conditions, while other investigated complexes based on Ru, Pd, Fe or Re gave little or no product at all. This clearly shows that the here presented catalyst works under significantly milder conditions than most other catalysts known for this reaction.



Scheme 3.2.2 Performance of state-of-the-art catalysts under optimised reaction conditions. All reactions were carried out with **1a** (1.0 mmol), catalyst (0.02 mmol), NaOH (0.1 mmol) in MeOH (0.5 ml) at 60 °C for 22 h. Yields determined by GC using hexadecane as internal standard.

Next, to understand this superior performance compared to other known catalysts, we performed several mechanistic experiments. First, we wanted to rule out the possibility of

nanoparticles or heterogeneous materials formed under reaction conditions to be the main active catalyst species. Hence, the reaction was performed in the presence of one drop of mercury, which had no negative impact on the reaction^{33,34}. Because amalgam formation is not necessarily taking place for Ru particles, further control experiments under addition of strongly coordinating ligands were performed. Here, the addition of sub-stoichiometric amounts of triphenylphosphine as well as 1,10-phenanthroline led to slightly decreased yields of 78% or 68%, respectively. The addition of over-stoichiometric amounts of these ligands with respect to the catalyst however resulted in a complete shutdown of its reactivity. Overall, this behaviour is typical for homogenous catalysts, so that nanoparticles or even heterogeneous materials are unlikely to be the active catalysts in this transformation.

Instead, we believe the pre-catalyst becomes activated by the base as shown by an ¹H NMR experiment where only the catalyst and sodium hydroxide are suspended in MeOH-d₄. This immediately led to the formation of a clear orange solution (pre-catalyst **9** is insoluble in methanol), that was investigated via ¹H NMR spectroscopy. Here, the phenyl imidazole ligand as well as η⁶ coordinated *p*-cymene could be detected. The aromatic signals of *p*-cymene were relatively broad which indicated that the complex is dynamic in behaviour likely because the chloride of the precursor was abstracted and replaced by fluctuant solvent molecules. The possibility that phenyl imidazole as well as *p*-cymene remained bound to the metal centre over the whole course of the reaction was additionally supported by other experiments in which 10 mol% of these ligands were added under otherwise optimised reaction conditions. Would any of these ligands be released to form the active catalyst, the additional ligand should have suppressed this reaction by shifting its equilibrium. Instead, for *p*-cymene this did not lead to any decrease in product formation, while the yield only dropped to 79% when phenyl imidazole was added. We assume this slight decrease in product yield likely stems from the phenyl imidazole acting as a weak additional ligand competing for the catalyst's active site. To further investigate the mechanism, the model reaction was carried out with differently deuterated methanol derivatives and we investigated the deuteration pattern of the resulting *N*-methylaniline. While the amount of deuterium at the NH position can easily scramble with solvent molecules during workup, the deuteration pattern at the methyl group is a clear indication for the reaction mechanism. Surprisingly, when methanol with a deuterated methyl group was the starting material, a fully deuterated methyl group was found in the product (>98%), while methanol without deuterium at the methyl group did not produce any

deuteration at the product's methyl group (<1%). Overall, this means that there is no exchange between the hydrogen atoms stemming from methanol's CH₃ group and any other H atoms in the reaction solution. This occurs either if no actual methanol dehydrogenation takes place during the reaction or if the Ru hydride (deuteride) species formed by methanol dehydrogenation only transfers this hydride (deuteride) to the imine's α -carbon and is not able to release it as H₂.

To distinguish between these two possibilities, yield time plots of the reaction with differently deuterated methanol derivatives were recorded. As shown in Fig. 3.2.2, there is a clear reactivity difference between the reactions with CH₃OH and CH₃OD and the ones with CD₃-OH and CD₃-OD. More specifically, a kinetic isotope effect of 1.8 for MeOH-d₃ was found. This indicates that the C-H bond of the methyl group is involved in the rate determining step of the reaction, which likely corresponds to the β -hydride elimination of methanol bound to the catalyst forming a Ru hydride species and formaldehyde.

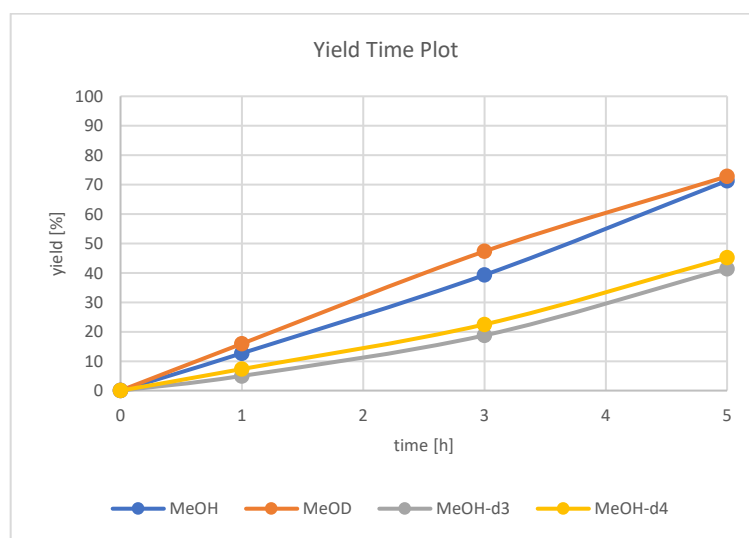
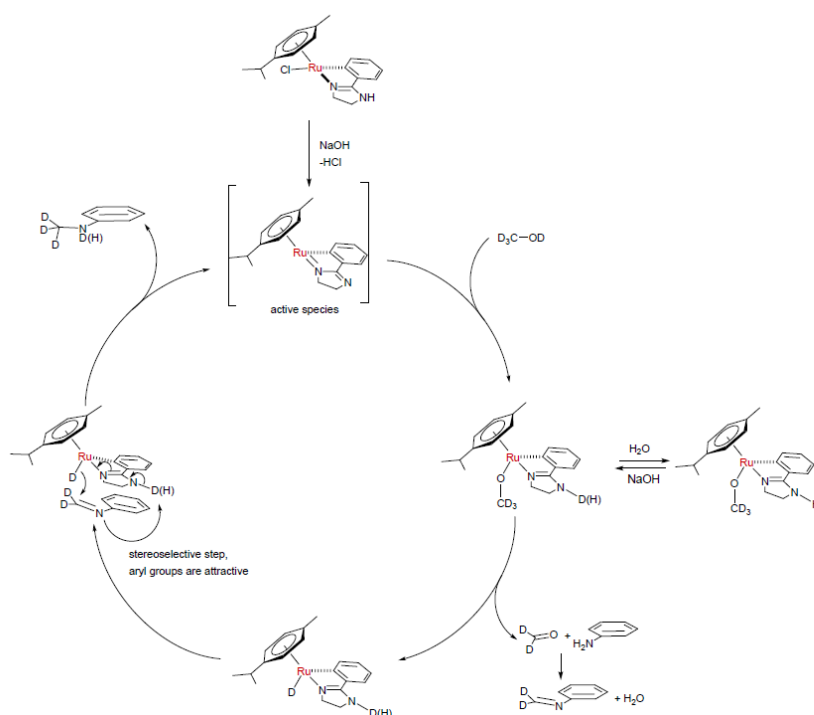


Fig. 3.2.2 Yield time plot of the reaction for differently deuterated methanol derivatives.

On the other hand, for MeOD no significant KIE was found, so the O-H bond does not play a significant role in the rate determining step, ruling out a concerted H₂ transfer from methanol to the catalyst. We believe that the reactivity differences between CH₃OH/CH₃OD as well as CD₃-OH/CD₃-OD are insignificant and can be explained by minor variations in the respective experiments. Besides these findings, the yield time plots show a nearly linear progress without a significant induction period. This again hints towards a homogeneously catalysed reaction

that probably is in a state of catalyst saturation and therefore shows zero-order influence of the substrate aniline.

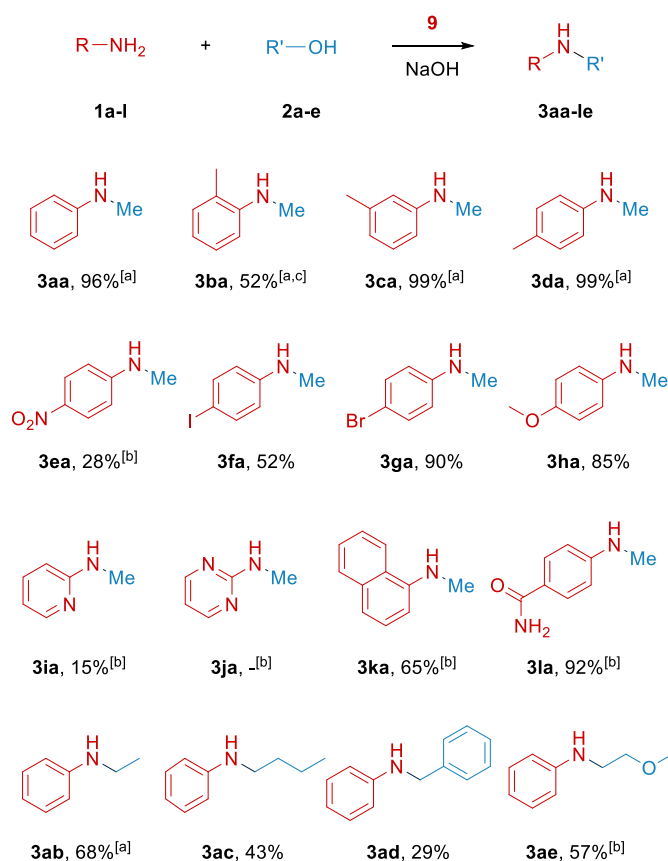
Overall, we explain these surprising results from the reactions with the different forms of deuterated methanol by a mechanistic proposal shown in Scheme 3.2.3. The selective hydrogenation/deuteration of the in situ generated imine can be explained by the attractive interaction of the aryl groups of the cyclometalated ligand and the imine. Notably, H/D-exchange is easily possible on the nitrogen atom of the imidazole ring while this is not possible for the Ru–H/D bond.



Scheme 3.2.3 Mechanistic proposal for a catalytic cycle.

Finally, we explored the substrate scope of the reaction (scheme 3.2.4). First, different toluidines were used. While the methyl group in ortho position caused a lower yield due to steric hindrance even when the temperature is elevated and more NaOH is used (**3ba**), meta- or para-methylation had no negative impact and the corresponding products were formed quantitatively (**3ca**, **3da**). An electron-withdrawing nitro group in aniline's 4-position led to lower 28% yield even with higher temperature and base loading (**3ea**). Interestingly, no significant hydrogenation of the nitro group was observed here. Halide-substituted anilines including 4-iodoaniline (**3fa**) were selectively methylated without significant dehalogenation

side-reactions. Additionally, electron-rich 4-methoxyaniline gave the corresponding product with a high yield or 85% (**3ha**). Furthermore, 2-aminopyridine allowed for methylation, albeit with lower reactivity, while the corresponding 2-amino pyrimidine was not methylated at all (**3ja**). On the other hand, 1-amino naphthalene did not cause many problems, so that the corresponding product was obtained in 65% yield (**3ka**). Interestingly, 4-amidoaniline gave very good 92% of the corresponding product without methylation of the amido-group (**3la**). Unfortunately testing primary aliphatic amines as substrates under analogous conditions revealed only negligible reactivity for methylation. Lastly, other aliphatic and benzylic alcohols were tested as alkylating agents. Without further optimization the corresponding products were formed in yields up to 68% (**3ab–3ae**).



Scheme 3.2.4 Scope of the N-alkylation of anilines with alcohols. Unless otherwise stated, reactions were carried out with **1a-l** (1.0 mmol), catalyst **9** (0.02 mmol) and NaOH (0.1 mmol) in **2a-e** (0.5 ml) at 60 °C for 22 h. Isolated yields. ^[a]Yields determined by GC using hexadecane as internal standard; ^[b] NaOH (0.3 mmol), 80 °C reaction temperature; ^[c] NaOH (0.3 mmol), 100 °C reaction temperature.

3.3 Conclusions

In conclusion, in this work cyclometalated ruthenium complexes have been established as novel catalysts for the methylation of anilines using methanol via a hydrogen autotransfer procedure. The optimal system **9** bearing a phenyl imidazoline as bidentate ligand likely works in a homogenous manner with β -hydride elimination of methanol to form a Ru–H species being the rate determining step. Compared to other known catalysts for this transformation, **9** allows to work under very mild reaction conditions without the necessity of strong/expensive bases.

3.4 Experimental section

3.4.1 General procedure for the synthesis of cyclometalated ruthenium complexes [Ru(C^N)(*p*-cym)Cl]

According to literature procedures³⁵, [Ru(*p*-cym)Cl₂]₂ (1.0 mmol), the aryl-substituted heterocycle (2.0 mmol) and KOAc (4.0 mmol) were dissolved in 50 ml of methanol and the resulting suspension stirred at room temperature for 4 days. Evaporation of the solvent provided the crude product as an orange solid which was purified either by column chromatography or washing with a suitable solvent mixture to remove impurities.

[Ru(2-phenyl pyridine)(*p*-cym)Cl], **4**: Following the general procedure³⁵, the reaction of [Ru(*p*-cym)Cl₂]₂ with 2-phenyl pyridine provided [Ru(2-phenyl pyridine)(*p*-cym)Cl] as an orange solid. The crude product was washed with a solution of heptane/ethyl acetate (1:1, 3 x 10 ml). The remaining solid was then dissolved in CH₂Cl₂ and the resulting solution filtered to remove insoluble impurities. After evaporation of the solvent, the pure product was obtained as an orange solid (742.4 mg, 87%).

[Ru(2-(4-methoxy phenyl) pyridine)(*p*-cym)Cl], **5**: Following the general procedure³⁵, the reaction of [Ru(*p*-cym)Cl₂]₂ with 2-(4-methoxy phenyl) pyridine provided [Ru(2-(4-methoxy phenyl) pyridine)(*p*-cym)Cl] as an orange solid. The crude product was washed with MeOH (3 x 5 ml). The remaining solid was then dissolved in CH₂Cl₂ and the resulting solution filtered to remove insoluble impurities. After evaporation of the solvent, the pure product was obtained as an orange solid (612.1 mg, 67%).

[Ru(2-(4-trifluoromethyl phenyl) pyridine)(*p*-cym)Cl], **6**: Following the general procedure³⁵, the reaction of [Ru(*p*-cym)Cl₂]₂ with 2-(4-trifluoromethyl phenyl) pyridine provided [Ru(2-(4-trifluoromethyl phenyl) pyridine)(*p*-cym)Cl] as an orange solid. The crude product was washed with MeOH (3 x 5 ml). The remaining solid was then dissolved in CH₂Cl₂ and the resulting solution filtered to remove insoluble impurities. After evaporation of the solvent, the pure product was obtained as an orange solid (731.2 mg, 74%).

[Ru(1-phenyl pyrazole)(*p*-cym)Cl], **7**: Following the general procedure³⁵, the reaction of [Ru(*p*-cym)Cl₂]₂ with 1-phenyl pyrazole provided [Ru(1-phenyl pyrazole)(*p*-cym)Cl] as a yellowish

orange solid. The crude product was washed with a solution of heptane/ethyl acetate (1:1, 3 x 10 ml). The remaining solid was then dissolved in CH₂Cl₂ and the resulting solution filtered to remove insoluble impurities. After evaporation of the solvent, the pure product was obtained as a yellowish orange solid (556.6 mg, 67%).

[Ru(2-phenyl-2-oxazoline)(p-cym)Cl], **8**: Following the general procedure³⁵, the reaction of [Ru(*p*-cym)Cl₂]₂ with 2-phenyl-2-oxazoline provided [Ru(2-phenyl-2-oxazoline)(*p*-cym)Cl] as an orange solid. The crude product was purified by column chromatography under an argon atmosphere using heptane/ethyl acetate (1:1) with 1% NEt₃ as eluent (412.2 mg, 49%).

[Ru(2-phenyl imidazoline)(p-cym)Cl], **9**: Following the general procedure³⁵, the reaction of [Ru(*p*-cym)Cl₂]₂ with 2-phenyl imidazoline provided [Ru(2-phenyl imidazoline)(*p*-cym)Cl] as an orange solid. The crude product was washed with MeOH (3 x 5 ml). The remaining solid was then dissolved in CH₂Cl₂ and the resulting solution filtered to remove insoluble impurities. After evaporation of the solvent, the product was obtained as an orange solid (300.3 mg, 72%). Crystals suitable for x-ray crystal structure analysis were obtained by slow evaporation of a solution of **9** in THF.

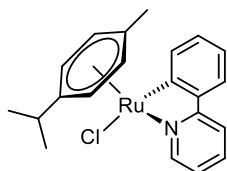
*[Ru(benzo[*h*]quinone)(p-cym)Cl]*, **10**: [1] Following the general procedure³⁵, the reaction of [Ru(*p*-cym)Cl₂]₂ with benzo[*h*]quinone provided [Ru(benzo[*h*]quinone)(*p*-cym)Cl] as a dark green solid. The crude product was purified by column chromatography under an argon atmosphere using heptane/ethyl acetate (1:1) with 1% NEt₃ as eluent (738.9 mg, 82%).

3.4.2 General Procedure for the Ruthenium-catalysed N-Methylation of Anilines

In a glass pressure tube (25 mL) under an argon atmosphere, ruthenium complex **9** (8.3 mg, 0.02 mmol), NaOH (4.0 mg, 0.1 mmol), and the aniline derivative (1.0 mmol) were dissolved in the respective alcohol (0.5 mL). Next, the pressure tube was closed, and the resulting mixture was stirred at 60 °C in an aluminium block for 22 hours. After cooling down to room temperature, the crude was directly purified by flash chromatography on silica gel to afford, after concentration and drying, the corresponding products were obtained in the reported yields.

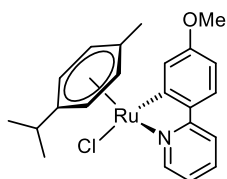
3.5 Characterization Data

3.5.1 Characterization of cyclometalated ruthenium complexes $[\text{Ru}(\text{C}^{\wedge}\text{N})(p\text{-cym})\text{Cl}]$, anilines (**1**) and N-alkylanilines (**3**)



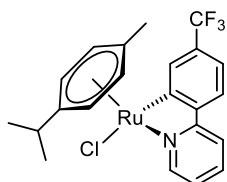
$[\text{Ru}(2\text{-phenyl pyridine})(p\text{-cym})\text{Cl}]$, **4**: orange solid.

^1H NMR (400 MHz, CDCl_3) δ = 0.88 (d, J = 6.9 Hz, 3H), 0.98 (d, J = 6.9 Hz, 3H), 2.04 (s, 3H), 2.43 (hept, J = 6.9 Hz, 1H), 4.98 (dd, J = 5.9, 1.3 Hz, 1H), 5.17 (dd, J = 5.9, 1.2 Hz, 1H), 5.57 (ddd, J = 10.4, 6.0, 1.2 Hz, 2H), 6.98 – 7.08 (m, 2H), 7.17 (td, J = 7.4, 1.4 Hz, 1H), 7.57 – 7.74 (m, 3H), 8.15 (ddd, J = 7.5, 1.2, 0.5 Hz, 1H), 9.23 (ddd, J = 5.7, 1.6, 0.8 Hz, 1H) ppm. ^{13}C NMR (101 MHz, CDCl_3) δ = 18.9 (CH₃), 21.9 (CH₃), 22.7 (CH₃), 30.9 (CH), 82.3 (CH), 84.2 (CH), 89.8 (CH), 90.9 (CH), 100.6 (C), 100.8 (C), 118.9 (CH), 121.5 (CH), 122.6 (CH), 124.0 (CH), 129.6 (CH), 136.7 (CH), 139.7 (CH), 143.4 (C), 154.7 (CH), 165.5 (C), 181.5 (Ru-C) ppm.



$[\text{Ru}(2\text{-}(4\text{-methoxy phenyl})\text{ pyridine})(p\text{-cym})\text{Cl}]$, **5**: orange solid.

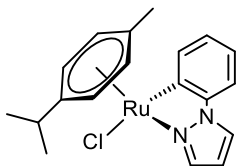
^1H NMR (300 MHz, CDCl_3) δ = 0.88 (d, J = 6.9, 3H), 0.98 (d, J = 6.9, 3H), 2.04 (s, 3H), 2.44 (hept, J = 7.0, 1H), 3.90 (s, 3H), 4.97 (dd, J = 6.0, 1.2, 1H), 5.17 (dd, J = 6.0, 1.2, 1H), 5.50 – 5.59 (m, 2H), 6.58 (dd, J = 8.5, 2.5, 1H), 6.95 (ddd, J = 6.2, 5.7, 2.3, 1H), 7.52 – 7.63 (m, 3H), 7.70 (d, J = 2.5, 1H), 9.10 – 9.19 (m, 1H) ppm; ^{13}C NMR (75 MHz, CDCl_3) δ = 18.9 (CH₃), 21.8 (CH₃), 22.7 (CH₃), 30.9 (CH), 55.3 (CH₃), 82.4 (CH), 84.4 (CH), 89.6 (CH), 90.6 (CH), 100.4 (C), 100.6 (C), 108.8 (CH), 118.2 (CH), 120.4 (CH), 124.0 (CH), 125.0 (CH), 136.5 (CH), 136.7 (C), 154.5 (CH), 159.7 (C), 165.0 (C), 183.4 (C-Ru) ppm.



$[\text{Ru}(2\text{-}(4\text{-trifluoromethyl phenyl})\text{ pyridine})(p\text{-cym})\text{Cl}]$, **6**: orange solid.

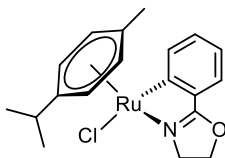
^1H NMR (300 MHz, CDCl_3) δ = 0.86 (d, J = 6.9, 3H), 0.97 (d, J = 6.9, 3H), 2.06 (s, 3H), 2.41 (hept, J = 6.9, 1H), 5.01 (dd, J = 6.0, 1.2, 1H), 5.20 (dd, J = 6.0, 1.1, 1H), 5.56 – 5.63 (m, 2H), 7.12 (ddd, J = 7.3, 5.7, 1.7, 1H), 7.24 (ddd, J = 8.1, 1.8, 0.7, 1H), 7.62 – 7.72 (m, 2H), 7.75 (ddd, J = 8.3, 1.7, 0.8, 1H), 8.38 (dd, J = 1.8, 0.9, 1H), 9.25 (ddd, J = 5.7, 1.5, 0.8, 1H) ppm; ^{13}C NMR (75 MHz, CDCl_3) δ = 18.9 (CH), 21.8 (CH₃), 22.6 (CH₃), 31.0 (CH), 82.2 (CH), 84.6 (CH), 89.9 (CH), 91.1 (CH), 101.4 (C), 101.7 (C), 119.6 (q, J = 4.0, CH), 119.7 (CH), 122.6 (CH), 123.5 (CH), 130.0 (q, J = 30.3, CCF₃),

135.6 (q, $J=3.5$, CH), 137.1 (CH), 146.7 (q, $J=1.6$, C), 154.9 (CH), 164.1 (C), 181.4 (Ru-C) ppm, CF_3 not detectable; ^{19}F NMR (282 MHz, CDCl_3) $\delta = -62.0$ ppm.



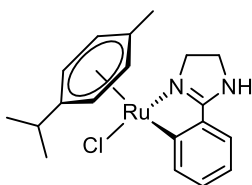
[Ru(1-phenyl pyrazole)(p-cym)Cl], **7**: orange solid.

^1H NMR (400 MHz, CDCl_3) $\delta = 0.94$ (dd, $J=14.2$, 6.9, 6H), 2.04 (s, 3H), 2.43 (hept, $J=6.9$, 1H), 5.05 – 5.10 (m, 1H), 5.26 – 5.30 (m, 1H), 5.55 (dd, $J=5.8$, 1.2, 2H), 6.46 (dd, $J=2.8$, 2.2, 1H), 6.99 – 7.05 (m, 1H), 7.10 (td, $J=7.3$, 1.4, 1H), 7.16 (dd, $J=7.7$, 1.3, 1H), 7.90 (dd, $J=2.8$, 0.7, 1H), 8.05 (dd, $J=2.2$, 0.7, 1H), 8.13 (dd, $J=7.3$, 1.3, 1H) ppm; ^{13}C NMR (101 MHz, CDCl_3) $\delta = 18.9$ (CH_3), 22.0 (CH_3), 22.5 (CH_3), 30.8 (CH), 82.3 (CH), 84.2 (CH), 88.2 (CH), 88.7 (CH), 100.1 (C), 100.1 (C), 108.4 (CH), 111.5 (CH), 123.2 (CH), 125.0 (CH), 126.1 (CH), 140.2 (CH), 141.9 (C), 142.2 (CH), 161.9 (Ru-C) ppm.



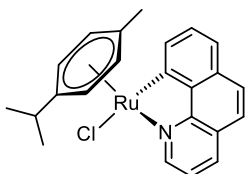
[Ru(2-phenyl-2-oxazoline)(p-cym)Cl], **8**: orange solid.

^1H NMR (400 MHz, CDCl_3) $\delta = 0.97$ (d, $J=6.8$, 3H), 1.08 (d, $J=6.9$, 3H), 2.03 (s, 3H), 2.53 (hept, $J=6.9$, 1H), 4.02 – 4.24 (m, 2H), 4.58 – 4.78 (m, 2H), 4.96 (dd, $J=5.8$, 1.2, 1H), 5.17 (dd, $J=5.9$, 1.2, 1H), 5.43 (dd, $J=5.9$, 1.2, 1H), 5.53 (dd, $J=5.8$, 1.2, 1H), 6.96 (td, $J=7.4$, 1.1, 1H), 7.19 (td, $J=7.4$, 1.5, 1H), 7.33 (ddd, $J=7.5$, 1.5, 0.6, 1H), 8.13 (ddd, $J=7.6$, 1.1, 0.5, 1H) ppm; ^{13}C NMR (101 MHz, CDCl_3) $\delta = 19.0$ (CH_3), 22.1 (CH_3), 22.7 (CH_3), 31.1 (CH), 54.4 (CH_2), 70.7 (CH_2), 80.9 (CH), 81.7 (CH), 87.5 (CH), 88.0 (CH), 99.2 (C), 101.3 (C), 122.3 (CH), 126.4 (CH), 130.6 (CH), 130.8 (C), 139.3 (CH), 174.2 (CH), 182.7 (CH) ppm.



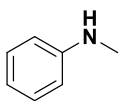
[Ru(2-phenyl imidazoline)(p-cym)Cl], **9**: orange solid.

^1H NMR (300 MHz, CDCl_3) $\delta = 0.95$ (dd, $J=18.4$, 6.9, 6H), 2.00 (s, 3H), 2.29 – 2.47 (m, 2H), 3.26 (dt, $J=10.9$, 9.0, 1H), 3.76 – 3.98 (m, 2H), 4.91 (dd, $J=5.7$, 1.2, 1H), 5.14 (dd, $J=5.9$, 1.2, 1H), 5.37 (dd, $J=5.8$, 1.2, 1H), 5.43 (dd, $J=5.7$, 1.2, 1H), 6.19 (d, $J=2.9$, 1H), 6.93 (td, $J=7.4$, 1.2, 1H), 7.12 (td, $J=7.4$, 1.5, 1H), 7.32 (ddd, $J=7.4$, 1.5, 0.5, 1H), 8.16 (ddd, $J=7.5$, 1.2, 0.5, 1H) ppm; ^{13}C NMR (75 MHz, CDCl_3) $\delta = 19.0$ (CH_3), 22.3 (CH_3), 22.6 (CH_3), 31.1 (CH), 44.3 (CH_2), 56.0 (CH_2), 80.6 (CH), 82.5 (CH), 87.3 (CH), 87.9 (CH), 99.1 (C), 99.3 (C), 121.7 (CH), 125.4 (CH), 129.4 (CH), 135.1 (C), 139.4 (CH), 172.3 (C), 182.6 (C-Ru) ppm; Elemental Anal. calcd. for $\text{C}_{19}\text{H}_{23}\text{ClN}_2\text{Ru}$: C, 54.87; H, 5.57; Cl, 8.52; N, 6.74; Ru, 24.30; found: C, 44.6; H, 4.4; Cl, 15.5; N, 5.2; Ru, 20.1. According to this, the sample contains ca. 82% of compound **9** and 18% of KCl. HRMS (ESI-TOF): m/z : calcd for $[\text{M}-\text{Cl}]^+$: 381.0905, found 381.0901.



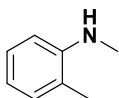
[Ru(benzo[h]quinone)(*p*-cym)Cl], **10**: dark green solid.

^1H NMR (400 MHz, CD_2Cl_2) δ = 0.80 (d, $J=6.9$, 3H), 0.93 (d, $J=6.9$, 3H), 2.00 (s, 3H), 2.44 (hept, $J=6.9$, 1H), 5.12 (dd, $J=5.9$, 1.2, 1H), 5.30 (dd, $J=5.9$, 1.2, 1H), 5.67 (dd, $J=5.9$, 1.2, 1H), 5.73 (dd, $J=5.9$, 1.3, 1H), 7.47 (dd, $J=8.0$, 5.3, 1H), 7.53 – 7.62 (m, 3H), 7.79 (d, $J=8.7$, 1H), 8.21 (dd, $J=8.0$, 1.3, 1H), 8.38 (dd, $J=6.4$, 1.7, 1H), 9.47 (dd, $J=5.3$, 1.3, 1H) ppm; ^{13}C NMR (101 MHz, CD_2Cl_2) δ = 19.0 (CH₃), 21.9 (CH₃), 22.7 (CH₃), 31.3 (CH), 82.6 (CH), 84.0 (CH), 89.7 (CH), 90.3 (CH), 100.3 (C), 101.6 (C), 120.9 (CH), 121.6 (CH), 123.3 (CH), 127.1 (C), 129.3 (CH), 129.7 (CH), 134.1 (C), 135.9 (CH), 136.9 (CH), 140.9 (C), 153.2 (CH), 155.5 (C), 179.3 (Ru-C) ppm.



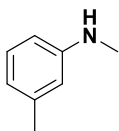
N-methylaniline (**1a**): colourless liquid (102.5 mg, 96%).

^1H NMR (300 MHz, CDCl_3) δ = 2.86 (s, 3H), 3.69 (s, 1H), 6.59 6.69 (m, 2H), 6.74 (tt, $J=7.5$, 1.1, 1H), 7.17 – 7.27 (m, 2H) ppm; ^{13}C NMR (75 MHz, CDCl_3) δ = 30.8 (CH₃), 112.5 (2 x CH), 117.4 (CH), 129.3 (2 x CH), 149.5 (C) ppm; GCMS (EI): m/z (%): 51 (8), 65 (7), 77 (20), 78 (7), 79 (16), 106 (100), 107 (79) [M^+], 108 (7); HRMS (ESI-TOF): m/z : calcd for $\text{C}_7\text{H}_9\text{N}$: 108.0813 [$\text{M}+\text{H}$]⁺; found: 108.0811.



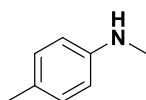
N,2-dimethylaniline (**1b**):

Following the general procedure except using 30 mol% NaOH and a reaction temperature of 100 °C, *N*,2-dimethylaniline was obtained as a colourless liquid (42.8 mg, 35%, determined by GC using hexadecane as internal standard). ^1H NMR (400 MHz, CDCl_3) δ = 2.16 (s, 3H), 2.92 (s, 3H), 3.58 (s, 1H), 6.64 (dd, $J=8.1$, 1.2, 1H), 6.70 (td, $J=7.4$, 1.2, 1H), 7.08 (ddq, $J=7.3$, 1.7, 0.8, 1H), 7.19 (dddd, $J=8.0$, 7.4, 1.6, 0.6, 1H) ppm; ^{13}C NMR (101 MHz, CDCl_3) δ = 17.5 (CH₃), 30.9 (CH₃), 109.2 (CH), 117.0 (CH), 122.0 (C), 127.3 (CH), 130.0 (CH), 147.3 (CH) ppm; GCMS (EI): m/z (%): 77 (12), 91 (26), 106 (79), 120 (63), 121 (100) [M^+]; HRMS (ESI-TOF): m/z : calcd for $\text{C}_8\text{H}_{11}\text{N}$: 122.0969 [$\text{M}+\text{H}$]⁺; found: 122.0972.



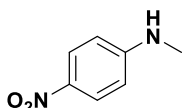
N,3-dimethylaniline (**1c**):

Following the general procedure, *N*,3-dimethylaniline was obtained as a colourless liquid (120.2 mg, 99%, determined by GC using hexadecane as internal standard). ^1H NMR (300 MHz, CDCl_3) δ = 2.31 (q, $J=0.7$, 3H), 2.84 (s, 3H), 3.60 (s, 1H), 6.40 – 6.50 (m, 2H), 6.51 – 6.61 (m, 1H), 7.04 – 7.16 (m, 1H) ppm; ^{13}C NMR (75 MHz, CDCl_3) δ = 21.8 (CH₃), 30.9 (CH₃), 109.8 (CH), 113.3 (CH), 118.3 (CH), 129.2 (CH), 139.1 (C), 149.5 (C) ppm; GCMS (EI): m/z (%): 65 (6), 77 (8), 91 (19), 92 (5), 106 (7), 120 (100), 121 (82) [M^+], 122 (7); HRMS (ESI-TOF): m/z : calcd for $\text{C}_8\text{H}_{11}\text{N}$: 122.0969 [$\text{M}+\text{H}$]⁺; found: 122.0973.



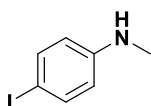
N,4-dimethylaniline (1d):

Following the general procedure, *N,4*-dimethylaniline was obtained as a yellowish liquid (120.1 mg, 99%, determined by GC using hexadecane as internal standard). ¹H NMR (300 MHz, CDCl₃) δ = 2.27 (d, *J*=0.9, 3H), 2.83 (s, 3H), 3.42 (s, 1H), 6.52 – 6.62 (m, 2H), 6.97 – 7.13 (m, 2H) ppm; ¹³C NMR (75 MHz, CDCl₃) δ = 20.5 (CH₃), 31.2 (CH₃), 112.7 (2 x CH), 126.6 (C), 129.8 (2 x CH), 147.3 (C) ppm; GCMS (EI): *m/z* (%): 77 (7), 91 (14), 106 (7), 120 (100), 121 (73) [M⁺], 122 (6); HRMS (ESI-TOF): *m/z*: calcd for C₈H₁₁N: 122.0969 [M+H]⁺; found: 122.0970.



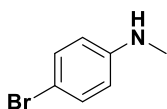
N-methyl-4-nitroaniline (1e):

Following the general procedure except using 30 mol% NaOH and a reaction temperature of 80 °C, *N*-methyl-4-nitroaniline was obtained as a yellow solid (42.8 mg, 28%). ¹H NMR (300 MHz, DMSO) δ = 2.78 (d, *J*=5.0, 3H), 6.53 – 6.65 (m, 2H), 7.25 – 7.31 (m, 1H), 7.94 – 8.05 (m, 2H) ppm; ¹³C NMR (75 MHz, DMSO) δ = 29.3 (CH₃), 126.4 (4 x CH), 135.7 (C), 155.4 (C) ppm; GCMS (EI): *m/z* (%): 65 (19), 77 (30), 79 (18), 105 (13), 106 (17), 122 (45), 152 (100) [M⁺]; HRMS (ESI-TOF): *m/z*: calcd for C₇H₈N₂O₂: 153.0664 [M+H]⁺; found: 153.0668.



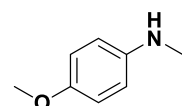
4-iodo-N-methylaniline (1f):

Following the general procedure, 4-iodo-*N*-methylaniline was obtained as a violet oil (121.5 mg, 52%). ¹H NMR (400 MHz, CDCl₃) δ = 2.80 (s, 3H), 3.69 (s, 1H), 6.35 – 6.43 (m, 2H), 7.38 – 7.48 (m, 2H) ppm; ¹³C NMR (101 MHz, CDCl₃) δ = 30.6 (CH₃), 77.8 (C), 114.7 (2 x CH), 137.8 (2 x CH), 148.9 (C) ppm; GCMS (EI): *m/z* (%): 77 (6), 105 (6), 106 (6), 232 (31), 233 (100) [M⁺], 234 (8); HRMS (ESI-TOF): *m/z*: calcd for C₇H₈NI: 233.9779 [M+H]⁺; found: 233.9777.



4-bromo-N-methylaniline (1g):

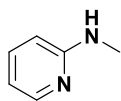
Following the general procedure, 4-bromo-*N*-methylaniline was obtained as a colourless liquid (177.0 mg, 95%). ¹H NMR (400 MHz, CDCl₃) δ = 2.81 (s, 3H), 3.73 (s, 1H), 6.44 – 6.53 (m, 2H), 7.22 – 7.31 (m, 2H) ppm; ¹³C NMR (101 MHz, CDCl₃) δ = 30.8 (CH₃), 108.9 (C), 114.0 (2 x CH), 132.0 (2 x CH), 148.4 (C) ppm; GCMS (EI): *m/z* (%): 104 (12), 105 (17), 184 (80), 185 (100) [M⁺], 186 (83), 187 (98); HRMS (ESI-TOF): *m/z*: calcd for C₇H₉BrN: 185.9918 [M+H]⁺; found: 185.9919.



4-methoxy-N-methylaniline (1h):

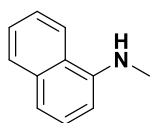
Following the general procedure, 4-methoxy-*N*-methylaniline was obtained as a yellowish liquid (116.7 mg, 85%). ¹H NMR (400 MHz, CDCl₃) δ = 2.82 (s, 3H), 3.38 (s, 1H), 3.77 (d, *J*=0.9, 3H), 6.56 – 6.65 (m, 2H), 6.79 – 6.85 (m, 2H) ppm; ¹³C NMR (101 MHz, CDCl₃) δ = 31.7 (CH₃), 55.9 (CH₃), 113.7 (2 x CH), 115.0 (2 x CH), 143.8 (C), 152.1 (C) ppm; GCMS (EI): *m/z* (%): 65 (6),

94 (20), 122 (100), 123 (8), 137 (65) [M⁺], 138 (6); HRMS (ESI-TOF): *m/z*: calcd for C₈H₁₁NO: 138.0919 [M+H]⁺; found: 138.0921.



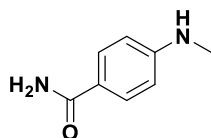
N-methylpyridin-2-amine (**1i**):

Following the general procedure except using 30 mol% NaOH and a reaction temperature of 80 °C, *N*-methylpyridin-2-amine was obtained as a yellowish oil (16.3 mg, 15%). ¹H NMR (400 MHz, CDCl₃) δ = 2.90 (s, 3H), 4.61 (s, 1H), 6.37 (dt, *J*=8.4, 1.0, 1H), 6.56 (ddd, *J*=7.1, 5.0, 1.0, 1H), 7.42 (ddd, *J*=8.4, 7.1, 1.9, 1H), 8.08 (ddd, *J*=5.0, 1.9, 0.9, 1H) ppm; ¹³C NMR (101 MHz, CDCl₃) δ = 29.2 (CH₃), 106.3 (CH), 112.8 (CH), 137.5 (CH), 148.3 (CH), 159.7 (C) ppm; GCMS (EI): *m/z* (%): 51 (11), 52 (19), 78 (34), 79 (76), 80 (51), 107 (57), 108 (100) [M⁺]; HRMS (ESI-TOF): *m/z*: calcd for C₆H₈N₂: 109.0765 [M+H]⁺; found: 109.0769.



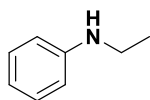
N-methylnaphthalen-1-amine (**1k**):

Following the general procedure except using 30 mol% NaOH and a reaction temperature of 80 °C, *N*-methylnaphthalen-1-amine was obtained as a reddish-brown liquid (102.8 mg, 65%). ¹H NMR (400 MHz, CDCl₃) δ = 3.04 (s, 3H), 4.43 (s, 1H), 6.64 (dd, *J*=7.6, 1.0, 1H), 7.26 – 7.33 (m, 1H), 7.39 – 7.54 (m, 3H), 7.75 – 7.90 (m, 2H) ppm; ¹³C NMR (101 MHz, CDCl₃) δ = 31.1 (CH₃), 103.9 (CH), 117.4 (CH), 119.9 (CH), 123.5 (C), 124.8 (CH), 125.8 (CH), 126.8 (CH), 128.8 (CH), 134.3 (C), 144.6 (C) ppm; GCMS (EI): *m/z* (%): 115 (25), 127 (10), 128 (23), 129 (21), 156 (43), 157 (100) [M⁺], 158 (12); HRMS (ESI-TOF): *m/z*: calcd for C₁₁H₁₁N: 158.0969 [M+H]⁺; found: 158.0969.



4-(methylamino)benzamide (**1l**):

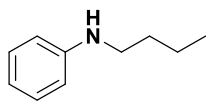
Following the general procedure except using 30 mol% NaOH and a reaction temperature of 80 °C, 4-(methylamino)benzamide was obtained as a faintly brownish solid (144.0 mg, 96%). ¹H NMR (300 MHz, DMSO) δ = 2.70 (d, *J*=5.0, 3H), 6.16 (q, *J*=5.0, 1H), 6.45 – 6.57 (m, 2H), 6.85 (s, 1H), 7.54 (s, 1H), 7.61 – 7.72 (m, 2H) ppm; ¹³C NMR (75 MHz, DMSO) δ = 29.3 (CH₃), 110.3 (2 x CH), 120.7 (C), 129.1 (2 x CH), 152.2 (C), 168.1 (C(O)NH₂) ppm; GCMS (EI): *m/z* (%): 65 (6), 77 (13), 79 (10), 106 (14), 131 (8), 132 (9), 134 (100), 135 (9), 149 (6), 150 (90) [M⁺], 151 (9); HRMS (ESI-TOF): *m/z*: calcd for C₈H₁₀N₂O: 151.0871 [M+H]⁺; found: 151.0870.



N-ethylaniline (**3a**):

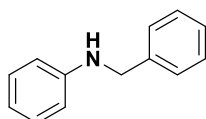
Following the general procedure, *N*-ethylaniline was obtained as a colorless liquid (82.1 mg, 68%, determined by GC using hexadecane as internal standard). ¹H NMR (400 MHz, CDCl₃) δ = 1.27 (t, *J*=7.1, 3H), 3.17 (q, *J*=7.1, 2H), 3.50 (s, 1H), 6.58 – 6.66 (m, 2H), 6.67 – 6.76 (m, 1H), 7.14 – 7.24 (m, 2H) ppm; ¹³C NMR (101 MHz, CDCl₃) δ = 15.0 (CH₃), 38.6 (CH₂), 112.9 (2 x CH), 117.3 (CH), 129.3 (2 x CH), 148.6 (C) ppm; GCMS (EI): *m/z* (%): 77 (16), 79 (8), 106 (100), 107

(8), 120 (6), 121 (43) [M⁺]; HRMS (ESI-TOF): *m/z*: calcd for C₈H₁₁N: 122.0969 [M+H]⁺; found: 122.0972.



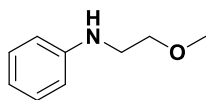
N-butylaniline (**3b**):

Following the general procedure, *N*-butylaniline was obtained as a colourless liquid (63.4 mg, 43%). ¹H NMR (300 MHz, CDCl₃) δ = 0.99 (t, *J*=7.3, 3H), 1.37 – 1.57 (m, 2H), 1.53 – 1.71 (m, 2H), 3.08 – 3.20 (m, 2H), 3.59 (s, 1H), 6.57 – 6.67 (m, 2H), 6.71 (tt, *J*=7.4, 1.1, 1H), 7.13 – 7.26 (m, 2H) ppm; ¹³C NMR (75 MHz, CDCl₃) δ = 14.0 (CH₃), 20.4 (CH₂), 31.8 (CH₂), 43.8 (CH₂), 112.8 (2 x CH), 117.2 (CH), 129.3 (2 x CH), 148.7 (C) ppm; GCMS (EI): *m/z* (%): 77 (10), 106 (100), 107 (9), 149 (25) [M⁺]; HRMS (ESI-TOF): *m/z*: calcd for C₁₀H₁₅N: 150.1283 [M+H]⁺; found: 150.1284.



N-benzylaniline (**3c**):

Following the general procedure, *N*-benzylaniline was obtained as a colourless oil (52.4 mg, 29%). ¹H NMR (400 MHz, CDCl₃) δ = 4.05 (s, 1H), 4.37 (s, 2H), 6.64 – 6.72 (m, 2H), 6.76 (tt, *J*=7.4, 1.1, 1H), 7.17 – 7.28 (m, 2H), 7.25 – 7.37 (m, 1H), 7.37 – 7.45 (m, 4H) ppm; ¹³C NMR (101 MHz, CDCl₃) δ = 48.4 (CH₃), 112.9 (2 x CH), 117.7 (CH), 127.3 (CH), 127.6 (2 x CH), 128.8 (2 x CH), 129.4 (2 x CH), 139.6 (C), 148.3 (C) ppm; GCMS (EI): *m/z* (%): 65 (11), 77 (13), 91 (83), 106 (18), 182 (37), 183 (100) [M⁺], 184 (14); HRMS (ESI-TOF): *m/z*: calcd for C₁₃H₁₃N: 184.1126 [M+H]⁺; found: 184.1122.



N-(2-methoxyethyl)aniline (**3d**):

Following the general procedure except using 30 mol% NaOH and a reaction temperature of 80 °C, *N*-(2-methoxyethyl)aniline was obtained as a colourless liquid (86.9 mg, 57%). ¹H NMR (400 MHz, CDCl₃) δ = 3.31 (dd, *J*=5.6, 4.8, 2H), 3.41 (s, 3H), 3.62 (dd, *J*=5.7, 4.8, 2H), 4.02 (s, 1H), 6.61 – 6.69 (m, 2H), 6.73 (tt, *J*=7.3, 1.1, 1H), 7.15 – 7.25 (m, 2H) ppm; ¹³C NMR (101 MHz, CDCl₃) δ = 43.6 (CH₂), 58.9 (CH₃), 71.1 (CH₂), 113.2 (2 x CH), 117.7 (CH), 129.3 (2 x CH), 148.3 (C) ppm; GCMS (EI): *m/z* (%): 77 (13), 79 (6), 106 (100), 107 (8), 151 (25) [M⁺]; HRMS (ESI-TOF): *m/z*: calcd for C₉H₁₃NO: 152.1075 [M+H]⁺; found: 152.1075.

3.6 References

- [1] M. A. W. Lawrence, K.-A. Green, P. N. Nelson and S. C. Lorraine, *Polyhedron*, **2018**, *143*, 11–27.
- [2] A. Ricci, *Modern Amination Methods*, Wiley-VCH, Weinheim, **2000**.
- [3] A. Ricci, *Wiley-VCH*, Weinheim, **2008**.
- [4] J. S. Carey, D. Laffan, C. Thomson and M. T. Williams, *Org. Biomol. Chem.*, **2006**, *4*, 2337–2347.
- [5] N. Schneider, D. M. Lowe, R. A. Sayle, M. A. Tarselli and G. A. Landrum, *J. Med. Chem.*, **2016**, *59*, 4385–4402.
- [6] S. D. Roughley and A. M. Jordan, *J. Med. Chem.*, **2011**, *54*, 3451–3479.
- [7] E. J. Barreiro, A. E. Kümmerle and C. A. M. Fraga, *Chem. Rev.*, **2011**, *111*, 5215–5246.
- [8] J. Chatterjee, F. Rechenmacher and H. Kessler, *Angew. Chem., Int. Ed.*, **2013**, *52*, 254–269.
- [9] F. Li, J. Xie, H. Shan, C. Sun and L. Chen, *RSC Adv.*, **2012**, *2*, 8645–8652.
- [10] D. Deng, B. Hu, M. Yang and D. Chen, *Organometallics*, **2018**, *37*, 3353–3359.
- [11] M. González-Lainez, M. V. Jiménez, V. Passarelli and J. J. Pérez-Torrente, *Catal. Sci. Technol.*, **2020**, *10*, 3458–3467.
- [12] T. T. Dang, B. Ramalingam and A. M. Seayad, *ACS Catal.*, **2015**, *5*, 4082–4088.
- [13] G. Choi and S. H. Hong, *Angew. Chem., Int. Ed.*, **2018**, *57*, 6166–6170.
- [14] O. Ogata, H. Nara, M. Fujiwhara, K. Matsumura and Y. Kayaki, *Org. Lett.*, **2018**, *20*, 3866–3870.
- [15] G. Choi and S. H. Hong, *ACS Sustainable Chem. Eng.*, **2019**, *7*, 716–723.
- [16] S. N. R. Donthireddy, P. Mathoor Illam and A. Rit, *Inorg. Chem.*, **2020**, *59*, 1835–1847.
- [17] M. Maji, K. Chakrabarti, B. Paul, B. C. Roy and S. Kundu, *Adv. Synth. Catal.*, **2018**, *360*, 722–729.
- [18] K. Polidano, B. D. W. Allen, J. M. J. Williams and L. C. Morrill, *ACS Catal.*, **2018**, *8*, 6440–6445.
- [19] A. Lator, S. Gaillard, A. Poater and J.-L. Renaud, *Org. Lett.*, **2018**, *20*, 5985–5990.
- [20] S. Elangovan, J. Neumann, J. B. Sortais, K. Junge, C. Darcel and M. Beller, *Nat. Commun.*, **2016**, *7*, 12641.
- [21] J. Neumann, S. Elangovan, A. Spannenberg, K. Junge and M. Beller, *Chem.–Eur. J.*, **2017**, *23*, 5410–5413.
- [22] A. Bruneau-Voisine, D. Wang, V. Dorcet, T. Roisnel, C. Darcel and J.-B. Sortais, *J. Catal.*, **2017**, *347*, 57–62.
- [23] M. Huang, Y. Li, Y. Li, J. Liu, S. Shu, Y. Liu and Z. Ke, *Chem. Commun.*, **2019**, *55*, 6213–6216.
- [24] Z. Liu, Z. Yang, X. Yu, H. Zhang, B. Yu, Y. Zhao and Z. Liu, *Adv. Synth. Catal.*, **2017**, *359*, 4278–4283.
- [25] D. Wei, O. Sadek, V. Dorcet, T. Roisnel, C. Darcel, E. Gras, E. Clot and J.-B. Sortais, *J. Catal.*, **2018**, *366*, 300–309.

- [26] L. Jiang, F. Guo, Y. Wang, J. Jiang, Y. Duan and Z. Hou, *Asian J. Org. Chem.*, **2019**, *8*, 2046–2049.
- [27] M. A. R. Jamil, A. S. Touchy, M. N. Rashed, K. W. Ting, S. M. A. H. Siddiki, T. Toyao, Z. Maeno and K.-i. Shimizu, *J. Catal.*, **2019**, *371*, 47–56
- [28] P. Piehl, R. Amuso, E. Alberico, H. Junge, B. Gabriele, H. Neumann and M. Beller, *Chem.–Eur. J.*, **2020**, *26*, 6050–6055.
- [29] P. Piehl, R. Amuso, A. Spannenberg B. Gabriele, H. Neumann and M. Beller, *Catal. Sci. Technol.*, **2021**, *11*, 2512–2517
- [30] B. Li, T. Roisnel, C. Darcel and P. H. Dixneuf, *Dalton Trans.*, **2012**, *41*, 10934–10937.
- [31] L. Kathuria, N. Reshi and A. Samuelson, *Chem. – Eur. J.*, **2020**, *26*, 7622–7630.
- [32] J. Neumann, S. Elangovan, A. Spannenberg, K. Junge and M. Beller, *Chem. – Eur. J.*, **2017**, *23*, 5410–5413.
- [33] L. Kathuria, N. Reshi and A. Samuelson, *Chem. – Eur. J.*, **2020**, *26*, 7622–7630.
- [34] J. A. Widegren and R. G. Finke, *J. Mol. Catal. A: Chem.*, **2003**, *198*, 317–341.
- [35] B. Li, T. Roisnel, C. Darcel, P. H. Dixneuf, *Dalton Trans.* **2012**, *41*, 10934–10937.

Chapter 4

Synthesis of 1,3-Oxazine-2,4-Diones by DBU-Catalyzed Incorporation of Carbon Dioxide Into 3-Ynamides

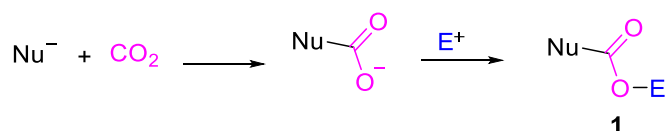
4.1 Introduction

4.1.1 CO₂: pollutant or precious resource?

Carbon dioxide is a gas that occurs naturally in the earth's atmosphere and is very important as it participates in numerous processes that regulate and promote life on the planet. The CO₂ is also termed as "greenhouse gas" because of its special properties to let pass the sun's rays coming from the high atmosphere. This phenomenon is fundamental in the natural thermoregulation of the temperature on the planet and contributes to increasing it in a not negligible way. The problem is that the concentration of atmospheric carbon dioxide has grown steadily since the industrial revolution, mainly because of the use of fossil fuels and deforestation¹. As main CO₂ greenhouse gases associated with global warming²⁻³, one of the most important issues for humans today. The average increase in global temperature in recent decades has been very pronounced while increasingly extreme weather phenomena have become much more frequent than in the recent past. All this has serious repercussions on the environment, social and political. A partial solution to the problem could be to find an innovative method that allows to reduce the concentration of CO₂ in the atmosphere and at the same time transform it into high value-added compounds. In the field of organic chemistry in recent years many research studies have been conducted in this direction, since carbon dioxide is an abundant, non-toxic and low-cost raw material⁴. In addition to the advantages from an environmental point of view, the incorporation of CO₂ in some particular substrates allows the formation of heterocycles with high added value, with potential properties in the pharmacological field. The synthesis of these compounds represents a great innovation in synthetic methodology, as it avoids the use of dangerous carbonylating reagents such as CO and phosgene. Furthermore, in recent years a set of techniques have been developed to convert CO₂ into molecules with high added value, polymers and fuels⁵. There are numerous reactions that allow the transformation of CO₂ into molecules with high added value and in particular in this chapter the carboxylation reactions will be discussed.

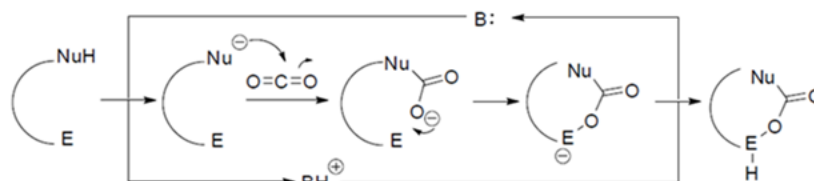
4.1.2 Carbon Dioxide in carboxylation reactions

The carbon dioxide is a non-polar molecule due to its symmetry but the difference in electronegativity between oxygen and carbon makes the C=O bond polar and gives the carbon the characteristic of being an electrophilic site. It can also be considered as an amphoteric molecule, in which the oxygens behave as Lewis bases having free doublets while the carbon is Lewis acid. Overall, the molecule is more likely to accept electrons than to donate them and therefore the total reactivity of CO₂ is determined by the electrophilic character of the carbon⁶. In this molecule, the carbon assumes its maximum oxidation number (+4) and this is the cause of two important characteristics, which greatly limit its reactivity and its use in organic synthesis reactions: high thermodynamic stability and kinetic inertia⁷. For this reason, the use of CO₂ in many cases involves the use of highly reactive substrates, relatively high temperatures and pressures or the use of catalysts. For example, one way to activate CO₂ is to use an appropriate organic superbases⁸, or an N-heterocyclic carbene (NHC)⁹, compounds capable of reacting with the electrophilic carbon of CO₂ or to activate the nucleophilic character of a substrate. The first step is precisely the nucleophilic attack on CO₂, with the formation of a nucleophilic intermediate to oxygen while subsequently the reaction with an electrophile allows the incorporation of CO₂, as described in the scheme 4.1.1:



Scheme 4.1.1 Incorporation of CO₂ into product **1** following nucleophilic attack.

If the nucleophilic and electrophilic site are present simultaneously on the same molecule, the formation of a heterocycle is possible, as shown in scheme 4.1.2:



Scheme 4.1.2¹⁰ Formation of a generic heterocycle by incorporation of CO₂.

4.1.3 Pharmacological importance of 1,3-Oxazinediones

Molecules with a 1,3-oxazine-2,4-dionic nucleus are the object of research as they are characterized by various types of pharmacological activity. For example, Oxazinomycin (figure 4.1.1), a C-nucleoside of natural origin¹¹, has highlighted antibacterial and antitumor properties thanks to its particular structure.

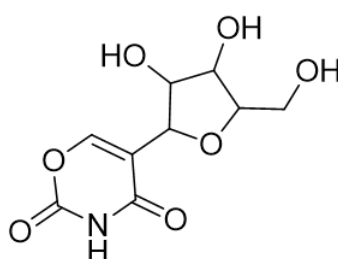


Fig. 4.1.1 Oxazinomycin structure

These molecules are also present in the literature as compounds characterized by a powerful anti-ulcer activity. A study demonstrates¹², after numerous tests on different molecules, the efficacy of the compound with 1,3-oxazine-2,4-dionic core shown below (figure 4.1.2):

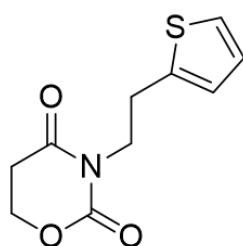


Fig. 4.1.2 1,3-Oxazine-2,4-diones derivatives with anti-ulcer activity

Furthermore, these derivatives also showed anticoagulant activity. A study tests some molecules with this structure as inhibitors against Factor Xa, endoprotease which plays a key role in the blood coagulation enzyme cascade, in order to obtain potential anticoagulant

agents useful in the treatment of thromboembolic disorders¹³. A final activity, albeit still little depth, is related to some central nervous system. The oxazindionic structural core is related to other heterocyclic systems that characterize drugs with sedative or anticonvulsive activity. A patent¹⁴ proposes some molecules as potential antiepileptic agents and associates them with other sedative, hypnotic and depressing properties of the central nervous system. A particular compound known as Dioxone (figure 4.1.3) is an exception, showing a stimulating action, in particular towards the central respiratory centers¹⁵:

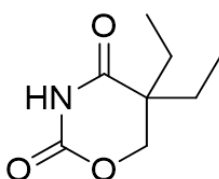


Fig. 4.1.3 Dioxone structure

In addition to having a direct pharmacological activity, many molecules with a 1,3-oxazine-2,4-dionic nucleus are important precursors in the synthesis of different heterocycles of relevant pharmacological interest. This nucleus can undergo ring transformations to convert into pyrimidine, pyridine and pyrazole nuclei after treatment with suitable amines¹⁶. This is also made possible by the presence of three electrophilic sites susceptible to nucleophilic attack by amines on the oxazindionic nucleus (figure 4.1.4):

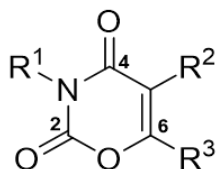


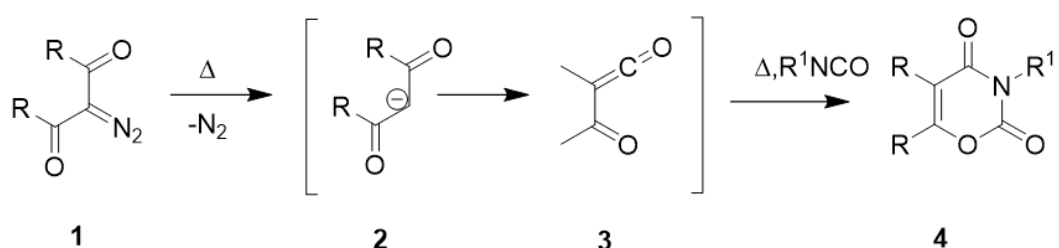
Fig. 4.1.4 Electrophilic sites on the oxazindionic nucleus

The positions of nucleophilic attack are determined by the strength of the base: the strong ones (such as ammonia or alkylamines) react mainly to C1 (with formation of pyrimidines,

pirazzoli and pyridines), the alcohols react primarily at C2 (alkyl carbamates are formed), while weak bases react to C3 (forming pyrroles).

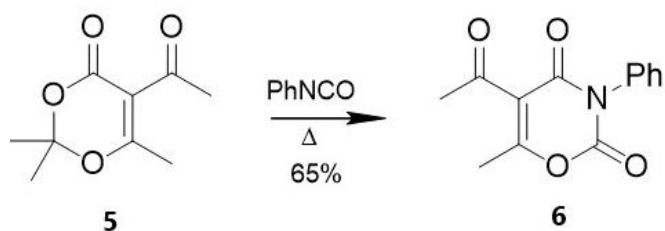
4.1.4 Synthesis of 1,3-Oxazinedione derivatives

Various methods of synthesis of the 1,3-oxazine-2,4-dionic nucleus are known in the literature, which differ in the reaction conditions and the type of substrate used. Many synthetic strategies use Diels-Alder cycloaddition reactions, which involve the use as reagents of a diene and an alkene bearing electron-withdrawing groups, defined as a dienophile. This type of reaction has a concerted mechanism (therefore takes place in a single stage) and is stereospecific, while if the dienophile contains a heteroatom there will be the formation of a heterocycle. The key precursor (which plays the role of diene) in the synthesis of the 1,3-oxazine-2,4-dionic nucleus is acyl-ketene. There are several ways of synthesizing this important intermediate, such as from acyl chlorides by means of elimination reactions or starting from α -diazoketones by Wolff rearrangement. In the latter case, for example, starts from 2-diazo-1,3-diketone in the presence of arylisocyanate at a temperature of 140 ° C, with the formation of the oxazindionic nucleus¹⁷ following a 1,4-cycloaddition. The process is catalyzed by light, heat or metal complexes, with the formation of nitrogen gas (scheme 4.1.3):



Scheme 4.1.3 Formation of the oxazindionic nucleus¹⁷ starting from 2-diazo-1,3-diketone in the presence of arylisocyanate

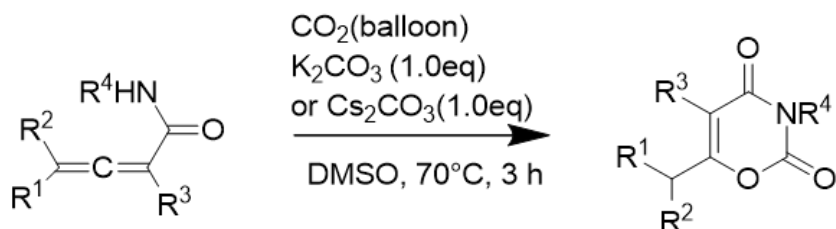
Another interesting precursor is 2,2,6-trimethyl-1,3-dioxin-4-one which, in the presence of phenylisocyanate, leads to the formation of the 1,3-oxazine-2,4-dionic nucleus with yields of 65%¹⁸(scheme 4.1.4):



Scheme 4.1.4 Formation of 1,3-oxazine-2,4-diones derivatives **6** from 2,2,6-trimethyl-1,3-dioxin-4-one **5**

A very important parameter of this reaction is the temperature, which depends on the nature of the substituents on the ring¹⁹. In fact, the temperature varies from 80 °C if there is no substituent in positions 5 and 6 of the ring, at 120 °C if there is only one substituent in position 5 or 6 or up to 160 °C if the ring is alkylated in both position 5 and position 6.

Recent studies have shown that the synthesis of the 1,3-oxazine-2,4-dionic nucleus can be carried out, under particular conditions, starting from a new type of substrate, the 2,3-allenamides²⁰. Their particular structure and their high reactivity are crucial for the success of the reaction, considering that analogous reactions with α,β -unsaturated alkenamides or alkynamides do not occur. The reaction object of study in this article employs as a starting substrate the *N*-benzyl-4-methyl-2,3-pentadienamide. A screening of the parameters was carried out, which showed that the best solvent is DMSO while the base is K_2CO_3 or alternatively Cs_2CO_3 . The reaction is carried out for three hours at a temperature of 70 °C, using 1 atm of CO_2 and obtaining a yield of 75% (scheme 4.1.5).

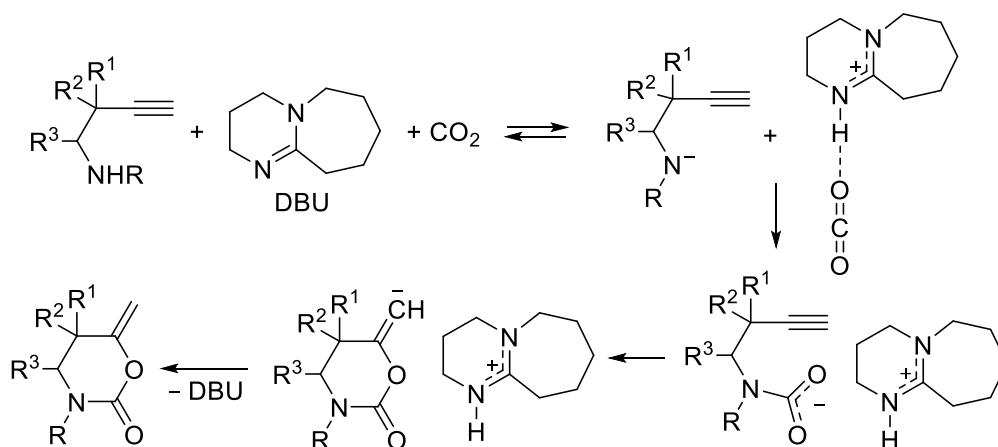


Scheme 4.1.5 Synthesis of the 1,3-oxazine-2,4-dionic nucleus starting from 2,3-allenamide²⁰

Numerous substrates have been tested and it has been noted that the increase in steric hindrance on the allenic structure causes a substantial decrease in yields.

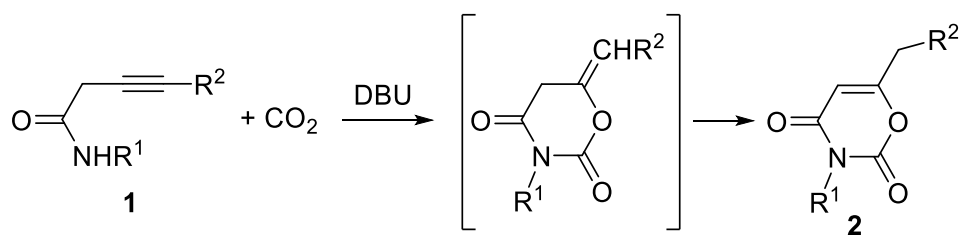
4.2 Results and Discussion

Recently, Gabriele's research group reported the carboxylation of homopropargylic amines to give 6-methylene-1,3-oxazin-2-ones, under the cooperative catalysis of 1,8-diazabicyclo[5.4.0]undec-7-ene (DBU) and CuCl_2 (Scheme 4.2.1)²¹. The role of the superbase was to deprotonate the amino group of the substrate to give, in the presence of CO_2 , the corresponding nitrogen anion and protonated DBU (DBUH^+), stabilized by the hydrogen bonding with CO_2 to give a $\text{DBUH}^+\text{-CO}_2$ complex. In this manner, CO_2 was activated toward the nucleophilic attack by the anion to give a carbamate intermediate, from which the final product was formed by 6-*exo-dig* cyclization followed by protonolysis (Scheme 4.2.1). On the other hand, the use of CuCl_2 together with DBU ensured higher product yields, most probably by activating the triple bond toward the intramolecular nucleophilic attack by the carbamate intermediate in the annulation step²¹.



Scheme 4.2.1 DBU-catalyzed carboxylation of homopropargylic amines leading to 6-methylene-1,3-oxazin-2-ones²¹.

In this work, we have studied the possibility to extend this method to the use of 3-ynamides **1**, with the aim of developing a new approach to 2*H*-1,3-oxazine-2,4(3*H*)-diones **2** (by carboxylative 6-*exo-dig* cyclization followed by in situ isomerization) starting from simple and readily available substrates under organocatalytic CO_2 activation conditions, according to Scheme 4.2.2.

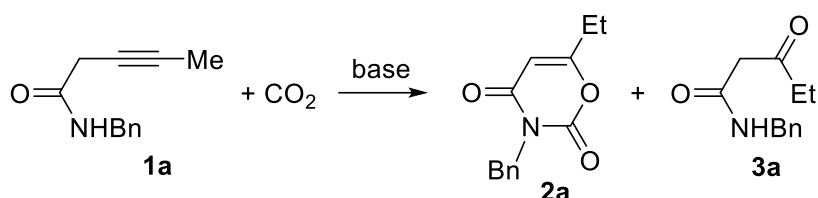


Scheme 4.2.2 This work: Synthesis of 1,3-oxazine-2,4-diones **2** from 3-ynamides **1** by DBU-catalyzed carboxylative cyclization followed by in situ isomerization.

Our initial experiments were carried out with *N*-benzylpent-3-ynamide **1a** as the model substrate. This 3-ynamide was allowed to react in MeCN (0.1 mmol of **1a**/mL of solvent) with CO₂ (30 atm) at 100 °C in the presence of 0.4 equiv of DBU. After 15 h, analysis of the reaction mixture revealed the formation of two products, which have been separated and characterized by spectroscopic techniques. The major compound corresponded to the desired cyclization product deriving from CO₂ incorporation and 6-*exo-dig* cyclization (3-benzyl-6-ethyl-2*H*-1,3-oxazine-2,4(3*H*)dione **2a**, 24% yield), while the minor product was identified as *N*-benzyl-3-oxopentanamide **3a**, clearly deriving from water addition to the triple bond (Table 4.1, entry 1; water being present in the reaction mixture as impurity). In order to improve the yield and selectivity of the process toward **2a**, we then changed the reaction conditions. In particular, to hinder the formation of **3a**, we carried out an experiment in the presence of a dehydrating agent as trimethyl orthoformate. Using a 3:1 mixture of MeCN–HC(OMe)₃, the formation of **3a** was indeed suppressed, with formation of **2a** in 35% yield (Table 4.1, entry 2). No further improvement in the yield of **2a** was observed working in pure HC(OMe)₃ as the solvent (Table 4.1, entry 3), while the use of MeOH as cosolvent instead of MeCN did not lead to any product formation (Table 4.1, entry 4). In DMSO–HC(OMe)₃, **2a** and **3a** were formed in 20% and 15% yields, respectively (Table 4.1, entry 5). The use of a lower CO₂ pressure (10 atm, Table 4.1, entry 6) as well as of a different base (MTBD, Table 4.1, entry 7, or DIPEA, Table 1, entry 8) led to less satisfactory results with respect to the same reaction carried out with DBU (Table 4.1, entry 2). Inferior results in terms of **2a** yield were also observed with a lower amount of DBU (0.2 equiv, Table 4.1, entry 9) or by increasing the substrate concentration (from 0.1 to 0.3 mmol/mL of solvent, entry 10). On the other hand, an augment in **2a** yield was observed by decreasing the substrate concentration to 0.05 mmol/mL solvent (Table 4.1, entry 11) and by decreasing the reaction temperature to 80 °C (Table 4.1, entry 12; no further

improvement was observed at 60 °C, Table 4.1, entry 13), while practically the same results as those of Table 4.1, entry 2, were obtained by adding 0.01 equiv of CuCl₂ as possible cocatalyst (Table 4.1, entry 14).

TABLE 4.1 Reactions of N-benzylpent-3-ynamide **1a** with CO₂ under different conditions^a



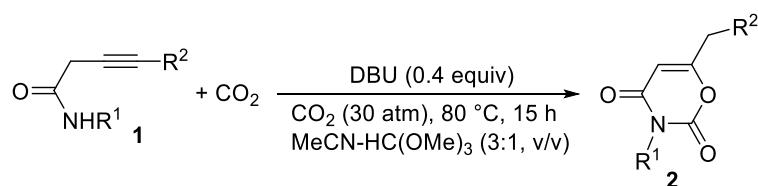
Entry	Base [equiv]	Solvent	Concn. of 1a ^b	P[CO ₂] [atm]	T[°C]	Conversion of 1a [%] ^c	Yield of 2 [%] ^d	Yield of 3 [%] ^d
1	DBU [0.4]	MeCN	0.1	30	100	100	24	8
2	DBU [0.4]	MeCN/HC(OMe) ₃ , 3:1 v/v	0.1	30	100	100	35	-
3	DBU [0.4]	HC(OMe) ₃	0.1	30	100	100	28	-
4	DBU [0.4]	MeOH/HC(OMe) ₃ , 3:1 v/v	0.1	30	100	4	-	-
5	DBU [0.4]	DMSO/HC(OMe) ₃ , 3:1 v/v	0.1	30	100	100	20	15
6	DBU [0.4]	MeCN/HC(OMe) ₃ , 3:1 v/v	0.1	10	100	98	14	4
7	MTDB [0.4]	MeCN/HC(OMe) ₃ , 3:1 v/v	0.1	30	100	100	27	8
8	DIPEA [0.4]	MeCN/HC(OMe) ₃ , 3:1 v/v	0.1	30	100	5	-	-
9	DBU [0.2]	MeCN/HC(OMe) ₃ , 3:1 v/v	0.1	30	100	100	17	-
10	DBU [0.4]	MeCN/HC(OMe) ₃ , 3:1 v/v	0.3	30	100	100	16	-
11	DBU [0.4]	MeCN/HC(OMe) ₃ , 3:1 v/v	0.05	30	100	100	50	-
12	DBU [0.4]	MeCN/HC(OMe) ₃ , 3:1 v/v	0.1	30	80	100	45	-

13	DBU [0.4]	MeCN/HC(OMe) ₃ , 3:1 v/v	0.1	30	60	100	40	-
14 ^e	DBU [0.4]	MeCN/HC(OMe) ₃ , 3:1 v/v	0.1	30	100	100	36	-

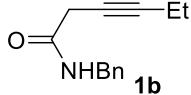
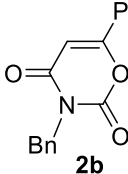
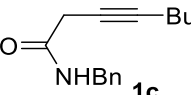
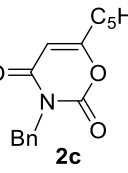
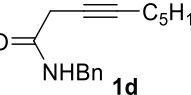
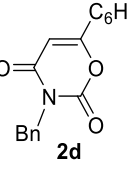
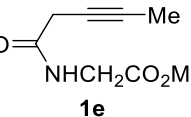
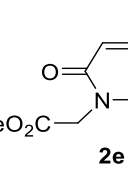
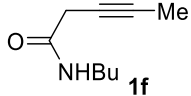
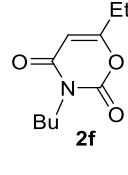
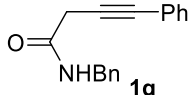
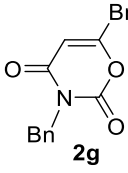
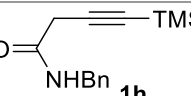
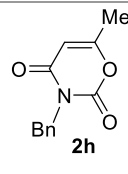
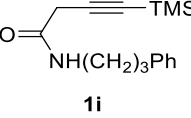
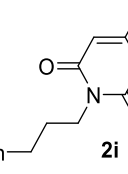
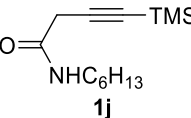
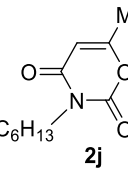
^aAll reactions were carried out for 15 h. ^b Mmol of **1a**/mL of solvent ^cDetermined by GLC ^dIsolated yield ^eThe reaction was carried out in the presence of 0.01 equiv of CuCl₂.

Therefore, the optimized reaction conditions corresponded to MeCN–HC(OMe)₃ as the solvent (0.05 mmol of **1a**/mL of solvent) under 30 atm of CO₂ at 80 °C for 15 h in the presence of 0.4 equiv of DBU. Under these conditions, the reaction of ynamide **1a** selectively led to the formation of oxazinedione **2a** in 66% yield (Table 4.2, entry 1). The extension of the method to other differently substituted substrates demonstrated that the process was quite general (Table 4.2). In particular, the yields in the corresponding oxazinediones **2b–e** were around 60–65% when the triple bond was substituted with an alkyl group and the nitrogen with a benzyl or a (methoxycarbonyl)methyl group (Table 4.2, entries 2–5). On the other hand, the product yields tended to be lower when the substituent on nitrogen was butyl (yield of **2f**, 50%; Table 4.2, entry 6) or when the triple bond was conjugated with a phenyl group (yield of **2g**, 51%; Table 4.2, entry 7).

Table 4.2. Synthesis of 2*H*-1,3-oxazine-2,4(3*H*)-diones **2** by DBU-catalyzed incorporation of CO₂ into 3-ynamides **1**^[a]



Entry	1	2	Yield of 2 [%] ^[b]
1	 1a	 2a	66

2	 1b	 2b	66
3	 1c	 2c	60
4	 1d	 2d	67
5	 1e	 2e	69
6 ^c	 1f	 2f	50
7	 1g	 2g	51
8	 1h	 2h	84
9	 1i	 2i	79
10	 1j	 2j	87

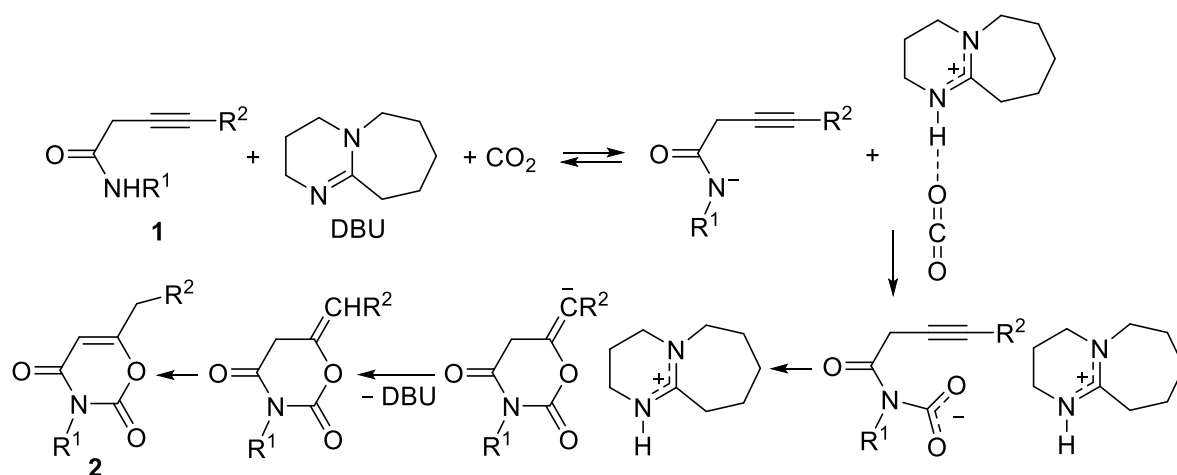
11			81
12			85
13			77
14			82
15			74
16			44

^[a] Unless otherwise noted, all reactions were carried out in a MeCN-HC(OMe)₃ mixture (3:1, v/v) (substrate concentration = 0.05 mmol / mL solvent) at 80 °C for 15 h, in the presence of DBU (0.4 equiv), under 30 atm of CO₂. ^[b] Isolated yield based on starting **1**. ^[c] The reaction was carried out for 24 h.

Interestingly, significantly higher yields were obtained when starting from 3-ynamides substituted with a trimethylsilyl group on the triple bond. In this case, the trimethylsilyl group was lost during the carboxylation process (probably due by DBU-promoted desilylation), so the final products **2h-o** were unsubstituted at C-6 (Table 4.2, entries 8-15). Yields ranging from 74% to 87% were obtained with different groups on nitrogen, including benzyl (yield of **2h**, 84%; Table 4.2, entry 8), 3-phenylpropyl (yield of **2i**, 79%; Table 4.2, entry 9), pentyl (yield of **2j**, 87%; Table 4.2, entry 10), isobutyl (yield of **2k**, 81%; Table 4.2, entry 11), isopentyl (yield of **2l**, 85%; Table 4.2, entry 12), cyclohexylmethyl (yield of **2m**, 77%; Table 4.2, entry 13) and functionalized substituents such as 3-methoxypropyl (yield of **2n**, 82%; Table 4.2, entry 14)

and 2-furylmethyl (yield of **2o**, 74%; Table 4.2, entry 15). This was probably due to the increased stability of the TMS-substituted triple bond in **1h-o**, which disfavored substrate degradation under the reaction conditions. The process, however, was quite sensitive to the steric effect of the substituent on nitrogen, which affected nitrogen nucleophilicity, as shown by the lower yield obtained with *N*-isopropyl-4-(trimethylsilyl)but-3-ynamide **1p** (yield of **2p**, 44%; Table 4.2, entry 16).

Mechanistically, in agreement with the previously reported DBU-catalyzed carboxylation of homopropargylic amines (Scheme 4.2.1), the process may involve substrate deprotonation by DBU followed by attack of the anionic nitrogen on carbon dioxide activated by hydrogen bonding with protonated DBU. This leads to the formation of a carbamate intermediate, which then undergoes 6-*endo-dig* cyclization and protonolysis by DBUH⁺ to give the final product with regeneration of DBU (Scheme 4.2.3).



Scheme 4.2.3 Mechanistic proposal for the DBU-catalyzed carboxylation of 3-ynamides **1** to 1,3-oxazine-2,4-diones **2**.

4.3 Conclusions

In conclusion, we have reported a new approach for CO₂ utilization and valorization, which consists in its catalytic incorporation into readily available 3-ynamides to give high value-added 3-oxazine-2,4-diones. The reaction, promoted by DBU as simple and commercially available organocatalyst (0.4 equiv), takes place in a 3:1 MeCN–HC(OMe)₃ mixture under relatively mild conditions (30 atm of CO₂, at 80 °C for 15 h), and proceeds through a mechanism involving substrate deprotonation by DBU followed by attack of the anionic nitrogen on carbon dioxide, *6-endo-dig* cyclization, and protonolysis.

Differently substituted 3-ynamide substrates, bearing various substituents on nitrogen or on the triple bond, have been converted into the corresponding oxazindiones in isolated yields ranging from 44% to 87% over 16 examples. The yields were higher when the substrate triple bond was protected with a trimethylsilyl group and the nitrogen was bonded to a sterically unhindered substituent, to give the corresponding oxazinediones in 74-87% yields, while lower yields (44-69%) were observed in the case of substrates bearing an alkyl or phenyl substituent on the triple bond or a sterically bulky group on nitrogen.

4.4 Experimental Section

4.4.1 General procedure for the synthesis of 3-ynamides **1a**, **1b**, **1d**, **1f**, **1i-p**

To a stirred solution of alk-3-ynoic acids (10,2 mmol) [pent-3-ynoic acid: 1 g; dec-3-ynoic acid²²: 1.72 g; oct-3-ynoic acid²²: 1.43 g; hex-3-ynoic acid²²: 1.14 g; 4-phenylbut-3-ynoic acid²²: 1.63 g; 4-(trimethylsilyl)but-3-ynoic acid²³: 1.59 g] and amine (10,2 mmol) [benzylamine: 1.09 g; butylamine: 0.75 g; isopentylamine: 0.89 g; hexylamine: 1.03 g; isobutylamine: 0.75 g; 3-phenylpropan-1-amine: 1,38 g; 3-methoxypropan-1-amine: 0.91 g; furfurylamine: 0.99 g; cyclohexylmethanamine: 1.15 g; cyclopentanamine: 0.86 g; isopropylamine: 0.60 g] in anhydrous CH₂Cl₂ (52 mL), was added under nitrogen EDC·HCl (7.95 mmol; 1,52 g). The resulting mixture was stirred at room temperature for 3 h. Then, water (20 mL) was added and the phases were separated. The aqueous phase was extracted twice with CH₂Cl₂ (2 × 10 mL) and the combined organic phases were washed with water (20 mL) and then were dried over Na₂SO₄. After filtration and evaporation of the solvent, the crude products were purified by column chromatography on silica gel using 8:2 hexane-AcOEt as eluent.

Substrates **1c**, **1g** and **1h**, were prepared according a known procedure²⁴⁻²⁶.

4.4.2 Preparation of methyl pent-3-ynoylglycinate **1e**

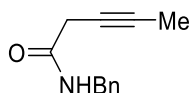
To a stirred solution of pent-3-ynoic acid (0.5 g; 5,1 mmol) and glycine methylester hydrochloride (0.64 g; 5.1 mmol) in anhydrous CH₂Cl₂ (45 mL), was added, under nitrogen, DMAP (1.13 g; 9.28 mmol) at 0°C. Then always at 0°C EDC·HCl (0.98 g; 5.1 mmol) was added portionwise. The resulting mixture was stirred at 0°C for 0.5 h and then at room temperature for 15 h. Then, a 1M aqueous solution of HCl (56 mL) was added and the phases were separated. The aqueous phase was extracted twice with CH₂Cl₂ (2 × 20 mL) and the combined organic phases were washed with a saturated solution of NaHCO₃ (20 mL) and then were dried over Na₂SO₄. After filtration and evaporation of the solvent, the crude product was purified by column chromatography on silica gel using 6:4 hexane-AcOEt as eluent.

4.4.3 General procedure for the carboxylation of alk-3-ynamides **1** to give 1,3-oxazine-2,4-diones **2a-p** (Table 4.2)

A 250 stainless steel autoclave was charged with a solution of **1** (0.6 mmol)[**1a**: 112.3 mg; **1b**: 120.8 mg; **1c**: 137.6 mg; **1d**: 154.4 mg; **1e**: 101.5 mg; **1f**: 91.9 mg; **1g**: 149.6 mg; **1h**: 147.2 mg; **1i**: 164.1 mg; **1j**: 143.7 mg; **1k**: 126.8 mg; **1l**: 135.2 mg; **1m**: 150.9; **1n**: 136.4; **1o**: 141.2; **1p**: 118.4] in a 1-3 mixture of CH(OMe)₃-CH₃CN (12 mL) and DBU (36,5 mg, 0,24 mmol). The autoclave was sealed, purged at room temperature several times with CO₂ with stirring (5 atm), and finally pressurized with CO₂ (30 atm). After being stirred at 80 °C for 15 h, the autoclave was cooled, degassed and opened. The solvent was evaporated and the products were purified by column chromatography on silica gel using as eluent: 7:3 hexane – AcOEt for **2a, 2d-f, 2h, 2j-o** and 8:2 hexane – AcOEt for **2b-c, 2g, 2i, 2p**.

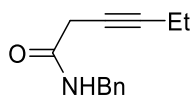
4.5 Characterization Data

Characterization of 3-ynamides **1a-o** and 1,3-oxazine-2,4-diones **2a-p**



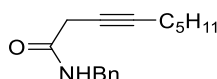
N-benzylpent-3-ynamide (**1a**).

Yield: 1.25 g, starting from 1.00 g of pent-3-ynoic acid (65%). Colourless solid, mp: 84 - 86°C; ¹H NMR (300 MHz, CDCl₃): δ = 7.40 – 7.24 (m, 5 H, Ph), 6.92 (br s, 1 H, NH), 4.47 (d, *J* = 5.9, 2 H, CH₂Ph), 3.19 (q, *J* = 2.6, 2 H, COCH₂), 1.81 (t, *J* = 2.6, 3 H, Me); ¹³C NMR (75 MHz, CDCl₃): δ = 167.5, 138.0, 128.7, 127.6, 127.5, 81.7, 72.1, 43.6, 27.7, 3.6; GC/MS (EI): *m/z* = 187 (M⁺, 1), 172 (5), 143 (52), 129 (11), 104 (4), 91 (100), 77 (7).



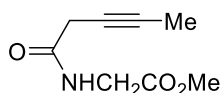
N-benzylhex-3-ynamide (**1b**).

Yield: 1.03 g, starting from 1.14 g of hex-3-ynoic acid (50%). Colorless solid, mp: 65 - 68°C; IR (KBr): ν = 3286 (m), 1635 (s), 1543 (m), 1458 (m), 1373 (m), 1242 (m), 1064 (w), 748 (m), 694 (m); ¹H NMR (300 MHz, CDCl₃): δ = 7.38 – 7.24 (m, 5 H aromatic), 6.90 (br s, 1 H, NH), 4.47 (d, *J* = 5.9, 2 H, CH₂ Ph), 3.21 (t, *J* = 2.4, 2 H, COCH₂), 2.18 (qt, *J* = 7.5, 2.4, 2H, ≡CCH₂), 1.10 (t, *J* = 7.5, 3H, CH₃); ¹³C NMR (75 MHz, CDCl₃): δ = 167.5, 138.0, 128.7, 127.6, 127.5, 87.7, 72.4, 43.7, 27.8, 13.8, 12.4; GC/MS (EI): *m/z* = 201 (M⁺, 1), 157 (21), 142 (18), 129 (10), 91 (100).



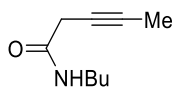
N-benzyldec-3-ynamide (**1d**).

Yield: 1.79 g, starting from 1.72 g of dec-3-ynoic acid (68%). Colorless solid, mp: 40-42°C. IR (film): ν = 3924 (m), 2932 (m), 2180 (vw), 1651 (s), 1551 (m), 1458 (m), 1373 (m), 1342 (m), 1242 (m), 1065 (w), 988 (w), 748 (s), 703 (s); ¹H NMR (300 MHz, CDCl₃): δ = 7.40 – 7.28 (m, 5 H, Ph), 6.88 (br s, 1 H, NH), 4.98 (d, *J* = 5.8, 2 H, CH₂Ph), 3.23 (t, *J* = 2.4, 2 H, COCH₂), 2.21 – 2.12 (m, 2 H, C≡CCH₂), 1.46 (quint, *J* = 7.2, 2 H, C≡CCH₂CH₂), 1.38 – 1.18 (m, 6 H, C≡CCH₂CH₂CH₂CH₂CH₂), 0.87 (t, *J* = 6.5, 3 H, Me); ¹³C NMR (75 MHz, CDCl₃): δ = 167.5, 137.9, 128.7, 127.60, 127.56, 86.6, 73.0, 43.7, 31.3, 28.57, 28.55, 27.8, 22.5, 18.7, 14.1; GC/MS: *m/z* = 257 (M⁺, 1), 186 (9), 172 (4), 160 (2), 149 (6), 129 (8), 106 (5), 91 (100), 77 (7).

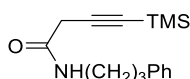


Methyl pent-3-ynoylglycinate (**1e**).

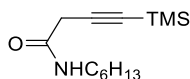
Yield: 0.69 g, starting from 0.64 g of glycine methylester hydrochloride (80%). Colourless solid, mp: 41 - 43°C; IR (film): ν = 3333 (m), 3062.96 (m), 2955 (m), 2237 (w), 1751. (s), 1667 (s), 1535 (m), 1435 (m), 1373 (m), 1211 (s), 1034 (w), 988 (w), 733 (m); ¹H NMR (300 MHz, CDCl₃): δ = 7.12 (br s, 1 H, NH), 4.08 (d, *J* = 5.3, 2 H, NCH₂), 3.78 (s, 3 H, OMe), 3.21 (q, *J* = 2.6, 2 H, COCH₂C≡C), 1.88 (t, *J* = 2.6, 3 H, C≡CCH₃); ¹³C NMR (75 MHz, CDCl₃): δ = 170.2, 167.9, 81.9, 71.7, 52.5, 41.4, 27.5, 3.6; GC/MS = 169 (M⁺, 14), 137 (6), 116 (95), 110 (24), 88 (100).



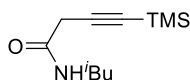
N-butylpent-3-ynamide (**1f**). Yield: 0.81 g, starting from 1 g of pent-3-ynoic acid (52%). Colorless solid, mp: 26 - 27°C; IR (film): $\nu = 3294$ (m), 2955(m), 2932 (m), 1651 (s), 1543 (m), 1265 (w), 741(w), 579(w); ^1H NMR (300 MHz, CDCl_3): $\delta = 6.60$ (br s, 1 H, NH), 3.28 (q, $J = 7.1$, 2 H, NCH_2), 3.19 (q, $J = 2.6$, 2 H, COCH_2), 1.87 (t, $J = 2.6$, 3 H, $\text{C}\equiv\text{CCH}_3$), 1.52 (quint, $J = 7.1$, 2 H, NCH_2CH_2), 1.37 (sext, $J = 7.3$, 2 H, CH_2CH_3), 0.94 (t, $J = 7.3$, 3 H, CH_2CH_3); ^{13}C NMR (75 MHz, CDCl_3): $\delta = 167.4$, 81.6, 72.4, 39.5, 31.6, 27.7, 20.1, 13.8, 3.6; GC/MS (EI): $m/z = 153$ (M^+ , 2), 138 (2), 124 (8), 111 (19), 100 (49), 96 (5), 81 (5), 67 (9), 57 (100).



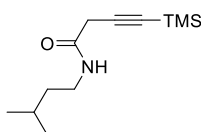
N-(3-phenylpropyl)-4-(trimethylsilyl)but-3-ynamide (**1i**). Yield: 1.45 g starting from 1.59 g of 4-(trimethylsilyl)but-3-ynoic acid (52%). Yellow oil. IR (film) $\nu = 3294$ (m), 2183 (w), 1666 (s), 1527 (m), 1249 (m), 1033 (w), 840 (s), 756 (w), 702 (w); ^1H NMR (300 MHz, CDCl_3): $\delta = 7.32$ -7.23 (m, 2 H aromatic), 7.22-7.12 (m, 3 H aromatic), 6.69 (br s, 1 H, NH), 3.32 - 3.21 (m, 2 H, CH_2NH), 3.20 (s, 2 H, COCH_2), 2.65 (t, $J=7.5$, CH_2Ph), 1.85 (quint, $J=7.5$, 2 H, $\text{CH}_2\text{CH}_2\text{NH}$), 0.20 (s, 9H, SiMe_3); ^{13}C NMR (75 MHz, CDCl_3): $\delta = 166.3$, 141.1, 128.4, 128.2, 126.0, 99.5, 90.8, 39.1, 32.9, 30.8, 28.7, -0.2; GC/MS: $m/z = 273$ (M^+ , 20), 258 (10), 169 (33), 162 (36), 117 (27), 91 (100), 73 (73).



N-hexyl-4-(trimethylsilyl)but-3-ynamide (**1j**). Yield: 1.81 g, starting from 1.59 g of 4-(trimethylsilyl)but-3-ynoic acid (74%). Yellow oil; IR (film): $\nu = 3294$ (m), 2183 (w), 1659 (s), 1551 (m), 1250 (m), 1042 (w), 849 (s); ^1H -NMR (500 MHz, CDCl_3): $\delta = 6.59$ (br s, 1 H, NH), 3.30 - 3.25 (m, 2 H, CH_2NH), 3.21 (s, 2 H, COCH_2), 1.53 (quint, $J = 7.1$, 2 H, $\text{CH}_2\text{CH}_2\text{NH}$), 1.38 - 1.28 (m, 6 H, $\text{CH}_2\text{CH}_2\text{CH}_2\text{CH}_3$), 0.90 (t, $J = 7.0$, 3 H, CH_3), 0.19 (s, 9H, SiMe_3); ^{13}C -NMR (125 MHz, CDCl_3): $\delta = 166.2$, 99.8, 91.0, 39.8, 31.5, 29.3, 28.8, 26.5, 22.6, 14.0, -0.16; GC/MS (EI): $m/z = 239$ (M^+ , 6), 224 (27), 200 (22), 182 (10), 169 (11), 128 (38), 112 (51), 85 (30) 73 (100).

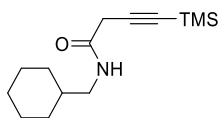


N-isobutyl-4-(trimethylsilyl)but-3-ynamide (**1k**). Yield: 0.97 g, starting from 1.59 g of 4-(trimethylsilyl)but-3-ynoic acid (45%). Colourless solid, mp: 55 - 60°C. IR (KBr): $\nu = 3287$ (m), 2183 (w), 1651 (s), 1558 (m), 1465 (w), 1250 (m), 1026 (w), 849 (s); ^1H -NMR (500 MHz, CDCl_3): $\delta = 6.68$ (br s, 1 H, NH), 3.23 (s, 2 H, COCH_2), 3.14 - 3.10 (m, 2 H, CH_2NH), 1.81 (nonuplet, $J = 6.7$, 1 H, $\text{CH}(\text{CH}_3)_2$), 0.95 (d, $J = 6.7$, 6 H, 2 CH_3), 0.19 (s, 9H, SiMe_3); ^{13}C -NMR (125 MHz, CDCl_3): $\delta = 166.2$, 99.8, 91.2, 46.9, 28.9, 28.3, 20.0, 19.9, -0.17; GC/MS (EI): $m/z = 211$ (M^+ , 5), 196 (15), 140 (7), 116 (7), 112 (39), 97 (12), 83 (15), 73 (100).



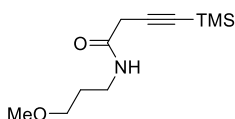
N-isopentyl-4-(trimethylsilyl)but-3-ynamide (**1l**). Yield: 1.03 g starting from 1.59 g of 4-(trimethylsilyl)but-3-ynoic acid (45%). Colorless solid, mp: 44 - 48°C; IR (KBr): $\nu = 3264$ (m), 2183 (w), 1651 (s), 1574 (m), 1466 (m), 1250 (m), 1042 (w),

849 (s); $^1\text{H-NMR}$ (300 MHz, CDCl_3): δ = 6.55 (br s, 1 H, NH), 3.36 – 3.26 (m, 2 H, CH_2NH), 3.22 (s, 2 H, COCH_2), 1.66 (nonuplet, J = 6.6, 1 H, $\text{CH}(\text{CH}_3)_2$), 1.49 – 1.38 (m, 2 H, $\text{CH}_2\text{CH}_2\text{NH}$), 0.94 (d, J = 6.6, 6 H, 2 CH_3), 0.20 (s, 9 H, SiMe_3); GC/MS (EI): m/z = 225 (M^+ , 2), 210 (18), 186 (13), 169 (15), 140 (4), 114 (21), 112 (36), 97 (12), 83 (14), 73 (100).



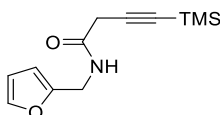
N-(cyclohexylmethyl)-4-(trimethylsilyl)but-3-ynamide (**1m**).

Yield: 1.80 g, starting from 1.59 g of 4-(trimethylsilyl)but-3-ynoic acid (70%). Colorless solid, mp: 79-81°C; IR (KBr): ν = 3271 (m), 2183 (w), 1651 (s), 1574 (m), 1450 (m), 1250 (m), 1072 (w), 980 (m), 841 (s); $^1\text{H-NMR}$ (500 MHz, CDCl_3): δ = 6.65 (br s, 1 H, NH), 3.22 (s, 2 H, COCH_2), 3.13 (t, J = 6.3, 2 H, CH_2NH), 1.79 – 1.64 (m, 5 H, cyclohexyl), 1.55 – 1.44 (m, 1 H, cyclohexyl), 1.30 – 1.12 (m, 3 H, cyclohexyl), 1.02 – 0.92 (m, 2 H, cyclohexyl), 0.19 (s, 9H, SiMe_3); $^{13}\text{C-NMR}$ (125 MHz, CDCl_3): δ = 166.2, 100.0, 91.3, 45.9, 37.9, 30.8, 28.9, 26.4, 25.9, -0.13; GC/MS (EI): m/z = 251 (M^+ , 4), 236 (13), 212 (15), 169 (10), 156 (38), 140 (28), 112 (41), 97 (63), 73 (100).



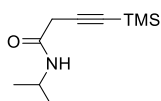
N-(3-methoxypropyl)-4-(trimethylsilyl)but-3-ynamide (**1n**).

Yield: 1.41 g starting from 1.59 g of 4-(trimethylsilyl)but-3-ynoic acid (61%). Yellow oil. IR (film): ν = 3302 (m), 2183 (w), 1659 (s), 1535 (m), 1250 (m), 1119 (m), 1042 (w), 849 (s); $^1\text{H-NMR}$ (500 MHz, CDCl_3): δ = 6.94 (br s, 1 H, NH), 3.48 (t, J = 5.9, 2 H, CH_2OCH_3), 3.39 (q, J = 6.2, 2 H, CH_2NH), 3.35 (s, 3 H, OCH_3), 3.22 (s, 2 H, COCH_2), 1.83 – 1.77 (m, 2 H, $\text{CH}_2\text{CH}_2\text{NH}$), 0.20 (s, 9H, SiMe_3); $^{13}\text{C-NMR}$ (125 MHz, CDCl_3): δ = 166.4, 99.5, 90.6, 71.2, 58.8, 38.1, 29.0, 28.8, -0.15; GC/MS (EI): m/z = 227 (M^+ , 10), 212 (10), 188 (8), 169 (11), 152 (6), 129 (7), 116 (71), 112 (18), 97 (15), 84 (70), 73 (100).



N-(furan-2-ylmethyl)-4-(trimethylsilyl)but-3-ynamide (**1o**).

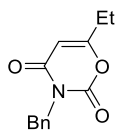
Yield: 1.85 g starting from 1.59 g of 4-(trimethylsilyl)but-3-ynoic acid (77%). Yellow oil. IR (KBr): ν = 3294 (m), 2183 (w), 1666 (s), 1535 (m), 1404 (w), 1250 (m), 1018 (w), 849 (s); $^1\text{H-NMR}$ (500 MHz, CDCl_3): δ = 7.37 (dd, J = 1.9, 0.8, 1 H, H-4), 6.89 (br s, 1 H, NH), 6.33 (dd, J = 3.2, 1.9, 1 H, H-3), 6.26 – 6.24 (m, 1 H, H-2), 4.46 (d, J = 5.5, 2 H, CH_2NH), 3.25 (s, 2 H, COCH_2), 0.17 (s, 9H, SiMe_3); $^{13}\text{C-NMR}$ (125 MHz, CDCl_3): δ = 166.3, 150.9, 142.4, 110.6, 107.5, 99.4, 91.5, 37.0, 28.8, -0.19. GC/MS (EI): m/z = 235 (M^+ , 20), 234 (21), 218 (22), 162 (26), 145 (12), 96 (9), 81 (100), 73 (39).



N-isopropyl-4-(trimethylsilyl)but-3-ynamide (**1p**).

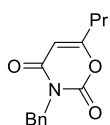
Yield: 1.17 g starting from 1.59 g of 4-(trimethylsilyl)but-3-ynoic acid (58%). Colorless solid, mp: 66-70 °C; IR (KBr): ν = 3279 (m), 2183 (w), 1651 (s), 1558 (m), 1250 (m), 1049 (w), 849 (s); $^1\text{H-NMR}$ (500 MHz, CDCl_3): δ = 6.39 (br s, 1 H, NH), 4.10 – 3.99 (m, 1 H, $\text{CH}(\text{CH}_3)_2$), 3.19 (s, 2 H, COCH_2), 1.19 (d, J = 6.6, 2 H, 2 CH_3), 0.20 (s, 9H, SiMe_3); $^{13}\text{C-NMR}$ (125 MHz, CDCl_3): δ = 166.4,

100.0, 91.3, 41.7, 29.0, 22.6, -0.15; GC/MS (EI): m/z = 197 (M^+ , 4), 182 (17), 158 (23), 140 (10), 112 (48), 97 (14), 86 (18), 73 (100).



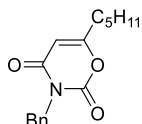
3-benzyl-6-ethyl-2H-1,3-oxazine-2,4(3H)-dione (2a).

Yield: 91.6 mg starting from 112.3 mg g of **1a** (66%). Colorless oil. IR (film): ν = 1759 (s), 1697 (s), 1396 (m), 1342 (m), 1196 (m), 1072 (m), 833 (m), 733 (m); ^1H NMR (300 MHz, CDCl_3): δ = 7.51 – 7.43 (m, 2 H aromatic), 7.36 – 7.24 (m, 3 H aromatic), 5.76 (s, 1 H, CH), 5.03 (s, 2 H, CH_2Ph), 2.43 (qd, J = 7.5, 0.9, 2 H, CH_2CH_3), 1.20 (t, J = 7.5, 3 H, Me); ^{13}C NMR (75 MHz, CDCl_3): δ = 169.2, 161.4, 149.1, 135.7, 129.2, 128.5, 128.1, 99.8, 44.9, 26.0, 10.0; GC/MS (EI): m/z = 231 (M^+ , 49), 133 (22), 105 (16), 91 (100), 69 (14).



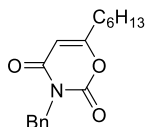
3-benzyl-6-propyl-2H-1,3-oxazine-2,4(3H)-dione (2b).

Yield: 97.1 mg starting from 120.8 mg g of **1b** (66%). Colorless solid, mp: 56 -59 °C. IR (KBr) ν = 1751 (s), 1697 (s), 1396 (m), 1195 (w), 1134 (w), 995 (w), 756 (m), 732 (m); ^1H NMR (300 MHz, CDCl_3): δ = 7.50 – 7.43 (m, 2 H aromatic), 7.37 – 7.23 (m, 3 H aromatic), 5.76 (s, 1 H, CH), 5.02 (s, 2H, CH_2Ph), 2.36 (t, J = 7.4, 2H, = CCH_2), 1.65 (hex, J = 7.4, 2H, CH_2CH_3), 0.98 (t, J = 7.4, 3H, Me); ^{13}C NMR (75 MHz, CDCl_3): δ = 167.9, 161.3, 149.1, 135.7, 129.2, 128.5, 128.1, 100.6, 44.9, 34.6, 19.2, 13.4.; GC/MS (EI): m/z = 245 (M^+ , 25), 133 (15), 113 (41), 105 (12), 91 (100), 77 (11).



3-Benzyl-6-pentyl-2H-1,3-oxazine-2,4(3H)-dione (2c).

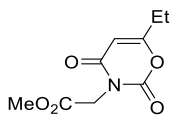
Yield: 98.4 mg starting from 137.6 mg g of **1c** (60%). Colorless solid, mp: 45 -49 °C. IR (KBr) ν = 1751 (s), 1697 (s), 1658 (m), 1396 (m), 1350 (m), 1195 (m), 995 (m), 756 (m), 601 (m); ^1H NMR (300 MHz, CDCl_3): δ = 7.50 – 7.44 (m, 2 H aromatic), 7.36 – 7.27 (m, 3 H aromatic), 5.76 (s, 1 H, CH), 5.03 (s, 2 H, CH_2Ph), 2.38 (t, J = 7.6, 2 H, = CCH_2), 1.67 – 1.54 (m, 2 H, $\text{CH}_2\text{CH}_2\text{CH}_2\text{CH}_3$), 1.40 – 1.26 (m, 4 H, $\text{CH}_2\text{CH}_2\text{CH}_3$), 0.90 (t, J = 6.9, 3 H, Me); ^{13}C NMR (75 MHz, CDCl_3): δ = 168.2, 161.4, 149.1, 135.7, 129.3, 128.5, 128.1, 100.5, 44.9, 32.7, 31.0, 25.5, 22.2, 13.8; GC/MS (EI): m/z = 273 (M^+ , 27), 141 (40), 133 (18), 105 (11), 91 (100), 84 (16).



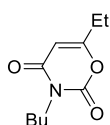
3-Benzyl-6-heptyl-2H-1,3-oxazine-2,4(3H)-dione (2d).

Yield: 121.2 mg starting from 154.4 mg of **1d** (67%). Colorless solid, mp: 38 – 40 °C. IR (KBr): ν = 1751 (s), 1697 (s), 1396 (m), 1196 (m), 1134 (m), 1072 (m), 864 (m), 756 (m), 725 (m); ^1H NMR (300 MHz, CDCl_3): δ = 7.51 – 7.44 (m, 2 H aromatic), 7.36 – 7.27 (m, 3 H aromatic), 5.76 (s, 1 H, CH), 5.03 (s, 2 H, CH_2Ph), 2.39 (t, J = 7.5, 2 H, C= CCH_2), 1.61 (quint, J = 7.5, 2 H, C= CCH_2CH_2), 1.42 – 1.22 (m, 8 H, C= $\text{CCH}_2\text{CH}_2\text{CH}_2\text{CH}_2\text{CH}_2\text{CH}_2$), 0.88 (t, J = 7.0, 3 H, Me); ^{13}C NMR (75 MHz, CDCl_3): δ = 168.2, 161.4, 149.2, 135.7, 129.3, 128.5, 128.1, 100.5, 44.9, 32.8, 31.6,

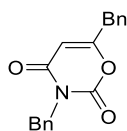
28.8, 25.8, 22.6 14.4; GC/MS (EI): m/z = 301 (M^+ , 23), 217 (2), 169 (33), 150 (7), 133 (19), 105 (12), 91 (100), 84 (17), 69 (20).



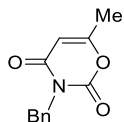
Methyl 2-(6-ethyl-2,4-dioxo-2H-1,3-oxazin-3(4H)-yl)acetate (2e). Yield: 88.3 mg starting from 101.5 mg of **1e** (69%). Colorless oil. IR (film): ν = 1751 (s), 1697 (s), 1412 (m), 1389 (m), 1219 (m), 1011 (w), 795 (m). ^1H NMR (300 MHz, CDCl_3): δ = 5.82 (t, J = 0.9, 1 H, CH), 5.63 (s, 2 H, NCH_2), 3.78 (s, 3 H, CO_2Me), 2.51 (qd, J = 7.5, 0.9, 2 H, CH_2CH_3), 1.25 (t, J = 7.5, 3 H, CH_2CH_3); ^{13}C NMR (75 MHz, CDCl_3): δ = 169.8, 167.4, 160.8, 148.8, 99.4, 52.7, 42.2, 26.2, 10.0; GC/MS (EI): m/z = 213 (M^+ , 9), 181 (34), 154 (13), 116 (5), 110 (2), 98 (68), 88 (18), 69 (100), 57 (77).



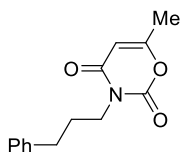
3-Butyl-6-ethyl-2H-1,3-oxazine-2,4(3H)-dione (2f). Yield: 59.2 mg starting from 91.9 mg g of **1f** (50%). Colorless solid, mp: 26 - 27 °C. IR (KBr): ν = 1766 (s), 1697 (s), 1396 (m), 1366 (m), 1204 (m), 833 (m), 756 (m); ^1H NMR (300 MHz, CDCl_3): δ = 5.75 (t, J = 0.9, 1 H, CH), 3.87 (t, J = 7.5, 2 H, NCH_2), 2.47 (qd, J = 7.5, 0.9, 2 H, CH_2CH_3), 1.69 – 1.56 (m, 2 H, NCH_2CH_2), 1.36 (sept, J = 7.3, 2 H, $\text{NCH}_2\text{CH}_2\text{CH}_3$), 1.23 (t, J = 7.5, 3 H, CH_2CH_3), 0.95 (t, J = 7.3, 3 H, $\text{NCH}_2\text{CH}_2\text{CH}_3$); ^{13}C NMR (75 MHz, CDCl_3): δ = 169.1, 161.5, 149.1, 99.7, 41.7, 29.4, 26.0, 20.0, 13.7, 10.0; GC/MS (EI): m/z = 197 (M^+ , 2), 180 (2), 168 (5), 155 (8), 142 (100), 128 (7), 112 (8), 98 (43), 69 (88).



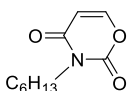
3,6-Dibenzyl-2H-1,3-oxazine-2,4(3H)-dione (2g). Yield: 89.8 mg starting from 149.6 mg g of **1g** (51%). Yellow solid, mp = 45 – 49 °C. IR (KBr) ν = 1767 (s), 1697 (s), 1396 (m), 1196 (w), 1003 (m), 864 (m), 725 (s); ^1H NMR (500 MHz, CDCl_3): δ = 7.50 – 7.18 (m, 10 H aromatic), 5.62 (s, 1 H, CH), 5.00 (s, 2 H, NCH_2Ph), 3.66 (s, 2 H, CH_2Ph); ^{13}C NMR (125 MHz, CDCl_3): δ = 167.0, 161.2, 148.9, 135.6, 133.0, 129.4, 129.3, 129.1, 128.6, 128.1, 127.9, 101.4, 45.0, 39.1; GC/MS (EI): m/z = 293 (M^+ , 45), 202 (3), 161 (21), 133 (12), 105 (7), 91 (100).



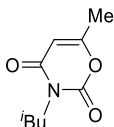
3-benzyl-6-methyl-2H-1,3-oxazine-2,4(3H)-dione (2h). Yield: 109.5 mg starting from 147.2 mg g of **1h** (84%). Colorless solid, mp = 82 - 87 °C. IR (KBr): ν = 1759 (s), 1690 (s), 1389 (m), 1350 (m), 1204 (w), 1080 (w), 996 (m), 733 (m); ^1H NMR (300 MHz, CDCl_3): δ = 7.50 – 7.43 (m, 2 H aromatic), 7.37 – 7.28 (m, 3 H aromatic), 5.80 – 5.76 (m, 1 H, CH), 5.03 (s, 2 H, CH_2Ph), 2.17 (d, J = 0.9, 3 H, Me); ^{13}C NMR (75 MHz, CDCl_3): δ = 164.6, 161.2, 150.0, 135.6, 129.2, 128.6, 128.1, 101.4, 44.9, 19.1; GC/MS (EI): m/z = 217 (M^+ , 52), 133 (18), 105 (16), 91 (100), 88 (11), 65 (15).



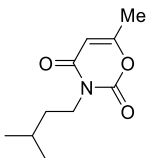
6-Methyl-3-(3-phenylpropyl)-2H-1,3-oxazine-2,4(3H)-dione (2i). Yield: 116.3 mg starting from 164.1 mg g of **1i** (79%). Colorless solid, mp = 35-37°C. IR (KBr): ν = 1774 (s), 1697 (s), 1651 (m), 1396 (m), 1365 (m), 1134 (w), 1002 (w), 864 (m), 756 (m), 702 (m), 625 (w); ^1H NMR (300 MHz, CDCl_3): δ = 7.32 – 7.22 (m, 3 H aromatic), 7.22 – 7.15 (m, 2 H aromatic), 5.70 (s, 1 H, CH), 3.92 (t, $J=7.6$, 2 H, CH_2N), 2.67 (t, $J=7.6$ 2 H, CH_2Ph), 2.13 (s, 3 H, Me), 1.99 (quint, $J=7.6$, 2 H, $\text{CH}_2\text{CH}_2\text{N}$); ^{13}C NMR (75 MHz, CDCl_3): δ = 164.5, 161.2, 148.9, 141.0, 128.4, 128.2, 125.9, 101.3, 41.7, 33.0, 28.5, 19.0; GC/MS (EI): m/z = 245 (M^+ , 27), 161 (15), 141 (21), 128 (52), 118 (100), 117 (95), 91 (53).



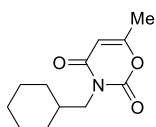
3-Hexyl-6-methyl-2H-1,3-oxazine-2,4(3H)-dione (2j). Yield: 110.3 mg starting from 143.7 mg g of **1j** (87%). Colorless solid, mp = 68-71°C. IR (KBr) ν = 1751 (s), 1697 (s), 1396 (m), 1358 (m), 1319 (m), 1196 (w), 1057 (w), 995 (w), 856 (m), 756 (s); ^1H NMR (500 MHz, CDCl_3): δ = 5.75 (q, $J = 0.9$, 1 H, CH), 3.88 – 3.82 (m, 2 H, NCH_2), 2.19 (d, $J = 0.9$, 3 H, Me), 1.67 – 1.59 (m, 2H, NCH_2CH_2), 1.38 – 1.27 (m, 6 H, $\text{CH}_2\text{CH}_2\text{CH}_2\text{CH}_3$), 0.88 (s, 3 H, CH_2CH_3); ^{13}C NMR (125 MHz, CDCl_3): δ = 164.4, 161.3, 149.0, 101.5, 42.0, 31.4, 27.3, 26.4, 22.5, 19.1, 14.0; GC/MS (EI): m/z = 211 (M^+ , 1), 169 (8), 141 (13), 128 (100), 85 (41).



3-Isobutyl-6-methyl-2H-1,3-oxazine-2,4(3H)-dione (2k). Yield: 89.0 mg starting from 126.8 mg g of **1k** (81%). Colorless solid, mp = 60 – 63°C. IR (KBr): ν = 1759 (s), 1697 (s), 1396 (m), 1342 (m), 1219 (w), 1065 (m), 864 (m), 756 (m); ^1H NMR (300 MHz, CDCl_3): δ = 5.77 – 5.75 (m, 1 H, C=CH), 3.72 (d, $J = 7.5$, 2 H, NCH_2), 2.20 (d, $J = 0.9$, 3 H, C=CCH₃) 2.22 – 2.05 (m, 1 H, $\text{CH}(\text{CH}_3)_2$), 0.93 (d, $J = 6.8$, 6 H, $\text{CH}(\text{CH}_3)_2$); ^{13}C NMR (75 MHz, CDCl_3): δ = 164.5, 161.6, 149.3, 101.4, 48.6, 26.7, 19.9, 19.1; GC/MS (EI): m/z = 183 (M^+ , absent), 168 (2), 141 (7), 128 (100), 110 (2), 100 (3), 85 (48), 69 (33).

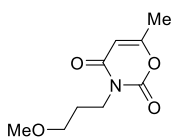


3-Isopentyl-6-methyl-2H-1,3-oxazine-2,4(3H)-dione (2l). Yield: 100.6 mg starting from 135.2 mg g of **1l** (85%). Colorless solid, mp = 36 – 39°C. IR (KBr): ν = 1767 (s), 1697 (s), 1435 (m), 1396 (m), 1366 (m), 1204 (m), 1126 (m), 995 (m), 825 (m), 756 (m); ^1H NMR (300 MHz, CDCl_3): δ = 5.77 – 5.76 (m, 1 H, C=CH), 3.91 – 3.84 (m, 2 H, NCH_2), 2.19 (d, $J = 0.9$, 3 H, C=CCH₃) 1.71 – 1.56 (m, 1 H, $\text{CH}(\text{CH}_3)_2$), 1.56 – 1.47 (m, 2 H, NCH_2CH_2), 0.96 (d, $J = 6.5$, 6 H, $\text{CH}(\text{CH}_3)_2$); ^{13}C NMR (75 MHz, CDCl_3): δ = 164.4, 161.2, 148.9, 101.4, 40.5, 36.0, 26.1, 22.4, 19.1; GC/MS (EI): m/z = 197 (M^+ , 1), 154 (5), 141 (16), 128 (100), 114 (5), 85 (42), 69 (31).



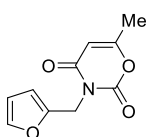
3-(Cyclohexylmethyl)-6-methyl-2H-1,3-oxazine-2,4(3H)-dione (2m).

Yield: 103.2 mg starting from 150.9 mg of **1m** (77%). Colorless solid, mp = 88 -90°C. IR (KBr): $\nu = 1744$ (s), 1713 (s), 1443 (m), 1396 (m), 1350 (m), 1204 (m), 1042 (m), 856 (m), 756 (m); ^1H NMR (500 MHz, CDCl_3): $\delta = 5.75$ (q, $J = 0.9$, 1 H, C=CH), 3.73 (d, $J = 7.4$, 2 H, NCH_2), 2.19 (d, $J = 0.9$, 3 H, C=CCH₃), 1.85 – 1.75 (m, 1 H, CHCH₂), 1.74 – 1.68 (m, 2 H, cyclohexyl), 1.66 – 1.60 (m, 2 H, cyclohexyl), 1.27 – 1.11 (m, 4 H, cyclohexyl), 1.07 – 0.98 (m, 2 H, cyclohexyl); ^{13}C NMR (125 MHz, CDCl_3): $\delta = 164.4$, 161.6, 149.3, 101.4, 47.5, 36.0, 30.6, 26.3, 25.7, 19.1; GC/MS (EI): $m/z = 223$ (M^+ , 3), 141 (28), 128 (100), 96 (13), 85 (30).



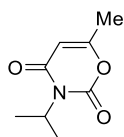
3-(3-Methoxypropyl)-6-methyl-2H-1,3-oxazine-2,4(3H)-dione (2n).

Yield: 98.0 mg starting from 136.4 mg of **1n** (82%). Colorless solid, mp : 60 -61°C. IR (KBr): $\nu = 1751$ (s), 1697 (s), 1396 (m), 1358 (m), 1119 (m), 1056 (m), 1003 (m), 856 (m), 756 (m); ^1H NMR (500 MHz, CDCl_3): $\delta = 5.76$ (q, $J = 0.9$, 1 H, C=CH), 3.97 (t, $J = 7.0$, 2 H, NCH_2), 3.44 (t, $J = 6.1$, 2 H, CH_2OMe), 3.31 (s, 3 H, OMe), 2.19 (d, $J = 0.9$, 3 H, C=CCH₃), 1.94 – 1.88 (m, 2 H, NCH_2CH_2); ^{13}C NMR (125 MHz, CDCl_3): $\delta = 164.5$, 161.3, 149.0, 101.4, 70.3, 58.6, 39.7, 27.4, 19.1; GC/MS (EI): $m/z = 199$ (M^+ , absent), 184 (24), 169 (21), 141 (27), 128 (79), 85 (100).



3-(Furan-2-ylmethyl)-6-methyl-2H-1,3-oxazine-2,4(3H)-dione (2o).

Yield: 92.0 mg starting from 141.2 mg of **1o** (74%). Colorless solid, mp: 69 – 73°C. IR (KBr): $\nu = 1751$ (s), 1705 (s), 1381 (m), 1343 (m), 995 (m), 856 (m), 748 (s); ^1H NMR (500 MHz, CDCl_3): $\delta = 7.34$ (dd, $J = 1.9, 0.9$, 1 H, H-5), 6.41 – 6.38 (m, 1 H, H-4), 6.31 (dd, $J = 3.2, 1.9$, 1 H, H-3), 5.78 (q, $J = 0.9$, 1 H, C=CH), 5.05 (s, 2 H, NCH_2), 2.18 (d, $J = 0.9$, 3 H, C=CCH₃); ^{13}C NMR (125 MHz, CDCl_3): $\delta = 164.8$, 160.7, 148.8, 142.5, 110.5, 109.9, 101.4, 37.7, 19.1; GC/MS (EI): $m/z = 207$ (M^+ , 39), 123 (41), 85 (45), 81 (100).



3-Isopropyl-6-methyl-2H-1,3-oxazine-2,4(3H)-dione (2p).

Yield: 44.7 mg starting from 118.4 mg of **1p** (44%). Yellow solid, mp: 53 – 57°C. IR (KBr): $\nu = 1712$ (s), 1659 (s), 1365 (m), 1227 (w), 1065 (m), 856 (m), 764 (m); ^1H NMR (500 MHz, CDCl_3): $\delta = 5.71$ (q, $J = 0.9$, 1 H, C=CH), 5.06 (quint, $J = 6.9$, 1 H, NCH), 2.16 (d, $J = 0.9$, 3 H, C=CCH₃), 1.45 (d, $J = 6.9$, 6 H, $\text{CH}(\text{CH}_3)_2$); ^{13}C NMR (125 MHz, CDCl_3): $\delta = 164.4$, 161.8, 148.0, 101.6, 45.9, 29.7, 18.94, 18.88; GC/MS (EI): $m/z = 169$ (M^+ , 13), 128 (100), 85 (75)

4.6 References

- [1] C. Federsel; R. Jackstell; M. Beller; *Angew. Chem.* **2010**, *122*, 6392-6295.
- [2] D.W. Keith *Science*, **2009**, *325*, 1654-1655.
- [3] D.R. Ahuja, *Nature* ,**1990**, *344*, 529-531
- [4] G.A. Olah; A. Goepfert; G.K.S. Prakash *J. Org. Chem.* **2009**, *74*, 487-498.
- [5] A. Correa; T. Leon; R. Martin *J. Am. Chem. Soc.* **2014**, *136*, 1062-1069.
- [6] R. Francke, B. Schille and M. Roemelt, *Chemical Reviews* **2018**, *118*, 4631-4701.
- [7] Q. Liu, L. Wu, R. Jackstell and M. Beller, *Nature Communications* **2015**; *6*, 1-15.
- [8] C. Villiers, J.-P. Dognon, R. Pollet, P. Thuery, M. Ephritikhine, *Angew. Chem. Int. Ed.* **2010**, *49*, 3465 –3468; *Angew. Chem.* **2010**, *122*, 3543 – 3546.
- [9] Y. Kayaki, M. Yamamoto, T. Ikariya, *Angew. Chem. Int. Ed.* **2009**, *48*, 4194 –4197; *Angew. Chem.* **2009**, *121*, 4258 –4261.
- [10] R. Dalpozzo, N. della Ca', B. Gabriele and R. Mancuso, *Catalysts* **2019**, *9*, 1-59.
- [11] a) M. E. Dyen, D. Swern, *Chem. Rev.* **1967**, *67*, 197 –246; b) T. A. Mukhtar, G. D. Wright, *Chem. Rev.* **2005**, *105*, 529–542.
- [11] V. Ji Ram, A. Sethi, M. Nath, R. Pratap, *The Chemistry of Heterocycles, Chemistry of Six-to-Eight-Membered N, O, S, P and Se Heterocycles* **2019**, *1*^o, Elsevier, 306-318.
- [12] M. Kobayashi, M. Kitazawa and T. Saito, *Yakugaku Zasshi* **1984**, *104*, 680-690.
- [13] J. Irinia C., W. Ruth R., Q. Jennifer, N. Suanne, Q. Mimi L., W. Shuaige, S.H.Joanne M., *Word Intellectual Property Organization* **2002**.
- [14] S. R. Safir, R. Edge, R. J. Lopresti, *United States Patent Office* **1957**.
- [15] G. Maffii, G. Bianchi, P. Schiatti and B. Silvestrini, *British Journal of Pharmacology* **1961**, *16*, 231-243.
- [16] M. Yogo, K. Hirota and Y. Maki, *Journal of the Chemical Society, Perkin Transactions 1* **1984**, 2097-2102.
- [17] L. Capuano, H. Reiner Kirn and R. Zander, *Chemische Berichte* **1976**, *109*, 2456-2461.
- [18] R. Daniel Little and Wade A. Russu, *Journal of Organic Chemistry* **2000**, *65*, 8096-8099.
- [19] M. Sato, N. Katagiri, K. Takayama, M. Hirose and C. Kaneko, *Chemical and Pharmaceutical Bulletin* **1989**, *37*, 665-669.
- [20] G. Chen, C. Fu, and S. Ma, *Organic Letters* **2009**, *11*, 2900-2903.
- [21] R. Mancuso, I. Ziccarelli, C.S. Pomelli, C. Cuocci, N. Della Ca', D. Olivieri, C. Carfagna, B. Gabriele, *J. Catal.* (**2020**) *387*, 145-153.
- [22] Weiwei Fang, B. Breit, *S.I. Angewandte Chemie International Edition*, **2018**, *57*, 14817-14821.
- [23] H.M Davies, T.A. Boebel *Tetrahedron Lett.*, **2000**, *41*, 8189
- [24] W. Shi, C. Liu, Z. Yu, A. Lei *Chem. Comm.*, **2007**, 2342.
- [25] G.A. Molander, K.M. Traister *Org. Lett.*, **2013**, *15*, 5052
- [26] S. Usugi, H. Yorimitsu, H. Shinokubo, K. Oshima, *Bull. Chem. Soc. Jap.*, **2002**, *75*, 2687.

Chapter 5

Synthesis of Oxazinobenzimidazolone Derivatives by ZnCl₂-Promoted Cyclization

5.1 Introduction

5.1.1 Pharmacological importance of Oxazinones

1,3-Oxazinan-2-one derivatives are an important class of heterocycles, which possess remarkable biological activities, including antibacterial, anticancer, and antidiabetic activity.

In a recent work¹, have been reported molecules containing chiral nucleus 1,3-oxazinan-2-one that exhibit potent antibacterial activities against the tested Gram-positive bacteria, including *Staphylococcus aureus*, *Enterococcus faecalis*, and *Bacillus subtilis*. These compounds have been designed based on structural features of existing synthetic antibacterial agents.

The basic structure of these compound is a tertiary amine composed of a 1,3-oxazinan-2-one and two aromatic groups (Figure 5.1.1).

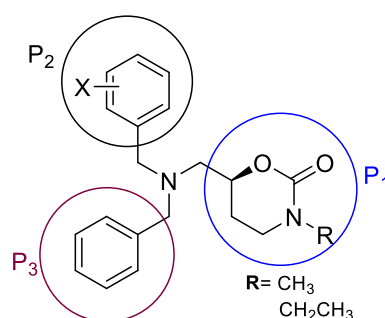
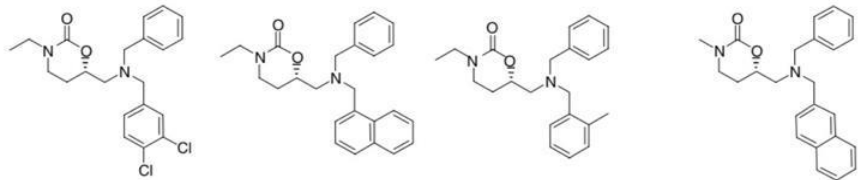


Fig.5.1.1 Basic structure of 1,3-oxazinan-2-one derivatives with antibacterial activities

As reported in the literature¹, the activities of different derivatives with chiral 1,3-oxazinan-2-one core were evaluated with standard methods, which include testing against different strains of Gram-positive bacteria from the American Type Culture Collection (ATCC), *S. aureus* 29213, *S. aureus* 43300, *E. faecalis* 29212 and *Bacillus subtilis* PY79.

The results obtained showed that the various compounds have moderate to potent activity against all four bacterial strains and, in particular, the most potent compounds, A11, A13, A17 and B9, with the related MIC₉₀ of *S. aureus* 29213 and *B. Subtilis* 79 are shown in the following Figure 5.1.2.



		A11	A13	A17	B9
MIC ₉₀ µg/mL	<i>S. aureus</i> 29213	9.85	14.9	29.8	14.9
	<i>B. subtilis</i> PY79	7.44	30.0	59.5	30.0

Fig.5.1.2 MIC₉₀ for *S. aureus* 29213 and *B. Subtilis* 79 of the most potent compounds A11, A13, A17 and B9

Among the molecules of natural origin characterized by a 1,3-oxazinane-2-one nucleus is the powerful antimetabolic agent Maytansine (Figure 5.1.3).

Maytansine is a benzoansamamcrolide antibiotic originally isolated from the African shrub *Maytenus ovatus*. The antimetabolic effect is due to its ability to bind tubulin in or near the Vinblastine binding site and inhibit the assembly of microtubules, causing mitosis to be stopped. Maytansine exhibits cytotoxicity against many tumor cell lines and can inhibit tumor growth *in vivo*².

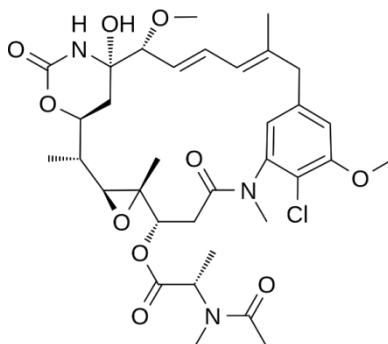


Fig.5.1.3 Structure of Maytansine

Although maytansine has not been successful in clinical use, the unusually high cytotoxic activity of maitansinoids, chemical derivatives of maitansin, makes them interesting candidates for tissue-specific delivery, as in an antibody-drug conjugate. Selective delivery to tumor tissue has the effect of modifying the distribution and pharmacokinetics of the cytotoxic agent *in vivo*. Humanized monoclonal antibodies typically have a circulation half-life of approximately two weeks in humans. Hence, the binding of a small drug molecule to the antibody will prevent penetration into healthy tissue and can extend the *in vivo* half-life of the

drug (typically minutes to hours for unconjugated drug) up to two weeks, accumulating thus a proportionately larger amount in malignant tissue than in healthy tissue. Preclinical evaluations of a series of antibody-maytansinoid conjugates have shown that this specific delivery approach significantly improves the specificity for the tumor and the antitumor activity of maytansinoids.

Several conjugates have shown promising clinical results. In particular, the thiomethyl derivatives of maitansin, S-methyl-DM1 and S-methyl-DM4 (Figure 5.1.4), are the main cellular or hepatic metabolites of antibody-maitansinoid conjugates, prepared with maitansinoids containing thiol DM1 and DM4, respectively ³.

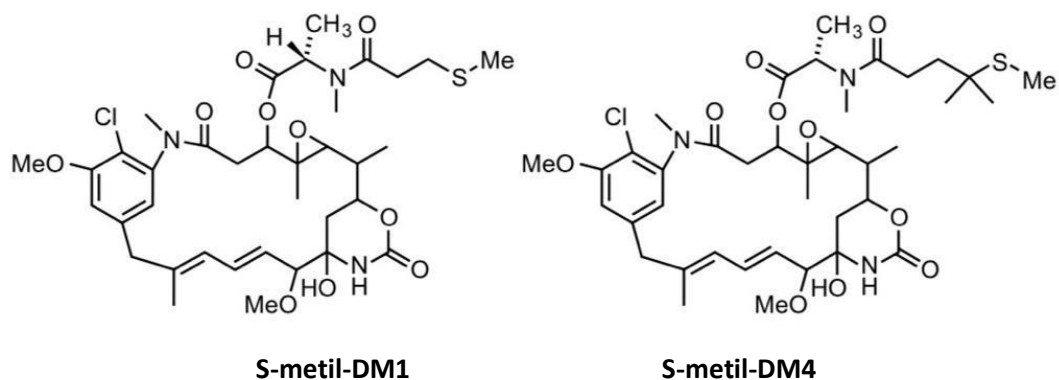


Fig.5.1.4 Thiomethyl derivatives of maitansin

The antibody-conjugates of DM1 and DM4 are able to kill different types of cancer cells in the concentration range from nanomolar to picomolar.

A potent inhibitor of 11- β -hydroxysteroid dehydrogenase type 1 (11 β HSD1) with nucleus 1,3-oxazinan-2-one was recently discovered, for the treatment of diabetes, defined as BI-135585 (Figure 5.1.5). The inhibitory activity of BI-135585 was tested in human preadipocytes, adipocyte and liver tissues of the monkey cynomolgus ex vivo, and the results indicated that substantial inhibition of 11 β -HSD1 activity was achieved after treatment with BI- 135585. The compound inhibited 11 β HSD1 activity in human adipocytes with an IC₅₀ of 4.3 nM and in human primary adipose tissue with an IC₈₀ of 53 nM.

The molecule showed excellent potency against 11 β -HSD1 in human adipocytes, with 1000 times greater selectivity than three other hydroxysteroid dehydrogenases, including 11 β -HSD2⁴.

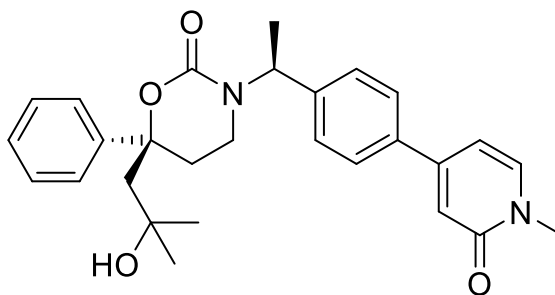


Fig.5.1.5 Structure of potent inhibitor of 11 β HSD1 with nucleus 1,3-oxazinan-2-one

Diabetes is a chronic disease characterized by an excess of sugar (glucose) in the blood and is divided into two main forms: type 1 diabetes, characterized by an inability to produce sufficient insulin and type 2 diabetes characterized by an inability to respond adequately to insulin. Furthermore, diabetes is often associated with obesity, dyslipidemia and hypertension, which together are known as the metabolic syndrome. In recent years, research has shown that the aberrant overexpression of 11- β -HSD1 contributes to the development of the metabolic syndrome⁵. 11 β -hydroxysteroid dehydrogenase type 1 (11 β -HSD1) is a key enzyme in metabolism, belongs to the reductase family and catalyzes the intracellular conversion of the inactive glucocorticoid cortisone into the physiologically active cortisol, in the presence of nicotinamide adenine dinucleotide phosphate (NADPH). 11 β -HSD1 is expressed in almost all tissues, including adult brain, inflammatory cells and gonads, but mainly in the liver and adipose tissue⁶.

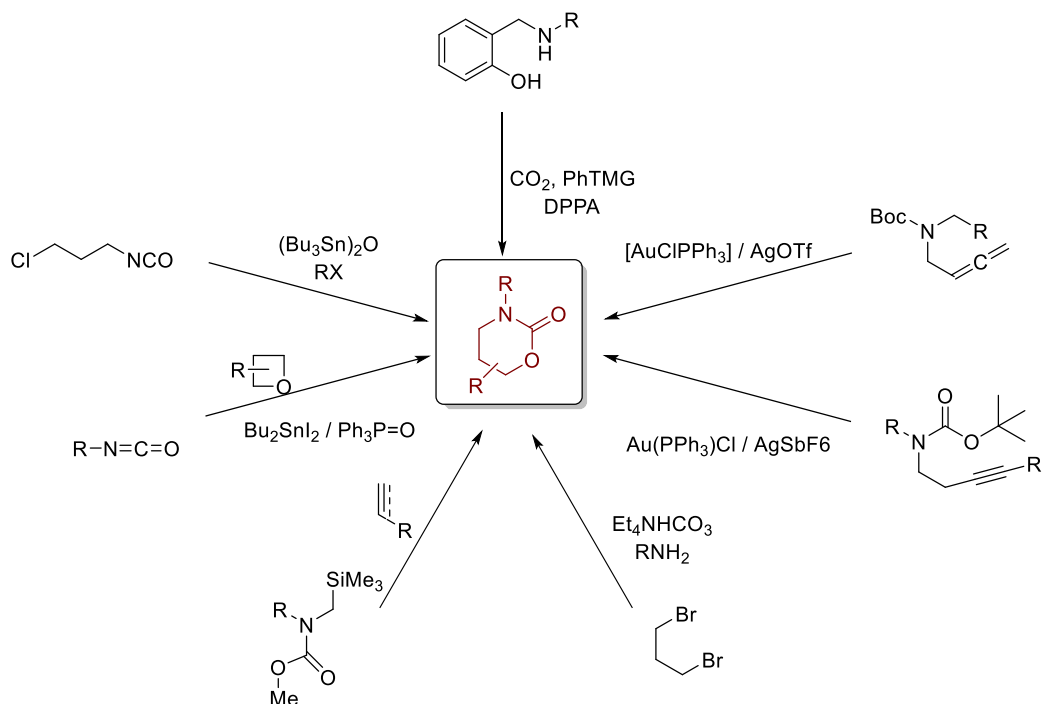
In the literature there are numerous studies that highlight the correlation between the overexpression of 11 β -HSD1 in adipose tissue with obesity, insulin resistance, diabetes and cardiovascular disease in humans.

5.1.2 Synthesis of Oxazinones derivatives

The search for new practical and efficient synthetic routes for the preparation of 1,3-oxazinan-2-one derivatives is of great interest, thanks to the exceptional biological activities shown by these molecules. Therefore, it is not surprising that various synthetic methods for building this heterocyclic system have been reported in the literature.

Among many current methodologies: reactions of CO₂ with amino alcohols⁷; gold-catalyzed synthetic routes from easily accessible allenic carbamates⁸ or N-Boc-protected

alkynylamines⁹; one-pot reaction of readily available tetraethylammonium bicarbonate, 1,3-dibromopropane, and a primary amine¹⁰; cycloaddition reaction with a variety of dienophiles such as alkenes and alkynes¹¹; cycloadditions of oxetanes with isocyanates¹², coupling of the adducts from the reaction between $(\text{Bu}_3\text{Sn})_2\text{O}$ and haloalkyl isocyanate with alkyl halides¹³, are the most interesting ones (Scheme 5.1.1)



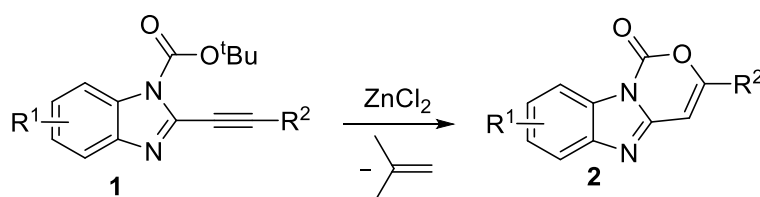
Scheme 5.1.1 Synthesis of various methodologies for the preparation of Oxazinones derivatives reported in the literature⁷⁻¹³

5.2 Results and discussion

Considering the importance of developing an efficient method for the synthesis of high value-added polycyclic heterocyclic derivatives, is particularly attractive the possibility to obtain them by a simple cyclization process by metal-promoted annulation of acyclic precursors, starting from readily available substrates¹⁴⁻¹⁸

Furthermore, among acyclic substrates able to undergo a metal-promoted cyclization to give a polycyclic heterocycle, functionalized alkynes bearing a suitably placed heteronucleophile play a major role, as the triple bond can be easily electrophilically activated by a suitable metal species thus promoting the cyclization by intramolecular nucleophilic attack¹⁹⁻²³. Usually, processes like these are promoted by costly metals, mainly gold^{24,25} and palladium²⁶, besides rhodium²⁷, platinum²⁸, and, occasionally, ruthenium²⁹. On the other hand, the use of less expensive metal species, such as cobalt³⁰, nickel³¹, copper³², zinc³³, and silver³⁴ compounds, has been scantily reported in the literature, and applied to a limited number of examples.

In this work³⁵, we have reported the use of very simple and inexpensive ZnCl_2 as a promoter for the efficient deprotective heterocyclization of *N*-Boc-2-alkynylbenzimidazoles **1**, to give access to novel polycyclic heterocycles, that are, 1*H*-benzo[4,5]imidazo[1,2-*c*][1,3]oxazin-1-ones **2** (Scheme 5.2.1). This synthesis method was accomplished exploiting the *tert*-butyloxycarbonyl protecting group as indirect carboxylation agent.

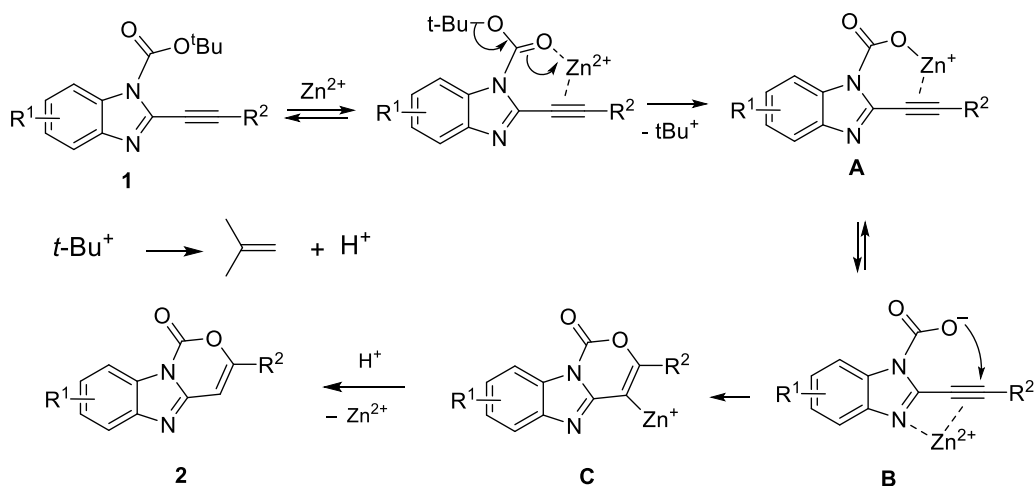


Scheme 5.2.1 ZnCl_2 -assisted heterocyclization of *N*-Boc-alkynylbenzimidazoles **1** to benzimidazoxazinones **2**.

It is known that zinc(II) compounds are able to promote Boc deprotection.³⁶⁻⁴¹ In particular, an excess of ZnBr_2 has been successfully employed for the deprotection of secondary amines³⁹ as well as of *tert*-butyl esters^{40,41}.

According to our rationale, the zinc center should play a double role, that is, to promote deprotection to give a carbamate species **A** (with elimination of isobutene and H^+ from the

ensuing *tert*-butyl carbocation) and then assist a 6-*endo-dig* heterocyclization by intramolecular nucleophilic attack of the free carbamate group of species **B** (in equilibrium with **A**) on the triple bond activated by coordination to Zn²⁺ (with the zinc center stabilized by chelation by the benzimidazole nitrogen). This would lead to organozinc intermediate **C**, whose protonolysis would then afford the polycyclic heterocycles **2** (Scheme 5.2.2; zinc counteranions have been omitted for clarity).



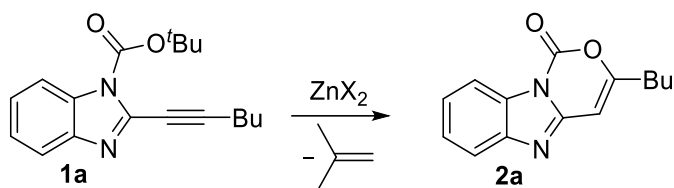
Scheme 5.2.2. Mechanistic hypothesis for the formation of polycyclic heterocycles **2** by Zn²⁺-mediated sequential deprotection-6-*endo-dig* heterocyclization of *N*-Boc-alkynylbenzimidazoles **1**

The first experiments were carried out with *N*-Boc-2-(hex-1-in-1-yl)-1*H*-benzo[*d*]imidazole **1a** as substrate (R¹=H, R²=Bu) (prepared by alkynylation of *N*-Boc-2-bromo-1*H*-benzo[*d*]imidazole), which was allowed to react in CH₂Cl₂ as the solvent at room temperature in the presence of ZnBr₂ (1 equiv). Under these conditions, after 3 h reaction time, substrate conversion was 51%, while the desired 3-butyl-1*H*-benzo[4,5]imidazo[1,2-*c*][1,3]oxazin-1-one **2a** was isolated in 25% yield. In spite of the low yield, this initial result was encouraging, since confirmed the validity of mentioned above work hypothesis and the possibility to synthesize a novel class of polycyclic heterocycles with a very simple approach and using an inexpensive promoter.

In order to improve the reaction performance, and achieve a higher **2a** yield, we then changed some operative parameters (Table 5.1, entries 2-9). Practically no reaction occurred by changing the solvent to MeOH (Table 5.1, entry 2), while only traces of **2a** were detected in acetone (Table 5.1, entry 3). Lowering the amount of ZnBr₂ significantly suppressed the

reaction (Table 5.1, entry 4). On the other hand, the use of 1.5 or 2 equiv of ZnBr_2 was beneficial, **2a** being formed in ca. 70% isolated yield (Table 5.1, entries 5 and 6, respectively). Better results with respect to the parent reaction (Table 5.1, entry 1) were also obtained by increasing the **1a** concentration from 0.5 (Table 5.1, entry 1) to 1 mmol / mL of CH_2Cl_2 (Table 5.1, entry 7), while more diluted conditions led to a lower **2a** yield (Table 5.1, entry 8). Predictably, a faster reaction was observed at 40 °C rather than 25 °C, with a higher yield of **2a** (Table 5.1, entry 9) with respect to the initial experiment (Table 5.1, entry 1). Under the optimized conditions (40 °C in CH_2Cl_2 in the presence of 1.5 equiv of ZnBr_2 , with a substrate concentration of 1 mmol per mL of solvent), **2a** could be finally obtained in a yield as high as 79% (Table 5.1, entry 10). The structure of **2a** was unequivocally confirmed by XRD analysis (figure 5.2.1).

Table 5.1. ZnX_2 -promoted deprotective heterocyclization of *N*-Boc-2-(hex-1-in-1-yl)-1*H*-benzo[*d*]imidazole **1a** under different conditions^[a]



Entry	ZnX_2 (equiv)	T (°C)	Solvent	Concentration of 1a ^[b]	Conversion of 1a [%] ^[c]	Yield of 2a [%] ^[d]
1	ZnBr_2 (1)	25	CH_2Cl_2	0.5	51	17
2	ZnBr_2 (1)	25	MeOH	0.5	3	0
3	ZnBr_2 (1)	25	acetone	0.5	12	traces
4	ZnBr_2 (0.5)	25	CH_2Cl_2	0.5	9	6
5	ZnBr_2 (1.5)	25	CH_2Cl_2	0.5	100	72
6	ZnBr_2 (2)	25	CH_2Cl_2	0.5	100	70
7	ZnBr_2 (1)	25	CH_2Cl_2	1	62	33
8	ZnBr_2 (1)	25	CH_2Cl_2	0.2	42	10
9	ZnBr_2 (1)	40	CH_2Cl_2	0.5	100	63
10	ZnBr_2 (1.5)	40	CH_2Cl_2	1	100	79
11	ZnCl_2 (1.5)	40	CH_2Cl_2	1	100	82
12	ZnI_2 (1.5)	40	CH_2Cl_2	1	100	77

^[a]All reactions were carried out for 3 h. ^[b]Mmol of starting **1a** per mL of solvent. ^[c]Based on unreacted **1a**, upon isolation from the reaction mixture. ^[d] Isolated yield based on starting **1a**.

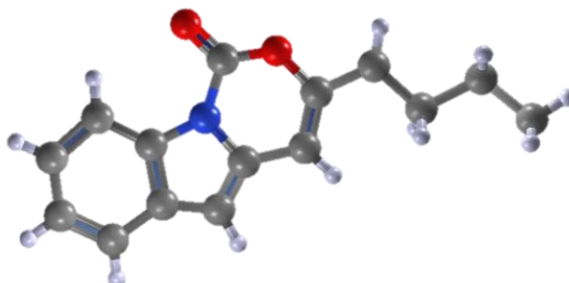
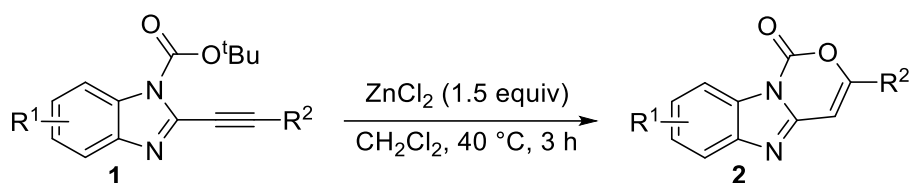


Fig. 5.2.1 Molecular structure of 3-butyl-1H-benzo[4,5]imidazo[1,2-c][1,3]oxazin-1-one **2a**. Color legend: carbon (light grey), hydrogen (white), oxygen (red), nitrogen (blue).

With considerable interest, the reaction was also performed successfully with ZnCl₂ (Table 5.1, entry 11) or ZnI₂ (Table 5.1, entry 12) and the best yield of **2a** being obtained with ZnCl₂ (82%, Table 5.1, entry 11). This result, in with the lower cost of ZnCl₂, made ZnCl₂ the promoter of choice for realizing the synthesis of **1a** into benzimidazoxazinone **2a** and for the subsequent generalization study to other differently substituted substrates (Table 5.2). Thus, to assess the generality of the reaction, various *N*-Boc-alkynylbenzimidazoles **1** (bearing different R¹ and R² groups) were subjected to the reaction conditions of Table 5.1, entry 11, with ZnCl₂ as the promoter (Table 5.2, entries 2-15).

Table 5.2. Synthesis of 1*H*-benzo[4,5]imidazo[1,2-*c*][1,3]oxazin-1-ones **2** by ZnCl₂-promoted deprotective heterocyclization of *N*-Boc-2-alkynylbenzimidazoles **1**.^[a]



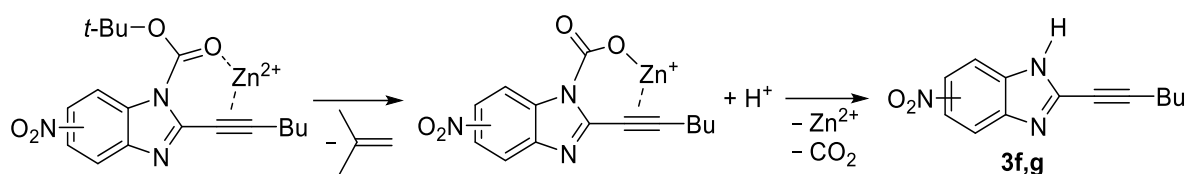
Entry	1	2	Yield of 2 [%] ^[b]
1			82
2			77
3			76
4			83
5			77
6			45 ^[c]
7			30 ^[d]
8			85

9			82
10			80
11			70
12			66
13			60
14			74
15			66

^{a)} All reactions were carried out in CH₂Cl₂ (1 mmol of **1** per mL of solvent) at 40 °C for 3 h. ^{b)} Isolated yield based on starting **1a**. ^{c)} The reaction led also to 2-(hex-1-yn-1-yl)-6-nitro-1*H*-benzo[d]imidazole **3f** in 20% isolated yield. ^{d)} The reaction led also to 2-(hex-1-yn-1-yl)-5-nitro-1*H*-benzo[d]imidazole **3g** in 31% isolated yield.

As can be seen from Table 5.2, entries 2-5, excellent results were obtained with substrates still with R² = Bu and bearing either electron-donating (methyl or methoxy; yields of the corresponding products **2b-d** were 76-83%, Table 5.2, entries 2-4) or electron-withdrawing chlorine substituents (yield of **2e** = 77%, Table 5.2, entry 5) on the aromatic ring. On the other hand, inferior results were observed with substrates **1f** and **1g**, bearing a strong electron-withdrawing group nitro substituent (yields of **2f** and **2g** were 45% and 30%, Table 5.2, entries 6 and 7, respectively). With these substrates, decarboxylation of the carbamate intermediate competed with heterocyclization, as confirmed by the formation of not negligible amounts of

deprotected compounds **3f** and **3g** (20% and 31%, respectively, Table 5.2, entries 6 and 7) (Scheme 5.2.3), not observed in other cases. The diminished nucleophilicity of the carbamate intermediate **B**, induced by the strong electron-withdrawing effect of the nitro group, bring the formation of byproducts **3f** and **3g** from substrates **1f** and **1g**. The structures of products **2c** and **2f** were confirmed by XRD analysis (Figures 5.2.2 and 5.2.3, respectively).



Scheme 5.2.3 Formation of byproducts **3f** and **3g** (Table 3.2, entries 6 and 7) by Boc-deprotection of nitro-substituted substrates **1f** and **1g**, competitive with heterocyclization.

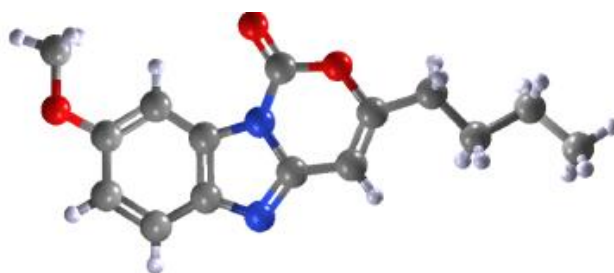


Fig. 5.2.2 Molecular structure of 3-butyl-8-methoxy-1H-benzo[4,5]imidazo[1,2-c][1,3]oxazin-1-one **2c**. Color legend: carbon (light grey), hydrogen (white), oxygen (red), nitrogen (blue)

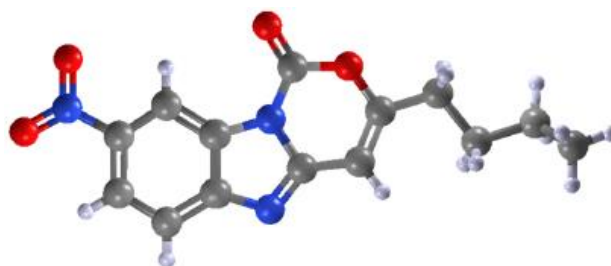
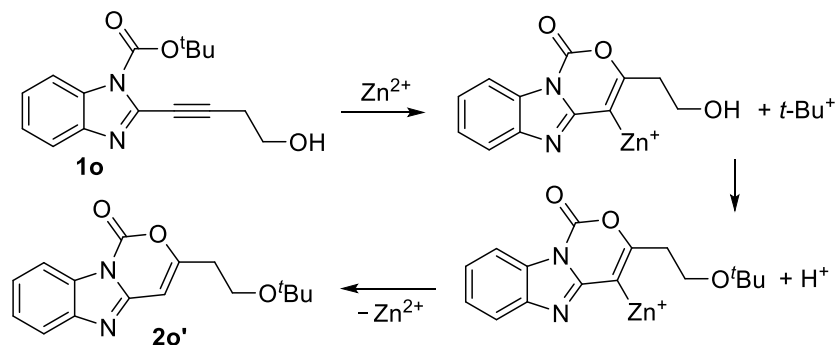


Fig. 5.2.3 Molecular structure of 3-butyl-8-nitro-1H-benzo[4,5]imidazo[1,2-c][1,3]oxazin-1-one **2f**. Color legend: carbon (light grey), hydrogen (white), oxygen (red), nitrogen (blue)

The corresponding benzimidazoxazinones were obtained with high yields changing the alkyl substituent on the triple bond R² to octyl (yield of **2h**, 85%; Table 5.2, entry 8), isopentyl (yield of **2i**, 82%; Table 5.2, entry 9), or phenethyl (yield of **2j**, 80%; Table 5.2, entry 10), while a slightly lower yield was observed with R² = cyclohexylmethyl (yield of **2k**, 70%; Table 5.2, entry 11). The use of a substrate with the triple bond conjugated with an alkenyl group, as in *N*-Boc-2-(cyclohex-1-en-1-ylethynyl)-1*H*-benzo[*d*]imidazole **1l**, led to a satisfactory yield of the corresponding polycyclic heterocycle **2l** (66%; Table 5.2, entry 12).

The method also worked nicely with substrates bearing a functionalized alkyl chain of the triple bond, as shown by the results obtained with a methoxymethyl (yield of **2m**, 60%; Table 5.2, entry 13) or a 2-(methoxycarbonyl)ethyl (yield of **2n**, 74%; Table 5.2, entry 14) group. Interestingly in the case of *N*-Boc-4-(1*H*-benzo[*d*]imidazol-2-yl)but-3-yn-1-ol **1o**, bearing a 2-hydroxyethyl group on the triple bond, the *tert*-butyl group was incorporated into the final product to give 3-(2-(*tert*-butoxy)ethyl)-1*H*-benzo[4,5]imidazo[1,2-*c*][1,3]oxazin-1-one **2o'** (66% yield; Table 5.2, entry 15). This is clearly due to the trapping of the *tert*-butyl carbocation, ensuing from deprotection by the nucleophilic hydroxyl group, as shown in Scheme 5.2.4.



Scheme 5.2.4 Plausible mechanism for the formation of product **2o'** (chloride anions are omitted for clarity).

5.3 Conclusions

In conclusion, in this work has been described the ZnCl₂-promoted heterocyclization with ZnCl₂ in under mild conditions (40 °C in CH₂Cl₂ for 3h), giving access to a new class of polycyclic heterocycles, 1*H*-benzo[4,5]imidazo[1,2-*c*][1,3]oxazin-1-ones. In the present study the ZnCl₂, simple and inexpensive, assisted the 6-*endo-dig* heterocyclization of the carbamate intermediate with incorporation of the carbamate group (as indirect carboxylation agent) into the final polyheterocyclic derivative, while in the previous literature ZnCl₂ was reported to promote complete N-Boc deprotection with elimination of isobutene and CO₂. ZnCl₂ thus played a dual role, by promoting the Boc deprotection of the substrate with elimination of the *tert*-butyl carbonation (which could be trapped by substrates bearing a nucleophilic group) and activating the triple bond toward the intramolecular nucleophilic attack by the carbamate moiety. The benzimidazoxazinone derivatives have been obtained in moderate to high yields starting from differently substituted substrates, and the structure of representative products was confirmed by X-ray diffraction analysis.

5.4 Experimental Section

5.4.1 General procedure for the preparation of *N*-Boc-alkynylbenzoimidazoles **1a-o**

Substrates **1a-1o** were prepared by Boc protection of 2-bromo-1*H*-benzo[*d*]imidazoles (as reported in the literature)¹⁴ followed by Sonogashira coupling reaction with terminal alkynes, as described below.

5.4.1.1 General procedure for the Boc protection of 2-bromo-1*H*-benzo[*d*]imidazoles

To a solution of the 2-bromo-1*H*-benzo[*d*]imidazole derivative (11.7 mmol) (2-bromo-1*H*-benzo[*d*]imidazole: 2.30 g; 2-bromo-5,6-dimethyl-1*H*-benzo[*d*]imidazole: 2.63 g; 2-bromo-5-methoxy-1*H*-benzo[*d*]imidazole: 2.11 g; 2-bromo-5,6-dichloro-1*H*-benzo[*d*]imidazole: 3.11 g; 2-bromo-5-nitro-1*H*-benzo[*d*]imidazole: 2.83 g) in an anhydrous DMF-CH₃CN mixture (1:1, v/v; 92 mL), was added triethylamine (2 mL, 14 mmol) under nitrogen. The mixture was allowed to stir for 30 min at room temperature and then solution of Boc₂O (3.82 g, 17.5 mmol) in anhydrous DMF (33 mL) was added dropwise. After the addition was complete, the reaction was allowed to stir at room temperature overnight. After evaporation of the solvent, products were purified by flash chromatography on silica gel using a 7:3 hexane-EtOAc (v/v) as eluent.

5.4.1.2 General procedure for coupling reaction of *N*-Boc-2-bromo-1*H*-benzo[*d*]imidazoles and 1-alkynes

To a stirred solution of *N*-Boc-2-bromo-1*H*-benzo[*d*]imidazole derivatives (3.36 mmol) [*N*-Boc-2-bromo-1*H*-benzo[*d*]imidazole: 1.00 g; *N*-Boc-2-bromo-5,6-dimethyl-1*H*-benzo[*d*]imidazole: 1.09 g; *N*-Boc-2-bromo-5,6-dichloro-1*H*-benzo[*d*]imidazole: 1.23 g; *N*-Boc-2-bromo-5-methoxy-1*H*-benzo[*d*]imidazole: 1.10 g; *N*-Boc-2-bromo-5-nitro-1*H*-benzo[*d*]imidazole: 1.15 g] in NEt₃ (34 mL) were added under nitrogen 1-alkyne (5.04 mmol) [hex-1-yne: 414.1 mg; dec-1-yne: 696.8 mg; 5-methylhex-1-yne: 484.7 mg; but-3-yn-1-ylbenzene: 656.2 mg; prop-2-yn-1-ylcyclohexane: 615.9 mg; 1-ethynylcyclohex-1-ene: 535.1 mg; 3-methoxyprop-1-yne: 353.3 mg; but-3-yn-1-ol: 353.3 mg; methyl pent-4-ynoate 565.1 mg], and CuI (96 mg, 0.504 mmol) and Pd(OAc)₂ (75 mg, 0.0336 mmol). The reaction mixture was stirred for 20 h under nitrogen at room temperature, and then was filtered on celite washing the precipitate several time

with 1:3 EtOAc-hexane mixture. The solvent was evaporated under reduce pressure and then the crude products were dissolved in AcOEt (250 ml). To the solution was added a 1% solution HCl (50 mL) and the organic layer was separated. The organic layer was then washed with water (50 mL) and brine (50mL). The resulting organic phase was dried with Na₂SO₄. After filtration and evaporation of the solvent, the products were purified by column chromatography on silica gel using 9:1 hexane-AcOEt as eluent for substrates **1a-c**, **1h-o** and 95:5 hexane-AcOEt for substrates **1d-g**.

5.4.2 General procedure for the synthesis of benzoimidazoxazinones derivatives 2

A Schlenk flask was charged under nitrogen with the *N*-Boc-2-alkynylbenzimidazole **1** (1 mmol) (**1a**: 298 mg; **1b**: 326 mg; **1c**: 328 mg; **1d**: 328 mg; **1e**: 367 mg; **1f**: 343 mg; **1g**: 343 mg; **1h**: 354 mg; **1i**: 312 mg; **1j**: 346 mg; **1k**: 338 mg; **1l**: 322 mg; **1m**: 286 mg; **1n**: 328 mg; **1o**: 286 mg), anhydrous CH₂Cl₂ (1 mL), and ZnCl₂ (204 mg, 1.5 mmol). The reaction mixture was heated at 40°C and then allowed to stir at this temperature for 3 h. After cooling, the reaction mixture was diluted with CH₂Cl₂ (5 mL) and water (5 mL) (for **2a-1**, **2n**, and **2o'**) or the solvent was evaporated and water was added to the residue (20 mL) (for **1m**). The phases were separated the aqueous phase was washed with CH₂Cl₂ (5 mL), and the combined organic phases were dried with Na₂SO₄; after filtration and evaporation of the solvent, the product was purified by column chromatography on silica gel using hexane/AcOEt (8:2, v/v) as the eluent (for **2a-2l**, **2n**, and **2o'**). For the purification of **2m**, the suspension obtained as seen above was filtered, the precipitate washed with water (3 × 5 mL) and then purified by column chromatography on silica gel using hexane/AcOEt (8:2, v/v) as eluent. With substrates **1f** and **1g**, the reaction also led to the formation of deprotected products **3f** and **3g**, respectively (Scheme 3.5) (order of elution: **3f** followed by **2f**; **2g** followed by **3g**).

5.5 Characterization Data

Characterization of 2-bromo-1*H*-benzo[*d*]imidazoles, *N*-Boc-alkynylbenzoimidazoles **1a-o**, benzoimidazoxazinones derivatives **2** and nitro-protected compounds **3f** and **3g**.

N-Boc-2-bromo-1*H*-benzo[*d*]imidazole. Yield: 3.30 g, starting from 2.30 g of 2-bromo-1*H*-benzo[*d*]imidazole (95%). ¹H NMR (300 MHz, CDCl₃): δ = 7.95 – 7.86 (m, 1 H aromatic), 7.72 – 7.66 (m, 1 H aromatic), 7.38 – 7.29 (m, 2 H aromatic), 1.75 (s, 9 H, *t*-Bu). ¹³C NMR (75 MHz, CDCl₃): δ = 147.7, 141.8, 132.3, 124.5, 124.4, 122.3, 118.2, 114.3, 87.8, 27.8. The spectroscopic data agreed with those reported in the literature⁴².

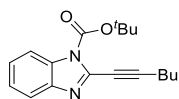
N-Boc-2-bromo-5,6-dimethyl-1*H*-benzo[*d*]imidazole. Yield: 2.59 g, starting from 2.63 g of 2-bromo-5,6-dimethyl-1*H*-benzo[*d*]imidazole (68%). Colorless solid, mp: 140 - 144 °C; IR (KBr): ν = 1744 (s), 1396 (m), 1342 (s), 1281 (m), 1196 (w), 1150 (s), 1119 (s), 841 (m) cm⁻¹; ¹H NMR (300 MHz, CDCl₃): δ = 7.70 (s, 1 H, aromatic), 7.41 (s, 1 H, aromatic), 2.36 (s, 3 H, CH₃), 2.34 (s, 3 H, CH₃), 1.72 (s, 9 H, *t*-Bu); ¹³C NMR (75 MHz, CDCl₃): δ = 147.6, 141.2, 134.4, 133.6, 132.3, 125.6, 119.6, 115.2, 86.6, 28.1, 20.8, 20.2; HRMS (ESI - TOF) *m/z*: [M+Na]⁺ Calcd for C₁₄H₁₇BrN₂NaO₂⁺ 347.0366; Found: 347.0365.

Mixture of Regioisomers N-Boc-2-bromo-6-methoxy-1*H*-benzo[*d*]imidazole (**A**) and *N*-Boc-2-bromo-5-methoxy-1*H*-benzo[*d*]imidazole (**B**) and (*A/B* ratio ca. 1, by ¹H NMR). Yield: 2.83 g, starting from 2.11 g of 2-bromo-5-methoxy-1*H*-benzo[*d*]imidazole (74%). Colorless solid, mp: 64 - 67 °C; IR (KBr): ν = 1744 (s), 1620 (m), 1435 (m), 1397 (w), 1350 (w), 1319 (m), 1211 (m), 1150 (s), 825 (m) cm⁻¹; ¹H-NMR (500 MHz, CDCl₃): δ = 7.76 [d, *J* = 9.1, 1 H, H-4 (**A**) or H-7 (**B**)], 7.54 [(d, *J* = 8.7, 1 H, H-7 (**B**) or H-4 (**A**)), 7.47 [(d, *J* = 2.5, 1 H, H-7 (**A**) or H-4 (**B**)), 7.14 [(d, *J* = 2.5, 1 H, H-4 (**B**) or H-7 (**A**))], 6.98 – 6.90 [(m, 2 H, H-5 (**A**) + H-6 (**B**)), 3.86 [s, 3 H, OCH₃ (**A** or **B**)], 3.85 [s, 3 H, OCH₃ (**B** or **A**)], 1.73 [s, 9 H, *t*-Bu (**A** + **B**)]; ¹³C NMR (125 MHz, CDCl₃): δ = 158.0, 157.3, 147.5, 147.3, 143.7, 137.2, 134.7, 128.2, 126.9, 124.5, 119.9, 115.3, 114.1, 113.3, 102.3, 99.1, 86.7, 55.8, 55.7, 28.1; HRMS (ESI - TOF) *m/z*: [M+Na]⁺ Calcd for C₁₃H₁₅BrN₂NaO₃⁺ 349.0158; Found: 349.0161.

N-Boc-2-bromo-5,6-dichloro-1*H*-benzo[*d*]imidazole. Yield: 2.57 g, starting from 3.11 g of 2-bromo-5,6-dichloro-1*H*-benzo[*d*]imidazole (60%). Colorless solid, mp: 157 – 160 °C; IR (KBr): ν = 1751 (s), 1435 (w), 1373 (w), 1119 (s), 1072 (s), 849 (m) cm⁻¹; ¹H NMR (300 MHz, CDCl₃): δ = 8.07 (s, 1 H, aromatic), 7.74 (s, 1 H, aromatic), 1.74 (s, 9 H, *t*-Bu); ¹³C NMR (75 MHz, CDCl₃): δ = 146.6, 141.8, 132.8, 129.5, 128.9, 128.7, 120.5, 116.5, 87.9, 28.0; HRMS (ESI - TOF) *m/z*: [M-*t*-Bu]⁻ Calcd for C₇H₂BrCl₂N₂⁻ 262.8784; Found: 262.8784.

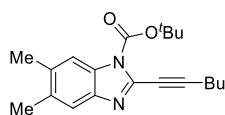
Mixture of Regioisomers N-Boc-2-bromo-6-nitro-1*H*-benzo[*d*]imidazole (**A**) and *N*-Boc-2-bromo-5-nitro-1*H*-benzo[*d*]imidazole (**B**) (*A/B* Ratio ca. 1, by ¹H NMR). Yield: 2.12 g, starting from 2.83 g of 2-bromo-5-nitro-1*H*-benzo[*d*]imidazole (53%). Yellow solid, mp: 240 - 243 °C; IR (KBr): ν = 1751 (s), 1528 (s), 1474 (w), 1435 (m), 1327 (s), 1273 (m), 1150 (m), 826 (m) cm⁻¹; ¹H-NMR (500 MHz, CDCl₃): δ = 8.89 [d, *J* = 2.1, 1 H, H-7 (**A**) or H-4 (**B**)], 8.55 [d, *J* = 1.9, 1 H, H-4 (**B**) or H-7 (**A**)], 8.33 – 8.23 [m, 2 H, H-5 (**A**) + H-6 (**B**)], 8.09 [d, *J* = 9.1, 1 H, H-4 (**A**) or H-7 (**B**)], 7.78 [d, *J* = 8.9, 1 H, H-7 (**B**) or H-4 (**A**)], 1.78 [s, 9 H, *t*-Bu (**A** or **B**)], 1.76 [s, 9 H, *t*-Bu (**B** or **A**)];

^{13}C NMR (75 MHz, CDCl_3): $\delta = 146.8, 146.7, 146.5, 146.4, 145.1, 142.3, 137.9, 133.2, 131.9, 130.4, 120.4, 120.3, 119.7, 115.5, 115.1, 111.7, 88.6, 85.2, 28.0, 27.5$; HRMS (ESI - TOF) m/z : $[\text{M} - t\text{-Bu}]^-$ Calcd for $\text{C}_7\text{H}_3\text{BrN}_3\text{O}_2^-$ 239.9414; Found: 239.9413



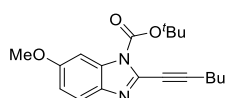
N-Boc-2-(hex-1-yn-1-yl)-1H-benzo[d]imidazole (**1a**).

Yield: 890 mg, starting from 1.00 g of *N*-Boc-2-bromo-1H-benzo[d]imidazole (89%). Yellow solid, mp: 48-53°C; IR (KBr): $\nu = 2222$ (w), 1728 (s), 1450 (m), 1342 (m), 1250 (m), 1134 (m), 918 (w), 764 (s) cm^{-1} ; ^1H NMR (300 MHz, CDCl_3): $\delta = 8.00 - 7.92$ (m, 1 H aromatic), 7.74 - 7.66 (m, 1 H aromatic), 7.40 - 7.30 (m, 2 H aromatic), 2.53 (t, $J = 7.1$, 2 H, $=\text{CCH}_2$), 1.80 - 1.61 (m, 2 H, $=\text{CCH}_2\text{CH}_2$), 1.71 (s, 9 H, *t*-Bu), 1.52 (hex, $J = 7.2$, 2 H, CH_2CH_3), 0.95 (t, $J = 7.2$, 3 H, CH_3); ^{13}C NMR (75 MHz, CDCl_3): $\delta = 147.9, 142.6, 136.3, 132.0, 125.5, 124.6, 120.0, 114.8, 97.8, 85.5, 72.3, 30.0, 28.1, 22.1, 19.5, 13.6$; HRMS (ESI-TOF) m/z : $[\text{M} + \text{Na}]^+$ Calcd for $\text{C}_{18}\text{H}_{22}\text{N}_2\text{O}_2\text{Na}^+$ 321.1573; Found: 321.1579.



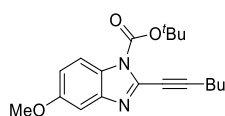
N-Boc-2-(hex-1-yn-1-yl)-5,6-dimethyl-1H-benzo[d]imidazole (**1b**).

Yield: 968 mg, starting from 1.09 g of *N*-Boc-2-bromo-5,6-dimethyl-1H-benzo[d]imidazole (88%). Colorless solid, mp: 73 - 75 °C; IR (KBr): $\nu = 2230$ (w), 1751 (s), 1458 (m), 1350 (s), 1228 (m), 1157 (m), 1134 (m), 1026 (m), 849 (s) cm^{-1} ; ^1H NMR (300 MHz, CDCl_3): $\delta = 7.75$ (s, 1 H, H-6 or H-9), 7.43 (s, 1 H, H-9 or H-6), 2.51 (t, $J = 7.2$, 2 H, $=\text{CCH}_2$), 2.37 (s, 3 H, CH_3 at C-7 or C-8), 2.34 (s, 3 H, CH_3 at C-8 or C-7), 1.75 - 1.60 (m, 2 H, $=\text{CCH}_2\text{CH}_2$), 1.70 (s, 9 H, *t*-Bu), 1.51 (hex, $J = 7.3$, 2 H, CH_2CH_3), 0.95 (t, $J = 7.3$, 3 H, CH_3); ^{13}C NMR (75 MHz, CDCl_3): $\delta = 148.1, 141.1, 135.4, 134.9, 133.5, 130.5, 120.0, 115.1, 97.0, 85.2, 72.5, 30.1, 28.1, 22.1, 20.7, 20.2, 19.5, 13.6$; HRMS (ESI - TOF) m/z : $[\text{M} + \text{Na}]^+$ Calcd for $\text{C}_{20}\text{H}_{26}\text{N}_2\text{O}_2\text{Na}^+$ 349.1886; Found: 349.1891



N-Boc-2-(hex-1-yn-1-yl)-6-methoxy-1H-benzo[d]imidazole (**1c**).

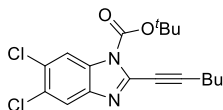
Yield: 423 mg, starting from 1.10 g of *N*-Boc-2-bromo-6-methoxy-1H-benzo[d]imidazole (38%). Colorless solid, mp: 54 - 55°C; IR (KBr): $\nu = 2237$ (w), 1744 (s), 1612 (m), 1481 (m), 1435 (m), 1350 (m), 1335 (s), 1281 (w), 1219 (m), 1150 (s), 1026 (w), 849 (m) cm^{-1} ; ^1H NMR (500 MHz, CDCl_3): $\delta = 7.56$ (d, $J = 8.8$, 1 H, H-4), 7.51 (d, $J = 2.4$, 1 H, H-7), 6.95 (dd, $J = 8.8, 2.4$, 1 H, H-5), 3.86 (s, 3 H, OCH_3), 2.51 (t, $J = 7.3$, 2 H, $\equiv\text{CCH}_2$), 1.75 - 1.61 (m, 2 H, $\text{CH}_2\text{CH}_2\text{CH}_3$), 1.71 (s, 9 H, *t*-Bu), 1.52 (hexuplet, $J = 7.3$, 2 H, CH_2CH_3), 0.95 (t, $J = 7.3$, 3 H, CH_2CH_3); ^{13}C NMR (75 MHz, CDCl_3): $\delta = 158.6, 148.1, 136.9, 135.1, 133.0, 120.4, 113.9, 98.6, 96.8, 85.4, 72.5, 55.7, 30.1, 28.1, 22.1, 19.5, 13.6$; HRMS (ESI - TOF) m/z : $[\text{M} + \text{Na}]^+$ Calcd for $\text{C}_{19}\text{H}_{24}\text{N}_2\text{O}_3\text{Na}^+$ 351.1679; Found: 351.1685.



N-Boc-2-(hex-1-yn-1-yl)-5-methoxy-1H-benzo[d]imidazole (**1d**).

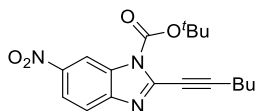
Yield: 230 mg, starting from 1.10 g of *N*-Boc-2-bromo-5-methoxy-1H-benzo[d]imidazole (21%). Yellow oil; IR (KBr): $\nu = 2237$ (w), 1751 (s), 1612 (w), 1489 (m), 1435 (m), 1327 (s), 1288 (m), 1219 (m), 1150 (s), 1026 (m), 849 (m) cm^{-1} ; ^1H NMR (500 MHz, CDCl_3): $\delta = 7.82$ (d, $J = 9.0$, 1 H, H-7), 7.15 (d, $J = 2.5$, 1 H, H-4), 6.98 (dd, $J = 9.0, 2.5$, 1 H, H-6), 3.85 (s, 3 H, OCH_3), 2.52 (t,

$J = 7.3$, 2 H, $\equiv\text{CCH}_2$), 1.75 – 1.62 (m, 2 H, $\text{CH}_2\text{CH}_2\text{CH}_3$), 1.71 (s, 9 H, *t*-Bu), 1.53 (hexuplet, $J = 7.3$, 2 H, CH_2CH_3), 0.95 (t, $J = 7.3$, 3 H, CH_2CH_3); ^{13}C NMR (125 MHz, CDCl_3): $\delta = 157.5$, 147.9, 143.6, 136.6, 126.4, 115.2, 115.0, 102.3, 97.8, 85.4, 72.4, 55.7, 30.1, 28.1, 22.1, 19.5, 13.6; HRMS (ESI - TOF) m/z : $[\text{M} + \text{Na}]^+$ Calcd for $\text{C}_{19}\text{H}_{24}\text{N}_2\text{O}_3\text{Na}^+$ 351.1679; Found: 351.1686.



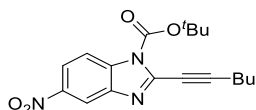
N-Boc-5,6-dichloro-2-(hex-1-yn-1-yl)-1H-benzo[d]imidazole (**1e**).

Yield: 976 mg, starting from 1.23 g of *N*-Boc-2-bromo-5,6-dichloro-1H-benzo[d]imidazole (79%). Colorless solid, mp: 70-71°C; IR (KBr): $\nu = 2237$ (w), 1751 (s), 1504 (m), 1443 (m), 1335 (s), 1219 (m), 1150 (s), 872 (m) cm^{-1} ; ^1H NMR (300 MHz, CDCl_3): $\delta = 8.10$ (s, 1 H, H-4 or H-7), 7.74 (s, 1 H, H-7 or H-4), 2.53 (t, $J = 7.1$, 2 H, $\equiv\text{CCH}_2$), 1.75 – 1.61 (m, 2 H, $\text{CH}_2\text{CH}_2\text{CH}_3$), 1.71 (s, 9 H, *t*-Bu), 1.59 – 1.44 (m, 2 H, CH_2CH_3), 0.96 (t, $J = 7.2$, 3 H, CH_2CH_3); ^{13}C NMR (75 MHz, CDCl_3): $\delta = 147.2$, 141.8, 137.7, 131.1, 129.6, 128.8, 120.8, 116.4, 99.3, 86.5, 71.9, 29.9, 28.0, 22.1, 19.5, 13.6; HRMS (ESI - TOF) m/z : $[\text{M} + \text{Na}]^+$ Calcd for $\text{C}_{18}\text{H}_{20}\text{Cl}_2\text{N}_2\text{O}_2\text{Na}^+$ 389.0794; Found: 389.0796.



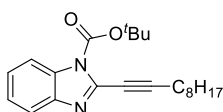
N-Boc-2-(hex-1-yn-1-yl)-6-nitro-1H-benzo[d]imidazole (**1f**).

Yield: 427 mg, starting from 1.15 g of *N*-Boc-2-bromo-6-nitro-1H-benzo[d]imidazole (37%). Colorless solid, mp: 149 - 150°C; IR (KBr): $\nu = 2230$ (w), 1744 (s), 1520 (s), 1443 (w), 1342 (s), 1250 (w), 1157 (m), 756 (m) cm^{-1} ; ^1H NMR (300 MHz, CDCl_3): $\delta = 8.92$ (d, $J = 2.2$, 1 H, H-7), 8.27 (dd, $J = 8.9$, 2.2, 1 H, H-5), 7.77 (d, $J = 8.9$, 1 H, H-4), 2.57 (t, $J = 7.1$, 2 H, $\equiv\text{CCH}_2$), 1.81 – 1.62 (m, 2 H, $\text{CH}_2\text{CH}_2\text{CH}_3$), 1.75 (s, 9 H, *t*-Bu), 1.60 – 1.45 (m, 2 H, CH_2CH_3), 0.97 (t, $J = 7.2$, 3 H, CH_2CH_3); ^{13}C NMR (75 MHz, CDCl_3): $\delta = 147.0$, 146.8, 145.5, 140.4, 131.5, 120.3, 120.0, 111.8, 101.1, 87.1, 71.9, 29.9, 28.0, 22.1, 19.6, 13.6; HRMS (ESI - TOF) m/z : $[\text{M} + \text{Na}]^+$ Calcd for $\text{C}_{18}\text{H}_{21}\text{N}_3\text{O}_4\text{Na}^+$ 366.1424; Found: 366.1433.



N-Boc-2-(hex-1-yn-1-yl)-5-nitro-1H-benzo[d]imidazole (**1g**).

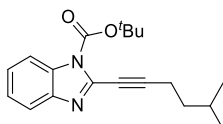
Yield: 431 mg, starting from 1.15 g of *N*-Boc-2-bromo-5-nitro-1H-benzo[d]imidazole (37%). Colorless solid, mp: 103 - 106°C; IR (KBr): $\nu = 2237$ (w), 1751 (s), 1528 (s), 1373 (w), 1335 (s), 1150 (s), 741 (m) cm^{-1} ; ^1H NMR (300 MHz, CDCl_3): $\delta = 8.55$ (d, $J = 2.0$, 1 H, H-4), 8.27 (dd, $J = 9.0$, 2.0, 1 H, H-6), 8.10 (distorted d, $J = 9.0$, 1 H, H-7), 2.56 (t, $J = 7.0$, 2 H, $\equiv\text{CCH}_2$), 1.83 – 1.62 (m, 2 H, $\text{CH}_2\text{CH}_2\text{CH}_3$), 1.74 (s, 9 H, *t*-Bu), 1.61 – 1.45 (m, 2 H, CH_2CH_3), 0.97 (t, $J = 7.2$, 3 H, CH_2CH_3); ^{13}C NMR (75 MHz, CDCl_3): $\delta = 147.1$, 145.2, 142.3, 139.2, 136.2, 120.7, 116.0, 115.1, 100.2, 87.1, 71.7, 29.9, 28.0, 22.1, 19.5, 13.6; HRMS(ESI-TOF) m/z : $[\text{M} + \text{Na}]^+$ Calcd for $\text{C}_{18}\text{H}_{21}\text{N}_3\text{O}_4\text{Na}^+$ 366.1424; Found: 366.1433.



N-Boc-2-(dec-1-yn-1-yl)-1H-benzo[d]imidazole (**1h**).

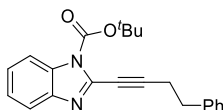
Yield: 910 mg, starting from 1.00 g of *N*-Boc-2-bromo-1H-benzo[d]imidazole (76%). Yellow oil; IR (KBr): $\nu = 2237$ (m), 1752 (s), 1504 (m), 1450 (m), 1340 (s), 1211 (m), 1158 (s), 849 (m), 764 (m) cm^{-1} ; ^1H NMR (300 MHz, CDCl_3) $\delta = 8.00$ – 7.92 (m, 1 H, aromatic), 7.73 – 7.66 (m, 1 H,

aromatic), 7.40 – 7.28 (m, 2 H, aromatic), 2.52 (t, $J = 7.1$, 2 H, $\equiv\text{CCH}_2$), 1.80 – 1.62 (m, 2 H, $\equiv\text{CCH}_2\text{CH}_2$), 1.71 (s, 9 H, *t*-Bu), 1.55 – 1.42 (m, 2 H, $\equiv\text{CCH}_2\text{CH}_2\text{CH}_2$), 1.39 – 1.20 (m, 8 H, $\text{CH}_2(\text{CH}_2)_4\text{CH}_3$), 0.93-0.83 (m, 3 H, CH_2CH_3); ^{13}C NMR (75 MHz, CDCl_3): $\delta = 147.9, 142.6, 136.4, 132.1, 125.6, 124.6, 120.0, 114.8, 97.9, 85.5, 72.3, 31.9, 29.18, 29.16, 29.07, 28.10, 28.06, 22.7, 19.8, 14.1$; HRMS (ESI - TOF) m/z : $[\text{M}+\text{Na}]^+$ Calcd for $\text{C}_{22}\text{H}_{30}\text{N}_2\text{O}_2\text{Na}^+$ 377.2199; Found: 377.2204.



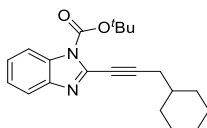
N-Boc-2-(5-methylhex-1-yn-1-yl)-1H-benzo[d]imidazole (**1i**).

Yield: 795 mg, starting from 1.00 g of *N*-Boc-2-bromo-1H-benzo[d]imidazole (76%). Colorless oil, IR (KBr): $\nu = 2237$ (m), 1751 (s), 1504 (m), 1450 (w), 1126 (m), 1011 (m), 849 (m), 738 (m) cm^{-1} ; ^1H NMR (300 MHz, CDCl_3): $\delta = 7.99 - 7.93$ (m, 1 H, aromatic), 7.73 – 7.66 (m, 1 H, aromatic), 7.41 – 7.29 (m, 2 H, aromatic), 2.53 (t, $J = 7.4$, 2 H, $\equiv\text{CCH}_2$), 1.88 – 1.66 (m, 10 H, *t*-Bu + $\text{CH}(\text{CH}_3)_2$), 1.59 (q, $J = 7.4$, 2 H, CH_2CH), 0.94 [d, $J = 6.6$, 6 H, $\text{CH}(\text{CH}_3)_2$]; ^{13}C NMR (75 MHz, CDCl_3): $\delta = 147.9, 142.6, 136.3, 132.1, 125.5, 124.6, 120.0, 114.8, 97.8, 85.5, 72.2, 36.8, 28.1, 27.3, 22.2, 17.8$. HRMS (ESI-TOF) m/z : $[\text{M}+\text{Na}]^+$ Calcd for $\text{C}_{19}\text{H}_{24}\text{N}_2\text{O}_2\text{Na}^+$ 335.1730; Found: 335.1736.



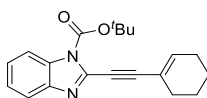
N-Boc-2-(4-phenylbut-1-yn-1-yl)-1H-benzo[d]imidazole (**1j**).

Yield: 1.09 g, starting from 1.00 g of *N*-Boc-2-bromo-1H-benzo[d]imidazole (94%). Colorless solid, mp: 53 - 54 °C; IR (KBr): $\nu = 2237$ (w), 1751 (s), 1504 (w), 1451 (m), 1320 (s), 1219 (m), 1157 (s), 1126 (s), 741 (s) cm^{-1} ; ^1H NMR (300 MHz, CDCl_3): $\delta = 8.01 - 7.92$ (m, 1 H, aromatic), 7.75 – 7.66 (m, 1 H, aromatic), 7.42 – 7.17 (m, 8 H, aromatic), 3.01 (t, $J = 7.5$, 2 H, $\equiv\text{CCH}_2$), 2.81 (t, $J = 7.5$, 2 H, CH_2Ph), 1.66 (s, 9 H, *t*-Bu); ^{13}C NMR (75 MHz, CDCl_3): $\delta = 147.9, 142.6, 140.1, 136.1, 132.1, 128.54, 128.46, 126.5, 125.6, 124.7, 120.1, 114.9, 96.6, 85.6, 72.9, 34.3, 28.0, 22.1$; HRMS (ESI-TOF) m/z : $[\text{M}+\text{Na}]^+$ Calcd for $\text{C}_{22}\text{H}_{22}\text{N}_2\text{O}_2\text{Na}^+$ 369.1573; Found: 369.1578



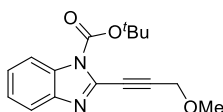
N-Boc-2-(3-cyclohexylprop-1-yn-1-yl)-1H-benzo[d]imidazole (**1k**).

Yield: 1.02 g, starting from 1.00 g of *N*-Boc-2-bromo-1H-benzo[d]imidazole (90%). Yellow solid, mp: 65-68°C; IR (KBr): $\nu = 2230$ (m), 1736 (s), 1504 (m), 1451 (m), 1360 (s), 1211 (m), 1134 (s), 1057 (w), 849 (m), 764 (s) cm^{-1} ; ^1H NMR (500 MHz, CDCl_3): $\delta = 7.97 - 7.94$ (m, 1 H, aromatic), 7.73 – 7.68 (m, 1 H, aromatic), 7.39 – 7.31 (m, 2 H, aromatic), 2.41 (d, $J = 6.8$, 2 H, $\equiv\text{CCH}_2$), 1.97 – 1.88 (m, 2 H, cyclohexyl ring), 1.80 – 1.62 (m, 4 H, cyclohexyl ring), 1.71 (s, 9 H, *t*-Bu), 1.34 – 1.24 (m, 2 H, cyclohexyl ring), 1.24 – 1.05 (m, 3 H, cyclohexyl ring); ^{13}C -NMR (125 MHz, CDCl_3): $\delta = 148.0, 142.7, 136.4, 132.1, 125.5, 124.6, 120.1, 114.8, 96.8, 85.5, 73.2, 37.2, 32.9, 28.1, 27.6, 26.2, 26.1$; HRMS (ESI-TOF) m/z : $[\text{M}+\text{Na}]^+$ Calcd for $\text{C}_{21}\text{H}_{26}\text{N}_2\text{O}_2\text{Na}^+$ 361.1892; Found: 361.1894.



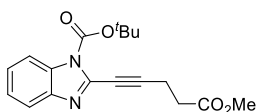
N-Boc-2-(cyclohex-1-en-1-ylethynyl)-1H-benzo[d]imidazole (**1l**).

Yield: 890 mg, starting from 1.00 g of *N*-Boc-2-bromo-1H-benzo[d]imidazole (82%). Yellow solid, mp: 78-80°C; IR (KBr): $\nu = 2199$ (w), 1736 (s), 1498 (m), 1451 (m), 1350 (s), 1227 (m), 1150 (s), 1111 (m), 849 (w), 764 (m) cm^{-1} ; ^1H NMR (500 MHz, CDCl_3): $\delta = 7.98 - 7.93$ (m, 1 H, aromatic), 7.74 – 7.68 (m, 1 H, aromatic), 7.41 – 7.32 (m, 2 H, aromatic), 6.45 (s, 1 H, =CH), 2.34 – 2.25 (m, 2 H, cyclohexenyl ring), 2.24 – 2.15 (m, 2 H, cyclohexenyl ring), 1.77 – 1.59 (m, 4 H, cyclohexenyl ring), 1.71 (s, 9 H, t-Bu); ^{13}C -NMR (125 MHz, CDCl_3): $\delta = 147.9, 143.0, 139.2, 139.1, 136.6, 132.2, 125.6, 124.7, 120.1, 114.9, 97.3, 85.7, 78.4, 28.5, 28.2, 26.0, 22.2, 21.4$; HRMS (ESI-TOF) m/z : $[\text{M} + \text{Na}]^+$ Calcd for $\text{C}_{20}\text{H}_{22}\text{N}_2\text{O}_2\text{Na}^+$ 345.1573; Found: 345.1581.



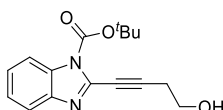
N-Boc-2-(3-methoxyprop-1-yn-1-yl)-1H-benzo[d]imidazole (**1m**).

Yield: 755 mg, starting from 1.00 g of *N*-Boc-2-bromo-1H-benzo[d]imidazole (78%). Colorless solid, mp: 63 - 67°C; IR (KBr): $\nu = 1751$ (s), 1504 (w), 1450 (m), 1335 (s), 1219 (m), 1157 (m), 1103 (m), 849 (w), 741 (m) cm^{-1} ; ^1H NMR (500 MHz, CDCl_3): $\delta = 8.03 - 7.96$ (m, 1 H, aromatic), 7.77 – 7.71 (m, 1 H, aromatic), 7.44 – 7.33 (m, 2 H, aromatic), 4.42 (s, 2 H, $\equiv\text{CCH}_2$), 3.51 (s, 3 H, OCH_3), 1.72 (s, 9 H, t-Bu); ^{13}C -NMR (125 MHz, CDCl_3): $\delta = 147.7, 142.7, 135.3, 132.2, 126.1, 124.8, 120.4, 115.0, 91.5, 86.1, 77.7, 60.3, 58.1, 28.1$; HRMS (ESI-TOF) m/z : $[\text{M} + \text{Na}]^+$ Calcd for $\text{C}_{16}\text{H}_{18}\text{N}_2\text{O}_3\text{Na}^+$ 309.1210; Found: 309.1217.



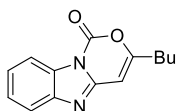
Methyl *N*-Boc-5-(1H-benzo[d]imidazol-2-yl)pent-4-ynoate (**1n**).

Yield: 890 mg, starting from 1.00 g of *N*-Boc-2-bromo-1H-benzo[d]imidazole (81%). Colorless solid, mp: 110 - 111°C; IR (KBr): $\nu = 2230$ (w), 1744 (s), 1504 (w), 1443 (m), 1343 (s), 1289 (w), 1180 (m), 1157 (s), 764 (m) cm^{-1} ; ^1H NMR (500 MHz, CDCl_3): $\delta = 7.98 - 7.93$ (m, 1 H, aromatic), 7.73 – 7.67 (m, 1 H, aromatic), 7.40 – 7.31 (m, 2 H, aromatic), 3.73 (s, 3 H, CO_2CH_3), 2.89 – 2.83 (m, 2 H, $\equiv\text{CCH}_2$), 2.76 – 2.70 (m, 2 H, $\text{CH}_2\text{CH}_2\text{CH}_3$), 1.71 (s, 9 H, t-Bu); ^{13}C -NMR (125 MHz, CDCl_3): $\delta = 171.9, 147.8, 142.6, 135.9, 132.1, 125.8, 124.7, 120.1, 114.9, 95.0, 85.7, 72.9, 52.0, 32.4, 28.1, 15.6$; HRMS (ESI-TOF) m/z : $[\text{M} + \text{Na}]^+$ Calcd for $\text{C}_{18}\text{H}_{20}\text{N}_2\text{O}_4\text{Na}^+$ 351.1315; Found: 351.1324.



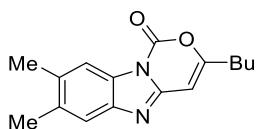
N-Boc-4-(1H-benzo[d]imidazol-2-yl)but-3-yn-1-ol (**1o**).

Yield: 800 mg, starting from 1.00 g of *N*-Boc-2-bromo-1H-benzo[d]imidazole (83%). Colorless solid, mp: 94 - 97°C; IR (KBr): $\nu = 3240$ (m, br), 2245 (w), 1767 (s), 1450 (m), 1350 (m), 1219 (w), 1126 (s), 1057 (m), 741 (m) cm^{-1} ; ^1H NMR (500 MHz, CDCl_3): $\delta = 7.92 - 7.87$ (m, 1 H, aromatic), 7.69 – 7.66 (m, 1 H, aromatic), 7.39 – 7.30 (m, 2 H, aromatic), 4.23 (s, br, 1 H, OH), 4.00 – 3.90 (m, 2 H, CH_2OH), 2.81 (t, $J = 6.3$, 2 H, $\equiv\text{CCH}_2$), 1.71 (s, 9 H, t-Bu); ^{13}C -NMR (125 MHz, CDCl_3): $\delta = 147.9, 142.2, 136.1, 125.8, 124.8, 120.0, 114.9, 95.5, 86.2, 73.8, 60.3, 28.1, 24.3$; HRMS (ESI-TOF) m/z : $[\text{M} + \text{Na}]^+$ Calcd for $\text{C}_{16}\text{H}_{18}\text{N}_2\text{O}_3\text{Na}^+$ 309.1210; Found: 309.1217.



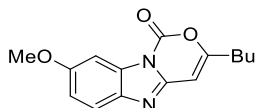
3-Butyl-1H-benzo[4,5]imidazo[1,2-c][1,3]oxazin-1-one (2a).

Yield: 198 mg, starting from 298 mg of **1a** (82%) (Table 2, entry 1). Colorless solid, mp: 92 - 94 °C; IR (KBr): $\nu = 1759$ (s), 1667 (m), 1551 (w), 1450 (w), 1366 (s), 1096 (m), 972 (w), 849 (w), 748 (m) cm^{-1} ; ^1H NMR (300 MHz, CDCl_3) $\delta = 8.24 - 8.13$ (m, 1 H, aromatic), 7.82 - 7.73 (m, 1 H, aromatic), 7.52 - 7.36 (m, 2 H, aromatic), 6.50 (s, 1 H, H-4), 2.61 (t, $J = 7.3$, 2 H, =CCH₂), 1.75 (quint, $J = 7.3$, 2 H, CH₂CH₂CH₃), 1.46 (hexuplet, $J = 7.3$, 2 H, CH₂CH₃), 0.98 (t, $J = 7.3$, 3 H, CH₃); ^{13}C NMR (75 MHz, CDCl_3): $\delta = 162.9, 147.4, 144.1, 129.3, 126.3, 124.9, 119.7, 114.6, 96.6, 32.8, 28.4, 22.1, 13.7$; GC/MS = 242 (M⁺, 100), 227 (2), 213 (3), 200 (42), 185 (31), 171 (6), 158 (43); 144 (4), 130 (12); HRMS (ESI-TOF) m/z : [M+H]⁺ Calcd for C₁₄H₁₅N₂O₂⁺ 243.1128; Found: 243.1132.



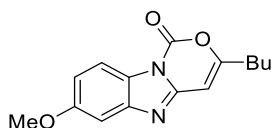
3-Butyl-7,8-dimethyl-1H-benzo[4,5]imidazo[1,2-c][1,3]oxazin-1-one (2b).

Yield: 208 mg, starting from 326 mg of **1b** (77%) (Table 2, entry 2). Colorless solid, mp: 133-137 °C; IR (KBr): $\nu = 1768$ (s), 1667 (m), 1558 (w), 1450 (m), 1381 (s), 1111 (w), 741 (w) cm^{-1} ; ^1H NMR (300 MHz, CDCl_3): $\delta = 7.92$ (s, 1 H, H-6 or H-9), 7.48 (s, 1 H, H-9 or H-6), 6.44 (s, 1 H, H-4), 2.59 (t, $J = 7.5$, 2 H, =CCH₂), 2.40 (s, 3 H, CH₃ at C-7 or C-8), 2.38 (s, 3 H, CH₃ at C-8 or C-7), 1.72 (quint, $J = 7.5$, 2 H, CH₂CH₂CH₃), 1.44 (hexuplet, $J = 7.5$, 2 H, CH₂CH₃), 0.98 (t, $J = 7.5$, 3 H, CH₃); ^{13}C NMR (75 MHz, CDCl_3): $\delta = 162.0, 146.6, 144.2, 142.5, 135.3, 134.3, 127.6, 119.8, 114.7, 96.7, 32.8, 28.5, 22.1, 20.4, 13.7$; GC/MS = 270 (M⁺, 100); 255 (3), 228 (29), 213 (24), 199 (5), 186 (19), 172 (3), 158 (6), 143 (1), 130 (2), 118 (8); HRMS (ESI - TOF) m/z : [M + H]⁺ Calcd for C₁₆H₁₉N₂O₂⁺ 271.1441; Found: 271.1446.



3-Butyl-8-methoxy-1H-benzo[4,5]imidazo[1,2-c][1,3]oxazin-1-one (2c).

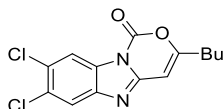
Yield: 207 mg, starting from 328 mg of **1c** (76%) (Table 2, entry 3). Colorless solid, mp: 96-99 °C; IR (KBr): $\nu = 1767$ (s), 1667 (m), 1489 (m), 1443 (w), 1366 (m), 1281 (m), 1204 (w), 1026 (w), 818 (m) cm^{-1} ; ^1H NMR (500 MHz, CDCl_3) $\delta = 7.70$ (d, $J = 2.5$, 1 H, H-9), 7.63 (d, $J = 8.8$, 1 H, H-6), 7.06 (dd, $J = 8.8, 2.5$, 1 H, H-7), 6.46 - 6.44 (m, 1 H, H-4), 2.60 (t, $J = 7.5$, 2 H, =CCH₂), 1.72 (quint, $J = 7.5$, 2 H, CH₂CH₂CH₃), 1.45 (hexuplet, $J = 7.5$, 2 H, CH₂CH₃), 0.98 (t, $J = 7.5$, 3 H, CH₃); ^{13}C NMR (125 MHz, CDCl_3): $\delta = 161.7, 158.0, 146.3, 144.4, 138.3, 130.2, 120.2, 115.5, 98.3, 96.8, 56.0, 32.8, 28.5, 22.1, 13.7$; GC/MS : $m/z = 272$ (M⁺, 100), 257 (17), 229 (29), 215 (22), 187 (14); HRMS (ESI - TOF) m/z : [M + H]⁺ Calcd for C₁₅H₁₇N₂O₃⁺ 273.1234; Found: 273.1237.



3-Butyl-7-methoxy-1H-benzo[4,5]imidazo[1,2-c][1,3]oxazin-1-one (2d).

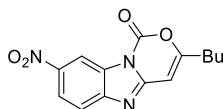
Yield: 226 mg, starting from 328 mg of **1d** (83%) (Table 3, entry 4) Colorless solid, mp: 93-97 °C; IR (KBr): $\nu = 1760$ (s), 1659 (m), 1558 (w), 1489 (m), 1435 (w), 1366 (m), 1281 (m), 1150 (m), 1103 (m) cm^{-1} ; ^1H NMR (500 MHz, CDCl_3) $\delta = 8.06$ (d, $J = 8.9$, 1 H, H-9), 7.24 (s, br, 1 H, H-6), 7.06 - 7.00 (m, 1 H, H-8), 6.50 - 6.47 (m, 1 H, H-4), 2.61 (t, $J = 7.5$, 2 H, =CCH₂), 1.73 (quint,

$J = 7.5$, 2 H, $\text{CH}_2\text{CH}_2\text{CH}_3$), 1.45 (hexuplet, $J = 7.5$, 2 H, CH_2CH_3), 0.98 (t, $J = 7.5$, 3 H, CH_3); ^{13}C NMR (125 MHz, CDCl_3): $\delta = 162.7, 158.9, 148.0, 145.5, 144.0, 123.5, 114.9, 113.8, 102.7, 96.6, 55.8, 32.8, 28.5, 22.1, 13.7$; GC/MS : $m/z = 272$ (M^+ , 100), 230 (20), 215 (15), 199 (11), 188 (19); HRMS (ESI - TOF) m/z : $[\text{M} + \text{H}]^+$ Calcd for $\text{C}_{15}\text{H}_{17}\text{N}_2\text{O}_3^+$ 273.1234; Found: 273.1242.



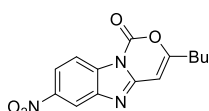
3-Butyl-7,8-dichloro-1H-benzo[4,5]imidazo[1,2-c][1,3]oxazin-1-one (2e).

Yield: 240 mg, starting from 367 mg of **1e** (77%) (Table 2, entry 5). Colorless solid, mp: 143-147 °C. IR (KBr): $\nu = 1775$ (s), 1667 (m), 1543 (w), 1435 (w), 1350 (m), 1134 (w), 1096 (m) cm^{-1} ; ^1H NMR (500 MHz, $\text{DMSO}-d_6$) $\delta = 8.18$ (s, 1 H, H-6 or H-9), 8.07 (s, 1 H, H-9 or H-6), 6.91 (s, 1 H, H-4), 2.63 (t, $J = 7.4$, 2 H, $=\text{CCH}_2$), 1.65 (quint, $J = 7.4$, 2 H, $=\text{CCH}_2\text{CH}_2$), 1.40 (hexuplet, $J = 7.4$, 2 H, CH_2CH_3), 0.93 (t, $J = 7.4$, 3 H, CH_3); ^{13}C NMR (125 MHz, $\text{DMSO}-d_6$): $\delta = 163.9, 150.0, 143.5, 128.7, 128.3, 126.3, 120.5, 114.9, 96.3, 31.8, 27.9, 21.3, 13.5$; GC/MS= 312 $[(\text{M}+2)^+$, 61], 310 (M^+ , 100), 268 (25), 253 (22), 226 (31), 202 (6); HRMS (ESI - TOF) m/z : $[\text{M} + \text{H}]^+$ Calcd for $\text{C}_{14}\text{H}_{13}\text{Cl}_2\text{N}_2\text{O}_2^+$ 311.0349; Found: 311.0348.



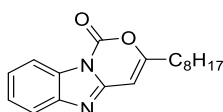
3-Butyl-8-nitro-1H-benzo[4,5]imidazo[1,2-c][1,3]oxazin-1-one (2f).

Yield: 129 mg, starting from 343 mg of **1f** (45%) (Table 2, entry 6). Colorless solid, mp: 165-168 °C; IR (KBr): $\nu = 1775$ (s), 1659 (m), 1543 (w), 1520 (m), 1343 (m), 748 (w) cm^{-1} ; ^1H NMR (300 MHz, CDCl_3) $\delta = 9.05$ (d, $J = 1.9$, 1 H, H-9), 8.39 (dd, $J = 8.8, 1.9$, 1 H, H-7), 7.83 (d, $J = 8.8$, 1 H, H-6), 6.63 (s, 1 H, H-4), 2.70 (t, $J = 7.4$, 2 H, $=\text{CCH}_2$), 1.76 (quint, $J = 7.4$, 2 H, $\text{CH}_2\text{CH}_2\text{CH}_3$), 1.49 (hexuplet, $J = 7.4$, 2 H, CH_2CH_3), 1.00 (t, $J = 7.4$, 3 H, CH_3); ^{13}C NMR (75 MHz, CDCl_3): $\delta = 165.6, 151.5, 148.6, 144.7, 143.2, 129.0, 122.1, 119.8, 111.0, 96.6, 33.1, 28.4, 22.1, 13.7$; GC/MS : $m/z = 287$ (M^+ , 100), 257 (11), 245 (49), 230 (27), 203 (23), 184 (16); HRMS (ESI - TOF) m/z : $[\text{M} + \text{Na} + \text{MeOH}]^+$ Calcd for $\text{C}_{15}\text{H}_{17}\text{N}_3\text{O}_5\text{Na}^+$ 342.1060; Found: 342.1064.



3-Butyl-7-nitro-1H-benzo[4,5]imidazo[1,2-c][1,3]oxazin-1-one(2g).

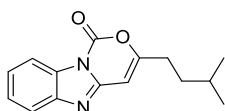
Yield: 86 mg, starting from 343 mg of **1g** (30%) (Table 2, entry 7). Yellow solid, mp: 144-147 °C; IR (KBr): 1775 (s), 1667 (m), 1520 (s), 1350 (s), 1173 (w), 1119 (w), 934 (w), 833 (m), 741 (m) cm^{-1} ; ^1H NMR (300 MHz, CDCl_3) $\delta = 8.62$ (s, 1 H, H-6), 8.38 – 8.30 (m, 2 H, H-8 + H-9), 6.60 (s, 1 H, H-4), 2.68 (t, $J = 7.4$, 2 H, $=\text{CCH}_2$), 1.76 (quint, $J = 7.4$, 2 H, $\text{CH}_2\text{CH}_2\text{CH}_3$), 1.49 (hexuplet, $J = 7.4$, 2 H, CH_2CH_3), 1.00 (t, $J = 7.4$, 3 H, CH_3); ^{13}C NMR (75 MHz, $\text{DMSO}-d_6$): $\delta = 164.7, 150.1, 146.4, 144.2, 143.5, 133.5, 120.2, 115.8, 114.7, 96.5, 33.0, 28.4, 22.1, 13.7$; GC/MS : $m/z = 287$ (M^+ , 100), 245 (50), 230 (29), 203 (31), 184 (13); HRMS (ESI - TOF) m/z : $[\text{M} + \text{Na} + \text{MeOH}]^+$ Calcd for $\text{C}_{15}\text{H}_{17}\text{N}_3\text{O}_5\text{Na}^+$ 342.1060; Found: 342.1064.



3-Octyl-1H-benzo[4,5]imidazo[1,2-c][1,3]oxazin-1-one (2h).

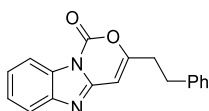
Yield: 254 mg, starting from 354 mg of **1h** (85%) (Table 2, entry 8). Colorless solid, mp: 90-94 °C; IR (KBr): $\nu = 1759$ (s), 1667 (m), 1551 (m), 1396 (m), 1373 (m), 1134 (m), 1103 (m), 964 (w),

756 (m) cm^{-1} ; ^1H NMR (300 MHz, CDCl_3): δ = 8.24 – 8.17 (m, 1 H, aromatic), 7.83 – 7.75 (m, 1 H, aromatic), 7.50 – 7.39 (m, 2 H, aromatic), 6.70 (s, 1 H, H-4), 2.62 (t, J = 7.6, 2 H, =CCH₂), 1.74 (quint, J = 7.6, 2 H, =CCH₂CH₂), 1.48 – 1.18 [m, 10 H, (CH₂)₅CH₃], 0.89 (t, J = 7.0, 3 H, CH₃); ^{13}C NMR (75 MHz, CDCl_3): δ = 163.4, 147.8, 143.9, 143.5, 129.1, 126.4, 125.1, 119.5, 114.6, 96.4, 33.2, 31.8, 29.2, 29.1, 28.9, 26.4, 22.6, 14.1; GC/MS = 298 (M^+ , 85), 283 (2), 269 (4), 255 (5), 239 (5), 225 (14), 213 (100), 200 (87), 185 (40), 171 (11), 158 (61), 130 (20); HRMS (ESI - TOF) m/z : [$\text{M} + \text{H}$]⁺ Calcd for $\text{C}_{18}\text{H}_{23}\text{N}_2\text{O}_2^+$ 299.1754; Found: 299.1757.



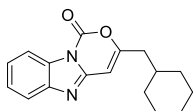
3-Isopentyl-1H-benzo[4,5]imidazo[1,2-c][1,3]oxazin-1-one (2i).

Yield: 210 mg, starting from 312 mg of **1i** (82%) (Table 2, entry 9). Colorless solid, mp: 102–104 °C; IR (KBr): ν = 1751 (s), 1667 (m), 1551 (w), 1451 (w), 1366 (s), 1134 (m), 1103 (m), 964 (w), 849 (w), 748 (m) cm^{-1} ; ^1H NMR (300 MHz, CDCl_3): δ = 8.21 – 8.15 (m, 1 H, aromatic), 7.77 – 7.72 (m, 1 H, aromatic), 7.50 – 7.37 (m, 2 H, aromatic), 6.48 (s, 1 H, H-4), 2.65 – 2.55 (m, 2 H, =CCH₂), 1.73 – 1.56 (m, 3 H, CH₂CH), 0.96 (d, J = 6.2, 6 H, 2 CH₃); ^{13}C NMR (75 MHz, CDCl_3): δ = 163.1, 147.4, 144.11, 144.03, 129.3, 126.2, 124.9, 119.7, 114.5, 96.5, 35.3, 31.1, 27.6, 22.3; GC/MS = 256 (M^+ , 100), 241 (6), 227 (2), 214 (10), 200 (56), 185 (25), 171 (5), 158 (61), 143 (4), 130 (14); HRMS (ESI - TOF) m/z : [$\text{M} + \text{H}$]⁺ Calcd for $\text{C}_{15}\text{H}_{17}\text{N}_2\text{O}_2^+$ 257.1285; Found: 257.1286.



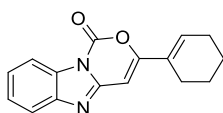
3-Phenethyl-1H-benzo[4,5]imidazo[1,2-c][1,3]oxazin-1-one (2j).

Yield: 232 mg, starting from 346 mg of **1j** (80%) (Table 2, entry 10). Colorless solid, mp: 159–162 °C; IR (KBr): ν = 1767 (s), 1667 (m), 1558 (w), 1451 (w), 1360 (s), 1103 (m), 988 (m), 864 (m), 756 (s), 694 (s) cm^{-1} ; ^1H NMR (300 MHz, CDCl_3): δ = 8.25 – 8.17 (m, 1 H, aromatic), 7.81 – 7.72 (m, 1 H, aromatic), 7.53 – 7.40 (m, 2 H aromatic), 7.35 – 7.13 (m, 5 H, Ph), 6.45 (s, 1 H, H-4), 3.06 (dist t, J = 7.6, 2 H, CH₂), 2.92 (dist t, J = 7.6, 2 H, CH₂); ^{13}C NMR (75 MHz, CDCl_3): δ = 161.4, 147.1, 144.0, 143.9, 139.2, 129.3, 128.7, 128.2, 126.7, 126.3, 125.0, 119.8, 114.6, 97.3, 34.8, 32.5; GC/MS = 290 (M^+ , 34), 245 (1), 199 (7), 185 (2), 155 (5), 129 (3), 102 (4), 91 (100); HRMS (ESI - TOF) m/z : [$\text{M} + \text{H}$]⁺ Calcd for $\text{C}_{18}\text{H}_{15}\text{N}_2\text{O}_2^+$ 291.1128; Found: 291.1126.



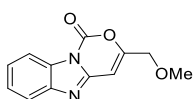
3-(Cyclohexylmethyl)-1H-benzo[4,5]imidazo[1,2-c][1,3]oxazin-1-one (2k).

Yield: 197 mg, starting from 338 mg of **1k** (70%) (Table 2, entry 11). Colorless solid, mp: 135–138 °C; IR (KBr): ν = 1767 (s), 1667 (m), 1559 (w), 1451 (w), 1389 (m), 1366 (m), 1096 (w), 964 (w), 748 (m) cm^{-1} ; ^1H NMR (500 MHz, CDCl_3) δ = 8.21 (d, J = 7.7, 1 H, aromatic), 7.77 (d, J = 8.1, 1 H, aromatic), 7.52 – 7.40 (m, 2 H, aromatic), 6.49 (s, 1 H, H-4), 2.48 (d, J = 7.0, 2 H, =CCH₂), 1.93 – 1.62 (m, 6 H, cyclohexyl), 1.39 – 0.96 (m, 5 H, cyclohexyl); ^{13}C NMR (125 MHz, CDCl_3): δ = 161.6, 147.3, 144.2, 129.4, 126.3, 124.9, 119.8, 114.6, 97.7, 41.0, 35.8, 33.0, 26.2, 26.0; GC/MS: m/z = 282 (M^+ , 67), 200 (100), 156 (24), 129 (5); HRMS (ESI - TOF) m/z : [$\text{M} + \text{H}$]⁺ Calcd for $\text{C}_{17}\text{H}_{19}\text{N}_2\text{O}_2^+$ 283.1441; Found: 283.1448.



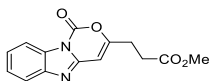
3-(Cyclohex-1-en-1-yl)-1H-benzo[4,5]imidazo[1,2-c][1,3]oxazin-1-one (2l).

Yield: 176 mg, starting from 322 mg of **1l** (66%) (Table 2, entry 12). Colorless solid, mp: 191-195 °C; IR (KBr): $\nu = 1767$ (s), 1636 (m), 1420 (w), 1366 (m), 1281 (w), 1180 (w), 1111 (m), 1026 (w), 833 (w), 748 (m) cm^{-1} ; ^1H NMR (300 MHz, CDCl_3) $\delta = 8.24 - 8.16$ (m, 1 H, aromatic), 7.81 - 7.71 (m, 1 H, aromatic), 7.53 - 7.39 (m, 2 H, aromatic), 7.00 - 6.90 (m, 1 H, =CH), 6.55 (s, 1 H, H-4), 2.40 - 2.24 (m, 4 H, cyclohexenyl), 1.86 - 1.74 (m, 2 H, cyclohexenyl), 1.74 - 1.62 (m, 2 H, cyclohexenyl); ^{13}C NMR (75 MHz, CDCl_3): $\delta = 157.7, 148.1, 144.5, 143.6, 134.0, 129.5, 127.1, 126.2, 124.9, 119.6, 114.5, 92.8, 25.9, 23.9, 22.0, 21.5$; GC/MS = 266 (M^+ , 100), 237 (7), 221 (23), 185 (26), 157 (9); HRMS (ESI - TOF) m/z : $[\text{M} + \text{H}]^+$ Calcd for $\text{C}_{16}\text{H}_{15}\text{N}_2\text{O}_2^+$ 267.1128; Found: 267.1129.



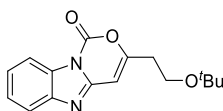
3-(Methoxymethyl)-1H-benzo[4,5]imidazo[1,2-c][1,3]oxazin-1-one (2m).

Yield: 138 mg, starting from 286 mg of **1m** (60%) (Table 2, entry 13). Yellow solid, mp: 122-125 °C; IR (KBr): $\nu = 1751$ (s), 1667 (m), 1558 (m), 1443 (m), 1381 (s), 1173 (m), 1103 (s), 957 (w), 748 (s) cm^{-1} ; ^1H NMR (500 MHz, CDCl_3) $\delta = 8.23 - 8.18$ (m, 1 H, aromatic), 7.82 - 7.75 (m, 1 H, aromatic), 7.53 - 7.43 (m, 2 H, aromatic), 6.81 - 6.78 (m, 1 H, H-4), 4.35 (s, 2 H, CH_2OCH_3), 3.53 (s, 3 H, OCH_3); ^{13}C NMR (125 MHz, CDCl_3): $\delta = 158.2, 146.8, 144.1, 143.5, 129.4, 126.4, 125.3, 120.0, 114.6, 97.2, 69.6, 59.4$; GC/MS: $m/z = 230$ (M^+ , 89), 199 (5), 185 (100), 171 (10), 157 (48), 129 (8); HRMS (ESI - TOF) m/z : $[\text{M} + \text{H}]^+$ Calcd for $\text{C}_{12}\text{H}_{11}\text{N}_2\text{O}_3^+$ 231.0764; Found: 231.0768.



Methyl 3-(1-oxo-1H-benzo[4,5]imidazo[1,2-c][1,3]oxazin-3-yl)propanoate (2n).

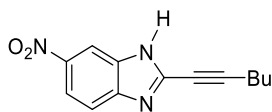
Yield: 201 mg, starting from 328 mg of **1n** (74%) (Table 2, entry 14). Colorless solid, mp: 189-193 °C; IR (KBr): $\nu = 1767$ (s), 1736 (s), 1667 (m), 1435 (w), 1366 (w), 1173 (m), 996 (m), 895 (w), 841 (w), 772 (m) cm^{-1} ; ^1H NMR (500 MHz, CDCl_3) $\delta = 8.19$ (d, $J = 7.7$, 1 H, aromatic), 7.77 (d, $J = 8.1$, 1 H, aromatic), 7.51 - 7.41 (m, 2 H, aromatic), 6.58 (s, 1 H, H-4), 3.72 (s, 3 H, CO_2CH_3), 2.97 (t, $J = 7.2$, 2 H, = CCH_2), 2.79 (t, $J = 7.2$, 2 H, $\text{CH}_2\text{CO}_2\text{CH}_3$); ^{13}C NMR (125 MHz, CDCl_3): $\delta = 171.8, 160.4, 147.0, 144.1, 143.7, 126.4, 125.2, 119.9, 114.6, 97.5, 52.1, 30.5, 28.4$; GC/MS: $m/z = 272$ (M^+ , 61), 243 (15), 212 (100), 199 (35), 185 (33), 169 (20), 157 (35); HRMS (ESI - TOF) m/z : $[\text{M} + \text{H}]^+$ Calcd for $\text{C}_{14}\text{H}_{13}\text{N}_2\text{O}_4^+$ 273.0870; Found: 273.0874.



3-(2-(tert-Butoxy)ethyl)-1H-benzo[4,5]imidazo[1,2-c][1,3]oxazin-1-one (2o').

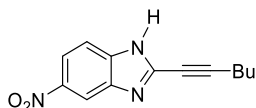
Yield: 189 mg, starting from 286 mg of **1o** (66%) (Table 2, entry 15). Colorless solid, mp: 189-193 °C; IR (KBr): $\nu = 1774$ (s), 1666 (m), 1551 (w), 1389 (w), 1366 (m), 1204 (w), 1111 (w), 1080 (m), 756 (m) cm^{-1} ; ^1H NMR (500 MHz, CDCl_3) $\delta = 8.25 - 8.21$ (m, 1 H, aromatic), 7.82 - 7.77 (m, 1 H, aromatic), 7.52 - 7.42 (m, 2 H, aromatic), 6.65 (dist t, $J = 0.8$, 1 H, H-4), 3.73 (t, $J = 6.1$, 2 H, $\text{CH}_2\text{Ot-Bu}$), 2.83 (td, $J = 6.1, 0.8$, 2 H, = CCH_2), 1.20 (s, 9 H,); ^{13}C NMR (125 MHz, CDCl_3): $\delta = 160.5, 147.4, 144.2, 144.0, 129.4, 126.3, 125.0, 119.8, 114.6, 98.0, 73.5, 57.7, 34.5$,

27.4; GC/MS: $m/z = 286$ (M^+ , 21), 213 (12), 200 (100), 171 (16), 156 (22); HRMS (ESI - TOF) m/z : $[M + H]^+$ Calcd for $C_{16}H_{19}N_2O_3^+$ 287.1390; Found: 287.1395.



2-(Hex-1-yn-1-yl)-6-nitro-1H-benzo[d]imidazole (3f).

Yield: 49 mg, starting from 343 mg of **1f** (20%) (Table 2, entry 6). Colorless solid, mp: 138-140 °C; IR (KBr): $\nu = 2230$ (w), 1520 (s), 1474 (w), 1435 (w), 1343 (s), 1065 (w), 818 (m) cm^{-1} ; 1H NMR (500 MHz, DMSO- d_6): $\delta = 8.41$ (s, br, 1 H, H-3), 8.14 (dd, $J = 8.9, 2.2$, 1 H, H-5), 7.69 (d, $J = 8.9$, 1 H, H-4), 2.58 (t, $J = 7.2$, 2 H, $\equiv CCH_2$), 1.60 (quint, $J = 7.2$, 2 H, $CH_2CH_2CH_3$), 1.49 (hexuplet, $J = 7.2$, 2 H, CH_2CH_3), 0.95 (t, $J = 7.2$, 3 H, CH_3) (Note: the NH signal was incorporated into the broad HOD signal at 3.49 ppm); ^{13}C NMR (125 MHz, DMSO- d_6): $\delta = 143.1, 139.6, 118.3, 114.3$ (br), 95.8, 71.6, 29.5, 21.4, 18.1, 13.3; GC/MS: $m/z = 243$ (M^+ , 100), 228 (48), 214 (73), 201 (93), 182 (41), 168 (54), 155 (57), 127 (27); HRMS (ESI - TOF) m/z : $[M + H]^+$ Calcd for $C_{13}H_{14}N_3O_2^+$ 244.1081; Found: 244.1081.



2-(Hex-1-yn-1-yl)-5-nitro-1H-benzo[d]imidazole (3g).

Yield: 75 mg, starting from 343 mg of **1g** (31%) (Table 2, entry 7). Yellow solid, mp: 145-148 °C; IR (KBr): $\nu = 2237$ (w), 1520 (s), 1474 (w), 1435 (w), 1366 (w), 1342 (s), 1065 (m), 818 (m), 741 (m) cm^{-1} ; 1H NMR (500 MHz, $CDCl_3$): $\delta = 8.75$ (s, 1 H, H-4), 8.29 (d, $J = 8.8$, 1 H, H-6), 7.83 (d, $J = 8.8$, 1 H, H-7), 2.48 (t, $J = 7.3$, 2 H, $\equiv CCH_2$), 1.50 (quint, $J = 7.3$, 2 H, $CH_2CH_2CH_3$), 1.33 (hexuplet, $J = 7.3$, 2 H, CH_2CH_3), 0.78 (t, $J = 7.3$, 3 H, CH_3) (Note: the NH signal was too broad to be detected); ^{13}C NMR (125 MHz, $CDCl_3$): $\delta = 144.4, 140.4, 119.2, 115.1$ (br), 112.6 (br), 98.2, 71.0, 29.9, 22.0, 19.1, 13.4; GC/MS: $m/z = 243$ (M^+ , 100), 228 (44), 214 (71), 201 (96), 182 (40), 168 (54), 155 (56); HRMS (ESI - TOF) m/z : $[M + H]^+$ Calcd for $C_{13}H_{14}N_3O_2^+$ 244.1081; Found: 244.1082.

5.6 References

- [1] G. Wang, J.R.E Menye and V. Sharma, *Bioorganic & Medicinal Chemistry Letters* **16**, **2006**, 2177–2181.
- [2] W.C. Widdison, S. D. Wilhelm, E. E. Cavanagh, K. R. Whiteman, B. A. Leece, Y. Kovtun, V. S. Goldmacher, H. Xie, R. M. Steeves, R. J. Lutz, R. Zhao, L. Wang, W. A. Blattler, and R. V. J. Chari, *Med. Chem.* **2006**, *49*, 4392–4408.
- [3] M. Lopus, E. Oroudjev, L. Wilson, S. Wilhelm, W. Widdison, R. Chari, and M. A. Jordan, *Mol Cancer Ther.* **2010**, *9* (10), 2689–99.
- [4] L. Zhuang et al., *Bioorganic & Medicinal Chemistry* **2017**.
- [5] Z. Xu et al., *J. Med. Chem.* **2011**, *54*, 6050–6062.
- [6] Z. Chuanxin, W. Shengzheng, D. Lei, X. Duoli, L. Jin, R. Fuzeng, L. Aiping, Z. Ge, *European Journal of Medicinal Chemistry*, **2020**.
- [7] J. Paz, C. P. Balado, B. Iglesias, and L. Muñoz, *J. Org. Chem.* **2010**, *75*, 3037–3046.
- [8] B. Alcaide, P. Almendros, M. T. Quirós and I. Fernández, *Beilstein J. Org. Chem.* **2013**, *9*, 818–826.
- [9] R. R. Machin, J. Adrio, and J. C. Carretero, *J. Org. Chem.* **2006**, *71*, 5023–5026.
- [10] S. Trifunović, D. Dimitrijević, G. Vasić, N. Radulović, M. Vukićević, F. W. Heinemann, R. D. Vukićević, *Synthesis* **2010**, *6*, 943–946.
- [11] J. Paz, C. P. Balado, B. Iglesias, and L. Muñoz, *J. Org. Chem.* **2010**, *75*, 3037–3046.
- [12] A. Baba, I. Shibata, M. Fujiwara and H. Matsuda, *Tetrahedron Letters*, **1985**, *26*, 42, pp 5167–5170.
- [13] I. Shibata, K. Nakamura, A. Baba, and H. Matsuda, *Bull. Chem. Soc. Jpn.*, **1989**, *62*, 853–859.
- [14] L. Zheng, R. Hua, *Front. Chem.* **2020**, *8*, 580355.
- [15] F.L. Hong, L.W Ye, *Acc. Chem. Res.* **2020**, *53*, 2003–2019.
- [16] N. Kaur, Y. Verma, P. Grewal, N. Ahlawat, P. Bhardwaj, N.K. Jangid, *Synth. Commun.* **2020**, *50*, 1567–1621.
- [17] B. Gabriele, R. Mancuso, L. Veltri, I. Zicarelli, N. Della Ca', *Eur. J. Org. Chem.* **2019**, 5073–5092.
- [18] R. Wang, X. Xie, H. Liu, Y. Zhou, *Catalysts* **2019**, *9*, 823.
- [19] L. Zheng, R. Hua, *Front. Chem.*, **2020**, *8*, 580355.
- [20] F.-L. Hong, L.W Ye, *Acc. Chem. Res.*, **2020**, *53*, 2003–2019.
- [21] N. Kaur, Y. Verma, P. Grewal, N. Ahlawat, P. Bhardwaj, N.K. Jangid, *Synth. Commun.* **2020**, *50*, 1567–1621.
- [22] B. Gabriele, R. Mancuso, L. Veltri, I. Zicarelli, N. Della Ca', *Eur. J. Org. Chem.* **2019**, 5073–5092.
- [23] R. Wang, X. Xie; H. Liu, Y. Zhou, *Catalysts* **2019**, *9*, 823.
- [24] J. Li, F. Yang, W. Hu, B. Ren, Z.S. Chen, K. Ji, *Chem. Commun.* **2020**, *56*, 9154–9157.
- [25] Li, Z.; Song, L.; Van Meervelt, L.; Tian, G.; Van der Eycken, E.V. Cationic Gold(I)-Catalyzed Cascade Bicyclizations for Divergent Synthesis of (Spiro)polyheterocycles. *ACS Catal.* **2018**, *8*, 6388–6393.

- [26] S.W Youn, H.J. Yoo, *Adv. Synth. Catal.* **2017**, *359*, 2176–2183.
- [27] V. Mamane, P. Hannen, A. Fürstner, A. *Chem. Eur. J.* **2004**, *10*, 4556–4575.
- [28] K. Ghosh, M. Shankar, R.K. Rit, G. Dubey, P.V. Bharatam, A.K. Sahoo, *J. Org. Chem.* **2018**, *83*, 9667–9681.
- [29] Y. Miclo; P. Garcia, Y. Evanno, P. George, M. Sevrin, M. Malacria, V. Gandon, C. Aubert, *Synlett* **2010**, 314–2318.
- [30] Y. Hoshimoto, K. Ashida, Y. Sasaoka, R. Kumar, K. Kamikawa, X. Verdagner, A. Riera, M. Ohashi, S. Ogoshi, *Angew. Chem. Int. Ed.* **2017**, *56*, 8206–8210.
- [31] X.F Mao, X.P. Zhu, D.Y. Li, P.N. Liu, *J. Org. Chem.* **2017**, *82*, 7032–7039.
- [32] A.K. Mandadapu, S.K. Sharma, S. Gupta, D.G.V. Krishna, B. Kundu, *Org. Lett.* **2011**, *13*, 3162–3165.
- [33] L. Habert, R. Sallio, M. Durandetti, C. Gosmini, I. Gillaizeau, *Eur. J. Org. Chem.* **2019**, 5175–5179.
- [34] Y. Liu, W. Zhen, W. Dai, F. Wang, X. Li, *Org. Lett.* **2013**, *15*, 874–877.
- [35] L. Veltri, R. Amuso, M. Petrilli, C. Cuocci, M. A. Chiacchio, P. Vitale, B. Gabriele, *Molecules*, **2021**, *26*, 2318.
- [36] Wutts, *JohnWiley & Sons, Inc.: Hoboken, NJ, USA*, **2014**; pp. 755–939.
- [37] E. Langille; C.S. Bottaro; A. Drouin, A. *J. Flow Chem.* **2020**, *10*, 377–387.
- [38] H.-D. Vu, J. Renault, T. Roisnel, C. Robert, P. Jéhan, N. Gouault, P. Uriac; *Eur. J. Org. Chem.* **2015**, 4868–4875.
- [39] S.C. Nigam, A. Mann, M. Taddei, C-G. Wermuth, *Synth. Commun.* **1989**, *19*, 3139–3142.
- [40] Y.-Q Wu, D.C. Limburg, D.E. Wilkinson, M.J. Vaal, G.S.A Hamilton, *Tetrahedron Lett.* **2000**, *41*, 2847–2849.
- [41] Kaul, R.; Brouillette, Y.; Sajjadi, Z.; Hansford, K.A.; Lubell, W.D. *J. Org. Chem.* **2004**, *69*, 6131–6133.
- [42] V. Bacauanu, S. Cardinal, M. Yamauchi, M. Kondo, D.F. Fernández, R. Remy, D.W.C. MacMillan, *Angew. Chem. Int. Ed.* **2018**, *57*, 12543-12548.

Chapter 6

Conclusions

In this PhD thesis have been developed various processes, which led in a one synthetic step, to the formation of high added-value molecules, with important pharmacological properties. In the first chapter we have developed a novel cyclocarbonylative method for the direct synthesis of thiadiazafluorenones **2** starting from readily available 2-(propynylthio)-1*H*-benzimidazoles **1** bearing internal and terminal triple bond. The process is catalyzed by the simple catalytic system PdI₂/KI and occurs in MeOH under relatively mild conditions (80 °C, under 30 atm of CO). Product formation, whose structure has been confirmed by XRD analysis by the most representative products, must ensue from some unexpected kind of structural rearrangement, most likely occurring through palladium-promoted propargyl–allene rearrangement to give a thiolate and an allenylpalladium intermediate, followed by thiolate addition to the central allenic carbon and cyclocarbonylation. The corresponding 3-alkyl-2-methyl-1-thia-4a,9-diazafluoren-4-ones **2** were obtained in fair yields (50–74%). To the best of our knowledge, this is the first example of synthesis of polyheterocycles **2** by a direct additive carbonylation approach.

In the second chapter, cyclometalated aryl heterocycles can be used as a tunable mimic of carbonyl and hydride ligands in popular ruthenium pincer complexes. Following this concept, a series of novel potent catalysts **[Ru]-5-[Ru]-12** for (de)hydrogenations have been obtained. The general advantage of such catalysts compared to the parent complex is demonstrated for the green α -alkylation of ketones with alcohols, obtained with satisfactory yields. Plausible reaction intermediates were investigated for this, all still involving the intact phenyl heterocycle and the pincer ligand. This catalyst design can be used as a guideline for the creation of a variety of other pincer complexes, too; thus, opening the door for more effective catalysis.

In third chapter other cyclometalated ruthenium complexes have been established as novel catalysts for the methylation of anilines using methanol via a hydrogen autotransfer procedure. The optimal system **9** bearing a phenyl imidazoline as bidentate ligand likely works in a homogenous manner with β -hydride elimination of methanol to form a Ru–H species being the rate determining step. Compared to other known catalysts for this transformation, **[Ru]-9** allows to work under very mild reaction conditions without the necessity of strong/expensive bases.

In the fourth part, we have reported a new approach for CO₂ utilization and valorization, which consists in its catalytic incorporation into readily available 3-ynamides to give high value-

added 3-oxazine-2,4-diones. The reaction, promoted by DBU as simple and commercially available organocatalyst (0.4 equiv), takes place in a 3:1 MeCN–HC(OMe)₃ mixture under relatively mild conditions (30 atm of CO₂, at 80 °C for 15 h), and proceeds through a mechanism involving substrate deprotonation by DBU followed by attack of the anionic nitrogen on carbon dioxide, 6-*endo-dig* cyclization, and protonolysis. Differently substituted 3-ynamide substrates, bearing various substituents on nitrogen or on the triple bond, have been converted into the corresponding oxazindiones in isolated yields ranging from 44% to 87% over 16 examples. The yields were higher when the substrate triple bond was protected with a trimethylsilyl group and the nitrogen was bonded to a sterically unhindered substituent, to give the corresponding oxazindiones in 74-87% yields, while lower yields (44-69%) were observed in the case of substrates bearing an alkyl or phenyl substituent on the triple bond or a sterically bulky group on nitrogen.

In the last work has been described the ZnCl₂-promoted heterocyclization with ZnCl₂ in under mild conditions (40 °C in CH₂Cl₂ for 3h), giving access to a new class of polycyclic heterocycles, 1*H*-benzo[4,5]imidazo[1,2-*c*][1,3]oxazin-1-ones. In the present study the ZnCl₂, simple and inexpensive, assisted the 6-*endo-dig* heterocyclization of the carbamate intermediate with incorporation of the carbamate group (as indirect carboxylation agent) into the final polyheterocyclic derivative, while in the previous literature ZnCl₂ was reported to promote complete *N*-Boc deprotection with elimination of isobutene and CO₂. ZnCl₂ thus played a dual role, by promoting the Boc deprotection of the substrate with elimination of the *tert*-butyl carbonation (which could be trapped by substrates bearing a nucleophilic group) and activating the triple bond toward the intramolecular nucleophilic attack by the carbamate moiety. The benzimidazoxazinone derivatives have been obtained in moderate to high yields starting from differently substituted substrates, and the structure of representative products was confirmed by X-ray diffraction analysis.